Theses

Electronic Theses and Dissertations

6-2014

Development of a Process for Producing Biodiesel from Microalgae Lipids with Supercritical Carbon Dioxide Extraction and Enzyme-Catalyzed Transesterification

Hanifa Easa Taher Al Belooshi

Follow this and additional works at: https://scholarworks.uaeu.ac.ae/all_theses

Part of the Engineering Commons

DEVELOPMENT OF A PROCESS FOR PRODUCING BIODIESEL FROM MICROALGAE LIPIDS WITH SUPERCRITICAL CARBON DIOXIDE EXTRACTION AND ENZYME-CATALYZED TRANSESTERIFICATION

Hanifa Easa Taher Al Belooshi

This dissertation is submitted in partial fulfillment of the requirements for the degree of Doctor of Philosophy

Under the direction of Dr. Sulaiman Al-Zuhair

June 2014

DECLARATION OF ORIGINAL WORK

I Hanifa Taher, the undersigned, a graduate student at the United Arab Emirates University (UAEU) and the author of the dissertation entitled " Development of a process for producing biodiesel from microalgae lipids with supercritical carbon dioxide extraction and enzyme-catalyzed transesterification", hereby solemnly declare that this dissertation is an original work done and prepared by me under the guidance of Dr. Sulaiman Al-Zuhair, in the College of Engineering at UAEU. This work has not previously formed the basis for the award of any degree, diploma or similar title at this or any other university. The materials borrowed from other sources and included in my dissertation have been properly acknowledged.

Student's Signature.................................... Date...11 - 06 - 2014

Approved by

PhD Examining Committee:

1) Advisor (Committee Chair): Dr. Sulaiman Al-Zuhair

Title: Associate Professor

Department of Chemical and Petroleum Engineering

College of Engineering

Signature……………………… Date ……………………………..

2) Member: Prof. Muftah El-Naas

Title: Professor

Department of Chemical and Petroleum Engineering

College of Engineering

Signature……………………… Date ……………………………..

3) Member: Dr. Mohammed Hamdan

Title: Associate professor

Department of Mechanical Engineering

College of Engineering

Signature……………………… Date ……………………………..

4) Member: Prof. Richard Lee Smith, Jr.

Title: Professor

Department of Chemical Engineering

Graduate School of Environmental Studies

Institution: Tohoku University

Signature……………………… Date ……………………………..

Accepted by

Dean of the College of Engineering: Prof. Amr Salah El-Dieb

Signature………………………… Date ……………………………..

Dean of the College of Graduate Studies: Prof. Nagi Wakim

Signature………………………… Date ……………………………..

Copy   of

ABSTRACT

Lipids were extracted from microalgae using supercritical carbon dioxide ($SC-CO_2$), and used for enzymatic biodiesel production in $SC-CO_2$. The growth of several fresh water and marine strains was tested under aeration with different CO_2 enrichments. The highest growth found was for *Chlorella* sp. grown at 27 ^{o}C, 1 % CO_2 enrichment and 460 mM NaCl concentration, at which carbon fixation rate was 1.7 g L^{-1} d^{-1}. The highest enhancement of lipids content by nitrogen starvation was found with *Scenedesmus* sp., but with a lower growth rate. Two step cultivation of *Scenedesmus* sp. was carried out in a 5 L internally-illuminated photobioreactor, to combine high growth rate with high lipids content.

$SC-CO_2$ extraction of lipids from lyophilized microalgae at 50 °C, 350 bar and a flow rate of 2.69 g min^{-1} was found to be more effective than conventional extraction techniques. The effects of extraction conditions, namely 200–500 bar; 35–65 °C and CO_2 flow rate of 1.38–4.02 g min^{-1}, on extraction yield were investigated. The optimum yield was found to be 7.4 at 53 °C and 500 bar after 1 h. The possibility of extracting lipids directly from wet cells, avoiding the drying step, was studied. Lytic enzymes were efficient in disrupting the cell walls and enhancing the extraction. Lipids extraction yield from wet cells was found to be 12.5% using $SC-CO_2$ compared to 16.6 % using *n*-hexane.

Enzymatic production of biodiesel from extracted lipids in a $SC-CO_2$ medium was studied in a batch reactor. The effect of enzyme loading (15-50 % wt), temperature (35-55 ^{o}C) and methanol to lipid (M:L) molar ratio (3-15:1)

were investigated. A reaction yield of 82 % was obtained at 50 $^{\circ}$C, 200 bar, 35% enzyme loading, and 9:1 M:L molar ratio after 4 h. The extraction and reaction processes were combined in a continuous integrated process, and the best M:L ratio was found to be 10:1, and the enzyme was reused for 6 cycles retaining 78 % of its original activity. The enzyme washed with *tert*-butanol at the end of the sixth cycle and was successfully reused for 24 cycles retaining 70% of its activity.

Keywords: Biodiesel, microalgae lipids, supercritical CO_2, transesterification, process scale-up, process integration

iii

الملخص

تم إستخلاص الدهون من الطحالب الدقيقة بإستخدام ثاني أكسيد الكربون في الحالة فوق الحرجة (SC-CO$_2$) وأستخدمت لتعزيز أسترة الدهن المستخلص إلى ديزل حيوي في وجود لييبز (lipase). تمت دراسة نمو عدة سلالات من الطحالب الدقيقة و تحديد أفضل الظروف. كان أعلى معدل نمو للطحلب كولوريلا (Chlorella sp) عند 27 °م، 1 % تركيز لثاني أكسيد الكربون بالهواء و مستوى ملوحة تقدر ب 460 حجم مولي بتثبيت 1.7 جرام لتر$^{-1}$ يوم بتثبيت لثاني أكسيد الكربون الجوي. كذلك، كان أعلى زياده لمحتوى الدهن لدى Scenedesmus sp.، لكن بمعدل نمو أقل. فلذلك تم زراعتها في مفاعل حيوي ضوئي (سعة 5 لتر) على خطوتين لتعزيز كل من معدل النمو و المحتوى الدهني.

تمت دراسة إستخلاص الدهون من الطحالب المجففة عند 50 °م ، 350 ضغط جوي باستخدام ثاني اكسد الكربون في الحالة الفوق حرجة و وجد أنه ذو كفاءة أعلى من الطرق التقليدية. تمت دراسة ضروف الاستخلاص ، بالتحديد 200-500 ضغط جوي، 35-65 °م وتدفق كتلي 4.02-1.38 جرام لكل دقيقه . و كانت أعلى كمية للإستخلاص 7.34 عند 53 °م، 500 ضغط لمدة 60 دقيقة. بناء ع ذلك تم دراسة إمكانية إستخلاص الدهون من الخلايا الغير مجففة و المعالجة إنزيمياً، و كانت أعلى حصيلة للاستخلاص، باستخدام ثاني اكسيد كربون في الحالة الحرجة، 12.5% مقارنة ب 16.6% باستخدام المذيب العضوي (الهكسان).

علاوة على ذلك، تم دراسة الإنتاج الأنزيمي للديزل الحيوي من الدهون المستخلصة بوساطة SC-CO$_2$ في مفاعل حيوي، وتمت دراسة تأثير كميىة الأنزيم المستخدمة (15-50٪)، درجة الحرارة (35- 55 °م) و النسبة المولارية بين الميثانول و الدهن (3:1-15:1). وتم الحصول على أعلى كمية للديزل الجيوي بنسبة 82 % عند 47 °م ، 200 ضغط ، 35 % تركيز للانزيم و 9:1 نسبة مولارية بعد 4 ساعات من التفاعل، ومن ثم تم دمج العمليتان المذكورتان أعلاه (استخلاص وتفاعل) في عملية واحده مستمره، و تم التوصل لإمكانية إنتاج الوقود بفعالية عند 10:1 نسبة مولارية، و التمكن من إستخام الإنزيم نفسه في 6 دورات مستمرة. وكذلك تم بنجاح استخدام الانزيم ذاته في 24 دورات متتاليه والاحتفاظ ب 70 % من نشاطها بعد غسلها بالبيوتانول الثلاثي.

TABLE OF CONTENTS

ACKNOWLEDGMENTS

First and foremost, I would like to thank God for providing me a chance to have this graduate study opportunity to achieve my goals. It is always hard to look back and try to remember all of individuals who have assisted me during this journey. I would like to say "thank you" to all of them.

Words cannot express my deepest appreciation that I have for my main supervisor, Dr. Sulaiman Al-Zuhair for all his supports and possible conditions necessary for a good work. Special thanks are extended the advising committee, Dr. Ali Al-Marzouqi, Prof. Yousef Haik and Prof. Mohammed Farid for their valuable supervision, support and help during my study. Their continuous support and advices provided me vital guidance and motivation. Without their support, I wasn't able to successfully complete this work.

Appreciation is extended to my committee members, Prof. Muftah Al-Naas, Dr. Mohammed O. Hamdan and Prof. Richard Smith for their time. Also, I would like thank all lab technicians in chemical & petroleum engineering and Food science departments within United Arab Emirates University for their helps in samples preparation and analysis.

Last but not the least, I would like to admit that this would not have been possible without the family encouragement. A special acknowledgement is made to my parents, brothers and sisters.

LISTS OF FIGURES

LISTS OF TABLES

ABBREVIATIONS

ASTM	American Society for Testing and Materials
ANOVA	Analysis of Variance
BIC	Broken and intact cells
CN	Cetane number
DAG	Diacylglycerol
EN	European standard
GC	Gas chromatography
FAAE	Fatty acid alkyl ester
FAME	Fatty acid methyl ester
FID	Flame ionization detector
FFA	Free fatty acid
IC	Inorganic carbon
IV	iodine value
LSD	Least significant differences
LOI	Loss of ignition
M:L	Methanol to lipid
MAG	Monoacylglycerol
NO_x	Nitrogen oxides
NIST	National Institute of Standards and Technology
NREL	National Renewable Energy Laboratory
OF	Objective function
PM	Particular matter

RSM	Response surface methodology
SV	Saponification value
SO_x	Sulfur oxides
SCA	Supercritical alcohol
$SC\text{-}CO_2$	Supercritical carbon dioxide
SCE	Supercritical ethanol
SCF	Supercritical fluids
SCM	Supercritical methanol
TIC	Total inorganic carbon
TAG	Triglyceride

NOMENCLATURE

[A]	Alcohol concentration	[mol L^{-1}]
[S]	Substrate concentration	[mol L^{-1}]
[M]*	Initial mass concentration of methanol	[g g^{-1}]
a_o	Specific surface area	[m^2 m^{-3}]
a and b	Fitting parameters	
C$_o$, C$_1$ and C$_2$	Fitting parameters	
k_o, k_1 and k_2	Fitting parameters	
d	Screen size	[mm]
d_p	Particle size	[mm]
d_{sv}	Surface-volume mean diameter	[mm]
D_{12}	Mass diffusivity	[m^2 s^{-1}]
E	Amount of extracted lipids	[g g^{-1}]
h	Axial coordinate	[cm]
H	Bed height	[cm]
H	Henry constant	[mol L^{-1} atm^{-1}]
k_f	Mass transfer coefficient in fluid phase	[m s^{-1}]
k_s	Mass transfer coefficient in solid phase	[m s^{-1}]
K_M	Michaelis constant	[mol L^{-1}]
K_i	Inhibition constant	[mol L^{-1}]
$K_{m,l}$	Apparent Michaelis–Menten constant for the substrate	[g g^{-1}]
K_{iA}	Apparent methanol inhibition constant for alcohol	[g g^{-1}]
$K_{m,A}$	Apparent Michaelis–Menten constants for methanol	[g g^{-1}]

K_s	Monod half-saturation constant	[mol L^{-1}]
m_{CO_2}	Mass of passed SC-CO_2	[g]
m_{bed}	Mass of solute free biomass	[g]
m_{lipid}	Extract weight	[g]
$m_{biomass}$	Biomass weight	[g]
$\dot{m}_{i+1}$	FAME production rate in batch $i+1$	[mg min^{-1}]
$\dot{m}_{i=1}$	FAME production rate in batch i	[mg min^{-1}]
m_{FAME}	produced FAME	[mg]
n	uniformity factor	[-]
q	Specific amount of CO_2 passed through the extractor	[g g^{-1}]
q_m	Specific amount of CO_2 when extraction in intact cells started	[g g^{-1}]
q_n	Specific amount of CO_2 at end of sond stage	[g g^{-1}]
R	Retained biomass on sieve	[%]
R_{CO_2}	CO_2 fixation rate	[g L^{-1} d^{-1}]
RA	Regeneration activity	[-]
Re	Reynolds number	[-]
$R_{TG/L}$	Triglycerides content of extracted lipids	[g g^{-1}]
Sc	Schmidt number	[-]
Sh	Sherwood number	[-]
sv	specific surface area	[m^2 g^{-1}]
W	Dimensionless parameters proportional to the fluid phase coefficient	[-]
x_k	Inaccessible lipid concentration inside the solid particle	[g g^{-1}]
x_o	Extractable lipids concentration in the bed	[g g^{-1}]

x_p	Accessible specific solute concentration	[g g^{-1}]
$Y_{FAME,b}$	FAME production yield in batch system	[g g^{-1}]
$Y_{FAME,c}$	FAME production yield in continuous system	[g g^{-1}]
Z	Dimensionless parameters proportional to the fluid phase coefficient	[-]
Z_w	Dimensionless axial coordinate between fast and slow extractions	[-]

GREEK SYMBOLS

ε	Bed porosity	[-]
ρ_b	Bulk density	[kg m^{-3}]
Γ	Gamma function	[-]
v_i	Initial reaction rate	[g g^{-1} h^{-1}]
v_{max}	Maximum reaction velocity	[g g^{-1} h^{-1}]
$\bar{\mu}_{max}$	Maximum specific growth rate	[d^{-1}]
ρ	SC-CO$_2$ density	[kg m^{-3}]
μ	SC-CO$_2$ viscosity	
ρ_s	Solid density	[kg m^{-3}]
$\bar{\mu}$	Specific growth rate	[d^{-1}]

CHAPTER 1: INTRODUCTION

1.1 MOTIVATION

Currently, the world energy demand is mainly met by fossil fuels, which are being depleted, resulting in an increase in their prices. At the same time, the global environment is threatened by the increase in emissions of harmful gases associated with fossil fuel combustion, which accounts for 75 % of the total reported carbon dioxide (CO_2) emissions [1]. Thus, reducing the dependency on fossil fuels is crucial to reduce CO_2 emissions. The most sufficient way to achieve this goal is to find alternative fuels that are sustainable, cost-effective and environmentally-friendly.

Triglycerides (TAGs), which account for more than 90 % of vegetable oils content, hold the promise as alternative diesel engine fuels due to the advantages of being available, renewable and biodegradable [2]. Nevertheless, oils have high viscosity and low volatility [3, 4], which hinder their direct use in diesel engine. On the other hand, biodiesel produced by TAGs transesterification, has a lower viscosity and similar properties to petroleum diesel and promises to be a better alternative. It is biodegradable, non-toxic, safe, and, based on its chemical structure, can be used in diesel engines without further modification to the engine [4, 5]. Additionally, biodiesel results in a significant reduction of unburned hydrocarbons, carbon monoxide (CO) and particular matter (PM) formation [6, 7].

The commercial biodiesel production processes are carried out using alkali catalysts that reach high conversions of 98 % [8-12]. However, these

processes have several environmental issues and require feedstock pretreatment to remove the free fatty acids (FFAs), which otherwise would cause saponification as a side reaction. In addition, such processes require complex biodiesel purification, which further increases the production cost [3, 13]. A flowchart of the production process is shown in Figure 1.1 (a). These could be eliminated by carrying out non-catalytic reaction using supercritical alcohols in a short reaction time and without the need for reaction product purification. However, this process is energy intensive and not economically feasible.

Recently, enzymatic transesterification by lipases, which belong to hydrolytic enzymes group, has received considerable attention as an alternative approach for biodiesel production. Lipases can work at mild operating conditions, which lower the overall energy requirement. They could esterify the FFAs and transesterify TAGs, and therefore the feedstock pretreatment would not be required, as in the case of alkali catalysts reactions [14]. However, the common limitation of lipase-based processes is the high cost of the enzymes, which hinders process commercialization. This problem can be reduced by the repeated use of the enzyme, which is possible through the immobilization that is generally employed to attain the enzyme reuse with lower production cost [15]. Besides enzyme reusability, other benefits of using immobilized lipase are the enhanced activity and stability [16, 17]. However, immobilized lipase suffers from inhibition and mass transfer limitations that decrease the reaction rate. The use of hydrophobic solvents has been suggested to improve the diffusivity of substrates towards the enzyme active sites and the products away from them. Several organic solvents have been successfully tested such as *n*-hexane and *tert*-butanol

[18-22]. However, organic solvents are toxic and require separation from the reaction medium for their reuse and product purification.
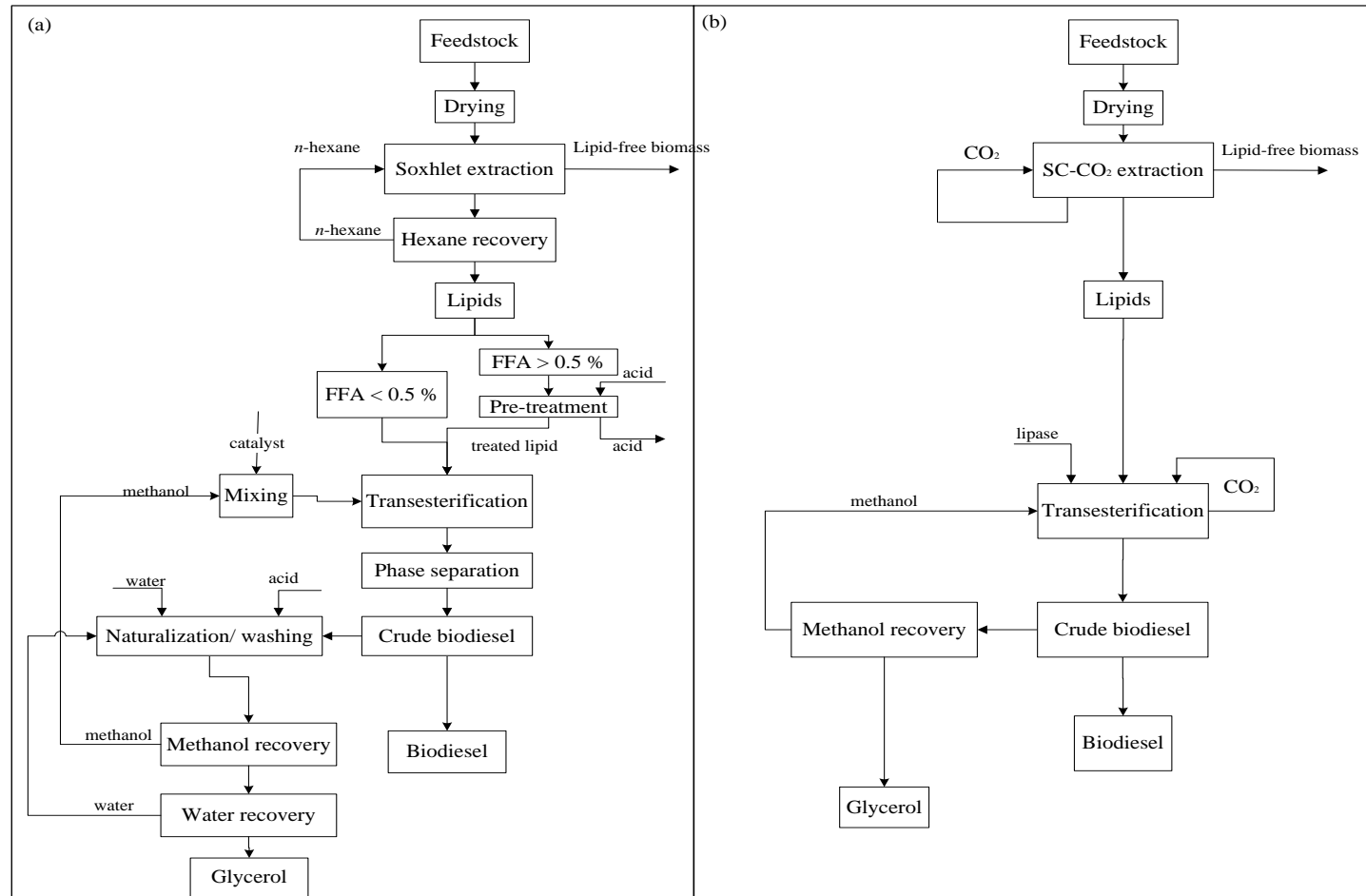
Figure 1.1: Process flowchart of: (a) conventional biodiesel production process, and (b) proposed enzymatic production process in SC-CO$_2$

Supercritical fluids (SCF) such as supercritical CO_2 (SC-CO_2), has received increasing attention in bio-catalysis applications as a green reaction medium [23, 24]. The first use of the enzyme in SC-CO_2 dated back to 1985 [25-27]. SC-CO_2 has many useful features such as being non-flammable, inexpensive, available in sufficient quantities, and CO_2 has moderate critical temperature (31.3 ^{o}C) and pressure (72.8 bar) with tunable properties. Compared to conventional reaction solvents, SC-CO_2 usually yields a faster reaction rate [28, 29], and offers easy product separation, while maintaining the same advantages for lipase catalysis as organic solvents do, such as solubilization of lipids and favoring esterification over hydrolysis. Another advantage of using SC-CO_2 is that the produced biodiesel dissolved in SC-CO_2 does not require a glycerol separation unit, as in conventional techniques, since the solubility of glycerol is low in SC-CO_2, and stay in the reactor resulting in the direct production of high purity biodiesel. A flowchart of enzymatic transesterification in SC-CO_2 is shown in Figure 1.1(b). SC-CO_2 has been used as a medium in lipase catalyzed reactions such as in esterification, and has proven to enhance the reaction rate [17, 30-32]. In most reported studies, SC-CO_2 showed the highest conversion, followed by *n*-hexane and then a solvent-free system. Nevertheless, limited work has been done on lipase catalyzed transesterification for biodiesel production [33-37]. This is mainly because SCF technology is considered unfeasible for energy production, despite its positive effect on reducing inhibition and easy product separation.

Apart from this, the use of conventional feedstocks for biodiesel production, which are vegetable oils, competes with their use as food stock. In addition, the use of conventional feedstocks requires the development of agricultural lands and need fertilization and high freshwater load for irrigation.

Moreover, the prices of vegetable oils are high and it was reported that 60-75 % of biodiesel cost comes from the cost of the vegetable oils [3, 38]. Therefore, waste oils and animal fats have been suggested [39]. Nevertheless, these alternatives suffer from inconsistent supply, difficulties in logistics, and cannot satisfy the existing global demand for diesel fuels [2, 40]. Microalgae, on the other hand, have proved to be the best source of lipid production with several promising features such as high growth rate and lipid content, faster production rate per unit area and seasonal tolerance [41]. The microalgae lipid production is reported to be ten times higher than that of the best oil crops, and their lipids have similar composition to that of vegetable oils [6, 42, 43]. By photosynthesis, microalgae can utilize CO_2 as a sole carbon source, which has the concurrent advantages of reducing harmful emissions and the dependency on organic substrates, such as glucose, that may compete with their use as a food source. Furthermore, microalgae are capable of growing in saline water, which reduce the fresh water loading, and do not require agricultural land development.

Various species of microalgae have been cultivated for biofuel production. The National Renewable Energy Laboratory (NREL) has identified over 3,000 microalgal strains [44], which makes the selection of a suitable strain not an easy task, and requires the evaluation of various parameters, including lipid productivity, CO_2 fixation rate and adaptability to grow in harsh conditions, such as high temperature and salinity [45]. Generally, the microalgal biodiesel production process requires biomass cultivation and harvesting, drying and cell disruption, lipid extraction and conversion to biodiesel, and finally biodiesel purification. The steps of the microalgae to biodiesel process are shown in Figure 1.2. The figure also shows the tasks performed in each step of this work. The

dashed lines represent suggested recycling streams, which were not used in this work.
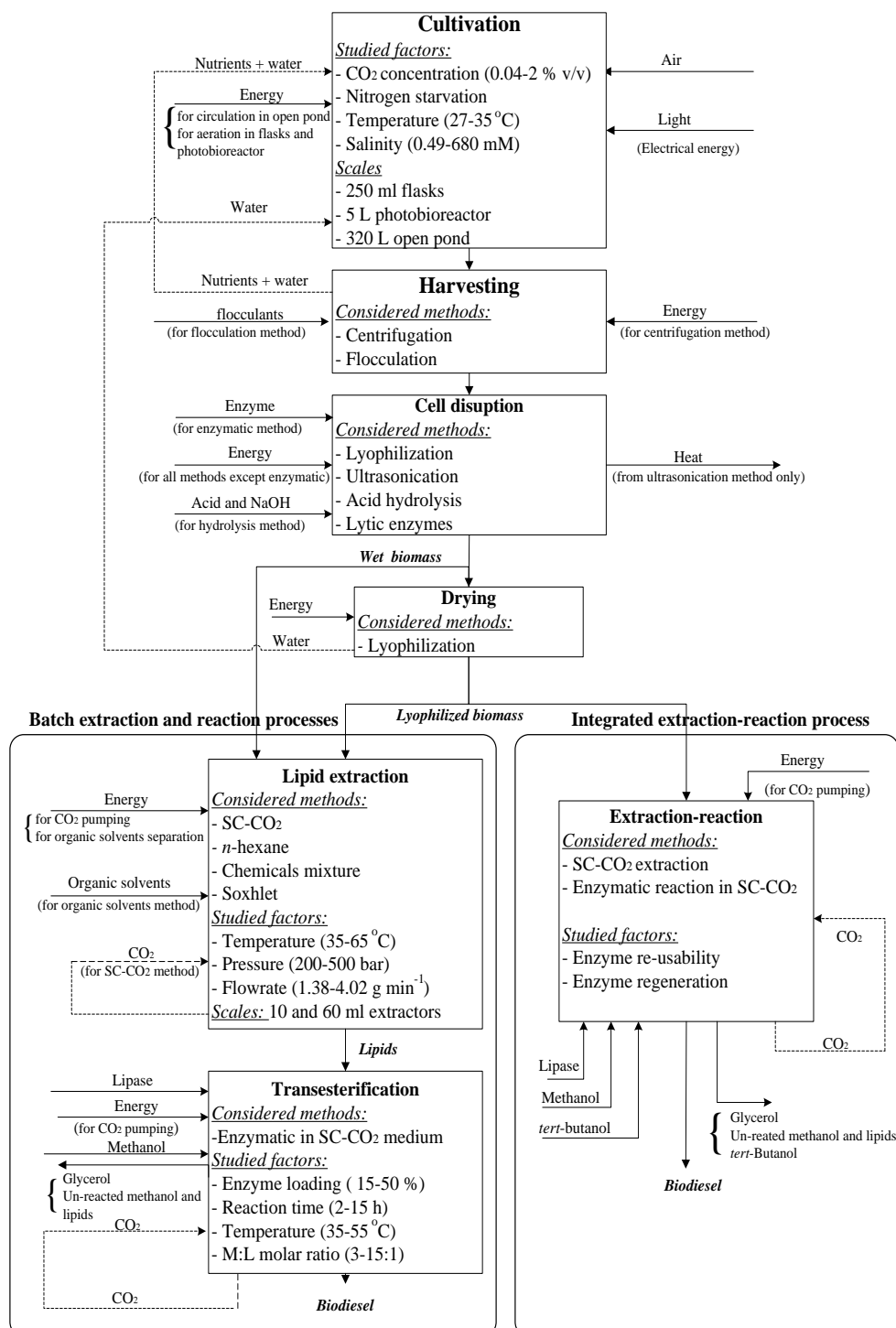
All recycling dashed lines presented in the diagram were not cosidered in this work, but optional for commercialization

Figure 1.2: Research steps of enzymatic biodiesel production from microalgae in SC-CO$_2$

Although microalgae showed their promising effect in enhancing biodiesel production sustainability and reducing the competition with the food and arable lands [46], the main challenges of process commercialization are associated with the effective extraction of the lipids from the rigid and robust cells. The conventional chemical extractions are carried out by organic solvents using Bligh and Dyer [47], Floch [48], or Soxhlet [49] extraction techniques, which are time consuming. In addition, the spent protein rich biomass after extraction is usually contaminated with used solvents, which limits their further uses in pharmaceutical or food industries. In addition, carrying out extraction at elevated temperatures, as done in conventional organic solvent methods, damages the proteins and other thermal sensitive compounds found in the leftover. Recently, SC-CO_2 has received considerable attention in extracting seeds oils due to its tunable solvation power and environmental benign features [50-52]. In addition, the process is fast, and extraction that requires 24 h using conventional techniques is completed within 30-60 min. This technique also does not require solvent separation as CO_2 is separated from the extracted lipid by simple depressurization. Furthermore, as shown in Figure 1.1(b), there is no contamination of the leftover biomass with the extraction solvent. The critical temperature of CO_2 is 31.1 ^{o}C, which is below the denaturation temperature of proteins, and its relatively high critical pressure of 73.8 bar, has an insignificant effect on the proteins structure and nature [24]. Extracting lipids from many strains has also been reported; including *Chlorella. vulgaris* [53, 54]*, Nannochloropsis* sp. [55], *Spirulina. platensis* [56] and *Spirulina. maxima* [54]. Although SC-CO_2 shows promising features, reported lipid yields from some

strains such as *Crypthecodinium cohnii* was much lower than employing the Bligh and Dyer method [57].

As mentioned earlier, lipids extraction from microalgae is carried out using conventional methods where lyophilization is employed to disrupt and dry the cell in order to enhance the extraction efficiency. However, this is an energy intensive process that usually counts for almost 70-75% of total processing cost [58]. This topic of research is still in the early stages and many processes have been investigated to directly convert wet algae to biodiesel [59, 60]. In addition, a lipid extraction step that eliminates biomass drying and the use of organic solvents could lead to significant energy and cost savings.

1.2   RESEARCH GOAL AND OBJECTIVES

The goal of this work is to develop environmentally-friendly extraction and reaction process for biodiesel production from microalgae biomass that does not compete with food, freshwater or arable lands. In addition, proteins in the spent biomass can possibly be used in pharmaceutical and food applications. In this work, CO_2 is considered as a key solvent. The work is divided into three parts; namely biomass production, lipid extraction and biodiesel production. The three steps are described below and are depicted in Figure 1.2. The diagram clearly shows selected research design and steps. Technical objectives for each step are given below.

1. Microalgae strains cultivation:

   a. To measure the ability of available microalgae strains to grow under aeration enriched with CO_2 and test their CO_2 biofixation rate

   b. To enhance cells' lipid content by growing in a nitrogen deficient medium

c. To test the ability of a freshwater strain to grow in water of high salinity, and at elevated temperature

d. To grow a microalgae strain in a two-steps culturing process that combines high biomass and high lipid productivities

e. To produce sufficient biomass of high lipid content to be used in subsequent lipid extraction experiments

2. Microalgae lipids extraction:

a. To use SC-CO$_2$ for extracting lipids of high TAGs content and to compare its effectiveness with conventional extraction methods

b. To study the effect of temperature, pressure and flowrate on SC-CO$_2$ extraction yield and optimize them using RSM

c. To apply the determined optimum extraction conditions in a scaled up extraction process for larger production of lipids for subsequent transesterification experiments

d. To use the experimental data from the small scale extration unit to estimate the parameters of a mass transfer correlation and validate it against the results of the large scale extraction unit

e. To test the possibility of extracting lipids from wet biomass, avoiding the drying step

3. Enzymatic biodiesel prodction from extracted microalgae lipids:

a. To successfully produce biodiesel from extracted lipids in a SC-CO$_2$ medium with a high reaction rate

b. To study the effect of enzyme loading, reaction time, temperature and methanol to lipids (M:L) molar ratio on the production yield, and to optimize the process conditions using RSM

c. To use the experimental results in determining the parameters of a suitable kinetic model that incorporates methanol inhibition

d. To test the properties of the produced biodiesel and compare them to ASTM and EN fuels standards

4. Integrated extraction-reaction system:

a. To test the integrataed extraction-reaction to continuously produce biodiesel from microalgae cells

b. To study the effect of M:L molar ratio of the FAMEs production rate and yield

c. To study enzyme re-usability and stability

d. To invistigate the effect of using *tert*-butanol in regenerating the emzyme bed activity

The success of this work will result in the production of sustainable fuel that reduces dependency on fossil fuels, which utilize a feedstock that does not compete with food stock, and, at same time, contributes to the reduction of CO_2 emissions.

1.3   THESIS SIGNIFICANCE

Although UAE is one of the largest oil exporters, the production of biodiesel falls within the country's visions to satisfy the coming generation's needs for clean energy. The re-shaping of the available technologies to greener

alternatives is needed for sustainable fuel production. Utilization of microalgae as a feedstock for biodiesel production is well known worldwide, but the production process is not yet economical, where the biodiesel cost from microalgae is still high compared to petroleum diesel. Compared to other countries, UAE enjoys abundant and continuous sunlight, combined with the availability of seawater, which makes the nation an ideal place for microalgae cultivation. Moreover, arable lands in the country are scarce, which favors the idea of microalgae cultivation.

The use of microalgae for fuel production would decrease the dependency on food stock, reduce the freshwater load, and assist in CO_2 mitigation. In addition, extraction of microalgae lipids using SC-CO_2 eliminates the need for using toxic organic chemicals. Moreover, integrating microalgae lipids extraction with enzymatic transesterification in one unit renders the use of such expensive process justified. However, the process still needs extensive studies and developments before being commercialized. The results of this work will lead to a major development in sustainable biodiesel production.

1.4   THESIS ORGANIZATION

The thesis is organized as follows:

Chapter 1 (Introduction): This chapter presents the motivation and objectives of the work. The chapter starts with explaining the demands for alternatives to fossil fuels, and gives an overview of the biodiesel production technologies. The chapter ends by stating the work's objectives and significance.

Chapter 2 (Literature Review): This chapter is a review of previous research works related to the topic of the thesis. An overview on the applications

of SCFs in lipids extraction and biodiesel production are provided. The theoretical backgrounds of cell growth, overall extraction and reaction kinetic models are also presented. The chapter also discusses the different technologies of biodiesel production and possible feedstocks.

Chapter 3 (Material and Methods): In this chapter, the materials used and the testing methods followed are presented. This includes the methods of biomass production and harvesting, sample preparation prior to extraction, lipid extraction and biodiesel production, as well as the applied statistical analyses. The description of the approaches carried out to analyze mathematical models and to determine kinetics models parametric is also presented.

Chapter 4 (Results and Discussion): Obtained results and research findings are shown and discussed in this chapter. The results of the microalgae cultivation, lipid productivity and CO_2 fixation rate are presented. The SC-CO_2 extraction results showing the effect of different biomass pre-treatment methods are also presented, followed by an optimization of SC-CO_2 extraction conditions. This is followed by showing the effect of selected operating conditions on the enzymatic transesterification of extracted microalgae lipids. The examined parameters are M:L molar ratio, reaction time and temperature, immobilized enzyme loading and enzyme reusability. The developed integrated continuous extraction-reaction system is also presented in this chapter, and the effect of enzyme reusability, M:L molar ratio, and bed regeneration by washing with *tert*-butanol are discussed.

Chapter 5 (Conclusions and Future Works): This chapter is the last chapter in the thesis that wraps up all the research findings, and relates them to the technical objectives presented in the first chapter.

CHAPTER 2: LITREATURE REVIEW

2.1 BIODIESEL

Limited fossil fuels reserves and their increasing demand, the ever-increasing of world population and environmental pollution and global warming worries due to greenhouse gases emission have all raised several issues at economic, environmental and social levels. Based on recent updates, the available fossil fuels may last for less than 50 years [61]. The transportation sector is one of the main fossil fuels consumers and, at the same time, the biggest contributor to environmental pollution. These challenges call for the development of alternative renewable and sustainable fuels that can meet the increased energy need. Among acceptable and notable substitutes is biodiesel, which is a mixture of mono-alkyl esters, that can be used in car and bus diesel engines [6, 62].

2.1.1 Biodiesel features and relevance

Biodiesel fuel has received increasing attention worldwide in recent years. It has many advantages over petroleum fuel; for example it is renewable, non-toxic, biodegradable and does not contribute to the net accumulation of te greenhouse gases [62, 63]. The physical and chemical properties of biodiesel are quite similar to those of petroleum diesel; thus, it has been suggested as a possible replacement for transportation fuels, and can be used without the need for any modifications or interventions in the engine [64, 65]. Also, biodiesel has no sulfur and lower aromatic (80-90 % less) content, higher cetane number and flash point than petroleum diesel [3, 6, 66, 67]. Other benefits of biodiesel include better lubricity and lower emissions of certain harmful gases [6].

Compared to petroleum diesel, 42.7-47.5 % reduction in CO and 55.3-66.7 % reduction in PMs emissions were reported [6, 7]. However, with the use of biodiesel, slightly higher levels of nitrogen oxides (NO_x) by 11.5 % have been reported [68]. Nevertheless, this can be enhanced by some modifications in combustion temperatures and injection timing [68, 69]. Therefore, the use of biodiesel will not only decrease the dependency on fossil fuels, but will also significantly reduce the greenhouse gases and other pollutant emissions.

The inventor of the diesel engine, Rudolf Diesel, was the first to use vegetable oils, when he tested peanut oil in 1900. Though the oil could be used directly in the engine, it was problematic and had many shortcomings such as high viscosity and low volatility, which caused poor atomization leading to incomplete combustion and operation problems such as carbon deposits [8, 66, 70, 71]. However, these problems could be overcome if the oil is mixed with the conventional diesel in an appropriate ratio, but this approach is still impractical for a long term use [34, 64, 72, 73]. Therefore, considerable efforts have been made to develop vegetable oil derivatives that have properties similar to those of the petroleum diesel fuels.

Recent approaches to minimize the problems associated with the direct use of vegetable oils have been addressed by pyrolysis (cracking), micro-emulsion and transesterification [13, 66, 74]. Pyrolysis and micro-emulsion have received little attention because they are costly and yield low quality biodiesel compared to the transesterification method that yields fatty acid alkyl esters (FAAE). Thus, the main focus of this research work was on the transesterification approach.

2.1.2 Transesterification: production techniques

Transesterification, also known as alcoholysis, is a chemical reaction between TAG and alcohols [74, 75]. The typical form of this reaction is shown in Figure 2.1, where R_1, R_2 and R_3 represent the fatty acid chains present in the feedstock that usually ranges from 12 to 22 carbon atoms. In this type of reaction, large and branched TAGs are transformed into smaller and straight chain molecules by exchanging the alcohol from an ester by another alcohol in a process similar to hydrolysis, except that an alcohol is used instead of water. The final product is always similar in size to the molecules of the species present in diesel fuel [76, 77]. Therefore, such products can be used in normal engines without any modifications.

$$
\begin{array}{c}
CH_2-O-\overset{\overset{\textstyle O}{\|}}{C}-R_1 \\
CH-O-\overset{\overset{\textstyle O}{\|}}{C}-R_2 \; + \; 3\,CH_3OH \\
CH_2-O-\overset{\overset{\textstyle O}{\|}}{C}-R_3
\end{array}
\quad \underset{\xrightarrow{\hspace{1cm}}}{\overset{\text{catalyst}}{\xleftarrow{\hspace{1cm}}}} \quad
\begin{array}{c}
CH_3-O-\overset{\overset{\textstyle O}{\|}}{C}-R_1 \\
CH_3-O-\overset{\overset{\textstyle O}{\|}}{C}-R_2 \; + \;
\begin{array}{c} CH_2-OH \\ CH-OH \\ CH_2-OH \end{array} \\
CH_3-O-\overset{\overset{\textstyle O}{\|}}{C}-R_3
\end{array}
$$
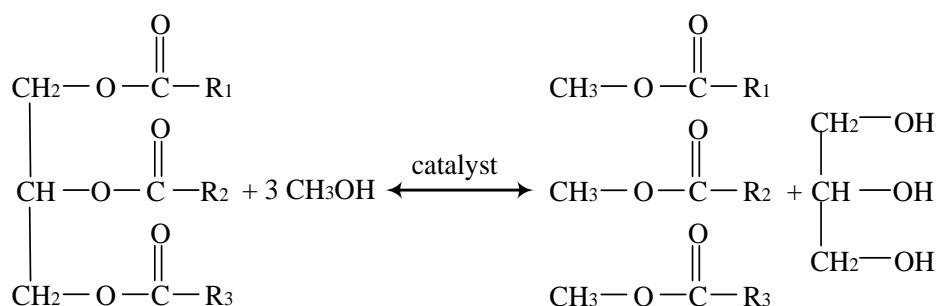
Figure 2.1: General transesterification reaction of triglycerides with alcohol to produce fatty acid alkyl esters

In the stoichiometry of transesterification reactions, each mole of TAG reacts with three moles of alcohol. However, a higher molar ratio of alcohol to oil is usually required to shift the reaction into more biodiesel production. Methanol, ethanol and propanol are the most commonly used alcohols. Ethanol use has been gaining popularity in recent years due to its production possibility from renewable and low toxicity sources, compared to methanol. However, methanol is most commonly used due to its low cost and industrial availability, which are

essential for industrial large scale production. It is worth mentioning also that transesterification differ from esterification reaction, where in transesterification the ester bonds in the TAG are broken first, then followed by the hydroxyl bond, whereas in esterification the hydroxyl bonds are broken before ester bonds, resulting in glycerol as a by-product in transesterification and water in esterification [3].

TAG and alcohol are immiscible in each other resulting in the formation of two phases with poor surface contact, which yields relatively slow reactions. However, these rates can be increased significantly by introducing a catalyst. The reaction can be carried out either using an alkali, acid or bio-catalyst, or using alcohols in their supercritical state [65, 78], as summarized in Figure 2.2.
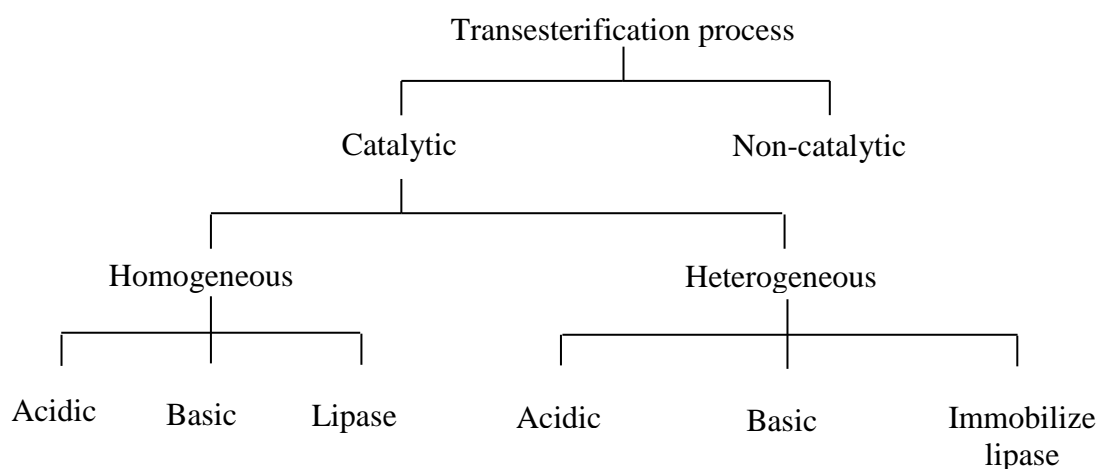
Figure 2.2: Triglycerides transesterification methods for biodiesel production

Processes that use a catalyst are called catalytic transesterification processes, in contrast to those without a catalyst, referred to as non-catalytic transesterification processes [13, 79-81]. Catalytic processes are divided into two types; homogenous and heterogeneous processes, depending on the form of the catalyst used. In both cases, the transesterification is a sequence of three reactions

by which driacylglycerol (DAG) and monoacylglycerol (MAG) are formed as intermediates. Briefly, TAG is first converted to a DAG and one FAAE, and then the DAG is converted to MAG giving an additional FAAE, and finally the MAG is converted to glycerol giving the last FAAE. By the end of the reaction, produced biodiesel and glycerol have to be separated and purified to remove the catalyst. The process selection depends on various factors, which are: (1) free fatty acids and moisture content of the feedstock, (2) the type of the catalyst and concentration, (3) molar ratio of alcohol to oil, (4) type of alcohol used, and (5) reaction time and temperature.

2.1.2.1 Alkali catalyzed transesterification

The conventional approach to increase the transesterification reaction rate is through the use of homogeneous chemical catalysts. This involves the use of alkali (base) and acid catalysts, where the former is the most commonly used because of its relative low cost and easy handling [82]. In addition, it can be performed at low temperature and pressure with a very high conversion reaching 98% within a short time [66]. Sodium hydroxide (NaOH), potassium hydroxide (KOH) and sodium methoxide (CH_3ONa) are the most common homogeneous base catalysts employed in alkaline transesterification [64, 71, 72, 74]. Table 2.1 summarizes some of the transesterification studies using homogeneous alkali catalysts.

Although by using alkali catalyst biodiesel can commercially be produced with high yields, this type of reaction has several limitations, where the process is energy intensive and sensitive to the FFAs and water content of the feedstocks. It works perfectly when the FFAs and moisture contents are less than certain limits,

usually below 0.5 wt % for FFAs [83, 84]. The presence of FFAs promotes soap formation, which consumes and hinders the catalyst, lowers the production yield, and more importantly cause difficulties in downstream separation of formed esters from glycerol due to the formation of complex emulsions [3, 13]. The higher the acidity of the feedstock oil, the lower the reaction conversion and, as a result, refined feedstocks are required, as can be seen in Figure 1.1. The refining is usually carried out by distillation at high temperatures under reduced pressure, which may cause degradation of temperature sensitive compounds and add cost to the overall process. In addition, such processes require purification of the products to remove the catalyst, which requires large quantities of water resulting in the need for wastewater treatment as well. Nevertheless, some vegetable oils contain phospholipids that need a degumming step prior to use. The degumming is usually carried out by hydration, where hot water is added to the oil, and by stirring the solubility of phospholipids would reduce, resulting in their separation from the oil when allowed to settle [85]. Having said that, not all phospholipids are hydratable, which suggests the use of citric or phosphoric acids to convert them into hydratable gums [86].

Sodium hydroxide is a widely used base catalyst and it has been tested with several feedstocks. The quality of the feedstocks has a significant effect on the reaction yield, where FFA and moisture content showed to be the key parameters to define the feedstock feasibility. For example, the production of FAMES from duck tallow [87] at 65 ^{o}C and 6:1 methanol to oil molar ratio resulted in 62 % conversion, whereas sunflower [88] resulted in 86 % conversion at the same conditions. Nevertheless, when KOH or CH_3NaO were used, the yield from duck tallow increased significantly, reaching 80% at the same

conditions. The yield from sunflower [88] was also increased when CH_3NaO was used. This might be due to the saponification and/or neutralization of the FFAs that decreases the yield.

Table 2.1: Summary of previous works using homogeneous chemical catalyzed transesterification of different feedstocks for biodiesel production

Catalyst	Feedstock	Alcohol	Temperature (^{o}C)	Molar ratio (alcohol:oil)	Reaction time	% Yield	References
Base catalysts							
NaOH	Duck tallow	Methanol	65	6:1	3 h	62.3	[87]
	Treated waste cooking oil	Methanol	50	7:1	1 h	88.9	[89]
	Sunflower oil	Methanol	65	6:1	--	86.7	[88]
	Neat canola oil	Methanol	70	6:1	15 min	93.5	[90]
	Treated used frying oil	Methanol	60	7:1	20 min	88.8	[90]
	Soybean oil	Methanol	45	6:1	20 min	100	[91]
	Sunflower oil	Methanol	60	6:1	1.5 h	97.1	[92]
	Sunflower oil	Ethanol	50	12:1	10 min	99	[93]
	Soybean oil	Ethanol	70	12:1	1 h	97.2	[94]
	Waste cooking oil	Methanol	50	6:1	1.5 h	86	[89]
KOH	Duck tallow	Methanol	65	6:1	3 h	79.7	[87]
	Karanja oil	Methanol	65	6:1	3 h	97-98	[95]
	Pongamia pinnata	Methanol	45	10:1	1.5 h	83	[96]

Table 2.1: Summary of previous works using homogeneous chemical catalyzed transesterification of different feedstocks for biodiesel production (cont.)

KOH	Soybean oil	Ethanol	70	12:1	-	95.6	[94]
	Pongamia pinnata	Methanol	60	10:1	1.5 h	92	[96]
	Mixture of castor and soybean	Ethanol	-	19:2	4 h	97	[97]
	Sunflower oil	Methanol	65	6:1	-	91.6	[88]
	Fish oil	Ethanol	60	6:1	30 min	98	[98]
	Waste cooking oil	Methanol	65	6:1	1 h	98.16	[99]
CH_3NaO	Duck tallow	Methanol	65	6:1	3 h	79.3	[87]
	Sunflower oil	Methanol	65	6:1	-	99.3	[88]
	Castor oil	Ethanol	80	6:1	3 h	80	[100]
	Coriander seed oil	Methanol	60	6:1	1.5 h	94	[101]
Acid catalysts							
H_2SO_4	Waste cooking oil	Methanol	95	20:1	20 h	90	[102]
	Used sunflower oil	Methanol	65	30:1	69 h	99	[103]
	Waste frying oil	Methanol	70	245:1	4 h	99	[104]
H_2SO_4	Rice Bran oil	Methanol	60	5:1	12	99	[105]

Table 2.1: Summary of previous works using homogeneous chemical catalyzed transesterification of different feedstocks for biodiesel production

(cont.)

Two steps: acid catalysis followed by alkali catalysis

H$_2$SO$_4$	Karanja	Methanol	60	6:1	1 h	FFAs	[106]
KOH			60	8:1	1 h	96	
HCL	Fish frying oil	Methanol	60	6:1	1	FFAs	[107]
KOH			60	6:1	1	94	
Ferric sulfate	Waste cooking oil	Methanol	95	10:1	2 h	FFAs	[102]
KOH			65	6:1	1 h	97	
Ferric sulfate		Methanol	100	9:1	2 h	FFAs	[108]
KOH	Waste cooking oil		100	7.5:1	1 h	96	

To overcome problems associated with catalyst recovery, heterogeneous catalysts, which at the end of the process by filtration can be separated and reused easily have been suggested [71, 109]. Such processes are environmentally more benign and can be employed either in a batch or a continuous mode. In addition, wastewater requirement is minimized. Alkaline earth oxides [110], zeolites [5], calcined hydrotalcites [12, 111] and magnesium and calcium oxides [10, 109] have been extensively tested. Among all, calcium oxide (CaO) has received much attention due to its relatively low cost, high basic strength, and low solubility in methanol [112]. Liu et al. [113] investigated the use of CaO in the transesterification of soybean oils to biodiesel and the effects of the molar ratio of methanol to oil, reaction temperature, and water content were investigated. Increasing the reaction temperature also from 50 to 65 $^{\circ}$C resulted in an increase of 2.4 times in the yield at 6:1 molar ratio; however, further increase resulted in a significant drop in the yield due to methanol vaporization. The biodiesel yield at 65 $^{\circ}$C also increased from 61 to 97 % with the increase in methanol to oil molar ratio from 3 to 12:1. It was also found that CaO maintained it's activity for 20 cycles without a significant drop in the activity. Table 2.2 shows a summary of some works that have been done using heterogeneous alkali catalysts. On the other hand, the most obvious problem of using heterogeneous base catalysts is the slower reaction rate compared to homogeneous catalyst, which is due to the three phase system that causes diffusion problems and require higher reaction temperature, catalyst loading and alcohol to oil molar ratio. Although the use of heterogeneous catalysts minimized the environmental issues, the high cost of the feedstock purification remains the main problem facing such process.

Table 2.2: Summary of previous works using conventional heterogeneous chemical catalyzed reaction of different feedstocks for

biodiesel production

Catalyst	Feedstock	Alcohol	Temperature (^{o}C)	Molar ratio (alcohol:oil)	Reaction time (h)	% Yield	Reference (s)
Heterogeneous base catalysts							
CaO	Soybean oil	Methanol	60-65	12:1	1	66	[114]
	refined soybean oil	Methanol	60-65	12:1	1	93	[114]
	Refined soybean oil	Methanol	65	12:1	3	95	[113, 115]
Li/CaO	Karanja	Methanol	65	12:1	8	95	[115]
K_3PO_4	Waste cooking oil	Methanol	60	18:1	2	97.3	[116]
Heterogeneous acid catalysts							
WO_3/ZrO_2	Unspecified vegetable oil	Methanol	75	19.4:1	20	85.1	[117]
ZrHPW	Waste cooking oil	Methanol	65	20:1	8	98.9	[118]
ZS/Si	Waste cooking oil	Methanol	200	18:1	5	98	[119]
$SO_4^{2-}/TiO_2–SiO_2$	Waste cooking oil	Methanol	500	9:1	4	90	[120]
$SO_4^{2-}/SnO_2–SiO_2$	Waste cooking oil	Methanol	150	15:1	3	92.3	[121]

2.1.2.2 Acid catalyst transesterification

The reaction of TAGs and alcohol may also be catalyzed with an acid catalyst instead of a base. Acid-catalyzed transesterification is more suitable with feedstocks of high FFAs, which are of low grade and inexpensive [2, 3, 122]. The most commonly used acids are strong acids like sulphuric, sulphonic, phosphoric and hydrochloric acids [13, 66, 115]. These kinds of processes are not as popular as the alkaline catalyzed processes, mainly because strong acids are corrosive, which requires specific equipments that in turn increases the overall production cost. In addition, acid catalyzed reactions are too slow, and reported to be 4000 times slower than the base catalyst process [3, 8, 80]. Moreover, usually acid catalyzed reactions are performed at high alcohol to oil molar ratios reaching 30:1 with high catalyst concentrations and requires neutralization and removal of the catalyst [8, 74]. In some case, the required alcohol to oil molar ratio reached up to 245 [104], which limits their use.. A summary of works on using acid catalysts is shown in Table 2.1.

The heterogeneous acid catalysts, which are less corrosive and toxic than homogeneous acid catalysts mentioned earlier with less environmental effects, have been also used. Sulphated tin oxide has been used as a catalyst to transesterified waste cooking oil [121]. Sulphated zirconias was also used as a catalyst in the alcoholysis of soybean oil and in the esterification of oleic acid [123]; heteropolyacid was used to transesterify yellow horn oil [124], and ion and cataion exchange resins were used for triolein transesterification reactions with ethanol to produce ethyl oleate [125]. The latter are becoming popular due to their ability to catalyze both esterification and transesterification reactions under

mild conditions [126]. The results of shibasaki-Kitakawa et al. [125] showed a very low conversion of triolein with cation-exchange resin, compared to ion exchange resins that exhibited high conversions reaching above 80%. The use of cation exchange resins was also tested by Feng et al. [127], and a high conversion of 90 % was achieved from acidified oils generated from waste frying oils esterification at 66 $^{\circ}$C, 7:1 molar ratio and a reaction time of 2 h. Besides the catalytic function, resins also showed an showed as good adsorbent, where the of feedstock impurities, FFAs, water and glycerin can be removed from the final product by the adsorption on the resin [128].

2.1.2.3 A two step catalyzed transesterification

As mentioned earlier, alkali catalyzed transesterification of high FFAs feedstock requires a pre-treatment step, whereas acid catalyzed reactions are very slow. Therefore, a two-step transesterification process was developed [129], where in the first step the FFAs are esterified to FAMEs, followed by alkali transesterification after separating the acid catalyst and producing water [74]. Water separation is considered an important step prior to using an alkali catalyst to avoid soap formation. This was reported by Liu et al. [130], where the catalytic activity was strongly inhibited by water. Several studies have been carried out using this approach with high reported yields reaching 98 % [129, 131-134]. Some of these works are tabulated in Table 2.1.

2.1.2.4 Non-catalytic transesterification

Although catalysts reduce the reaction time, their presence complicates final product purification, which results in increased production cost. To avoid this, the use of supercritical alcohol (SCA), which is above the critical

temperature and pressure of the fluid, was suggested [6, 72, 135]. Details about the supercritical fluids and critical points can be found in section 2.5. The SCA transesterification is a one-step conversion process performed at high pressure and temperature in the absence of a catalyst. Table 2.3 shows a summary of some studies using SCA. Both tested alcohols resulted in a much faster (within 5-15 min), simpler and environmentally-friendly product separation compared to the catalyzed processes, where pretreating the feedstock and removing of produced wastes and the generated waste water from the process were not required. Most studies have focused on methanol and ethanol as selected alcohols, where the typical operating conditions are 250-400 ^{o}C and 150-400 bar.

Saka and Kudiana [136] investigated biodiesel production from rapeseed oil above the supercritical conditions, and a high conversion of 95 % was achieved. Demirbas [135] also studied the transesterification of cotton seed, hazelnut kernel, poppy seed, rapeseed, safflower seed and sunflower seed and reported that increasing the reaction temperature above the supercritical condition had a favorable influence on the conversion. Compared to catalytic reactions, SCA reactions are fast and can achieve high conversions in a very short time. However, the reaction requires higher temperatures, pressures and alcohol to oil molar ratios reaching 42:1 in the case of methanol, which result in a high production cost [76, 77]. In addition, performing at elevated temperatures may lead to the possible generation of thermal degradation of heat sensitive products. Generally, the three transesterification processes, namely alkaline and acid catalyzed and supercritical non-catalytic processes have several drawbacks. The use of lipases can overcome these problems, and presents a more friendly alternative at lower temperature [3, 137].

Table 2.3: Non-catalytic vegetable oils transesterification using supercritical methanol and supercritical ethanol

Feedstock	Alcohol	Molar ratio (alcohol:oil)	Reaction conditions		Time (min)	% Yield	Reference
			Temperature (^{o}C)	Pressure (bar)			
Palm	Methanol	40:1	360	-	15	81.1	[138]
Krating	Methanol	40:1	260	160	10	90.4	[139]
Jatropha	Methanol	40:1	320	150	5	84.6	[139]
Soybean	Ethanol	40:1	350	200	-	77.5	[140]
Palm	Ethanol	40:1	360	-	150	79.5	[141]
Rapeseed	Ethanol	42:1	300	250	12	100	[142]
Rapeseed	Ethanol	42:1	300	400	20	80	[142]
Cottonseed	Ethanol	41:1	250	-	8	85	[142]
Linseed	Ethanol	41:1	250	-	8	85	[72]
Sunflower	Ethanol	40:1	300	200	40	100	[143]

2.1.2.5 Enzymatic transesterification

There is a great interest in using biocatalysts to catalyze TAG transformation, which has the advantage of having low operating conditions and high product purity. Lipase belongs to a group of hydrolytic enzymes called hydrolases (E.C.3.1.1.3) that are capable of catalyzing transesterification reactions. It can be obtained from microbial organisms (bacteria, yeast and fungi), plants (wheat, oats, corns and palms) or animals (pancreas, stomach, pharynx and different tissues) [144]. However, commercially available industrial lipases are derived from microorganisms [145] due to their availability, versatility, non-seasonable and rapid growth. Regardless of their sources, they can hydrolyze TAG [80], work in mild conditions and have an ability to work with TAG from different origins, but to different extents. Contrary to chemical catalysts, enzymes do not form soaps and can simultaneously catalyze both TAG transesterification and FFA esterification without any need for the washing step. This diversity allows lipases to be used in various applications including chemical synthesis, which typically depend on the specificity of the lipase itself. It is worth mentioning also that lipases differ from esterase, which belongs to hydrolases group as well, where the latter act on short chains of TAG (water soluble) whereas lipases act on lipids (water insoluble) [146, 147]. In addition, they differ from phospholipases, in which the latter uses phospholipids as substrate, whereas lipases acts on TAGs and the presence of phospholipids negatively affect their activity [148]. Phospholipids are similar to TAG, but with one of the three fatty acids replaced by a phosphate functional group. Recently, however, Cesarini et al. [149] successfully used a combination of phospholipase

and lipase to degum and transesterify crude soybean oil, containing 900 ppm phosphorus, to biodiesel.

The extracted lipase is either extracellular or intracellular [66, 67]. Extracellular lipases refer to the enzymes produced by the microorganism in the growth medium, which is then purified. Intracellular lipases refer to the enzyme that remains within the producing cell walls and require disrupting the cells in order to extract the enzyme [73].

In term of the region-selectivity, lipases have been divided into three types [150]:

- sn-1,3-specific: hydrolyze ester bonds in positions R_1 or R_3 of TAG
- sn-2-specific: hydrolyze ester bond in position R_2 of TAG
- non-specific: do not distinguish between positions of ester

Lipase catalyzed reaction for biodiesel production was first reported in 1990 by Mittelbach [151]. For biodiesel production lipases should be non-specific where all TAG, DAG and MAG are attacked by the biocatalyst. Therefore, lipases from *Candida antartica*, which are known to be non-specific, are commonly used [65].

2.2   LIPASE CATALYZED TRANSESTERIFICATION

2.2.1   Challenges and aspects

Despite the lipases advantages over chemical catalysts, commercial production of biodiesel using lipases are not yet commercialized, where several technical and economical challenges still need to be overcome. The most important challenge is the high cost of lipases, approximately 1,000 $ kg^{-1} for Novozym®435 [65], compared to approximately 0.62 $ kg^{-1} for NaOH [152],

which limit their industrial use and possible inhibition by reaction mixture, alcohol, and products, glycerol [71, 73, 153-155]. For that reason, the reusability of the enzyme by using it in an immobilized form is essential. Furthermore, the production yield depends on several factors, including the nature, specificity, selectivity and structural properties of used enzyme and substrate and used alcohol quality. Another problem that faces the lipase catalyzed reactions is its inhibition by alcohol and the by-product glycerol.

2.2.2 Process developments

2.2.2.1 Immobilization

Usually lipases are dispersed in the solution and can move freely, however in such casees, they are difficult to separate and handle. One promising approach to overcome this difficulty is the immobilization of lipase in a way that it can be separated later by any simple separation method. Enzyme immobilization is a technique in which the free movement is restricted and localized on an inert support or carrier. This technique has many advantages, the most important of which is that the immobilized enzyme can be reused [156, 157]. In addition, by immobilization, the operating temperature of the process can be increased [65]. An immobilized enzyme has to perform two essential functions: namely, the non-catalytic functions that are designed to aid separation and the catalytic functions that are designed to convert the targeting substrates within a desired time [156]. Generally, the support material and immobilization method are the most important factors that have to be considered to attain the enzyme activity and stability [155].

Enzyme immobilization can be carried out in different ways, classified into chemical and physical methods, as shown in Figure 2.3. The criteria for the selection depends on the source of the lipase, reaction type and process conditions.
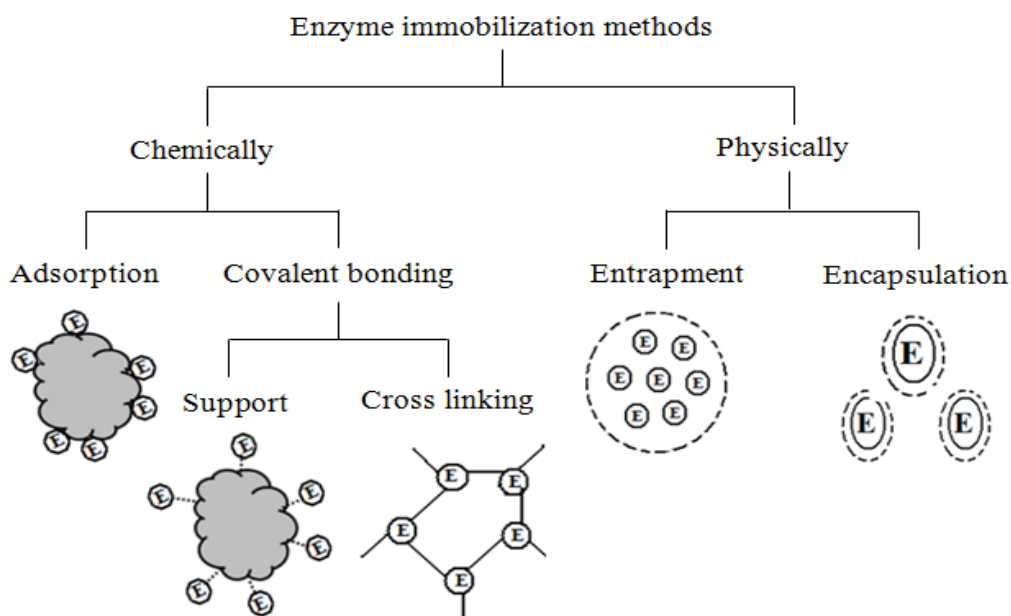
Figure 2.3: Enzyme immobilization methods [158]

The most commonly used lipases for commercial applications are Novozym®435 (*C. antartica* lipase immobilized on acrylic resin), Lipozyme IM (*Mucor miehei* lipase immobilized on a macroporous ion-exchange resin), Lipozyme TLIM (*Thermomyces lanuginosus* acrylic resin immobilized Lipase), Lipozyme RM IM (*Rhizomucor miehei* lipase immobilized on macroporous anion exchange resin) and *Candida* sp. 99–125 lipase, immobilized on textile membranes. In biodiesel enzymatic production, various immobilization techniques have been used. Amongst all, physical adsorption has been clearly selected by most researchers due to its ease, the absence of expensive and toxic chemicals and the ability to retain the activity and feasibility of regeneration [3]. Da Rós et al. [159] used an inorganic matrix of niobium oxide and a hybrid

matrix of polysiloxane–polyvinyl alcohol immobilized covalently for beef tallow transesterification using ethanol. Different yields were reported for the same reaction with the latter being found to be more stable (2 times more) compared to the former, and 17 times more stable than the free lipase, which is mainly because of the strong covalent binding of the enzyme on the support. Du et al. [160] used adsorption on macroporous resin, Noureddini et al. [155] worked on hydrophobic sol–gel support by entrapment and Orçaire et al. [161] worked on silica aerogel by encapsulation. Table 2.4 summarizes some of biodiesel previous works using different immobilization methods

The reusability of the immobilized lipases was investigated by several researchers. Lu et al. [162] transesterified lard using *Candida* sp. 99-125 with a step-wise methanol addition and found that the enzyme was reusable over seven repeated cycles (for 180 h) with no significant decrease in the lipase activity, and FAME yield was higher than 80%. Modi et al. [163] found similar stability when ethyl acetate was used instead of alcohol, where Novozym[®]435 was reused for 12 cycles without any loss in activity compared to ethanol that showed 40 % loss in the first re-use. On the other hand, Shimada et al. [164] have reported more than 95 % ester conversion even after 50 cycles (100 days) of the reaction. Table 2.5 shows a summary of different lipases tested with different feedstocks and conditions.

Table 2.4: Studies carried out for biodiesel production from different lipases immobilized by different methods

Lipase	Immobilization method	Carrier	Fat / Oil	Acyl acceptors	% Yield	Reference
C. antarctica	Adsorption	Silica gel	Soybean	Methanol	94	[165]
	Adsorption	Anion resin	Palm kern	Ethanol	63	[33]
	Adsorption	Acrylic resin	Soybean	Methyl acetate	92	[160]
	Adsorption	Acrylic resin	Soybean	Methanol	92.8	[166]
	Cross linking	Glutaraldehyde	Madhuca	Ethanol	92	[167]
Pseudomonas cepacia	Adsorption	Celite	Jatropha	Ethanol	98	[168]
	Entrapment	Hydrophobic sol-gel	Soybean	Methanol	56	[155]
	Entrapment	Phyllosilicate sol-gel	Tallow greases	Ethanol	94	[15]
	Encapsulation	Burkholderia cepacia	Sunflowe	Methyl acetate	64	[161]
Pseudomonas fluorescens	Adsorption	Polypropylene EP 100	Sunflower	Methanol	91	[169]
	Adsorption	Polypropylene MP1004	Soybean	Methanol	96	[170]
	Entrapment	Sodium alginate	Jatropha	Methanol	72	[171]

Table 2.5: Biodiesel production studies using different immobilized lipases and transesterification methods

Lipase	Fat/Oil	Alcohol	Solvent	Temperature (^{o}C)	Molar ratio (Alcohol:oil)	Time (h)	% Yield	Reference
Novozym®435	Cotton seed	Methanol	*tert*-butanol	50	4:01	24	97	[22]
	Cotton seed	Methanol	*tert*-butanol	51	5:01	25	95	[22]
	Jatropha	Ethyl acetate	-	50	11:01	12	91.3	[163]
	Soybean	Methanol	*tert*-butanol	50	4:01	12	65.8	[172]
	Soybean	Methyl acetate	-	40	12:01	14	92	[173]
	Soybean	Methyl acetate	-	40	12:01	14	92	[160]
	Palm kern	Ethanol	*n*-hexane	40	10:01	4	58.3	[33]
	Palm kern	Ethanol	SC-CO_2	40	10:01	4	63	[33]
	Sunflower	Methanol	SC-CO_2	45	5:01	6	23	[143]
	Soybean and rapeseed	Methanol	-	30	-	-	33.1	[164]
	Sunflower	Ethanol	SC-CO_2	45	5:01	6	27	[143]
	Soybean	Methanol	-	30	-	3.5	97	[174]
Pseudomonas	Sunflower	1-propanol	-	60	3:01	20	91	[157]
fluorescens	Soybean	Methanol	-	35	6:1	90	80	[175]

Table 2.5: Biodiesel production studies using different immobilized lipases and transesterification methods (cont.)

	Sunflower	Methanol	1,4-dioxane	50	3:01	80	70	[157]
	Jatropha	Methanol	n-hexane	40	4:1	48	71	[171]
P.cepacia	Tallow + Grease	Ethanol	-	50	4:01	20	94	[15]
	Soybean	Methanol	-	35	6:1	90	100	[175]
	Jatropha	Ethanol	-	50	4:01	12	98	[176]
	Sunflower	2-butanol	-	40	3:01	6	100	[177]
	Madhuca	Ethanol	-	40	4:01	2.5	92	[167]
	Soybean	Methanol	-	35	7.5:1	1	67	[155]
	Soybean	Ethanol	-	35	7.5:1	1	65	[155]
	Mahua	Ethanol	-	40	4:01	6	96	[167]
Lipozyme IM	Palm kern	Ethanol	n-hexane	40	3:01	4	77.5	[33]
	Palm kern	Ethanol	SC-CO_2	40	6.5:1	4	26.4	[33]
	Tallow	Methanol	-	45	3:1	5	19.4	[14]
	Tallow	Ethanol	-	45	3:1	5	65.5	[14]
	Tallow	Ethanol	n-hexane	45	3:1	5	98.3	[14]

Continued on next page

Table 2.5: Biodiesel production studies using different immobilized lipases and transesterification methods (cont.)

Lipozyme IM	Soybean	Methanol	-	40	3:1	12	98	[178]
	Soybean	Ethanol	*n*-hexane	45	3:1	5	97.4	[14]
Candidia sp. 99–125	Microalgae	Methanol	*n*-hexane	38	3:1	12	98.15	[179]
Lipozyme TL IM+Novozyme®435	Rapeseed	Methanol	*tert*-butanol	35	4:01	12	95	[180]

As can be concluded from the table, Novoyme®435 is the common tested immobilized lipase for biodiesel production. It has been tested with different acyl acceptors and under different reaction medium. Therefore, it has been used in this work.

2.2.2.2 Enzyme inhibitions

The activity and stability of lipases are mainly determined by the lipase native structure, which is mainly attributed to the change of confirmation [181]. Briefly, the 3-D structure of lipases used in biodiesel production displayed α/β hydrolase fold with Ser-His-Asp catalytic triad and a lid over the active site. The role of the lid is very important, where its movement allows un-shielding the active site from external environment or substrate availability to the active site. Lipase is inactive in organic media due to the lid coverage of the active site. However, the presence of water molecules opens up the structure and activates the enzyme. Although short-chain alcohols; specifically methanol, are preferable in conventional transesterification reactions, they negatively affect the lipase activity if used in excessive amounts. This is because short-chain alcohols have low solubility in oils resulting in their presence as a separate phase. The affinity of the alcohol to water is high, and this separate phase strips off the micro-layer of essential water surrounding the lipase needed to maintain the lipase conformation and catalytic activity, thus, reducing the activity and stability of the lipase [65, 160, 180, 182].

This is clearly reported in most studies, when methanol is used for biodiesel production. Santambrogio et al. [183] had studied the methanol effects on the activity and conformation of *Burkholderia glumae* lipase, and found that

the enzyme stability was negatively affected and assumed to be due to the negative effects on the conformational stability of the catalyst. Similar, but lower effects were reported when ethanol was tested due to the higher solubility of ethanol in vegetable oils than that of methanol [184, 185]. Abigor et al. [186] investigated the use of ethanol with *P.cepacia* lipase to convert palm kernel oil and found that a 5 times higher conversion was obtained when ethanol was used compared to methanol. Similar observation was reported by Nelson et al. [14] with the highest conversion of 65.5 and 19.4 % with ethanol and methanol, respectively, using Lipozyme IM60 for tallow conversion at 45 ^{o}C, stoichiometric ratio and 5 h reaction. This is mainly due to the decrease of system polarity with the increase of alcohol carbon chain; therefore the inhibitory effect becomes less.

This inhibition problem can be solved by different approaches, including the step wise addition of the alcohol, using other acyl acceptors, lipase pre-treatment, use of combined enzymes and reaction medium engineering.

A. Step-wise addition of alcohol

Among the several approaches to reduce the inhibition effect of the methanol, Shimada et al. [187] found that when the methanol concentration exceeded its solubility level, it deactivated the lipase irreversibly. They mentioned that the problem was due to contact of lipase with methanol, which was insoluble in reaction mixture, thus, proposed the methanol stepwise addition for catalyzed reaction Novozym$^®$435, where one-third of the molar ratio was suggested initially and after certain time of reaction the second portion was added, and this is repeated with the third portion, which was added later. The first portion of methanol was added at the beginning and after 7 h of reaction, where

33.1% conversion was obtained the second portion was added resulting in a 66.4% conversion after 10 h. This was followed by the addition of the last portion after 24 h where the reaction was allowed to continue for more 24 h in which 98.4 % conversion was accomplished. A comparable study was performed by Watanabe et al. [188] for a mixture of oils (soybean and rapeseed) by a two-step addition of methanol rather than three, where a yield of 98.5 % was achieved. The first portion was started at the beginning of the reaction and the second portion (two-thirds) was after 10 h. It was found that the solubility of the oil mixture increased by the presence of the produced biodiesel, which allowed more addition of methanol as the reaction proceeded. By doing this, the reaction time was reduced to 36 h, and enzymes were reused 70 times, compared to a 48 h reaction and 50 times f reuse as in Shimada et al. [187]. Similar observations were obtained using *P. fluorescens* [169] and *Rhizopus oryzae* [189]. As in the case of methanol, the step-wise addition of ethanol resulted in 60 % ethyl ester yield compared to 16.9 % when it was added in a single step at the beginning of the reaction [190]. Lee et al. [191] reported a higher conversion of 74 % using methanol compared to 43 % when ethanol was used in a three- step manner.

B. Different acyl acceptors use

The use of other acyl acceptors has been suggested as a way to eliminate the lipase inhibition effect. Methyl and ethyl acetates were the most used acceptors for interesterification of different oils and fats into biodiesel. Du et al. [160] performed a comparative study on Novozym$^®$435 transesterification of soybean oil with methanol and interesterification of the same oil with methyl acetate for biodiesel production. Methanol showed a negative effect on tested

enzymatic activity, whereas methyl acetate did not have any visible negative effects. Methyl acetate with Novozym[®]435 was also tested by Xu et al. [192] with soybean oil at 40 ^{o}C and similar results were found. Modi et al. [163, 166] also tested the use of ethyl acetate and propan-2-ol in converting oils from jatropha, karanja and sunflower using Novozym[®]435 at 50 ^{o}C, and found that both acceptors showed higher stabilities than ethanol and methanol. Despite methyl acetate clear advantages on enzyme activity, it gave results of a much slower reaction rate [160]. Tables 2.4 and 2.5 list examples of works done using ethyl acetate in lipase catalyzed biodiesel production.

C. Lipase pre-treatments

Numerous studies have reported that pre-treatment of the immobilized lipase affect the activity and stability. Samukawa et al. [174] studied the effect of pre-incubation of Novozym[®]435 on soybean oil transesterification with methanol. In their study, immobilized lipase was incubated in methyl oleate for 0.5 h and then in the oil for 12 h. When the enzyme was incubated in methyl oleate, 10% product content was achieved after 0.5 h of incubation and 20 % after 1h, whereas product contents 7.4 and 13.6 % were obtained, respectively, when transesterification was carried out without the incubation step. Within 3.5 h of reaction, 97 % of product was obtained by step-wise addition of 0.33 equivalent of methanol at 0.25-0.4 h intervals. Similar observation was obtained by Royon et al. [22] when Novozym[®]435 was immersed in *tert*-butanol, compared to complete inhibition of the lipase in *tert*-butanol absence. The positive effect might due to the *tert*-butanol ability to shield the enzyme vicinity from being inhibited by methanol. Moreover, by immersion in *tert*-butanol, high

catalytic activity and operation stability could be obtained [180], and was confirmed by many investigators [177]. Modi et al. [163] also studied similar pre-treatment effect, but using ethyl acetate with jatropha, karanj and sunflower oils, and their results showed insignificant effect on the relative activity of lipase, which indicates that ethyl acetate had no negative effect on enzyme activity.

D. Reaction engineering

The enzyme inhibition was overcome through medium engineering, specifically improving the medium polarity by the addition of an inert solvent. Generally, introducing organic solvents to synthetic reactions increase the solubility of the similar polarity substrate, so increasing reaction rate, and reducing water activity, which diminish hydrolysis during transesterification reactions [193]. Moreover, conducting the reactions in organic solvent media has many advantages compared to solvent free systems, such as reducing the reaction medium viscosity, allowing higher diffusion with less mass transfer limitations. In addition, better stability, and easy recovery and reuse of the immobilized enzyme from the reaction mixture have been reported [194, 195].

The selection of a proper solvent is critical as solvents may also strip off the essential hydration shell from the enzyme. The properties of the solvent such as hydrophobicity index, log P, which is the logarithm of n-octanol-water partition coefficient of the selected solvent between n-octanol and water, play vital role in the selection [196]. It is important to mention also that the Log P is only applicable for solvents of the same functionally [197]. Table 2.6 shows a list of common organic solvents and their respective log P values, including SC-CO$_2$ used in this work. Although numerous organic solvents can be used, several

aspects have to be considered in choosing the suitable solvent, including the solvent compatibility, inertness, low density, toxicity, and flammability [198]. Thus, lipases have been tested in organic solvents such as *tert*-butanol, *n*-hexane [180, 199, 200], ionic liquids [201, 202], supercritical fluids [203-205], and in gaseous media [206]. This is mainly applicable when short-chain alcohols are used in transesterification. Soumanou et al. [169] noted that the solubility of propanol and butanol in oils was much higher than that of methanol and ethanol, thus they do not need the additional organic solvent

Table 2.6: Common organic solvents and SC-CO_2 and their log P values [169, 207, 208]

Solvent	Log P
Iso-octane	4.7
n-heptane	4
Petroleum ether	≈3
n-hexane	3.5
Cyclohexane	3.2
Toluene	2.5
CO_2[a]	2
Benzene	2
Chloroform	2
CO_2[b]	0.9
tert-butanol	0.83

[a] at 50 °C and 118 bar
[b] at 50 °C and 3 bar

The importance of using a hydrophobic solvent has been well addressed in the literature. Köse et al. [209] investigated lipase catalyzed transesterification of cotton seed oil with methanol in solvent-free medium. Yield of 92.1 % was achieved in the presence of the Novozym®435 in 24 h reaction. This was performed at 50 °C, 4:1 alcohol to oil and 30% enzyme loading. In 2007, Royon

et al. [22] performed comparable work for cotton seed oil using Novozym®435 under the same conditions, but using *tert*-butanol as solvent. They noted that *tert*-butanol dissolved both methanol and glycerol that might inhibit enzyme activity and a higher conversion of 97 % was observed after 24 h of reaction. Similarly, Nelson et al. [14] tested the effect of using *n*-hexane with *Mucor miehei* lipase, yield of 94.8% compared to only 19.4 % yield obtained in a solvent free system after 5 h reaction of tallow with methanol at 3:1 molar ratio and 45 ^{o}C. On the other hand, with ethanol 65.5 % yield was achieved in a solvent free system and 98.0% in a *n*-hexane system within the first 5 h of the reaction. Using 80% *tert*-butanol (based on oil weight) improved biodiesel yield from soybean oil deodorizer distillate with 4 % Novozym®435 from 80 to 84 %. However, further increase in solvent use decreased the yield, which might be due to the dilution effect of reactants [102]. Soumanou et al. [169] tested the use of different solvents on Lipozyme TL activity and it was found that the yield increased with the hydrophobicity. In contrast, hydrophilic solvents are much less useful [210, 211]; for examples the use of acetone (log *P*=-0.23) showed less than 20 % yield compared 80 % when *n*-hexane was used. This is mainly due to the solvent interaction with the essential water layer surrounding the lipase molecule [157].

On the other hand, from an environmental point of view, the use of organic solvents has to be minimized because of their environmental impacts. In addition, they are usually expensive and require separation from the product. Hence, the need for high yields with better separation for higher purity products and environmentally friendly processes have led to the search for new technologies and solvents. The best choice of solvent to replace previously mentioned solvents should have the same advantages of dissolving both

substrates and reducing excess alcohol inhibition and, at the same time, avoiding the drawbacks of difficult separation of the solvent. In this regard, SCF have been suggested as alternative solvents [32]. SCFs have shown the potential as a better alternative to conventional co-solvent. The technology is rapidly developing, mainly, due to SCFs favorable properties. Further discussion on the use of SC-CO_2 as a reaction medium is found in section 2.5.2.

Compared to the suggested solutions to minimize the inhibition effects of short chain alcohols, this strategy is commonly used. This is mainly due to the shorter reaction time compared to step-wise additions. The pre-treatment enhances the stability; however it does not have to do with minimizing the inhibition. However, the use of acetates as acceptors promotes interesterification reaction, where the replacement of short chain alcohols with acetates results in triacetin production instead of glycerol. However, the triacetin separation is relatively more difficult than glycerol [212]. Therefore, the use of solvent was suggested in this work.

2.2.3   Modeling of lipase kinetics

Enzyme kinetics is the quantitative analysis of the factors affecting the enzyme activity. The thorough knowledge of the reaction kinetic is of great importance to get information about the rate of product formation required for any reactor design and process scale up. The first proposed study on enzyme catalytic potential was carried out by Henri 1903, who studied the effect of substrate concentration and found that the substrate conversion to product proceeded in a reversible reaction between the substrate and enzyme to form an intermediate that breaks down to deliver the product. From that, Michaelis and

Menten, who started the first formal theory for enzyme catalysis on a single substrate, established their first known equation, shown in Eq. (2.1), representing the parametric expression for the enzymatic reaction rate as a function of substrate concentration [213].

$$v_i = \frac{v_{max}\,[S]}{K_m + [S]} \tag{2.1}$$

where, K_m is the Michaelis constant, [S] is substrate concentration, v_i is the initial reaction rate and v_{max} is the maximum reaction velocity. This model is applicable to the case of a single substrate involved in the reaction without any inhibition effect to the enzyme. However, in some of enzymatic reactions the presence of excess substrate inactivates the enzyme by. For this case, the following model (Eq. 2.2) was proposed, where K_{IS} represents the inhibition constant.

$$v_i = \frac{v_{max}\,[S]}{K_m + [S]\left(1 + \frac{[S]}{K_{IS}}\right)} \tag{2.2}$$

For the enzymatic reactions presented by Eqs. (2.1 and 2.2), only one substrate is present; however, in most enzymatic reactions two or more substrates may take place, which is the case with lipase catalyzed transesterification. Several studies have focused on the kinetics of enzymatic transesterification of lipids for biodiesel production, where most of them confirmed that Ping-Pong Bi Bi with competitive alcohol inhibition best describes the reaction [35, 37, 122, 192, 214-217]. The Ping Pong Bi Bi model is a double displacement mechanism in which the first substrate, oil, combines with the enzyme forming fatty acid-

enzyme intermediate that forms the first product, leaving behind a modified enzyme intermediate (E-X). This modified intermediate then joins with the second substrate, alcohol, as illustrated in Eq. (2.3) to produce another intermediate, which produces the second product, and the enzyme returns to its natural state. The rate expression of the transesterification reaction of the lipids based on this model with competitive inhibition by the alcohol is given by Eq. (2.4).

(2.3)
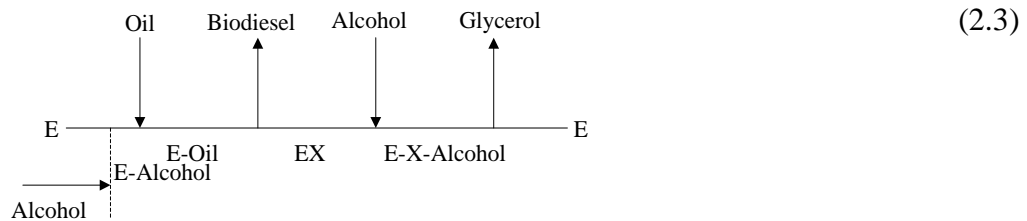
$$v_i = \frac{v_{max}[S][A]}{[S][A] + K_{m,A}[S] + K_{m,l}[A]\left\{1 + \frac{[A]}{K_{iA}}\right\}}$$

(2.4)

Where, $[A]$ is the concentration of alcohol, $K_{m,l}$ and $K_{m,A}$ are the apparent Michaelis–Menten constants for the substrate and methanol, respectively and K_{iA} is the apparent methanol inhibition constant. Hari et al. [218] proposed a development of the model (Eq. 2.4) by including a Ping Pong Bi Bi mechanism with both substrates inhibition. However, this modification was not valid for oil transesterification, and it has been confirmed experimentally that the oil does not exhibit any inhibition. In all of proven experiments, concentration of the oil substrate is considered constant, and only methanol concentration was varied taken into consideration [219]. Soumanou and Bornscheuer [169], who studied the effect of both substrate concentrations variation, and Al-Zuhair [219] who represented their initial reaction rate results versus substrate and methanol

concentrations to demonstrate the significance of the Krishna and Karanth modification and found that the substrate inhibition was independent of the type of lipase used.

Since the initial reaction rate is considered, the amount of produced glycerol is negligible, and its inhibitory effect can be eliminated. The classical studies were performed by investigating the independent effect of both substrates concentration on the reaction rate. In such cases, one of the substrates concentration was fixed and the concentration of the other substrate was varied, and vice versa. Several simplifications to Eq. (2.4) have been carried out. Among them is the one shown in Eq. (2.5) based on the initial mass concentrations, in term of the initial fixed lipid concentration, rather than initial molar concentrations [35]. By considering the concentration based on the initial oil concentration, and fixing the amount of oil, its concentration was taken as 1 and its effect did not appear in the modified equation (Eq. 2.5).The effect of methanol mass concentration on the reaction rate was investigated by transesterifying fixed initial quantities of lipids with various initial concentrations of methanol. This has been proved in earlier studies [35].

$$v_i = \frac{v_{max}[M]^*}{[M]^* + K_{m,m} + K_{m,l}[M]^* \left\{ 1 + \frac{[M]^*}{K_{im}} \right\}} \tag{2.5}$$

where, $[M]^*$ is the initial mass concentration of methanol in g g^{-1}.

2.3   FEEDSTOCKS

The major bottleneck in the biodiesel production is the supply and cost of the feedstock [220]. Biodiesel can be synthesized from a variety of feedstocks,

which include most vegetable oils and animal fats (tallow and lard). They can also be produced from other sources like non-edible oils, waste cooking oils, greases and algae oil [43]. Generally, oils and fats are esters of glycerol and fatty acids (saturated or unsaturated). As mentioned earlier, the direct use of vegetable oils is not practical and caused carbon deposition. The reason behind the carbon deposits is the glycerin part of the oil that has low caloric value. The glycerin part is responsible for the high viscosity of the oil as well. Thus, by eliminating the glycerin part from the vegetable oils, the residual FAAE can be used in engines [221]. The fatty acids present in oils are either saturated fatty acids that contain single carbon to carbon bonds (C-C), and unsaturated fatty acids that contain one or more double bonds (C=C). The main FAEE that are similar to petroleum diesel are steric, oleic linoleic and palmitic acids. The selection of the proper feedstock and reaction conditions depend on several factors such as the availability, oil characteristics, and the cost, which are the major barriers in process commercialization.

2.3.1   Conventional feedstocks

The conventional feedstocks for biodiesel production are vegetable oil seeds since they are available in large quantities. These include soybean seed [113, 222], canola [223], palm [122, 224, 225] and sunflower seed [226, 227], which contain oil that can be extracted. The typical fatty acids found in vegetable oils are presented in Tab;e 2.7.

Table 2.7: Chemical structure of common fatty acids presents in lipids used for biodiesel production [228]

Fatty Acid	Structure	Formula
Lauric	$C_{12:0}$	$C_{12}H_{24}O_2$
Myristic	$C_{14:0}$	$C_{14}H_{28}O_2$
Palmitic	$C_{16:0}$	$C_{16}H_{32}O_2$
Palmitoleic	$C_{16:1}$	$C_{16}H_{32}O_2$
Steric	$C_{18:0}$	$C_{18}H_{36}O_2$
Olieic	$C_{18:1}$	$C_{18}H_{34}O_2$
Linoleic	$C_{18:2}$	$C_{18}H_{32}O_2$
Linolenic	$C_{18:3}$	$C_{18}H_{30}O_2$
Arachidic	$C_{20:0}$	$C_{20}H_{40}O_2$
Archidonic	$C_{20:1}$	$C_{20}H_{40}O_2$
Behenic	$C_{22:0}$	$C_{22}H_{44}O_2$
Erucic	$C_{22:1}$	$C_{22}H_{42}O_2$

Table 2.8 shows the fatty acids profile of common oils used for biodiesel production. As can be seen, soybean and sunflower oils, which are the most common oils are composed of five main fatty acids, namely palmitic acid, stearic acid, oleic acid, linoleic acid, and linolenic acid. The composition is of great importance as it determines the derived biodiesel properties. The main disadvantages of using these vegetable oils for fuel production are the food-versus-fuel competition that increases the food prices.

Table 2.8: Fatty acid composition of lipids from common feedstocks tested for biodiesel productions [229-232]

Fatty acids	Fatty acid composition (*wt* %)										
	$C_{14:0}$	$C_{16:0}$	$C_{16:1}$	$C_{18:0}$	$C_{18:1}$	$C_{18:2}$	$C_{18:3}$	$C_{20:0}$	$C_{20:1}$	$C_{22:0}$	Others
Beef	4	26	4	20	28	3		-	-	-	14
Canola	-	4	-	2	61	22	10	-	1	-	
Chicken	1	25	8	6	41	18	1	-	-	-	-
Corn	-	11	-	2	28	58	1	-	-	-	-
Cotton	1	23	1	2	17	56	-	-	-	-	-
Groundnut	-	11.2	-	3.6	41.1	35.5	0.1	-	-	-	-
Lamb	2	19		26	44	2	4	-	-	-	-
Lineseed	-	5.6	-	3.2	17.7	15.7	57.8	-	-	-	-
Madhuca longifolia	-	18	-	14	46	18	-	-	-	-	-
Olive	-	13.8	1.4	2.8	71.6	9	1	-	-	-	-
Palm	1	45	-	4	39	11	-	-	-	-	-
Pongamia pinnata	-	9	-	8	66	12	-	1	1	3	-
Seseam	-	9.6	0.2	6.7	41.1	41.2	0.7	-	-	-	-
Soybean	-	11	-	4	23	54	8	-	-	-	-
Sunflower	-	6	-	5	29	58	1	-	-	1	-

Since biodiesel from food-grade oils is not economically competitive with petroleum-based diesel fuel, it is necessary to use lower-cost oil feedstocks. Thus, non-edible oils such as *Jatropha curcas, Pongamia pinnata, Madhuca indica* were suggested [96, 131, 133, 233, 234]. The use of non-edible oils for biodiesel production solves several problems, including food security and the utilization of unproductive lands that are not possible for edible oil cultivation. However, non-edible plantation competes with available lands, and requires fertilization, man-power and freshwater. Used cooking oils and fats are usually broken down after a period of use and become unsuitable for further cooking as a result of increasing FFAs content [235]. Once this reached, they are discarded or recycled. Thus, this type of feedstocks are cheap and reduces the waste product removal costs, which make them available for biodiesel production [39]. In addition, many animal processing and rendering companies create large amounts of waste fats. Utilization of such feedstocks can reduce the biodiesel production costs up to 60-90 % and helps in solving the waste disposal problems. Waste cooking oil conversion into biodiesel through the transesterification process reduces their molecular weight to approximately one-third, viscosity to about one-seventh, as well as reducing their flash point and volatility [64].

Using lipids extracted from algae, namely; macroalgae and microalgae, as a feedstock for biodiesel production has been started by the NREL research project [44]. Microalgae are small and unicellular organisms, and due to their simple cell structure, they are widely used and have been accepted as promising feedstock for biodiesel production. Generally, microalgae can produce both neutral lipids,

composed mainly of triglycerides that are used as energy storage, and polar lipids such as phospholipids, which are commonly produced in the cellular membrane, whereas the former usually accumulates as droplets in the cytoplasm [236].

2.3.2 General aspects of waste cooking oils

Many researchers have studied the use of alkaline catalysts in the transesterification reactions. However, these used oils have high free fatty acid contents that range from 5 to 15 wt% [108, 237, 238]. As mentioned earlier, the use of alkaline catalysts is not practical with feedstock of high FFA due to soap formation, which reduces the final product quality and adds difficulties in the separation step. Among the homogeneuous catalysts used with waste oils is sulfuric acid and high conversion reaching 99 % was obtained from used soybean oil at 28 ^{o}C with 9:1 molar ratio [239]. Similar conversions, but with a higher temperature (200 ^{o}C) and methanol to oil ratio requirement (18:1) were obtained when Zn/Si was used [119]. However, acid catalyzed reactions are slow. Furthermore, the supply of these sources is not continuous, where it is possible that suddenly a high bulk of material is available followed by a period with no supply [240]. Demirbas [72] carried out the supercritical methanol production of biodiesel using waste cooking oil at 287 ^{o}C, and obtained a yield close to 99 % in a 20 min reaction. Also, Yin et al. [241] tested the supercritical approach, and obtained 95 % conversion within 10 min of reaction with 42:1 methanol to oil molar ratio at 350 ^{o}C. Slightly higher conversion of 98 % was also obtained when KOH was added to the subcritical methanol at 160 ^{o}C. On the other hand, slightly lower conversions of 90-94 % but faster than acid catalyzed

reactions were achieved from waste cooking oil in organic solvents using immobilized lipases of from *Candida* sp., [242], Lipozyme TL-IM [243, 244] and Novozym[®]435 [245, 246]. In addition to the previously mentioned barriers, after reaction completion, produced biodiesel from waste cooking oil has to be left for hours to allow glycerol settling, which usually occurs much faster, but because of the feedstocks impurities this is usually a slow process with waste cooking oil [247].

2.3.3   Fuels properties

The fuel physico-chemical properties are important and depend on the properties and composition of the feedstock lipid. The most important properties that need to be considered are the density, viscosity, flash point, cetane number, cloud and pour points, and calorific value. Goering et al. [248] studied the use of straight vegetable oils; namely castor, corn, cotton seed, linseed, peanut, canola, safflower, sesame, soybean and sunflower, and determined their fuel properties. They had reported that the tested vegetable oils were much more viscous and reactive to excess oxygen and had higher cloud and pour points compared to commercial diesel fuel. The viscosities of vegetable oils were found to be 10–20 times greater than diesel fuel.

For commercial fuel use, the produced biodiesel must be analyzed. Several standards have been revised for fuels properties. Among these, ASTM D6751 [249] and EN14214 [249], shown in Table 2.9, are the most commonly used.

Table 2.9: Fuel standards and test methods for pure biodiesel

Property	Method		Limit	
	ASTM	EN	ASTM	EN
Acid value (mgKOH g^{-1})	ASTM D664	EN 14104	0.5 max	0.5 max
Water and sediment	ASTM D2709	EN ISO 12937	0.05[a] max	500[b] max
Ester content	-	EN 14103	-	96.5[d] min
Free glycerol	ASTM	EN 14105	0.02[c]	0.02 [d]
Total glycerol	ASTM	EN 14106	0.24 [c]	0.25 [d]
Sulfur content	ASTM D874	ISO 3897	0.02 [c]	0.02 [d]
Phosphorous content	ASTM D4951	EN 14107	0.001 [c] max	10[e] max
Cetane number	ASTM D613	EN ISO 5165	47.0 min	51.0 min
Cloud point	ASTM D2500	-	-	-
Oxidation stability (h)	-	EN 14112	3 min	6 min
Flash point (^{o}C)	ASTM D93	EN ISO 3679	93 min	120
Density, (kg m^{-3},15 ^{o}C)	-	EN ISO 3675	-	860-900
Kinematic viscosity, ($mm^2 s^{-1}$,40 ^{o}C)	ASM D445	EN ISO 3104	1.9-6.0	3.5-5.0

[a] *vol* %
[b] mg kg^{-1}
[c] % *wt*
[d] *mol* %
[e] mg kg^{-1}

The heating value is an important fuel combustion property used to assess produced biodiesel, in which the value of biodiesel is almost ten times that of petroleum diesel. The delay in ignition time between the fuels injection and ignition, called as cetane number, is another important property, wherein, the higher the cetane number indicates, the shorter ignition delay time. Most biodiesels produced from vegetable oils have cetane numbers higher than 50 [250, 251]. Another important property of fuel is the flow properties that determine the flow performance. This is usually evaluated by the viscosity that measures the fuel resistance to flow, where the higher value could reduce the performance, as attained from the direct use of vegetable oils. In cold environments, the cloud and pour points are of significance, which are the temperatures at which the wax formation might begin to plug the fuel filter and the fuel is no longer pumpable, respectively. In addition, biodiesel is subjected to oxidation, which might lead to degradation. Thus, it is crucial to determine the fuel resistance to chemical changes due to oxidation reactions. The flash point is the temperature required to which the produced fuel must be heated to form the flammable mixture of vapor and air that can be ignited, where the higher the flash point, the lower the risk of firing.

2.4 MICROALGAE

Algae are photosynthetic organisms that convert inorganic carbon, such as CO_2, in the presence of light, water and nutrients to algal biomass [252-257] with the majority live in aquatic environments [258]. They can grow either autotrophiclly or heterotrophically. The autotrophic growth of the algae requires CO_2, light and nutrients to grow, whereas the heterotrophic require an organic

carbon source, such as glucose, in addition to the nutrients [45, 256, 259, 260]. Thus, in the autotrophic algae the energy is gained through the supplied light, whereas in the heterotrophic it is gained from the dissolved organic matters. Typically, autotrophic growth is more favorable than the heterotrophic, as it does not require glucose which is a food source and, at the same time, fixes CO_2, which has a positive effect on the environment. In addition to these two types of growth, some algae are capable of behaving in both autotrophic and heterotrophic modes. These are called mixotrophic algae [255, 261].

Algae range from unicellular to multi-cellular forms [256]. They may exist as colonies, filaments or ameoboids [255]. Based on their internal structure, almost all algae are eukaryotes, where cells consist of cell wall, plasma membrane, cytoplasm, nucleus and organelles such as mitochondria, lysosomes and golgi. Algae cells are normally divided into several classes including blue-green (Cyanophyceae), green (Chlorophyceae), diatoms (Bacillariophyceae), yellow (Xanthophyceae), golden (Chrysophyceae), red (Rhodophyceae), brown (Phaeophyceae), dinoflagellates (Dinophyceae) and picoplankton (Prasinophyceae and Eustigmatophyceae) [262]. It was reported that there are over 40,000 species of algae, and only a limited number of these have been studied and have commercial significance [120, 263]. The most predominant group used for biodiesel production is the green microalgae.

The main components of any microalgae cell are protein, carbohydrates and lipids. The composition is species specific and varies between different microalgae depending on nutrient, salinity, medium pH, temperature, light intensity and growth phase, which allow microalgae to be used in different

applications ranging from food products to biofuels. Usually, they are used as animal feed [264], human health food [265] and as biofertilizer [42]. Additionally, microalgae can be used for atmospheric CO_2 mitigation. Table 2.10 shows the chemical composition of some studied microalgae strains.

Table 2.10: Chemical composition of various microalgae species (% dry weight)

Microalgae	Carbohydrates	Protein	Lipids	Reference(s)
Chaetoceros muelleri	19.3	46.9	33.2	[266]
Isochrysis galbana	26.8	47.9	14.5	[267]
Chaetoceros calcitrans	27.4	36.4	15.5	[267]
Isochrysis sp.	12.9	50.8	20.7	[268]
Prymnesiophyte (NT19)	8.4	41.3	14.7	[268]
Rhodomonas (NT15)	6.0	57.2	12	[268]
Cryptomonas (CRF101)	4.4	44.2	21.4	[268]
Chaetoceros (CS256)	13.1	57.3	16.8	[268]
C. protothecoides[a]	10.6	52.6	14.6	[269-271]
C. protothecoides[b]	15.4	10.3	55.2	[269, 270]
Microcystis aeruginosa	11.6	30.8	12.5	[269]
Nannochloropsis sp	29.0	10.7	60.7	[272]
S. obliquus	15	50.0	9.0	[273]
Oscillatoria limnetica	50	44.0	5.0	[273]
B. braunii	18.9	17.8	61.4	[274]
Botryococcus protuberans	16.8	14.2	52.2	[274]

[a] Autotrophic cultivation
[b] Heterotrophic cultivation

Among the biomass component, the lipids content, which is important for biodiesel production, is usually between 20-50 % of dry algae biomass weight, but may also exceed 80 % in some cases [42, 252, 275, 276]. Microalgae low with oil content (10 % *wt*) can still be used and produce four times the amount of oil that can be produced from best crop feedstock, which is palm. In addition, microalgae can grow very fast by doubling biomass within 24 h and during their

exponential growth phase they can double their biomass in about 3.5 h [42, 276-278].

Many microalgae can alter their metabolic pathway towards accumulations of lipids in form TAGs [120]. It is known that under stressed conditions, photosynthesis activity decreases, but lipid synthesis is enhanced. Generally, lipids may include neutral lipids, polar lipids, wax esters, sterols and hydrocarbons as well phenyl derivatives [220]. For biodiesel production, the natural lipids, which are non-polar, should always be targeted. Typically, most of microalgae produced lipids have fatty acid constitutions similar to most common vegetable oils [265, 279, 280]. They have a carbon chain range from C_{12} to C_{22}. Table 2.11 shows a summary of the lipid profile of some microalgae strains tested for biodiesel production.

Table 2.11: Fatty acid composition of lipids extracted different microalgae biomass [265, 280]

Fatty acid	*Spirulina platensis*	*Spirulina.maxima*	*S. obliquus*	*C.vulgaris*	*Dunaliella bardawil*
$C_{12:0}$	0.04	traces	0.3	-	-
$C_{14:0}$	0.7	0.3	0.6	0.9	-
$C_{14:1}$	0.2	0.1	0.1	2	-
$C_{15:0}$	traces	traces	-	1.6	-
$C_{16:0}$	45.5	45.1	16.0	20.4	41.7
$C_{16:1}$	9.6	6.8	8.0	5.8	7.3
$C_{16:2}$	1.2	traces	1.0	1.7	-
$C_{16:4}$	-	-	26.0	-	3.7
$C_{17:0}$	0.3	0.2	-	2.5	-
$C_{18:0}$	1.3	1.4	0.3	15.3	2.9
$C_{18:1}$	3.8	1.9	8.0	6.6	8.8
$C_{18:2}$	14.5	14.6	6.0	1.5	15.1
α-$C_{18:3}$	0.3	0.3	28.0	-	20.5
γ-$C_{18:3}$	21.1	20.3	-	-	-
$C_{20:2}$	-	-	-	1.5	-
$C_{20:3}$	0.4	0.8	-	20.8	-

Though microalgae contains a considerable amount of lipid with similar chemical composition to vegetable oils, the biodiesel production is not commercialized yet, which is mainly due to the high energy and costs from the both biomass and biodiesel productions. Thus, for sustainable fuel production from microalgae, the three main aspects have to be considered, which are the biomass production, recovery and processing. Typically, the microalgae biodiesel production process consists of several steps, which are strain selection, cultivation, harvesting, drying, cell disruption, lipid extraction and, at end, biodiesel production. Each step has its own technology, challenges and limitations.

2.4.1 Strain selection

Microalgae come in a variety of strains; each has different proportions of lipid, protein and carbohydrates contents. Due to their advantages, they have recently been suggested for biofuel production. Over 3,000 algal strains were collected, screened and characterized in the NREL sponsored project [44].

The selection of the most suitable strain needs certain parameters. These include; lipid content, growth rate and productivity, strain adaptableness and withstanding different weather conditions such as temperature, salinity and pH, high CO_2 capturing capacity, ease of biomass separation and processing and the possibility of obtaining valuable co-products [45].

Numerous researches have been carried out on different species environmental tolerance. Many of them were found to be suitable for biodiesel production. As shown in Table 2.10, some microalgae have high lipid content and others have high protein content, whereas others have high carbohydrate content.

Among the possible microalgae strains for biodiesel productions are *Chlorella, Nannochlorpsis* and *Scendensmus* species. Although high lipids content is always favorable, strains with low lipid usually grow faster [281]. Rodolfi et al. [282] have screened a variety of microalgal strains by evaluating their biomass productivity and lipid content in 250-ml flask laboratory cultures. They had clearly stated that microalgae cultures could become renewable source of fuel if the cultivation of the high productive strain succeeded on a large scale.

2.4.2   Cultivation and biomass production

For commercial biomass production, microalgal biomass must be easily cultivated at the required scale. The cultivation can be carried out in different types of systems, mainly open systems (open ponds) or closed systems (photobioreactors) [253, 283-285] in either phototrophic or heterotrophic approaches [179, 270]. Both methods and systems have different advantages and disadvantages, therefore, investigators are debating about which of the methods and systems is more favorable. Choosing the best production method or system depends on the selected algal strain and its integration with the appropriate downstream processing, which is the means for affordability and scalability of biodiesel production.

2.4.2.1   Cultivation systems

Open ponds are the most commonly used systems. Generally, ponds are made of a closed loop with recirculation channels. A paddle wheel that continuously operates is usually used to prevent sedimentation and provide the efficient circulation of the culture to maintain in suspension [286]. During daylight, the culture is fed continuously in front of the paddlewheel where the

flow begins and circulates through the loop to the harvesting point. On completion of the circulation loop, the broth is harvested [42, 253, 284, 287]. On the other hand, photobioreactors are closed bioreactors, which are designed as tabular, plate or bubble column reactors. Among these, the most common type is the tabular photobioreactors. These consist of less than 0.1 m diameter transparent tubes made from plastic or glass [42]. A photograph of both systems is shown in Figure 2.4.
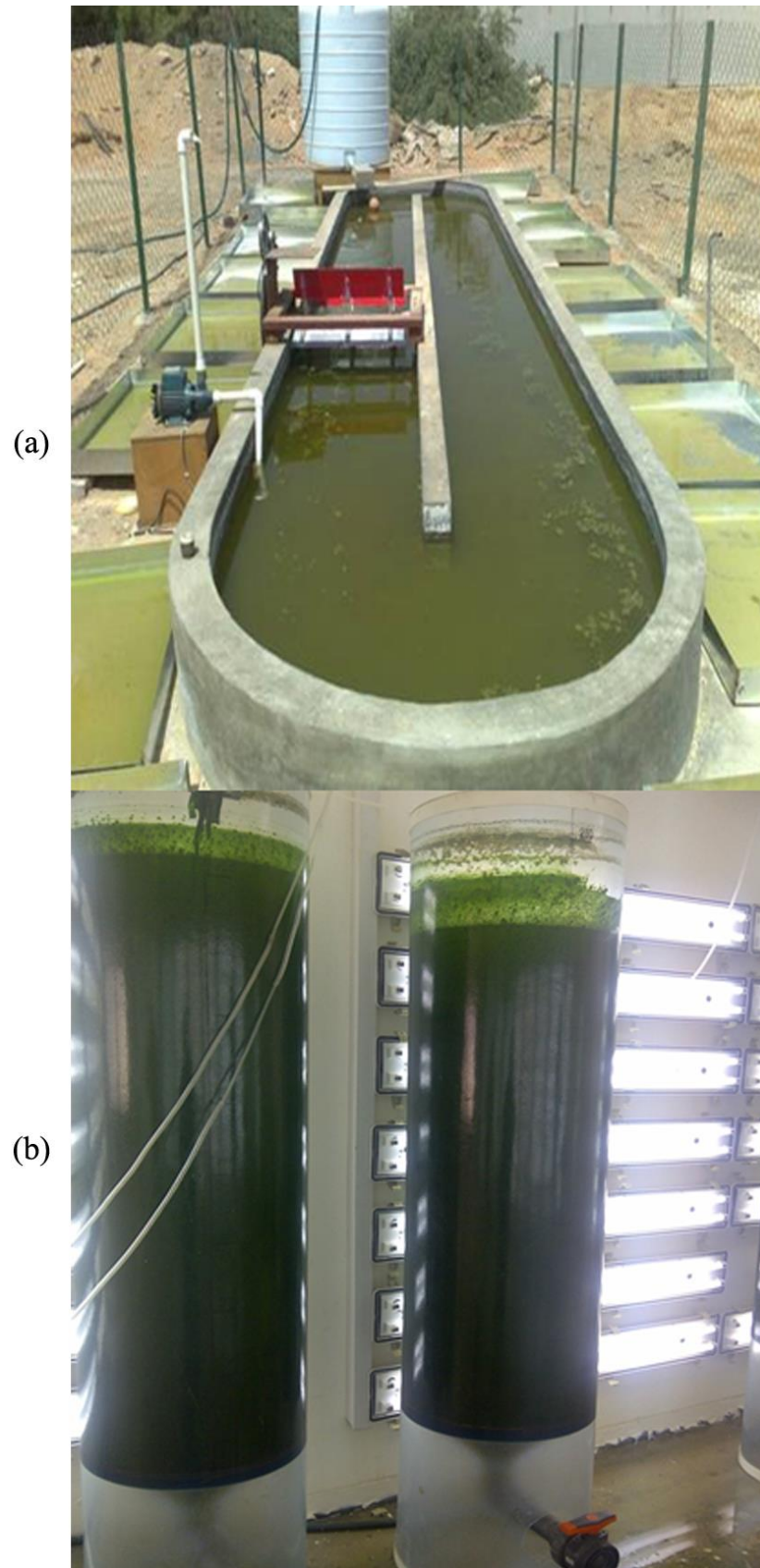
Figure 2.4: Photographs of; (a) open pond and (b) photobioreactor commonly used for biomass production

Typically, open ponds are preferred in large scale cultivation systems due to their simplicity and low construction and capital costs [42, 287]. However, these are open to the atmosphere, which lead to water evaporation and unwanted species contamination. The latter can be eliminated by growing at high salinities or pH, which are not practical for all strains. In addition, the cell's poor utilization of the light and low mass productivity due to the low light to volume ratio are the others limitations [288]. Therefore, for water, energy and chemicals saving purposes, photobioreactors have been proposed, but they are not yet commercialized. The main advantages of using photobioreactors are: better algal culture and environment control [287], large surface-to-volume ratio, less water evaporation, better isolation from outside contamination and higher mass productivity [289]. However, photobioreactors are usually made of plastic, and ultraviolet deterioration of the plastic surface is the main disadvantage. In addition, biofilm formation will require periodic cleaning, which is not easy [290]. A comparison between these two systems is summarized in Table 2.12.

Table 2.12: Comparison between open ponds and photobioreactors used for biomass production

System	Advantages	Limitations
Open ponds	- Simple - Cheap - Easy to operate and maintain - Low operation cost - No issues with cleaning	- Poor light utilization - Difficulties in light and temperature controlling - Water evaporation - May cause salt precipitation - Foreign species contaminations - Lower mass productivity (0.1-0.5 g L^{-1})

Continued on next page

Table 2.12: Comparison between open ponds and photobioreactors used for biomass production (cont.)

Photobioreactors	• High surface to volume ratio • Higher mass productivity • Less contaminations • Less water losses • Better light utilization	• Scalability problem • Costly • Complex • Cells damage • Biofilm formation • Cleaning problems

For a cost-effective cultivation process, a combination of the two previous mentioned systems, referred to as a hybrid system, was suggested [285]. In this type of system, microalgal strain with high lipids content are grow in photobioreactors in nutrient and CO_2 rich conditions, firstly to promote rapid reproduction with minimum contamination, then the microalgae enter an open system with limited nutrient to encourage their lipid production [291]. This process has been successfully verified by Huntley et al. [292]. In addition, open ponds covered with transparent sheets, and plastic bags photobioreactors were suggested to minimize contamination and maximize light utilization, respectively.

2.4.2.2 Cultivation conditions

Cultivation and growth conditions, such as temperature, light intensity, pH, water salinity, and nitrogen sources have significant effects on strain growth and lipid production. It has been reported that the lipid content in various green microalgae strains increased when growing in low nitrogen media compared to nitrogen rich media [293, 294].However, in these low nitrogen media, a reduction in growth rate is common [295]. Since the cell need sufficient nitrogen for growth, the cell production and division may reduce in the low nitrogen media. However, carbon metabolism continue leading to utilization of more energy for

lipid production rather than biomass growth [44, 296]. Other factors like CO_2, light intensity and temperature also significantly affect microalgae lipid content and composition. Renaud et al. [268] investigated the effect of temperature within the range of 25 to 35 $^\circ$C on *Rhodomonas* sp., *Chaetoceros* sp., *Cryptomonas* sp. and *Isochrysis* sp. growth rate and lipid content. Their results showed that optimum growth temperature was 25–27 °C for *Rhodomonas* sp., and 27–30 °C for *Cryptomonas* sp., *Chaetoceros* sp. and *Isochrysis* sp. Only *Chaetoceros* sp. was able to grow at 33 and 35 °C.

With the intent of providing sufficient light to the cultivation systems, open ponds are usually made shallow and tabular reactors are made small in diameter. Thus, the growth and productivity are highly affected by the light path. Tang et al. [297] studied the influence of the above mentioned parameters on *Dunaliella tertiolecta* growth, lipid content and fatty acid composition. They reported that increasing light intensity increases cell growth rate regardless of the light source. On the other hand, as for the CO_2 effect, the highest growth rate was found when CO_2 concentration was in the range of 2 to 6 %.

Although heterotrophic growth eliminates light requirement, not all strains are able to assimilate organic carbon. Thus, this cultivation method has been studied with a limited number of microalgae species [179, 270, 298], although it has been reported to provides high lipid content and biomass productivity [179, 269, 271, 299, 300], *C. protothecoides* lipid content was roughly 15% (% dry weight) under control conditions, but this reached around 44% [179, 301], 53% [302] and 55% [270] when grown heterotrophically. Liu et al. [303] compared the lipid content of *C. zofingiensis* cultivated under

heterotrophic and photoautotrophic conditions. Lipid content of 51.1 and 25.8 wt% were obtained, respectively. Liang et al. [304] compared *C. vulgaris* cell growth rate, lipid content and productivity under autotrophic and heterotrophic conditions and evaluated glucose, acetate, and glycerol carbon sources uptakes. They found that the biomass and lipid productivities are high under heterotrophic conditions with biomass productivity ranging from 22 to 27 mg $L^{-1} d^{-1}$, depending on the carbon source, whereas the highest lipid accumulation occurred at the autotrophic condition.

Furthermore, under stress conditions, microalgae can accumulate larger lipid content [305-308]. The primary stress applied to green microalgae is nitrogen deficiency, where accumulations of more than 50% (dry basis) have been reported [42, 309]. This is mainly due to the lack of nitrogen required for protein synthesis, and the excess carbon from photosynthesis is then diverted into lipid production pathway [310]. However, this is not always possible, as the high lipid content usually occurs under stress conditions, which results in low biomass productivity, yielding to low overall lipid productivity [311, 312]. Thus, it is important to work under condition where high lipid productivity is maintained. Moreover, in many cases, by the starvation, the polar lipids which are non-convertible to biodiesel are accumulated as well resulting in decreasing the quality of extracted lipids, and in some cases may result in inhibiting the enzymes. Therefore, monitoring the natural lipids accumulation is important.

2.4.2.3 Kinetic of cells growth

To design and scale up a cultivation system, the development of a kinetic model that adequately describes cells growth is essential. A microbial cell growth

kinetic study is commonly carried out in batch cultures. Among the several factors that limit microalgae growth rate, is the inorganic carbon (IC) concentration. CO_2 and HCO_3^- are the potential inorganic carbon sources for the photosynthesis in microalgae.

The common model of cell growth is the Monod model (Eq. 2.6) proposed in 1942, where the basic assumption was that the growth rate is dependent on a particular limiting substrate.

$$\bar{\mu} = \bar{\mu}_{max} \frac{[S]}{K_s + [S]}$$
(2.6)

where, $\bar{\mu}$ is specific growth rate, K_s is the Monod half-saturation constant, $[S]$ is limiting substrate concentration and μ_{max} is the maximum specific growth rate. The Monod model, however, fails to account for the substrate inhibition effect. Thus, correction for the inhibition effect was proposed by introducing the inhibition constant as in Haldane model, shown in Eq. (2.7).

$$\bar{\mu} = \bar{\mu}_{max} \frac{[S]}{K_s + [S]\left(1 + \frac{[S]}{K_i}\right)}$$
(2.7)

where, K_i is the substrate inhibition constant. Generally, enriched CO_2 is exchanged between the atmosphere and aquatic system via an equilibrium between the $CO_{2(g)}$ and dissolved $CO_{2(aq)}$, wherein the latter reacts with water forming H_2CO_3. The (TIC) concentration, shown in Eq. (2.8) is considered.

$$[TIC] = \left[CO_{2(aq)}\right] + [H_2CO_3] + [HCO_3^-] + [CO_3^{-2}]$$
(2.8)

$[CO_{2(aq)}]$ and $[H_2CO_3]$ are commonly denoted as $H_2CO_3^*$, as shown in Eq. (2.9). Thus, in equilibrium the gaseous CO_2 and dissolved $H_2CO_3^*$ are related by Henry's law (Eq.2.10);

$$CO_{2(g)} + H_2O \overset{H}{\leftrightarrow} H_2CO_3^*, \tag{2.9}$$

$$H = \frac{H_2CO_3^*}{pCO_2} \tag{2.10}$$

where H is the Henry constant and pCO_2 is the partial pressure. In any carbonate solution, $H_2CO_3^*$ releases H+ to the solution leaving HCO_3^-, which further dissociate to CO_3^{-2} with one more released H+ to the solution as shown in Eq. (2.11).

$$H_2CO_3^* \overset{K_1}{\leftrightarrow} H^+ + HCO_3^- \overset{K_2}{\leftrightarrow} H^+ + CO_3^{-2} \tag{2.11}$$

Where K_1 and K_2 are the dissociati(on constants determined using Millero et al. [313] correlations shown in Eqs. (2.12 and 2.13).

$$pK_1 = -126.34048 + \frac{6320.813}{T} + 19.56822 \, Ln \, T \tag{2.12}$$

$$pK_2 = -90.18333 + \frac{5143.692}{T} + 14.613358 \, Ln \, T \tag{2.13}$$

2.4.3 Harvesting and biomass concentration

For further processing of microalgal biomass to biodiesel, after cultivation and lipid synthesis, a harvesting step which comprises of separation and dewatering of the algae cells is essential. Due to the microalgae small size (3–30 µm) [253, 314, 315] and cultures medium dilution, which is usually less than 1 g l^{-1}, microalgae need to be concentrated to simplify the lipid extraction step.

However, this recovery step is difficult and requires dewatering using suitable harvesting method [42, 243, 316, 317]. The selection of the appropriate harvesting method is of great importance to the economics of biodiesel production. This mainly depends on the selected strain characteristics such as cell density and size, and growth environment. Generally, harvesting small size and diluted cultures is a challenge, especially when microalgae cells that normally carry negative charges that does not allow self-aggregate within suspension [316] The harvesting step accounts for almost 20–30 % of the total production cost [116, 318]. Thus, for cost-effective production, efficient harvesting method is essential.

Generally, harvesting can be divided into a two-step process. The first step is that the biomass is separated and concentrated, usually by flocculation, from the bulk culture to 2–7 % dry weight [45, 319]. In the second step, cells are further concentrated using conventional harvesting methods to get 15-25% solids [319]. Table 2.13 summarizes the advantages and disadvantages of each harvesting method.

Table 2.13: Advantages and disadvantages of different harvesting methods

Method	Advantage	Disadvantage
Flocculation	▪ High recovery yield (up to 22 TTS[a]) ▪ Low energy requirement	▪ Flocculants may be expensive ▪ Contamination issue may occur ▪ Marine environment high salinity may inhibit the process ▪ Long process period
Centrifugation	▪ Reliable ▪ Easy cleaning ▪ Rapid	▪ Energy intensive ▪ Expensive ▪ Cannot be used for species <30 μm

Filtration	▪ Reliable	▪ Filters may need to be replaced
	▪ Able to collect species of low density	periodically
		▪ Membrane blockage
		▪ High maintenance cost
		▪ Slow

[a] total suspended solids

2.4.3.1 Flocculation

Flocculation is a process where dispersed cells are collected into aggregate to form large particles that facilitate their separation, by addition of chemical additives, called flocculants. A large number of chemicals have been tested as flocculants for microalgal flocculation, where aluminum sulfate and cationic polymers are the most effective [320, 321]. Although chemical flocculants can enhance the separation, the main reported problems facing the flocculation step are the high cost and toxicity of the flocculent, which needs to be avoided [320]. In this work, it has been only used to harvest *Nannochlorpsis* sp. cells due to their very small sizes, less than 3 μm.

2.4.3.2 Filtration

In this method algae media pass through filters, which retain the biomass and allow the liquid to pass through. Surface and depth filtration systems are the two known types of filtration [322]. Grima et al. [318] studied microalgae recovery using filtration and they found that filters that operate in vacuum are suitable to recover *Dunaliella* through sand filters. Larger algae can be efficiently separated by vacuum filtration, whereas micro-filtration or ultrafiltrations are effective in recovering smaller algae. However, these are costly and requires filter cleaning or replacements. A filter bag made mad of polyester with 2 μm pore

diameter was tested in this work with *Nannochlorpsis* sp. and it does not work due to their small size, and sticking on the surface, which requires an additional cellulose paper.

2.4.3.3   Sedimentation

Sedimentation is a technique that separates microalgae biomass based on gravity action and particle diameter. Generally, when the cells are small in size, the settling rate is low and flocculants addition will be necessary. Although this is a high energy efficient and low cost process, its reliability is very low [323].

2.4.3.4   Centrifugation

Almost all types of microalgae can be separated from the culture medium by centrifugation. A centrifuge is mainly sedimentation with an enhanced gravitational force, by centrifugation, that increases the rate of sedimentation. Biomass recovery depends on the biomass residence time within the centrifugal field, settling rate and distance [318]. Sim et al. [324] stated that centrifugation is the most effective harvesting process with more than 90 % separation recovery within few minutes. This can be rapid, but it is energy intensive, which make it not feasible at industrial scale. Nevertheless, this process is the preferred method of recovering algal cells [318, 319]. Currently, there is no low cost harvesting method for all strains. This technique is mainly used in this work to get faster separation.

2.4.4   Drying and dehydration

In biodiesel production, lipid-rich biomass with low water content is always required; therefore, microalgae drying has to be carried out. Following the

harvesting of the biomass, algal slurry moisture content has to be reduced to at least 10 % of the total weight by drying and dehydration. Several techniques have been employed, such as sun drying, spray drying, drum drying and freeze-drying. Among all, sun drying is the cheapest and easiest, although it takes a long time and requires a large drying surface area. On the other hand, spray drying can be used for high value products, although it is expensive and might cause significant deterioration of algae [318]. In contrast, freeze drying has been commonly used by many investigators due to the ability to break-up cells [325]. Belarbi et al. [326] reported that a freeze dried sample can be subjected easily for lipid extraction without any additional cell disruption. Therefore, this technique has been used in algae lipid extraction from various microalgae sources*; Isochrysis galbana* [327], *P. tricornutum* [328], *C. vulgaris* [329], *S. platensis* [330] and *Chlorella sp*. [331]. Additionally, drying at low temperatures keeps the proteins in the biomass leftover preserved for further uses, and eliminates any possibility of lipid degradation**. Table 2.14 summarizes the advantages and disadvantages of each technique. Nevertheless, drying is energy intensive and adds additional cost to the overall production cost. It reported to counts for 89 % energy input [332], and 70-75 % of total processing cost [58]. Thus, it is considered as a major bottleneck of microalgae based biodiesel production [333]. The selection of the proper method depends on the energy requirement, operation scale and the desired final product value.

Table 2.14: Comparison between common drying methods used in microalgae
processes

Method	Advantages	Disadvantage
Sun drying	▪ Cheap (no running cost, low capital cost)	▪ Slow ▪ Weather dependent ▪ Require large surface ▪ Contamination
Spray drying	▪ Fast ▪ Continuous ▪ Efficient	▪ Cost intensive ▪ Species deterioration (i.e. pigments)
Drum drying	▪ Fast ▪ Efficient ▪ Sterilization advantage	▪ Cost intensive
Freeze drying	▪ Gentle ▪ Efficient ▪ Adds cell disuption with drying	▪ Cost intensive

This conventional biodiesel production process from dried biomass requires high energy consumption in both the up and down-stream processes in order to get high quality biodiesel. Thus, a positive net energy from microalgae biodiesel could be obtained if wet extraction is used. It would be economically favorable to avoid the drying step while maintaining an effective lipid extraction from the wet biomass. Lardon et al. [334] provided an analysis of environmental impacts of biodiesel production from microalgae, where he compared the total energy balance from dried and wet *Chlorella vulgaris*. According to life cycle assessment results, to produce 1 kg of biodiesel from lipids extracted by *n*-hexane from dried biomass, the total energy balance was -2.6 MJ compared to 105 MJ when wet biomass was considered using same extraction technique. The high energy contribution of almost 85 %, based on their analysis, was attributed to the

drying step. From this point of view, lipid extraction directly from wet biomass slurry will be promising, and suggests testing the use of wet biomass.

2.4.5 Cell disruption

The recovery of intracellular lipids from microalgae is usually difficult due to the rigid, robust and tough cell walls of microalgae cells that hinder the extraction of the cells lipids [317, 335]. These cell walls are mainly composed of 24–74 % neutral sugars, 1–24 % uronic acids, 2–16 % protein, and 0–15 % glucosamine [336]. In addition, the presence of water in wet harvested biomass forms a film preventing the solvent from reaching the lipid, which further prevents efficient lipid extraction. Thus, pre-treatment of the biomass prior to the lipid extraction is usually required to enhance the lipid recovery [318, 337]. Cell disruption is one of such pretreatment methods to breakdown the cells to liberate the lipid and allow them to come into contact with the solvent or weakening the cell wall structure to facilitate the extraction. Generally, the disruption efficiency differs from species to species, and usually depends on the extraction method that will be followed. This is conventionally done using wet milling [338], ultrasonication [339, 340], bead-beating [49], microwaves [339], autoclaving at a high temperature and pressure, and osmotic disruption by treatment with sodium chloride [317, 341]. Among them, homogenizers and bed mills are often preferred because of their short residence time and lower operating costs [298]. Lee et al. [341] tested the performance of different pretreatment methods in lipid extraction from *Botryococcus sp.,C. vulgaris, and Scenedesmus sp* lipids extraction by the modified Bligh and Dyer method [47]. They found that the microwave oven and bead beating resulted in higher extraction efficiency

compared to autoclaving, sonication and osmotic shock. Contradictory observation was reported by the recent work of Surendhiran et al. [342], who tested the pretreatment effect on *Nannochloropsis oculata* lipid extraction, and observed the lowest extraction yield was from microwave treated biomass. All these mechanical processes however, are energy intensive and may affect the properties of the triglycerides causing downstream difficulties in their transesterification to biodiesel. In addition, mechanical disruption usually results in excessive heat generation, which requires cooling. Freeze drying has also been suggested [339], wherein harvested cells are lyophilized, resulting in dried powder, prior to lipid extraction. Lyophilization, however, is energy intensive process that may not be justified in energy production processes.

Another technique, which is a chemical method, is acid treatment [343]. Usually, this is performed by soaking the biomass in diluted acid, commonly sulfuric acid, and then heating it at high temperature for a certain time. In many cases, this is followed by alkaline addition, commonly sodium hydroxide, thus leading to pores swelling and decreasing in cellulose crystallinity. Although this process is efficient in lignocellulose degradation, sulfuric acid is toxic and corrosive, which makes this process not recommended, either for fuel production or for the left biomass applications.

For an effective lipid extraction, efficient cell disruption, mild extraction conditions, and leftover biomass utilization are essential. Some enzymes have the potential to facilitate cell disruption. They can operate at low temperatures with high selectivity and fewer side products. Utilizing enzymes for cell disruption is expected to enhance the efficiency of lipid extraction under mild conditions.

Operation under mild conditions is less energy-intensive and also has a minimum effect on the triglycerides structure or the leftover residual biomass that can be utilized in pharmaceutical, food and fuel applications.

Several lysis enzymes can be used, such as cellulose, that can effectively hydrolyze the cellulosic structure of the cell walls, and lysozyme that can hydrolyze the linkage between peptidoglycan residues in the cell walls. Specifically, it degrades polymers containing N-acetylglucosamine, which is a derivative of glucosamine, a major component of the cell wall. The enzymes have been tested on *Chlorella species* and outer cell wall disruption was observed [344-347]. The recent work of Surendhiran et al. [342], which compares the enzymatic disruption to mechanical disruption techniques showed comparable results to conventional disruptions.

Although several initiations were carried out for enzyme utilization, they have still not been studied extensively. In most studies the superiority of the enzyme uses are addressed, however, not compared to the conventional disruption techniques in term of method efficiency, and energy and cost effectiveness, which are very important for commercialization. In addition, all these works were aimed to enhance the cell disruption for a specific strain, which may not be applicable for other strains. The optimal disruption depends on many factors, such as the cell wall rigidity and the lipid content that depends on the cultivation conditions.

On the other hand, cells disruption is followed by organic extraction of lipid, which is usually carried out by organic extraction, which is time consuming and uses toxic chemicals, which makes them not preferable on a large scale. The

use of fast, non-toxic solvents, which allows the utilization of the spent leftover biomass will be advantageous.

2.4.6 Lipid extraction

During the extraction, the extraction solvent dissolves soluble lipids and extracts them out from the cellular matrix, which are then separated from cellular debris and converted to biodiesel. This is considered a long and challenging step due to high costs and energy requirements. Thus, various technologies have been suggested. It is worth mentioning that microalgae lipids usually contain polar lipids, fraction of and non-acylglycerol neutral lipids, that are not convertible to biodiesel. Thus, for an efficient extraction, the selected extraction solvent should display high selectivity toward acylglycerol neutral lipids, which can be converted to biodiesel with minimum extraction of unwanted compounds and cost. For chemical extraction of microalgal lipids, organic solvents and SCFs can be used.

Microalgae lipid extraction using organic solvents is the most commonly used methods. These solvents have a high selectivity and solubility toward lipids, in which intracellular lipids can be extracted through diffusion across the cell wall [76]. Briefly, the dried biomass is exposed to an organic solvent, which penetrates through the cell wall and interact with the natural lipids forming asolvent-lipid complex, which then diffuses out into the bulk organic solvent. Based on the promising results obtained from crops oil extraction, the most commonly used solvent and method are *n*-hexane and Soxhlet extraction, respectively. The use of polar solvents has been suggested as well to break down the lipid protein complex by forming hydrogen bonds with the polar lipids in the

complex [348, 349] that enhances the extraction yield. The common protocols are those reported by Bligh and Dyer [47] and Folch et al. [48] with a mixture of chloroform and methanol, and Hara and Radin [350] with *n*-hexane and *iso*-propanol mixture.

As mentioned earlier, microalgae can produce both neutral lipids, composed mainly of triglycerides, and polar lipids such as phospholipids, which commonly produced in the cellular membrane, whereas the former usually accumulates as droplets in the cytoplasm [236]. Using a solvent mixture is reported to be ineffective in extracting microalgal lipids, due to its ability to solubilize phospholipids which cannot be converted to biodiesel. The unsaturated fatty acids has low solubility in *n*-hexane [351], whereas the Bligh and Dyer method [47] was reported to be the most effective method, where high extraction efficiency were attained from several strains. The employment of this method is, however, an unattractive from an environmental point of view, as chloroform is a highly toxic solvent. Table 2.15 shows a summary of published works on microalgae lipid extraction using different methods.

Table 2.15: Lipid extraction yields from different microalgae strains using different cell disruption and extraction techniques

Strain	Extraction solvent	Cell disruption	% Yield	Reference
Botryococcus braunii	*n*-hexane: chloroform: methanol	freeze-dried	2.7	[352]
	SC-CO$_2$		11	[353]
Botryococcus sp.	chloroform:methanol = 1:1	autoclave	8	[341]
		bead-beater	11	
		microwave	28	
		ultrasonication	8.5	
		osmotic shock	10	
Scenedesmus dimorphus	*n*-hexane	bead-beater	30	[338]
Scenedesmus sp.	chloroform:methanol = 1:1	autoclave	4	[341]
		bead-beater	8	
		microwave	10	
		ultrasonication	6	
		osmotic shock	5.8	
	n-hexane	Soxhlet	0.8	[76]
		ultrasonication	0.9	
	chloroform:methanol = 2:1	-	2	
		ultrasonication	6	

Continued on next page

Table 2.15: Lipid extraction yields from different microalgae strains using different cell disruption and extraction techniques (cont.)

Chlorella vulgaris	chloroform:methanol = 1:1	autoclave	10	[341]
		bead-beater	8	
		microwave	10	
		ultrasonication	6	
		osmotic shock	8	
	SC-CO$_2$	crushed	13	[53]
Chlorella protothecoides	*n*-hexane	bead-beater	25	[338]
	chloroform:methanol = 2:1	magnetic stirrring	19.7	[354]
	n-hexane		2.5	
	chloroform:methanol = 2:1	ultrasonication	19.4	
	n-hexane		1.5	
Chlorococcum sp.	*n*-hexane	-	1.5	[355]
	n-hexane/*iso*-propanol	-	5	
	n-hexane	Soxhlet	7.5	
	SC-CO$_2$		7.1	
Pavlova sp	*n*-hexane	-	13.5	[356]
	n-hexane	bead-beater	15.3	
	SC-CO$_2$		10.4	
	SC-CO$_2$		17.9	

Continued on next page

Table 2.15: Lipid extraction yields from different microalgae strains using different cell disruption and extraction techniques (cont.)

Crypthecodinium cohnii	chloroform:methanol = 1:1	freeze-dried	19.9	[57]
	SC-CO_2		8.6	
	SC-CO_2		8	

Generally, these organic solvents are toxic and the extraction is usually carried out at high temperatures, which may destroy the sensitive compounds. In addition, the technique requires a long extraction time and high solvent consumption. They are also labor intensive, difficult to automate, and often produce large amounts of solvent wastes, which are usually bulky and require a post-processing [357]. Furthermore, contamination of the de-lipidated with traces of solvent is inevitable, which limits their further uses. With these drawbacks, it is of value to find an alternative solvent that is more environmentally friendly. Supercritical fluid extraction, SFE, has been proposed using the extraction solvent in its supercritical state.

2.5   SUPERCRITICAL FLUIDS TECNOLOGY

2.5.1   Technology description

SCFs are fluids at pressures and temperatures above their critical values, which are the highest temperature and pressure at which the vapor and liquid phases exist in equilibrium. When the supercritical phase is reached, separation between liquid and vapor phases disappears. This can be demonstrated from the phase diagram shown in Figure 2.5.
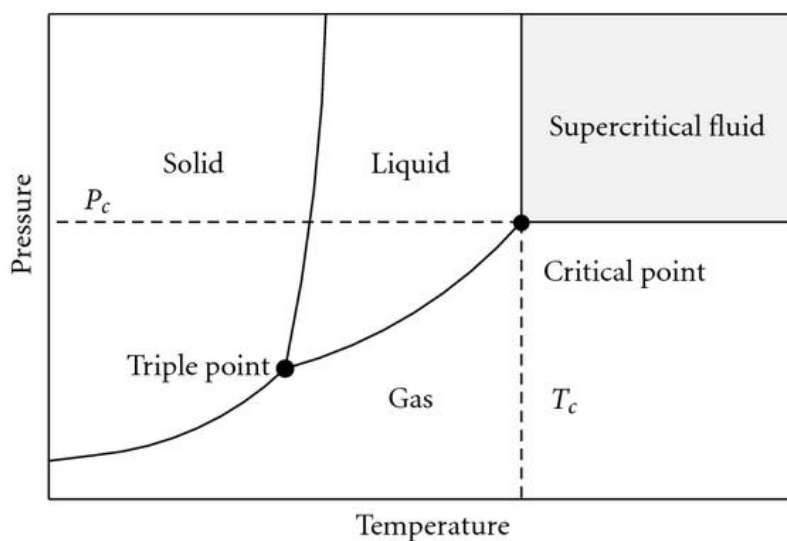
Figure 2.5: Pure component phase diagram [358]

As shown in the figure, there are three single phases, solid, liquid, and gas, where a substance may occur. If a mixture of two or more phases exists in these regions, a separation between the phases is distinct. Table 2.16 presents the values of the critical temperatures and pressures of substances commonly used as supercritical fluids.

Table 2.16: Critical data of some common solvents used in SCF sate [359]

Substance	Critical temperature (^{o}C)	Critical pressure (bar)
Xenon	16.7	59.2
Carbon dioxide	31.1	73.8
Ethane	32.4	49.5
Nitrous oxide	36.6	73.4
Chlorodifluoromethane	96.3	50.3
Ammonia	132.4	115.0
Methanol	240.1	82.0
Water	374.4	224.1

In the SCF region, the solvent displays physical properties which are intermediate to those of liquid and gaseous states. These properties can be easily

adjusted with simple changes in temperature and/or pressure. SCFs have more desirable transport properties than liquids and better solvent properties than gases, as can be seen in Table 2.17. The liquid-like density of the fluid gives high solvation power and facilitates the solute solubility, whereas the gas-like diffusivity gives excellent transport properties and increases the rates of solute mass transfer. Moreover, the low viscosity of the fluid gives rapid solvent penetration into a solid matrix.

Table 2.17: Physical properties of a gas, liquid and SCF [360, 361]

Property	Unit	State		
		Gas	SCF	Liquid
Density	$g\ cm^{-3}$	10^{-3}	0.3	1
Diffusivity	$cm^2\ s^{-1}$	0.2	10^{-3}	10^{-5}
Dynamic Viscosity	$g\ cm^{-1}\ s^{-1}$	10^{-4}	10^{-4}	10^{-2}

SCFs have been mostly used in extraction and chromatography purposes, where the lipid has received considerable attention, as a promising alternative to conventional solvent extraction. In addition, due to their interesting properties, they have recently been used for other applications, including reaction medium. Although a number of substances could serve as solvents, CO_2 is the most common. SC-CO_2 is inert under most conditions, and an inexpensive, non-toxic and environmentally friendly solvent [361, 362]. The critical temperature and pressure of CO_2 are 31.1 ^{o}C and 73.8 bar, respectively, which are not extremely high. Thus, SC-CO_2 has been identified as a good alternative for a number of applications including separation and reaction.

2.5.2   SC-CO$_2$: Extraction solvent

2.5.2.1   Process features

Distillation and use of organic solvent is the most common separation process operated in chemical industries. These types of processes are energy intensive and require large amount of solvents. If the separation can be carried out using a solvent that does not require separation, it will save energy. Among the common explored SCFs, SC-CO$_2$ has attracted considerable attention in lipid extraction, where the ability to extract the solute from a solid matrix depends mainly on the extract molecular weight and polarity. Near the critical point, CO$_2$ acts as a good solvent for non-polar to slightly polar solutes with low molecular weight [363]. In comparison with organic solvent extractions, no solvent residue remains in the extract since CO$_2$ is in a gaseous form at the ambient conditions, which allows its complete separation and results in solvent free extracts, simply by depressurizing. In addition, no oxidation or thermal degradation of the extracted lipids may occur. SC-CO$_2$ has been used to extract fats from meat samples to produce lean fat meat and high efficiency reaching 90 %, compared to Soxhlet extraction, which was achieved at 45 ^{o}C, 500 bar and 3 ml min^{-1}. The dried lean meat, after fat extraction, has longer shelf life, and when rehydrated it has similar characteristics to those of commercial low fat meats [364]. Thus, it has been considered as a better alternative to organic solvents.

Due to its obvious advantages, SC-CO$_2$ has been studied extensively for extracting essential oils [365, 366], vegetable oils [50-52] and animal fats [18, 35, 367] from various sources. In addition, it has been used to extract Astaxantine from *Haematococcus pluvialis* and Phycocyanine from *Spirulina maxima* [368],

β-carotene from *Chlorella vulgaris* [369] and lutein from *Chlorella pyrenoidose* [370]. It has been also tested to extract lipids from *C. vulgaris* [53, 54], *C. cohnii* and *C. protothecoides* [57], *Nannochloropsis* sp. [55], *S. platensis* [56], *Chlorococum* sp. [355] and *S. maxima* [54]. Table 2.18 shows the extraction yields of lipids from different strains using $SC-CO_2$, as compared to that of conventional solvent extraction. As shown, similar yields were reported when using $SC-CO_2$ and *n*-hexane for extracting lipids from *S. platensis* [56], *S. maxima* [54] and *Pavlova* sp. [356]. However, 25-40% lower yields were reported when comparing $SC-CO_2$ to *n*-hexane and acetone extractions, from *C. vulgaris* [53]. A lower yield was also reported when comparing $SC-CO_2$ and ethanol extractions from *S. maxima* [54]. However, other studies showed a better performance than *n*-hexane from *Chlorococum* sp. and *Nannochloropsis* sp. [55, 355]. The lipids were extracted from dried biomass in a temperature range of 40-80 °C and pressure range of 100 – 550 bar. The lower extract yield was due to the low lipid content of grown biomass.

Table 2.18: Comparison of $SC-CO_2$ performance and other conventional extraction solvents on lipids extraction yields from microalgae biomass

Microalgae species	$SC-CO_2$	Other conventional solvents			Reference
		acetone	ethanol	*n*-hexane	
C. vulgaris	13.3	16.8	-	18.5	[53]
Nannochloropsis sp	25	-	-	23	[55]
S. platensis	7.8	-	-	7.7	[56]
Chlorococum sp	5.8	-	-	3.2	[355]
S. maxima	2.5	4.7	5.7	2.6	[54]
Pavlova sp	17.9	-	-	18.5	[356]

Extracted lipid is a mixture of mainly TAG, FFAs and other minor components such as carotenoids, sterols, and squalene. The solubility of the lipid

depends on SC-CO$_2$ density and solute properties such as polarity and vapor pressure, where lipid components are soluble to different extents, depending on the temperature and pressure conditions [371]. Santana et al. [353] studied the effect of temperature, in the range of 50-80 ^{o}C, and pressure, in the range of 200-250 bar, on lipid extraction from *Botryococcus braunii.*

On the other hand, the use of non-polar CO$_2$ sometimes faces difficulties. To further enhance the SC-CO$_2$ extraction yields, the use of a co-solvent has been suggested to change the polarity SC-CO$_2$ and increase its solvating power towards lipid extraction. Methanol has been widely used with to extract nimbin from neem seeds [372], cocaine from human hair [373], and pennyroyal essential oil [374]. With microalgae lipids, so far, 10 % ethanol has been added to extract *S. maxima* lipids [375]. By doing so, the extraction yield increased by 24% from 2.5 % to reach 3.1%. This enhancement was explained by ethanol destruct effect on microalgal cellular walls.

As mentioned earlier, most lipid extractions were carried from lyophilized biomass, which is an energy intensive step. The use of enzymatically disputed biomass is advantageous. However, this has never been tested before with SC-CO$_2$. In addition, the success in extracting lipids from wet biomass using SC-CO$_2$ avoids the high organic solvent consumption and time consuming drying step. Moreover, the utilization of the spent leftover biomass in useful applications, or its conversion to a valuable product will add further enhancement to the overall algae biodiesel production process.

2.5.2.2   Extraction optimization

As mentioned earlier, the extraction yield and the characteristics of the extracted lipids are affected by several parameters, such as sample pre-treatment, extraction temperature, pressure and SC-CO_2 flow rate. The selection of the optimum condition for an efficient and cost effective process is not an easy task and needs screening experiments to develop reliable models with simplified assumptions. This is required to scale up processes from laboratory to pilot and industrial scales

The thermodynamic conditions of temperature and pressure, which affect the fluid density, are the main factors affecting the extraction process. Generally, it is well known that the extraction yields increase with the increase of pressure at fixed other factors due to the fact that the fluid density increases with the increase in pressure. However, there are opposite effects of temperature, where the increases in temperature results in a reduction in fluid density and, hence the extraction yield. However, one the other hand this may increase the solute vapor pressure resulting in enhanced solubility and yield. These two competing effects have same effectiveness at the crossover pressure, where the temperature does not show any influences. At lower pressure than the cross over pressure, the change in density is predominant whereas at higher pressures the vapor pressure effect is the predominant.

The flow rate effect is commonly used to determine whether the extraction is solubility and retention time controlled or diffusivity limited. The extraction rates that are controlled by the solubility show direct correlation with the flow rate, whereas the other shows no change in different flow rate. In

addition, the yield can be increased by using small particles when the diffusion is controlling the process, as the specific area increases. However, this is not always the case, as small particles may decreases the fluidized bed velocity causing channeling.

A.   Statistical modeling for conditions optimizations

Processes conditions optimization is usually assessed by altering one process variables while others are kept at constant value. However, this approach which is usually called as one-factor-at-a-time is unable to determine the interaction between process variables [376]. Therefore, experimental designs were proposed. In addition to interaction effect consideration, the design of experiments has the power to test the method robustness [377, 378].

As mentioned earlier, many factors may affect the extraction process and some of them do not have a significant effect. To overcome this, the optimization is usually carried out after the screening to determine the significant factors, which is important to minimize the large numbers of experiments. Among these designs are the full and factorial and Plackett–Burman designs are usually used for factors screening, whereas central composite, taguchi, and Box–Behnken designs for optimization. MiniTab, SPSS and other statistical softwares with design of experiment and process optimization packages are usually used. The most common technique in optimization is the response surface methodology (RSM), which is a collection of statistical and mathematical techniques.

2.5.2.3 Mathematical modeling of SC-CO₂ extraction

Due to the high capital investment of supercritical fluid extraction, the development of a reliable mathematical model to describe the process is needed to design and evaluate the scale up feasibility. In a packed bed extraction, first, the extraction fluid penetrates and diffuses into the solid matrix followed by the solute solubilization and movement from the solid matrix to the pores, and then diffusion inside the pores takes place and finally the fluid with the dissolved extract axially diffuses along the extraction bed

As the supercritical extraction in a mass transfer process with main transport mechanism through convection, the convective mass transfer coefficient is important and need to be determined to describe the process kinetic. Several approaches have been proposed for modeling the extraction, and each is based on certain postulations. They are mainly categorized into; empirical models, models based on heat and mass analogs and models based on differential mass balances. The empirical models that use exponential and hyperbolic correlations are the easiest; however they are not adequate for process scaling up, as they do not give any information of mass transfer, which is an important factor in large scale processes [279]. Bartle et al. [379] developed the hot ball model that was based on heat transfer analogy, where the extraction process is treated as heat transfer phenomena, in which all particles were considered spherical and equations covered by cooling down hot balls were applied to describe the solute concentration profile.

The most commonly used mass transfer models for process design and optimization are those based on a differential mass balance of the solute over a

control volume of the packed bed. Several differential mass balance models have been proposed to characterize the mass transfer kinetics. Among them, the model proposed by Sovova [380], which is based on extraction from broken and intact cells (BIC) is widely used in lipid extraction. In this model, the total available solutes are stored in the particle cells and protected by the cell wall. During the grinding step, to reduce the particle size and increase the surface area between the solute and fluid, some of those cells are broken, referred to by broken cells, and solutes become easily accessible to the fluid. These easily accessible lipids in the cells are denoted as x_p. The remaining lipids retained within unbroken cells, are referred to intact cells and defined as x_k. Thus, the extraction has been considered to be controlled by the internal and external resistances. Although, Sovova proposed a more complete model with additional parameters considering the equilibrium relationships in 2005 [381]. This modified model has not been widely used, due to its complexity, and most published works continued to use the old model with mass transfer coefficients in the fluid (k_f) and solid (k_s) phases, and x_k as the main fitting parameters. The commonly considered simplifying assumptions in this model are;

- Isothermal and isobaric process conditions
- Constant physical properties of SC-CO_2 during the extraction
- Uniform fluid velocity during the extraction
- Uniform initial lipid content and particle size distribution
- Constant bed porosity
- Negligible axial dispersion
- Negligible accumulation of lipids in SC-CO_2

The extraction process is divided into three periods, namely the constant extraction rate, falling extraction rate and diffusion periods [380]. In the first period, the easily accessible solutes are extracted at constant rate until the particles at the bed entrance lose all their accessible solutes. At this time, the diffusion extraction of the entrance part of the bed starts, combining with convection extraction of the rest of the bed. This results in continuing the extraction for broken cells, beyond the bed entrance, and at the same time extraction of cells starts in the bed entrance, and the rate of extraction decreases. At the end of this stage, all of broken cells are extracted and only the intact cells are there, thus the extraction become diffusion controlled. According to this, the simplified mass balances of the fluid and solid phases can be described by Eqs. (2.14 and 2.15), respectively.

$$u_{CO_2} \frac{\partial y}{\partial h} = \frac{j(x, y)}{\varepsilon} \qquad \text{for } 0 \leq h \leq H \qquad (2.14)$$

$$\frac{\partial x}{\partial t} = -\frac{j(x, y)}{(1 - \varepsilon)} \frac{\rho}{\rho_s} \qquad \text{for } t > 0 \qquad (2.15)$$

Where u_{CO_2} is the interstitial velocity of SC-CO_2, h and H are the axial coordinate and bed height, respectively, x and y are the concentration of the solute in the solid and SC-CO_2 phases, respectively, ε, ρ, and ρ_s are the bed porosity, SC-CO_2 density and solid density, respectively

For the solvent free solute at the entrance of the extraction bed with solids having the same initial solute concentration, the initial and boundary conditions are;

$$x_{(h,t=0)} = x_o \qquad (2.16)$$

$$y_{(h,t=0)} = y_{(h=0,t)} = 0 \qquad (2.17)$$

$$x_{(h=o,t)} = 0 \qquad (2.18)$$

The mass transfer flux, j, in the first extraction period, which is controlled by the convection mass transfer, depends on the solute concentration in the solid phase and is expressed by Eq. (2.19), whereas the flux inside the particles ,which depends on the solute diffusion from the interior of the solid to the surface, is expressed by Eq. (2.20).

$$j(x,y) = k_f a_o (y^* - y), \qquad \text{for } x > x_k \qquad (2.19)$$

$$j(x,y) = k_s a_o \left(1 - \frac{y}{y^*}\right), \qquad \text{for } x \le x_k \qquad (2.20)$$

where y^* is the solute solubility in the SC-CO$_2$, k_f and k_s are mass transfer coefficients in fluid and solid phases, respectively, a_o is the specific surface area.

The analytical solution of proposed model of the extraction curve for each extraction period is presented in term of the amount of extract verces the specific amount of SC-CO$_2$ (q-dependent), concentrations of the initial lipid (x_o) and less accessible concentrations, and parameters Z and W. Equations (2.21-2.23) show the proposed analytical solution in each stage

In the first stage, where $q < q_m$

$$E = q \times Y^* \times [1 - exp(-Z)] \qquad (2.21)$$

In the second stage ($q_m \leq q < q_n$), the unbroken cells starts to be extracted

$$E = Y^* \times [q - q_m \times exp(Z_w - Z)] \qquad (2.22)$$

In the last stage, $q \geq q_n$

$$E = x_o - \frac{Y^*}{W} ln \left\{ \frac{1 + \left[exp \left(W + \frac{x_o}{Y^*} \right) - 1 \right]}{exp \left[W \times (q_m - q) \times \frac{x_i}{x_o} \right]} \right\} \qquad (2.23)$$

where,

$$q = \frac{m_{CO_2}}{m_{bed}}, \dot{q} = \frac{q}{t}, \text{ and } q_m = \frac{x_o - x_i}{Y^* \times Z} \qquad (2.24)$$

$$q_n = q_m + \frac{1}{W} ln \left(\frac{x_i + (x_o - x_i) \times exp \left(\frac{W x_o}{Y^*} \right)}{x_o} \right) \qquad (2.25)$$

$$Z_w = \frac{Z \times Y^*}{W \times x_o} ln \left(\frac{x_o \times exp[W \times (q - q_m)] - x_i}{x_o - x_i} \right) \qquad (2.26)$$

The parameters Z and W are dimensionless parameters proportional to the fluid and solid phase mass transfer coefficients, respectively, according to Eqs. (2.27 and 2.28)

$$Z = \frac{k_f a_o \rho_f}{[\dot{q}(1 - \varepsilon)\rho_s]} \qquad (2.27)$$

$$W = \frac{k_s a_o}{[\dot{q}(1-\varepsilon)]} \qquad (2.28)$$

where, E is the amount of extract, m_{CO_2} is the mass of passed SC-CO$_2$, m_{bed} is the mass of lipids free biomass, q and $\dot{q}$ are the specific mass and specific rate per unit time lipid free biomass, passing through the extractor, respectively. q_m and q_n are the q-values representing the time at which the extraction begins inside the particles and easily accessible lipids are is all extracted, respectively, and Z_w is a dimensionless axial coordinate between fast and slow extractions.

Several approaches have been suggested to model the solute solubility in SC-CO$_2$, which are the thermodynamic, empirical and experimental approaches. The thermodynamic models, are based on equation of state along with various mixing rules. The second approach is through empirical models such as the one suggested by Chrastil [382], given in Eq. (2.29).

$$Y^* = \rho^{k_o} \, exp\left(a + \frac{b}{T}\right) \qquad (2.29)$$

Where Y^* ρ are the lipid solubility and SC-CO$_2$ density in kg m^{-3}, T is temperature in K, and k_o is an association constant that describes the number of fluid molecules in the solvated complex formed between the solute and solvent molecules at equilibrium. a is function of the enthalpy of the solvation and vaporization and b is related to the molecular weight of the solute. However, this model has some limitations, where it is not valid over a wide range of temperature and for the solubility higher than 100-200 kg m^{-3} [383]. Thus, some modifications were suggested.

This equation (Eq. 2.29) was modified by Adachi and Lu [384] and dell Valle and Aguilera [385], given in Eqs. (2.30 and 20.31), respectively. Adachi and Lu [384] considered the association parameter to be density dependent, whereas dell Valle and Aguilera [385] considered that the enthalpy changes with temperature, while keeping the association constant independent on the density.

$$Y^* = \rho^{k_o + k_1 \rho + k_2 \rho^2} \, exp\left(a + \frac{b}{T}\right) \tag{2.30}$$

$$Y^* = \rho^{k_o} \, exp\left(a + \frac{b}{T} + \frac{c}{T^2}\right) \tag{2.31}$$

where k_1, k_2, b and c are parameters adjusted to the experimental data.

In these two methods, the solubilities are usually determined using variable volume view cell equipped with sapphire window for visual observations, Another experimental approach is low flow rate extraction, In this approach, the slope of the linear part of the extraction curve that represent the amount of extracted solute verces the amount of passed solvent.

Presenting the process model by a mass transfer correlation is common. This requires understanding the processes physical properties, namely the density and viscosity of the SC-CO_2 and the mass diffusivity of the lipids in SC-CO_2. Dimensionless numbers; namely Reynolds (Re), Schmidt (Sc), Grashof (Gr) and Sherwood (Sh) are the considered numbers. It has been reported that in supercritical extraction, the natural convection is not significant [386]. However, at very low Reynolds number, this assumption is not readily verified [387]. In this case, the Sh is function of Re, Sc and Gr as well.

Sherwood number is related to mass transfer, Reynolds number is related to fluid flow, Schmidt number is related to mass diffusivity and Grashof number is related to mass transfer by buoyancy forces due to the density difference between saturated SC-CO$_2$ with lipids and pure SC-CO$_2$. When natural convection is not significant, the Sh would be related to Re and Sc only, as in Eq. (2.32)

$$Sh_F = C_O \, Re^{C_1} Sc^{C_2} \qquad (2.32)$$

where, Re, Sc and Sh$_F$ numbers are defined by Eqs. (2.33-2.35), respectively, and C$_o$, C$_1$ and C$_2$ are the adjustable parameters.

$$Re = \frac{\rho u_{CO_2} d_p}{\mu} \qquad (2.33)$$

$$Sc = \frac{\mu}{\rho D_{12}} \qquad (2.34)$$

$$Sh = \frac{k_f d_p}{D_{12}} \qquad (2.35)$$

Table 2.19 shows examples of proposed mass transfer correlations for SFE when the forced convection dominant. In all correlations the appropriate power for Sc is 1/3 and Re is between 0.5 and 0.8. However, negative values of the exponents were reported by Mongkholkhajornsilp et al. [388].

Table 2.19: Common correlations for forced convection mass transfer at supercritical conditions

Correlation	Applicability	Reference

$Sh_F = 0.38\,Re^{0.83}Sc^{1/3}$	$2 \leq Re \leq 40$	[138]
	$2 \leq Sc \leq 20$	
$Sh_F = 0.82\,Re^{0.6}Sc^{1/3}$	$1 \leq Re \leq 70$	[389]
	$3 \leq Sc \leq 11$	
$Sh_F = 0.2548\,Re^{0.5}Sc^{1/3}$	$1 \leq Re \leq 70$	[390]
	$3 \leq Sc \leq 11$	
$Sh_F = 0.206\,Re^{0.8}Sc^{1/3}$	$10 \leq Re \leq 100$	[391]
	$Sc < 10$	
$Sh_F = 3.173\,Re^{-0.06}Sc^{-0.85}$	-	[388]
$Sh_F = 0.085\,Re^{-0.298}Sc^{1/3}$	-	[388]
$Sh_F = 0.135\,Re^{0.5}Sc^{1/3}$	-	[388]

When small particle sizes are used and the fluid flows against the gravity, both forced and natural convection become important and need to be considered. Churchill et al. [392] developed an equation combining forced and natural convection, as shown in Eq. (2.36).

$$Sh = \sqrt[3]{Sh_F^3 + Sh_N^3} \qquad\qquad (2.36)$$

where Sh_N represents the natural convection Sherwood number given by Eq. (2.37).

$$Sh_N = C_3\,(Gr\,Re)^{C_4} \qquad\qquad (2.37)$$

and Gr is the Grashof number defined in Eq (2.38), and C_3 and C_3 are adjustable parameters.

$$Gr = d_p{}^3 \, g \, \Delta\rho \left(\frac{\rho}{\mu^2} \right) \tag{2.38}$$

where, g is the gravitational constant, and $\Delta\rho$ is the difference in mixture density between the saturated SC-CO$_2$ with lipids and pure SC-CO$_2$, could be found using Peng−Robinson equation of state (Eq. 2.39) with a suitable mixing rules [393].

$$P = \frac{R\,T}{V - b} - \frac{a\,\alpha(T)}{V(V + b) + b(V - b)} \tag{2.39}$$

$$a = 0.457 \frac{R^2 T_c^2}{P_c} \tag{2.40}$$

$$b = 0.00778 \, \frac{R\,T_c}{P_c} \tag{2.41}$$

$$a = \sum\sum y_i y_j a_{ij} \tag{2.42}$$

$$a_{ij} = \sqrt{a_i a_j} \tag{2.43}$$

$$b = \sum y_i b_i \tag{2.44}$$

2.5.3 SC-CO$_2$: Reaction medium

SCF plays a great role in reactions which are limited by mass transfer diffusion. This is mainly due to the gas-like viscosities, liquid-like solvation powers and high diffusivities of the SCFs. The first attempt to use of SCF as medium in enzymatic reaction dated back to 1985 [25, 26]. The most commonly used enzyme in supercritical fluid media is lipase in hydrolysis, esterification, transesterification, and enantioselective resolution of racemic alcohols and acids reactions. The investigated SCFs for use as reaction media for enzyme-catalyzed

reactions are small compared to those for extraction. This is mainly due to the characteristic nature of the enzymes that may unfold and become inactive at elevated temperatures. However, the effect of pressure has been generally shown not to affect the immobilized lipase activity [394, 395]. Although, several substances served as media in enzymatic reactions, CO_2 is the most advantageous. This is due to the low critical temperature, which is compatible with most enzymes.

Generally, the gas-like diffusivity and low viscosity of the supercritical fluids enhances reactions rates by reducing the mass resistance between the reaction mixture and the catalyst. The major disadvantage of SC-CO_2 use is the fluid non-polarity. However, this has recently been enhanced by surfactant developments, which allow the dissolution of both hydrophilic and hydrophobic materials in CO_2. The high pressure that requires expensive special equipment; however, this be reimbursed by the enzyme recycle and continuous production.

As mentioned earlier, one of the advantages of SCFs is their tunability properties, hence the solvent power, by changing in the pressure and/or the temperature. Using SC-CO_2 as a reaction medium adds to the advantages of organic solvents in saving downstream processing cost, where product purification is not necessary. Since solubility is greatly influenced by fluid temperature and pressure adjustments, separation can be easily achieved by a pressure reduction where the product and enzyme do not dissolve at room temperature. This adjustable property of the fluid allows the design of a production process with integrated downstream separation of products and un-reacted substrates.

Promising results have recently been reported for the use of lipase with SC-CO_2 in the production of biodiesel from vegetable oils and animal fats. Kumar et al. [17] esterified palmitic acid with ethanol at a temperature range of 35 to 70°C in the presence of three different lipases under SC-CO_2. Their results showed that Novozym$^®$435 was the best catalyst with highest (74 %) yield. Similar observation was observed by Romero et al. [32] who esterified isoamyl alcohol in SC-CO_2 and *n*-hexane, with initial reaction rate being higher in SC-CO_2. Higher yields were reported using SC-CO_2 compared to *n*-hexane and solvent free system by Laudani et al. [30] using Lipozyme RM IM.

Although SC-CO_2 has been used as a reaction medium for enzyme esterification of FFA, limited work has been done on the transesterification. Oliveira and Oliveira [33] compared enzymatic alcoholysis of palm kernel oil using *n*-hexane and SC-CO_2 systems where they showed the highest conversion of 63.2% using Novozym 435. Rathore et al. [34] used the same enzyme to transesterify *Jatropha* oil in SC-CO_2, and the highest conversions were in a range of 60-70 %. On the other hand, Varma et al. [37] tested linseed oils with Novozym$^®$435 in SC-CO_2. Varma et al. [36] synthesized biodiesel from mustard and sesame oils using different acyl acceptors at 50°C for 24 h reaction. Their results showed that using mustard oil, conversion of roughly 70 % and 65 % can be obtained using methanol and ethanol, respectively. Slightly lower observation was obtained from linseed oils, where the highest yield of 45% and 35% in methanol and ethanol were obtained, respectively. Similar yield was obtained from animal fat at 50 °C, 200 bar, 4:1 molar ratio and 30% loading of lipase enzyme, after 24 h of reaction. On the other hand, using sesame oil a conversion

of round 55% was obtained from ethanol, whereas only 45% conversion was obtained with methanol.

Despite the advantages of using SC-CO_2 in oils and fats transesterification for enzymatic biodiesel production, to the best of the knowledge of the investigators of this work, such process has never been tested with any of microalgae lipids. Thus, the use of use SC-CO_2 in lipid extraction and transesterification of microalgae lipids is considered in this work. The use of SC-CO_2, as mentioned earlier, was limited for transesterification reactions, where relatively low yields, in the presence of Novozym®435, were obtained compared to organic solvents. Thus, in this work, further investigations are aimed to enhance the production yield.

2.5.4 Integrated extraction-reaction under SC-CO2

Recently, several studies tested the use of continuous substrates flow in a reactor, packed with immobilized lipase. These types of continuous reactors are popular due to their easy operation and product separation, continuous removal of inhibitory products and reuse of the enzyme [30]. In addition, bed regeneration could be achieved by washing with a proper solvent, such as *tert*-butanol. The continuous production process using SC-CO_2 and immobilized lipase has been reported by many investigators. Dalla Rosa et al. [396] investigated a single continuous reactor to produce ethyl esters from soybean oil. More recently, Ciftci et al. [397, 398] investigated the conversion from corn oil in a similar system. Lubary et al. [399] and Rodrigues et al. [400] used similar reaction process for ethyl ester production from milk fat and sunflower oil, respectively.

In all these studies, the substrates mixture was initially mixed in an agitation system and then fed into the enzyme bed by a high pressure pump. Therefore, the feasibility of such process may not be obvious due to the high pumping cost, despite the positive effect on reducing inhibition and easy product separation. A combined continuous process of extracting lipid from the biomass using SC-CO_2 and the use of the extracted lipid for biodiesel production in SC-CO_2 in one integrated system would be feasible. Due to SC-CO_2 advantages over conventional organic solvents, the application of the high cost SC-CO_2 process may be justified in oil extraction. However, its justification for biodiesel production may not be evident, despite its positive effect on reducing inhibition effects and easy product separation. Nevertheless, a combined continuous process of extracting oil using SC-CO_2 and the use of the extracted oil for biodiesel production using immobilized lipase in SC-CO_2 in one integrated system would be feasible. In this continuous process, the oil that is extracted from microalgae is already dissolved in SC-CO_2, and can be fed directly to the enzymatic bioreactor to produce biodiesel without the need for further expensive pumping. In this way, the attractive advantages of performing the reaction in SC-CO_2 media will be gained, avoiding at the same time the disadvantage of high pumping cost. This continuous process is proposed and tested in this work.

2.6   PERSPECTIVE FOR FURTHER RESEARCH

As mentioned earlier in this chapter, lipid production per hectare from microalgae (of only 30% by weight lipids) is ten times higher than the best oil crop. This seems to be the best approach to satisfy the global demands for biodiesel. However, due to the process's high energy and cost demands,

associated with the drying and extraction steps, such process is not commercialized yet. Thus, further studies have to be carried out to investigate the possible ways of enhancing the efficiency of the process involved in microalgae biodiesel production. The potential depends on several factors; including cells growth rate and lipid content. In addition, the ability of the microalgae to grow at elevated temperatures and in saline environments is a crucial factor.

Using $SC\text{-}CO_2$ for lipids extraction and transesterification to biodiesel instead of the conventional organic chemicals that require final product separation and purification will be advantageous in saving downstream processing cost, as the purification is not required. Due to its advantages over conventional organic solvents, the application of the high cost $SC\text{-}CO_2$ process may be justified in lipid extraction from microalgae, especially if the leftover biomass, after lipid extraction, is to be used in pharmaceutical or food applications. However, for biodiesel production is not evident, despite its positive effect on reducing inhibition effects and easy product separation. Nevertheless, a combined continuous process of extracting oil from microalgae using $SC\text{-}CO_2$ and the use of the extracted lipids for biodiesel production in a one integrated system would be feasible. In this way, the attractive advantages of performing the reaction in $SC\text{-}CO_2$ media will be gained, avoiding at the same time the disadvantage of high pumping cost.

CHAPTER 3: MATERIALS AND METHODS

3.1 MATERIALS

3.1.1 Strains and culture media

In this work, both freshwater and marine strains have been tested. The fresh water strains were *Chlorella* sp. and *Pseudochlorococcum* sp. obtained from a local marine research center in Umm Al-Quwain, UAE, and *Scenedesmus* sp. provided by Algal Oil Limited, Philippines. The marine strains were *Tetraselmis* sp. and *Nannochloropsis* sp., obtained from the local marine research center in Umm Al-Quwain, UAE. The selection of these strains was based on their availability on the day of inoculum collection. The freshwater strains were grown phototrophically in modified Bold Bassel medium (+3N-BBM) consisting of (mM): 8.82 $NaNO_3$, 0.17 $CaCl_2 \cdot 2H_2O$, 0.3 $MgSO_4 \cdot 7H_2O$, 1.29 KH_2PO_4, 0.43 K_2HPO_4, 0.43 NaCl, 1 (ml L^{-1}) of Vitamine B_{12}, and 6 (ml L^{-1}) of P-IV solution that consisted of 2 $Na_2EDTA \cdot 2H_2O$, 0.36 $FeCl_3 \cdot 6H_2O$, 0.21 $MnCl_2 \cdot 4H_2O$, 0.37 $ZnCl_2$, 0.0084 $CoCl_2 \cdot 6H_2O$ and 0.017 $Na_2MoO_4 \cdot 2H_2O$. Marine strains were grown in F/2 medium (32 ppt salinity) consisting of (μM); 880 $NaNO_3$, 36 $NaH_2PO_4 \cdot H_2O$, 106 $Na_2SiO_3 \cdot 9H_2O$, 1 (ml L^{-1}) of; vitamine B_{12}, biotin vitamin and thiamine vitamin solutions, and 1 (ml L^{-1}) of trance metal solution that consisted of (μM); 0.08 $ZnSO_4 \cdot 7H_2O$, 0.9 $MnSO_4 \cdot H_2O$, 0.03 $Na_2MoO_4 \cdot 2H_2O$, 0.05 $CoSO_4 \cdot 7H_2O$, 0.04 $CuCl_2 \cdot 2H_2O$, 11.7 $Fe(NH_4)_2(SO_4)_2 \cdot 6H_2O$ and 11.7 $Na_2EDTA \cdot 2H_2O$. The prepared media, excluding vitamins, were sterilized in an autoclave (Hirayama HV-50, Japan) at 121 ^{o}C for 15 min and cooled to room temperature prior to use.

In addition, a mixed culture of microalgae was obtained from Ras Al-Khaimah Malaria Center, UAE. This culture was segregated by serial dilutions followed by streaking on an agar medium surface, as shown in Figure 3.1 and incubated until colonies appeared. Individual dominant colony was isolated and inoculated into a sterilized liquid medium of +3N-BBM, and referred in this work by M.C. sp. Agar medium was prepared by mixing 2 % (wt %) of the agar nutrient (No. 1, LAB M^{TM}) with prepared +3N-BBM in 250 ml flask and dissolved by heating, followed by sterilization. The sterilized medium was then poured into a petri dish, which was followed by the algae streaking.

| (a) | (b) |
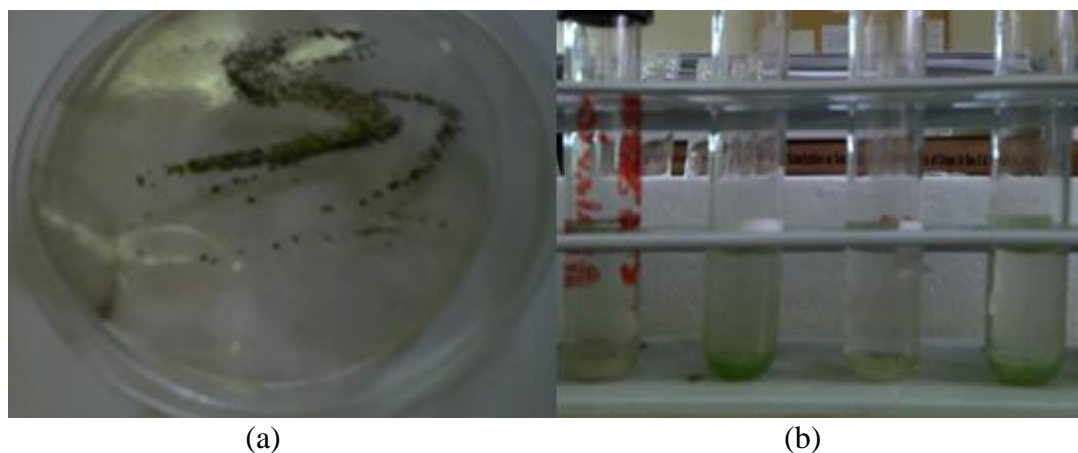
Figure 3.1: Photograph of; (a) streaked culture, and (b) sub-cultures colonies after two weeks of cultivation

For extensive lipid extraction experiments, 2 kg of sun-dried biomass of *Scenedesmus* sp. was provided by AlgaOil Limitted, Philippines. The provided biomass was cultivated in organic fertilizer (NPK, type 14 14 14), harvested by flocculation using potassium hydroxide and de-watered by sun drying.

3.1.2   Chemicals and reagents

n-Hexane (99 % assay), methanol (HPLC grade), acetone, sulfuric acid (95-98 % assay), sodium hydroxide (≥ 98 % assay), *tert*-butanol (99 % assay), chloroform (≥ 99.9 % assay), *iso*-propanol (≥ 99.5 % assay), ethanol (anhydrous

grade), HEPES (4-(2-hydroxyethyl)-1-piperazineethanesulfonic acid), 14 % boron tetraflouride- methanol mixture, sodium periodate ($\geq$99.8 % assay), acetylacetone ($\geq$99.8 % assay), glycerol ($\geq$99.5 % assay), Nile Red (9-diethylamino-5-benzo[α] phenoxazinone), and dimethyl sulfoxide (DMSO) were purchased from Sigma- Aldrich Inc., USA. Liquefied CO_2 (99.95 % purity) and hydrogen were supplied by Abu-Dhabi Oxygen Company, UAE. Ultra high purity helium and zero-air were supplied by Air Product Company, UAE. Standard mixture of high purity FAMEs, used for gas chromatography (GC) calibration and fatty acid compositional analysis, composed of (in wt %); 3.9 myristic acid methyl ester (C14:0), 9.9 palmitic acid methyl ester (C16:0), 6.0 stearic acid methyl ester (C18:0), 10 elaidic acid methyl ester (C18:1), 24.8 cis-9-oleic methyl ester (C18:1), 36.1 linoleic acid methyl ester (C18:2n6c), 1.9 linolelaidic acid methyl ester (C18:2), 2.1 arachidic acid methyl ester (C20:0), and 2.1 behenic acid methyl ester (C22:0) was obtained from Sigma-Aldrich Inc., USA.

3.1.3 Enzymes

Lysozyme from chicken egg white (activity > 40,000 U mg^{-1}) and cellulase from *Trichoderma longibrachiatum* (activity $\geq$ 1.0 U mg^{-1}) were purchased from Sigma-Aldrich Inc., USA, and stored below 8 $^{\circ}$C and above 0 $^{\circ}$C according to the supplier's instructions. Commercial lipase from *C. antarctica* (Novozym$^{\circledR}$435), with activity of 7000 U g^{-1} and 2% water content was obtained from Novozyms A/S, Denmark.

3.2   EXPERIMENTAL METHODS

3.2.1   Strains growth and productivity

3.2.1.1   Growth under different environmental conditions

Prior to any test, microalgal cells were first grown in 1 L of their corresponding sterilized medium for one to two weeks until sufficient turbidity was obtained. Photographs of the stock solutions are shown in Figure A.1, Appendix A. The examined strains were then inoculated into 250 ml Erlenmeyer flask at a ratio of 1:15 (v/v) with approximately 1×10^5 cells ml^{-1} and allowed to grow in a shaking water bath (Daihan Labtech, Korea) at 27 ^{o}C, 140 r min^{-1} with 150 ml sterilized medium, and exposed to 4 parallel white fluorescent light sources. The light sources were placed 22 cm above the culture surface to ensure that all cells were equally exposed to the light with 12/12 h light/dark photoperiod automatically controlled by 24 h timer (S2402, China). The light intensity was 136 μmol m^{-2} s^{-1}, measured from the culture surface using a light meter (model 472990, Extech Instruments, Massachusetts). Light was supplied in abundance and the culture was kept dilute enough to neglect self-shading, which allows ignoring the light effect on the photosynthesis and operating in the linear growth phase. Each culture was aerated by bubbling atmospheric air at a flow rate of 0.25 L min^{-1} controlled using calibrated mass flow controller (model MC-1SLPM-P-SV, Alicat Scientific, USA). Biological filter of 0.20 μm size (Nalgene, USA) and nickel valves were used to prevent any bacterial contaminations. The pH was maintained at 7.4 using HEPES buffering agent. Cell examination under 100X magnification was done to make sure that the

available strains were axenic and unicellular. These images of the cells can be found in Figure 3.2.

(a)   (b)   (c)

(d)   (e)   (f)
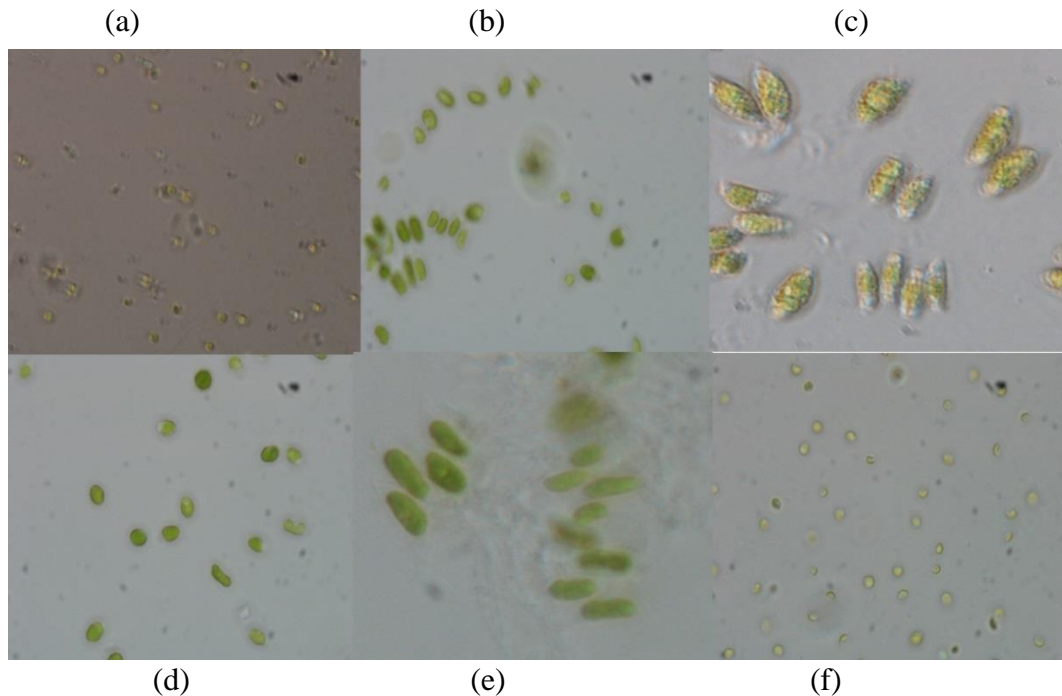
Figure 3.2: Cells cultures images under 100X magnifications

(a: *Chlorella* sp., b: *Pseudochlorococcum* sp., c: *Scenedesmus* sp., d: M.C. sp., e: *Tetraselmis* sp. and f: *Nannochloropsis* sp.)

The microalgae strains were allowed to grow for two continuous weeks and samples were collected daily to determine the cell concentrations. The ability of the strains to grow under different CO_2 enrichments were examined by growing under aeration with different CO_2 concentrations, ranging from ambient atmospheric air to 2% concentration. Air enrichments were obtained by mixing pure CO_2 with atmospheric air at specified concentrations using air and CO_2 mass flow controllers (model MC-1SLPM-P-SV, Alicat Scientific, USA). A photograph and schematic diagram of the experimental set-up are shown in Figure 3.3. Side views of the system can be found in Figure A.2

(a)
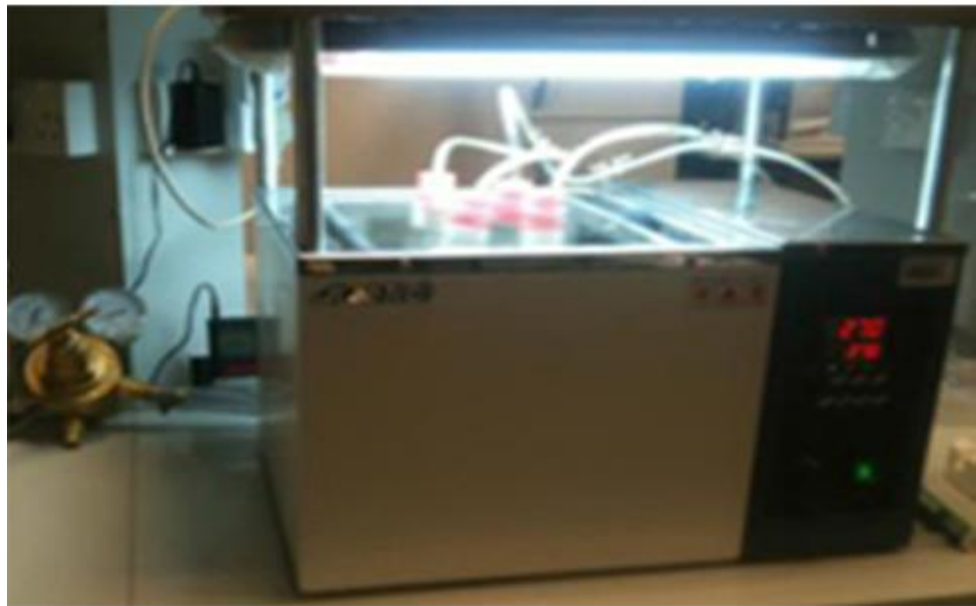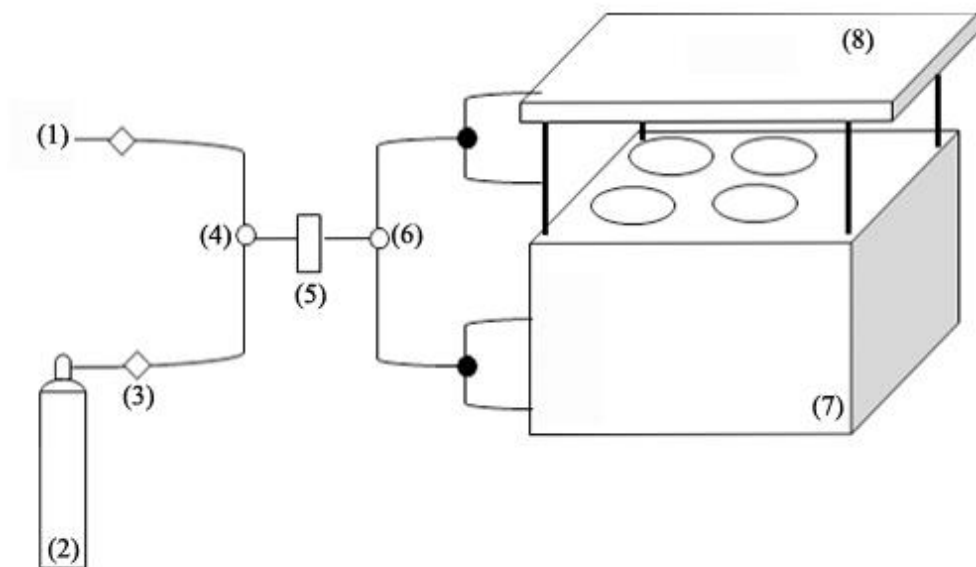
Figure 3.3: Photograph (a) and schematic diagram (b) of the 250 ml microalgae cultivation system used in the growth study

(1: air source, 2: CO_2 cylinder, 3: mass flow controller, 4: mixer, 5: filter, 6: splitter, 7: shaking water bath, and 8: lighting system)

To study the effect of nitrogen starvation, cells were cultured initially in a nitrogen sufficient medium (+3N-BBM for freshwater strains or F/2 for marine strains) for one week. At the end of the week, and while the cells were in their

exponential growth phase, the suspension was centrifuged at low speed of 3,000 r min^{-1} for 15 min using IEC CL31 multispeed centrifuge (Thermo Scientific, USA). The concentrated cells were then washed twice with distilled water and transferred to the pre-sterilized nitrogen-deficient medium (-N-BBM or -N-F/2) and allowed to grow for an additional two weeks. The nitrogen-deficient medium had the same nutrients as controlled nitrogen-sufficient medium, but with nitrogen sources elimination. Cells were grown under the same conditions as for controlled medium at 27 ^{o}C, and different CO_2 concentrations. Samples were collected daily to determine the cell concentration. Further study on the starvation effect on both growth rate and lipid accumulation were carried out in 5 L photobioreactor and 320 L open pond using *Scenedesmus* sp. as described in section 3.2.1.2

To investigate the medium salinity effects on the growth rate and lipid content, the freshwater strain *Chlorella* sp. was cultivated at different NaCl concentrations (0.49, 230 ,460 and 680 mM). *Chlorella* sp. was selected among other examined strains due to its high availability and fast growth rate at controlled conditions. The high salinity of 680 mM was selected to simulate the seawater (35-40 ppt) conditions. Pre-determined NaCl concentrations were added to the controlled medium before the sterilization step. In addition, the temperature effect on *Chlorella* sp. growth and lipid content was also investigated. The temperatures of 27, 31, and 35 ^{o}C were tested at the different salinities at the optimum pre-determined 1% CO_2 enrichment.

3.2.1.2 Biomass production in 5L photobioreactor and indoor open pond

For an effective biodiesel production from microalgae, high biomass productivity and lipid content are important. These two factors are difficult to achieve simultaneously, as conditions favoring high biomass productivity usually result in low lipid accumulation, and vice versa. To overcome this, a two stage cultivation approach has been used with *Scenedesmus* sp. In the first stage, cells were allowed to grow in the nutrient-rich medium (+3N-BBM) for two weeks in a 5 L bubble column photobioreactor to enhance the biomass productivity, and in the second stage cells, while cells were in their exponential growth phase, the were transferred to a nitrogen-deficient medium (-N-BBM) for three weeks to enhance and monitor the lipid accumulation.

The microalgae was first grown in 200 ml of +3N-BBM placed in 500 ml Erlermenary flasks with filtered air bubbling at a constant temperature of 25 ± 1 ^{o}C under light intensity of 75 µmol m^{-2} s^{-1} with an initial cell concentration of 3.2×10^{4} cells ml^{-1}. After 11 days of growth, the culture was transferred to the 5 L photobioreactor, where the cultivation was carried autotrophically, with CO_2 naturally present in bubbled air through the system being the sole carbon source. The photobioreactor was illuminated with one 50 cm, 60 watts, white fluorescent light at a light intensity of 120 µmol m^{-2} s^{-1}, measured using the light meter under12 h light/dark photoperiod automatically controlled by the 24 h timer. The photobioreactor had an outer diameter of 10 cm, an inner diameter of 5 cm and 40 cm height. The temperature inside the photobioreactor was controlled by circulating water from acontrolled temperature water bath through the jacket surrounding the reactor. A photograph and schematic diagram of the

photobioreactor are shown in Figure 3.4. More photos can be found in Figure A.3.

(a)

(b)
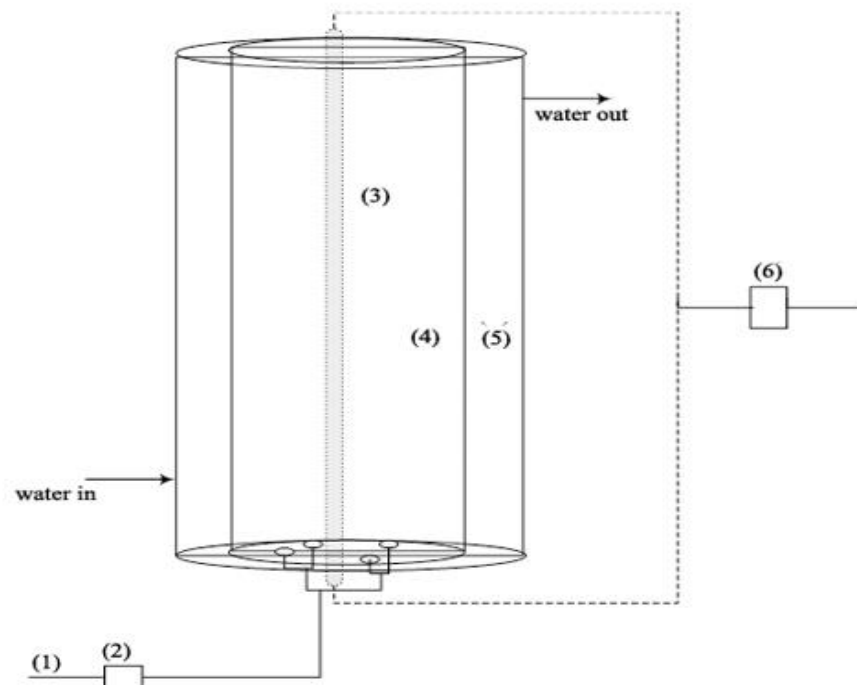
Figure 3.4: Photograph (a) and schematic diagram (b) of 5 L photobioreactor internally illuminated with white fluorescent light

(1: air source, 2: filter, 3: light source, 4: culture volume, 5: jacket, and 6: 24 h timer)

On day 14, while cells were still in their exponential growth phase, they were allowed to settle at the bottom of the photobioreactor, and were then collected and concentrated by centrifugation at low speed of 3000 r min^{-1} for 15 min. Concentrated microalgae cells were then cultivated back in a similar system in -N-BBM medium to enhance the lipid accumulation.

The lipids accumulations were monitored by staining constant cells concentration samples (1.5×10^6 cells ml^{-1}) with Nile Red that emits a yellow fluorescent signal in the presence of the natural lipid, and the fluorescents were visualized using fluorescence microscope (Olympus,USA). The Nile Red stock solution was prepared as described by Siaut et al. [401], by dissolving 0.1 mg of Nile Red in 1 ml acetone, and the solution was stored in the dark at 4 ^{o}C. Culture samples (500 µl) were placed in an eppendorf tube, span in a centrifuge (Sigma 113, Germany) for 30 s at 4,000 r min^{-1} and 410 µl of the supernatant were taken. DMSO (10 µl) was then added to promote the accessibility of Nile Red into the cells. The culture was then vortexed and 1 µl of Nile Red solution was added; followed by 20 min incubation in the dark. The lipid accumulations were then quantified using Multi-label Plate Reader (Perkin-Elmer, Boston) with black 96-well plates. Fluorescences were measured before and after Nile red staining and for Nile red stained −N-BBM medium. The intensity was considered after subtracting the stained medium and sample before staining intensities from the stained sample intensity at excitation and emission wavelengths of 485 and 590 nm, respectively.

The growth was also carried out in 320 L fiberglass indoor open pond (150 cm length, 80 cm width and 30 cm height) with a horizontal paddlewheel

agitating at 1400 r min^{-1}, used to mix the culture and run by a single phase electric motor (ML80B4, China). Lighting was supplied by a white fluorescent light tube of 202 µmol m^{-2} s^{-1} intensity, allocated 35 cm above culture surface and automatically alternated to 12/12 photoperiod using the 24 h timer. A photograph and top view of the pond are shown in Figure 3.5. More photographs can be found in Figure A.4

   Scenedesmus sp. was cultivated in sterilized +3N-BBM medium at room temperature for three continuous weeks, with 4.5 L inoculums collected from the photobioreactor. For sufficient lipid production, two-stage cultivation approach was also performed; where produced biomass was harvested after three weeks of cultivation by flocculation using 50 ml of 5M sodium hydroxide (NaOH) solution for each liter of culture. A photograph of the selected flocculants performance in enhancing the cells separation from the medium is shown in Figure A.5. Concentrated cells were washed with distilled water several times and re-cultivated in nitrogen deficient medium. In both stages, culture depth was maintained at 10 cm level, which corresponds to culture volume of 105 L.

(a)

(b)
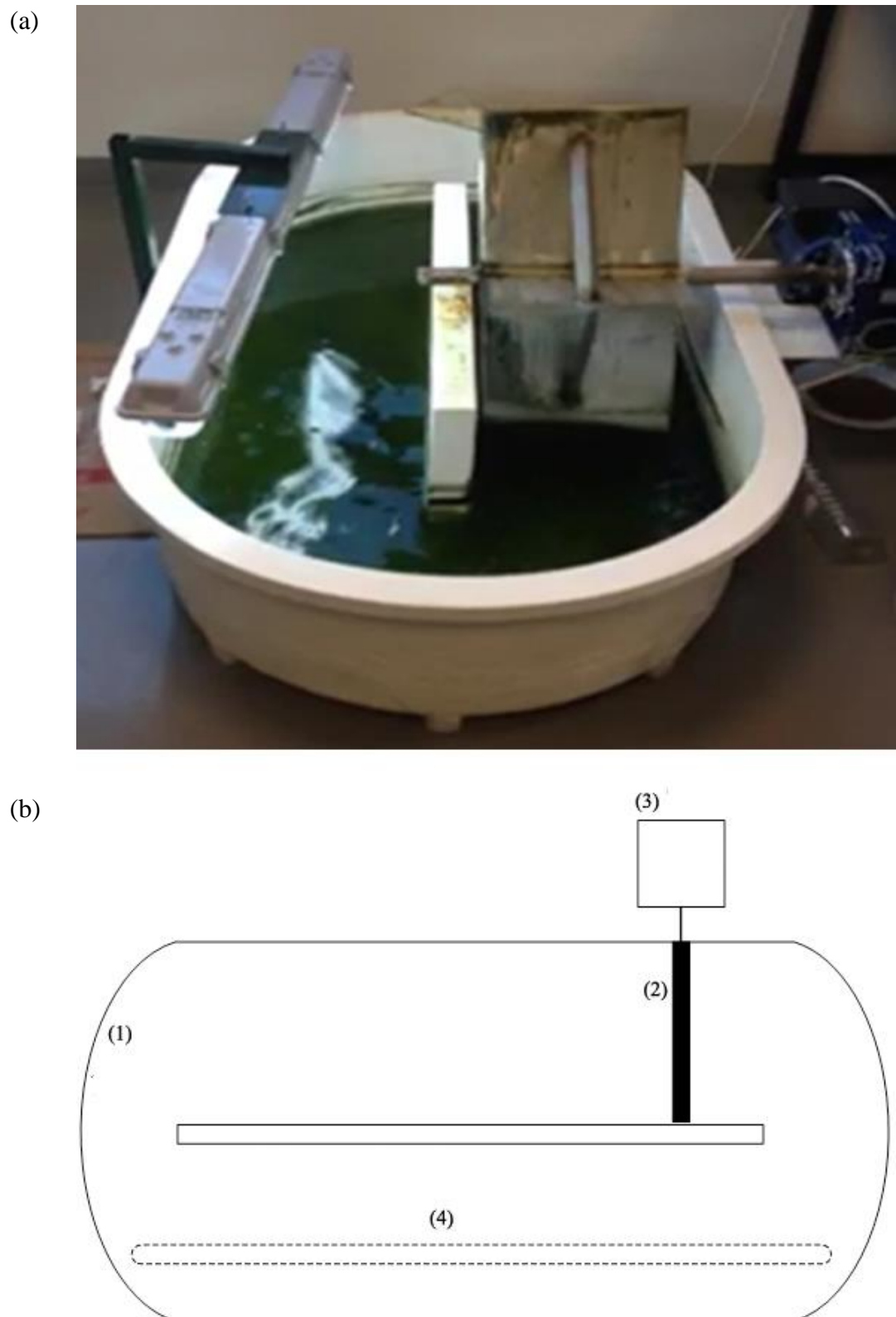
Figure 3.5: Photograph (a) and a top view (b) of used 320 L open pond supplied
with horizontal paddlewheel and a white fluorescent light
(1: Culture volume, 2: Paddle wheel, 3: Motor, 1: light source and 5: jacket)

3.2.1.3 Analytical methods

A. Cells concentrations

The cells concentration (cells ml^{-1}) of the culture was determined daily by measuring the optical density at 680 nm wavelength using UV-spectrophotometer (UV−1800, Shimadzu, Japan). The concentration at any given cultivation time was calculated from a pre-prepared calibration curve, shown in Figure (3.6a), between optical density at 680 nm and cell concentration determined using Neubauer Hemocytometer (PZO, Polandcountry), placed on a Nikon, Eclipse LV100 Pol microscope (Figure 3.7). For cell concentration determination by the cell counting technique, 0.1 mm deep hemocytometer was used. Two ml of the well mixed culture were diluted in 4 ml distilled water. This dilution step was repeated for several times, then 0.1 ml droplet of diluted samples was placed on a slide of 2.5×10^{-3} m^2, using pasteur pipette, and covered with 22×22 mm square cover slip. Cells were allowed to settle for 2 min and then the number of cells was counted in the four squares at the corner of the hemocytometer grid of four large squares of 1 mm^2 surface area. Figure 3.7 shows an example of the cell in the hemocytometer grid. Total cell concentration was then calculated, according to Strober [402] method using Eq. (3.1), from which the initial concentration was determined by multiplying the concentration with the dilution factor.
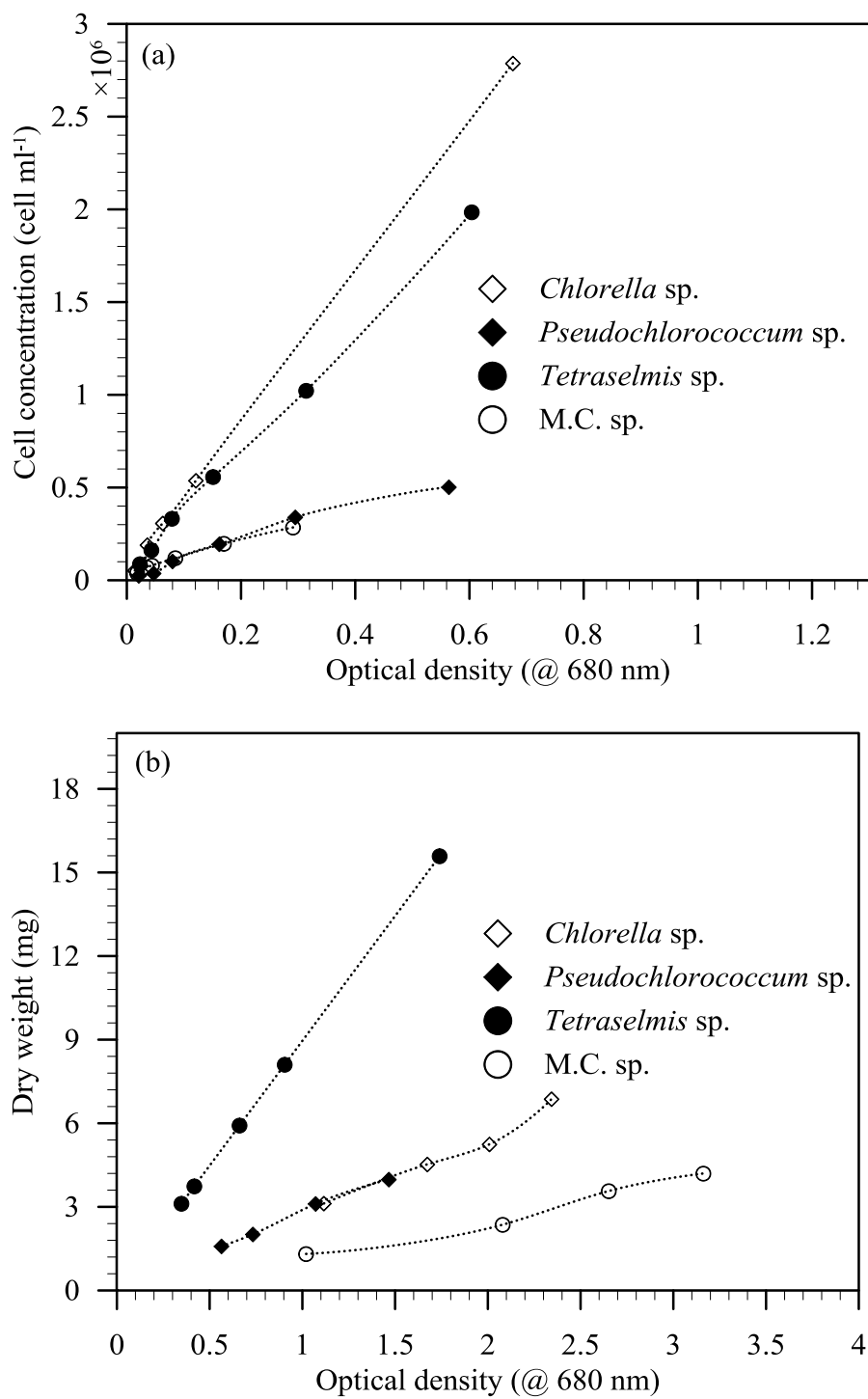
Figure 3.6: Correlations between; (a) cell concentration and (b) dry weigh and optical density at 680 nm
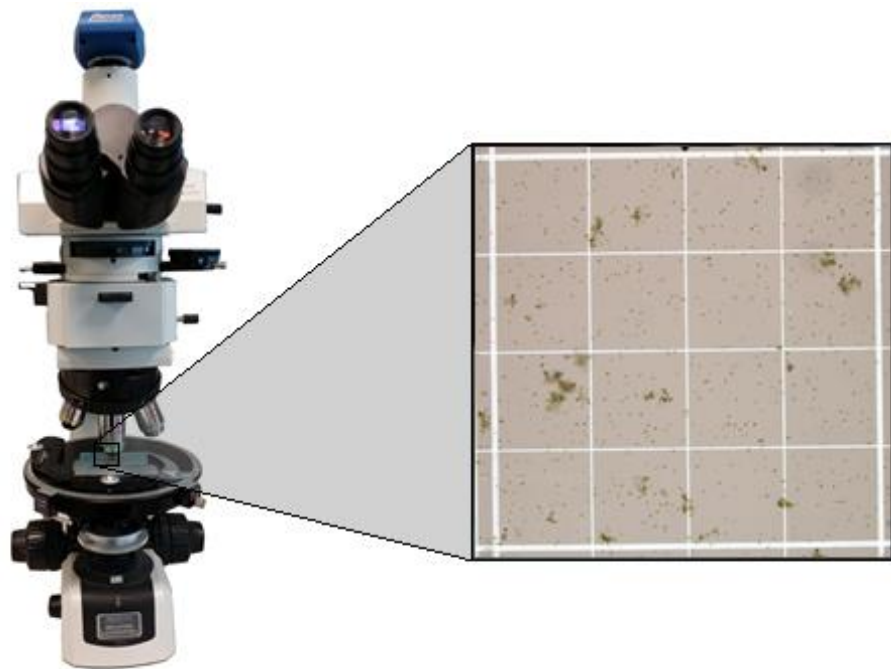
Figure 3.7: Photograph of used microscope use with an aenlargement of

hemocytometer grid

$$\text{Cell concentration (cell ml}^{-1}) \; = \frac{\text{Total counted cells}}{4} \times 10^4 \qquad (3.1)$$

The dry weight of algal biomass was also determined by filtering the algal suspension using a pre-washed and dried Whatman filter paper, dried overnight at 105 $^{\circ}$C in an oven (Memmert, Germany) until constant weight. A correlation between optical density and dry weight for each culture was generated, as shown in Figure (3.6b), and used in subsequent analysis for biomass concentration (g L^{-1}). Biomass productivity was determined from the slope of biomass concentration progress curve, whereas the specific growth rate was determined from the slop of logarithmic plot of biomass concentration over initial biomass concentration time progress.

B. Lipid content and productivity

At the end of each growth experiment, cells were harvested by centrifugation at 7000 rpm for 15 min, washed twice with distilled water, and lyophilized in a Telstar freeze drier (Spain), at -80 $^{\circ}$C for 6-8 h. This lyophilization step has the advantage of disrupting the cells in addition to drying, which enhances the lipid extraction. Lipid contents were determined by SC-CO_2 extraction in SFX-200 (ISCO, USA) system at 50 $^{\circ}$C, 300 bar and 1.5 ml min^{-1} for 90 min. Details about the extraction are found in section 3.2.4.2. The overall cell lipid productivity was calculated by multiplying the biomass productivity by lipid content.

C. CO_2 fixation rate

CO_2 fixation rate was calculated from the pre-determined carbon content and cells growth rate, as given by Eq. (3.2)

$$R_{CO_2} = P_M \times C_c \times \frac{M_{CO_2}}{M_C}$$
(3.2)

Where, R_{CO_2} (g L^{-1}d^{-1}) is the CO_2 fixation rate, P_M is the biomass productivity, C_c is the determined carbon content of the biomass, and M_{CO_2} and M_C represents CO_2 and elemental carbon molecular weights, respectively. Carbon content was determined by an elemental analysis using EURO Vector EA CHNSO Series 3000 elemental analyzer equipped with 18-6 mm packed reactor at temperature 980 °C; column: GC SS-2 m-6 ×5 mm.; oven temperature: 100 °C. The system was filled with; 1 cm Quartz wool, 10 cm Copper, 1 cm quartz wool , 4.5 cm Tungsten oxide , 0.5 cm Quartz wool, respectively from bottom to the top.

An L-cystine and sulfanilamide standards that contain 30 and 41.8% carbon contents, respectively, were used to calibrate the unit.

3.2.2 Biomass and extraction bed characterization

3.2.2.1 Chemical characterization

Prior to lipid extraction, untreated biomass were lyophilized using the Telstar freeze drier at -80 $^{\circ}$C for 6 h, and the moisture content was determined using moisture analyzer (Sartorius MA45-, Germany), to be 18.6 and 8% for the original untreated control and lyophilized samples, respectively. The protein content of the biomass was determined using the standard Kjeldahl method of nitrogen determination. The content was calculated from the measured total nitrogen using a conversion factor of 6.25. 1 gram of sample was digested with 15 ml of concentrated H_2SO_4 and 1 tablet of Selenium catalyst using a Kjeltec heating block digester unit (FOSS, 2020, Sweden) at 420 $^{\circ}$C for 1 h, followed by block cooling-down for 10 min and 20 ml of NaOH were then added. The nitrogen content of the digested sample were analyzed using Kjeltec Analyzer Unit (FOSS, 2300, Sweden) with automatic distillation and titration. The distillate was collected in 4 % boric acid solution containing an indicator and was titrated with 0.2N hydrochloric acid. The ash content of the sample was determined by weighting the sample before and after heating in a muffle furnace (Carbolite CWF 1200) at 550 $^{\circ}$C for 8 h. The crude fiber was determined by digesting 0.5 g of the sample in 0.255N H_2SO_4 followed by 0.313N NaOH with F57 filter bags using the Fibre Analyzer (Ankom 2000, US), according to the AOCS approved procedure Ba 6a- 05, and the total carbohydrate was calculated from the difference.

Thermal Gravimetric Analysis (TGA) was also used for proximate analysis. The test was carried out using Perkin Elmer thermal analyzer (USA), in which the biomass samples were heated under atmospheric nitrogen up to 875 ^{o}C with a heating rate of 10 ^{o}C min^{-1}, and the profile of percentage weight loss and its first derivative verses temperature were then obtained.

3.2.2.2 Physical characterization

Environmental scanning electron microscopy (eSEM) was used to investigate structure morphological changes due to the sample lyophilization step. Samples were dipped in Karnovsky's fixative at pH 7.2 and mixed on a rotamixer for 4 h at room temperature to preserve and stabilize their structure. After fixation, the specimens were washed twice for 15 min with 1 ml of 0.1 M phosphate buffer to remove excess fixative. The samples were recovered and post-fixed with 1 ml of buffered 1% osmium tetroxide and mixed for 1 h at room temperature on rotamixer, and then the osmium tetroxide solution was removed. Cells were washed with distilled water three times for 5 min and dehydrated through graded series of ethanol (30 % to 100 %). Samples were mounted on aluminum stubs, coated with gold layer and used for scanning using environmental Scanning Electron Microscope (Philip-XL30ESEM, Netherland) at an accelerating voltage of 18V.

Biomass was also grinded into small particles using AR1043 Moulinex grinder (China) for a short period of 15 s. Particles size distribution was then determined by sieve analysis (U.S.A. Standard Testing Sieves, W.S. Tyler Incorporated, USA), using three sieves of 355, 150 and 75 μm mesh size with 10 g sample, and used for average particle size determination. The distribution of the

particle sizes was as follow: 5.2 % > 355 µm, 46.7 % between 150 and 355 µm and 34.2 % > 75 µm.

For the evaluation of sieve analysis, Rosin-Rammler-Bennett distribution [403], shown in Eq. (3.3), was considered, in which the biomass retained on the sieves (R) were used to determine the distribution after normalization in respect to the total biomass weight.

$$R = 100 \, exp\left[-\left(\frac{d}{d_o}\right)^n\right]$$

(3.3)

Where, R is the percentage of sieve residue, d is the sieve screen size in mm, d_o is the average particle size in mm, corresponding to R=36.8% of the cumulative probability distribution, and n is the uniformity factor that controls the shape of the distribution function. The values of R were plotted verces the screen size and the particle size that corresponds to 36.8 of percentile of cumulative residue was considered the particle size diameter. The n value was determined by minimizing the sum of mean square errors using Solver tool in Excel. Table B.1 and Figure B.1 show the attained cumulative residue and screen size data. The bed porosity was determined using Eqs. (3.4 and 3.5).

$$\varepsilon = 1 - \frac{\rho_b}{\rho_s}$$

(3.4)

$$\rho_s = \frac{6}{s_v \, d_o}$$

(3.5)

where, ε is the porosity, ρ_s and ρ_b are the solid and bulk densities, respectively, and s_v is the specific surface area in m^2 g^{-1} obtained by the Dubinin-Radushkevich (DR) method using a Quantochrome Autosorb-1 volumetric gas

sorption instrument at 77.35 K for samples degassed at 150 ^{o}C for 1 h, and the specific surface area of the extraction bed (a_o) was determined using Eq. (3.6)

$$a_o = \frac{6}{d_{sv}}(1 - \varepsilon)$$ (3.6)

Where, d_{sv} is the surface area per unit volume evaluated using Eq. (3.7) after determining d_o and n values.

$$d_{sv} = \frac{1}{\frac{1}{d_o}\Gamma\left(1 - \frac{1}{n}\right)}$$ (3.7)

where, Γ is the gamma function evaluated using the exponential of the natural logarithm of gamma function.

3.2.3   Destruction of microalgal cells

In order to minimize the total production cost associated with high cell disruption and drying costs, wet cell biomass, shown in Figure A.6, were subjected to three different disruption methods, namely; (1) lyophilization (2) enzymatic disruption and (3) acid treatment. After getting a sufficient amount of biomass from *Scenedesmus* sp., cells were allowed to settle at the bottom of the photobioreactor, and were then concentrated by centrifugation at 3000 r min^{-1} for 15 min. Wet biomass was found to contain 0.068 g of solids per unit mass, which corresponds to 93 % water content. The lyophilization was carried out in the Telstar freeze drier operated at same conditions mentioned earlier. The enzymatic pre-treatments were carried as follow; 3.25 ml of 10 mg ml^{-1} of enzymatic (lysozyme or cellulase) solution was added to the wet biomass in the presence of 7.5 ml HEPES buffer solution (pH = 7.48). This corresponds to lysozyme and

cellulase loadings of 1.92×10^4 and 0.48 U mg^{-1} dry biomass, respectively, with 6.78 g l^{-1} biomass loading. The mixtures were then incubated in SI-300 shaker (Jeiotech, Japan) at 37 ^{o}C and 100 r min^{-1} for 30 min. The acid treatment was carried out by adding 1 ml of sulfuric acid (1 M) to the wet biomass and heating to 90 ^{o}C for 30 min in the shaking water bath (LabTech, DaihanlabTech Co. ltd., Koreas), followed by addition of 1 ml of sodium hydroxide (5 M) solution and further incubation at 90 °C for another 30 min [343].

3.2.4   Lipid extraction

3.2.4.1   Conventional organic extraction

Initially to assess the lipids extraction from microalgae biomass, conventional extractions from dried biomass were tested. Lipids were extracted from approximately 1 g of lyophilized biomass using pure *n*-hexane and solvents mixtures of different polarities in static extraction mode, where no continuous flow or circulation of the extraction solvent was employed. The tested solvents were *n*-hexane, chloroform/methanol/water (1:1:0.9), and *n*-hexane/*iso*-propanol (3:2). Protocols used for static solvent extraction were based on those reported by Bligh and Dyer [47], Folch et al. [48], and Hara and Radin [350] for the three solvents, respectively. Due to the lyophilization superiority in drying and disrupting cells, it was used exclusively in this part. Lyophilized biomass (containing 8 % water) were mixed with 40 ml of the solvent/mixture, ultra-sonicated for 30 min using Branson Sonifier 450 (Danbury, USA), and kept shaking horizontally in the LabTech shaking water bath at 150 r min^{-1} for 24 h. This was followed by centrifuging the mixture at 3,000 r min^{-1} for 5 min. In Chloroform/methanol/water test, the upper layer was removed and the lower

chloroform phase containing the extracted lipids was collected and transferred into a 30 ml tube. The solid material left at the bottom of extraction tube was extracted with the same procedure two more times. In the *n*-hexane/*iso*-propanol test, after shaking, 10 ml of water was added to induce biphasic layering. The *n*-hexane top layer was collected in a pre-weighed tube before it was heated to dryness in the oven at 60 ^{o}C. Whereas, when pure *n*-hexane was used, the solvent was evaporated after extraction.

Dynamic extraction was also tested using 75 ml of *n*-hexane in a Soxhlet apparatus (Lab-line instruments, Inc., Melrose Park Illinois, USA). Lyophilized biomass was placed in a cellulose thimble, which was initially dipped into *n*-hexane, so that the solvent diffused completely into the biomass. After 10 min, the thimble was subjected to the system that contained *n*-hexane at 80 ^{o}C for 12 h. It is worth mentioning that the ultra-sonication was not used in this test.

Static and Soxhlet extractions were also used when lipid extraction from wet biomass was tested. In the static mode, 30 ml of *n*-hexane was added to 1 g (containing 6.8 % solids) of the disrupted biomass; namely enzymatically or by sulfuric acid treatment and incubated in a SI-300 Benchtop Shaker at 50 ^{o}C and 100 r min^{-1} overnight. The wet samples had a water content of 93.2 % determined by drying a pre-weighed sample on a pre-dried Whatman filter paper overnight at 60 °C until a constant weight was reached. *n*-Hexane solvent was added directly to the treated sample, without removing the treating solutions. The mixture was then centrifuged at 3000 r min^{-1} for 5 min. The upper *n*-hexane layer containing the lipid was collected. The same approach was carried with lyophilized samples,

where lyophilized cells were extracted directly without any additional cell disruption step, as lyophilization can dry and disrupt cell.

Each extraction was performed at least in a duplicate and average values were considered with their respective measured uncertainties. The total lipids were measured gravimetrically, and then lipid yields were calculated according to Eq. (3.8).

$$\% \, Y = \frac{m_{lipid}}{m_{biomass}} \times 100 \qquad\qquad (\,3.8)$$

where m_{lipid} is the extract weight and $m_{biomass}$ is the subjected biomass to extraction.

3.2.4.2 Supercritical CO$_2$ extraction

SC-CO$_2$ extraction experiments were carried out in a 10 ml extraction cell using supercritical fluid extraction apparatus (ISCO, SFX 220, USA). The apparatus comprised of a syringe pump (Model 260D, ISCO, USA), heating chamber, an extractor with 10 ml stainless steel cell and a temperature controlled incubator. The pressure within the chamber was measured and controlled by the system and the flow rate was controlled manually using a micro-metering valve (HIP 15-12AF1-V). An Omega CN9000A thermocouple was connected to a scanning thermometer (Barnant , USA) to monitor the temperature on the surface of the valve. The maximum operating temperature, pressure and flow rate of the apparatus were 150 ^{o}C, 516 bar and 107 ml min^{-1}, respectively. To supply enough CO$_2$ to the syringe pump, the circulating water bath (Polystat, Cole-Parmer Instrument Company, Chicago) was connected to a heating coil surrounding the CO$_2$ cylinder was used. Figure 3.8 shows a photograph and

schematic diagram of the apparatus used. The dashed zoomed photo is an aenlargement of collected extract.

(a)

(b)
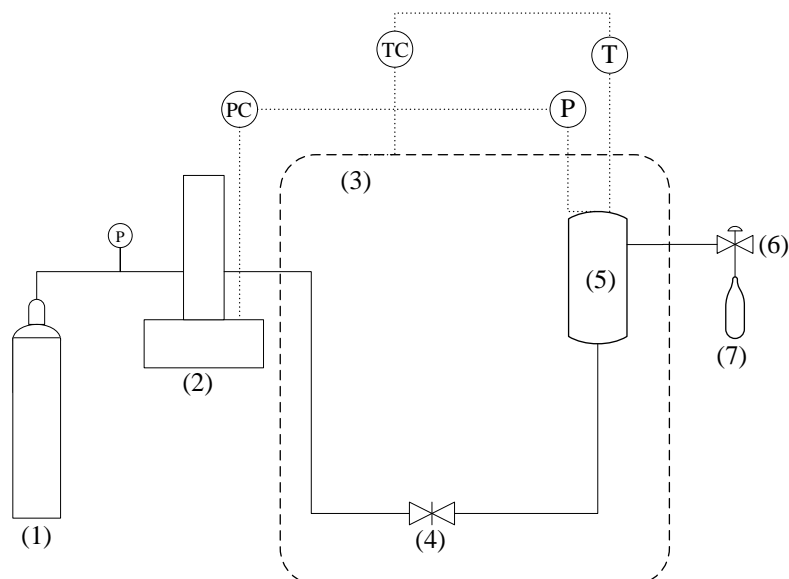
Figure 3.8: Photograph (a) and schematic diagram of supercritical CO_2 extraction apparatus used for lipid extraction

(1: CO_2 cylinder with dip tube, 2: Pump controller, 3: Temperature controller, 4: Pre-extraction valve, 5: Extraction cell, 6: Micro-metering Valve, 7: Extract collection vial)

In each experiment, approximately 3.0±0.06 g of the lyophilized biomass was placed in the extraction vessel with 5/8" filters placed at the top and bottom of the sample to prevent particles carryover. The extraction cell was placed in the heating chamber to maintain the temperature at the desired value. The system was allowed to equilibrate for 15 min before the extraction was followed by extract collection in a vial for every 5 ml of SC-CO$_2$ passed upward through the sample, and up to 120 ml, and weighed immediately after the collection using an analytical balance of 1×10^{-4} g precision (Model XB220A, Precisa, Switzerland). Extractions were conducted under pressures of 200-500 bar, temperatures of 35-65 ^{o}C and volumetric flow rates of 2-4 ml min^{-1}. The precision of temperature and pressure of the extraction system were ±0.1 ^{o}C and ±1 bar, respectively. It should be noted that the corresponding mass flow rates at each condition are function of the density, which in turn depends on the extraction temperature and pressure. The highest mass flow rate was 4.02 g min^{-1} at 35 ^{o}C and 500 bar, and the lowest was 1.38 g min^{-1} at 65 ^{o}C and 200 bar, resulting in a mean residence time in the range of 1.8 to 3.6 min.

The lipid solubility in SC-CO$_2$ was determined using the same SFX-200 extraction system at various temperature and pressure. Experiments were carried out at 0.5 ml min^{-1} flow rate with an equilibrium time of 15 min and the lipid solubilities were determined from the slope of the initial straight part of the overall extraction curve, represented as the amount of lipid extracted verses consumed SC-CO$_2$.

For sufficient extraction of lipids, a larger scale extraction cell was used. The system comprised of Teledyne ISCO syringe pump (Model 260D, USA), 120

ml high pressure extractor (740.5014-1-HM, SITEC Sieber engineering) with 60

ml cell, that holds 10 μm filter on both sides. The vessel used for extraction was

equipped with an electrical heating jacket, where the temperature was controlled

using a temperature controller (TC4S-14R, autonics) with Type K thermocouple

measuring the internal temperature. The temperature was also monitored by an

external Type J thermocouple, located at the surface of the vessel and connected

to the scanning thermometer. When both the desired temperature and pressure

were reached, the extraction started. Extracted lipids were separated through a

micro-metering valve (HIP 15-12AF1-V) wrapped with an electric heating tape

connected to a heater (Thermolyne 45500). Experiments were carried out in

duplicates at the optimum conditions, obtained from the 10 ml capacity cell. The

laboratory scale up was done by maintaining the bed height to diameter ratio the

same as those of the small scale. The 60 ml extraction cell has an inlet diameter

of 2.8 cm and a height of 9.2 cm; whereas the 10 ml extraction cell had an inlet

diameter of 1.7 cm and a length of 5.6 cm, which both resulted in a similar height

to diameter ratio of 3.3. In addition, solvent flow rate to biomass ratio used in the

60 ml was kept the same as that used in the 10 ml scale experiment, as suggested

by Prado et al. [404]. The weight of the sample used in this experiment was 25 g,

which is eight times larger than that used in the 10 ml cell experiment.

The SC-CO_2 extractions of wet biomass were conducted at a pressure of

500 bar, temperature of 50 ^{o}C and 2.88 g min $^{-1}$ that corresponds to 3 ml min^{-1}

flow of solvent in ISCO supercritical extraction unit (SFX-220, USA). Unlike in

the static *n*-hexane extraction, in the SC-CO_2 extraction, separating the wet

biomass from the enzyme solution, prior to extraction, was required. After the

incubation in the enzymatic solution for certain time, the sample was centrifuged

at 3000 r min^{-1} for 5 min. The supernatant was removed and the residual treated biomass was collected. The disrupted wet biomass was then placed in the 10 ml extraction cell with glass wool plugged in both extraction vessel sides to hold the sample in place.

Experiments were carried out in a random manner to minimize biases in the response, where at least each condition was carried out in duplicate, and the average values of the yield and uncertainties were considered. The extraction yield was calculated based on the cumulative mass of extract shown in Eq. (3.8). Since microalgae lipid contain large amount of polar lipids, the triglycerides content of extracted lipids were determined, as described in section 3.2.7.

3.2.5   Enzymatic transesterification of extracted lipids

3.2.5.1   Batch transesterification system

After collecting sufficient amount of lipids using the 60 ml capacity extraction cell, lipids were enzymatically transesterified to FAMEs. The transesterification reactions were carried out in a 10 ml reaction cell under SC-CO_2 medium. The reaction pressure was controlled by the Teledyne syringe pump (Model 260D, USA) with an electrical heating tape wrapped around the reaction cell and connected to a temperature controller (TC4S, autonics). The variation in temperature and pressure were ± 1 ^{o}C and $\pm$ 1 bar, respectively. Figure 3.9 and 3.10 show a photograph and schematic diagram of the apparatus used.

At each experimental condition, 0.8 g of extracted lipids were placed in the reaction cell with pre-specified amounts of Novozym$^{®}$435 and M:L molar

ratio. The cell was tightly sealed, heated up to the desired temperature and SC-CO_2 was then passed from the CO_2 cylinder into the high pressure syringe pump and pressurized to the desired pressure of 200 bar. The 200 bar pressure was used to avoid the negative effect of high pressure in enzyme activity. Once the desired pressure was reached, the reaction cell was filled with SC-CO_2 and the reaction was started. After a specified reaction time, the dissolved products in SC-CO_2 were eluted by depressurizing the cell through the micro-metering valve. Reaction products were diluted in 10 ml of *n*-hexane and taken for analysis to determine the FAMEs content using GC-FID. A preliminary study was first carried out to assess the enzyme loading effect on FAME yield (15-50 %). The optimum value was determined and then used in the following parametric study of temperature (35–55 ^{o}C) and M:L molar ratio (3:1-15:1). The operating conditions were optimized by carrying out a response surface methodology (RSM), as described in section 3.2.6. The production yield was determined using Eq. (3.9).

$$\% \, Y_{FAME,b} = \frac{m_{FAME}}{m_{lipid} \times R_{TG/L}} \times 100 \qquad (3.9)$$

where $Y_{FAME,b}$ is the batch production yield of FAME, m_{FAME} and m_{lipid} are the produced FAME determined by GC-FID and charged lipid, respectively, and $R_{TG/L}$ represent the triglycerides content of extracted lipids, which was determined from the GC quantitative analysis.
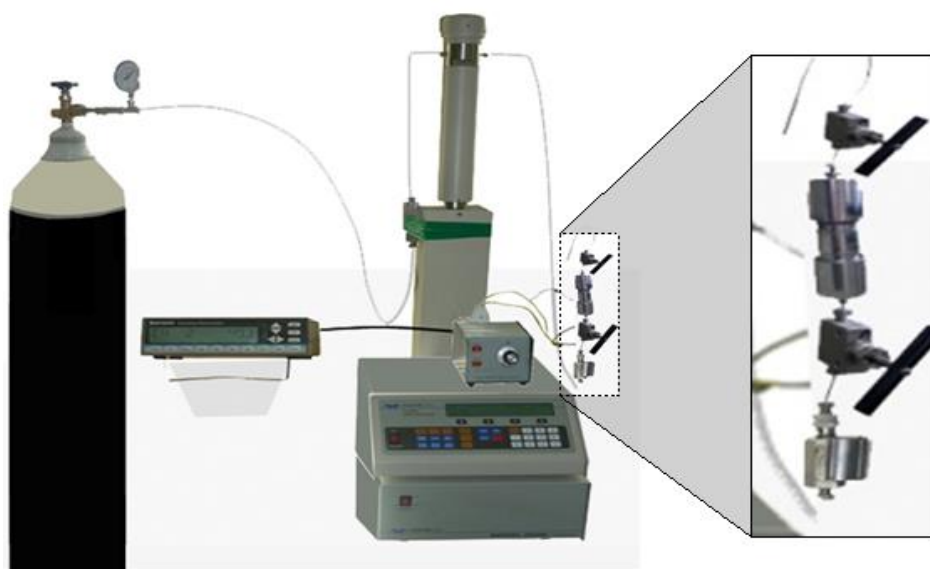
Figure 3.9: Photograph of the batch transesterification apparatus used for lipid conversion to biodiesel
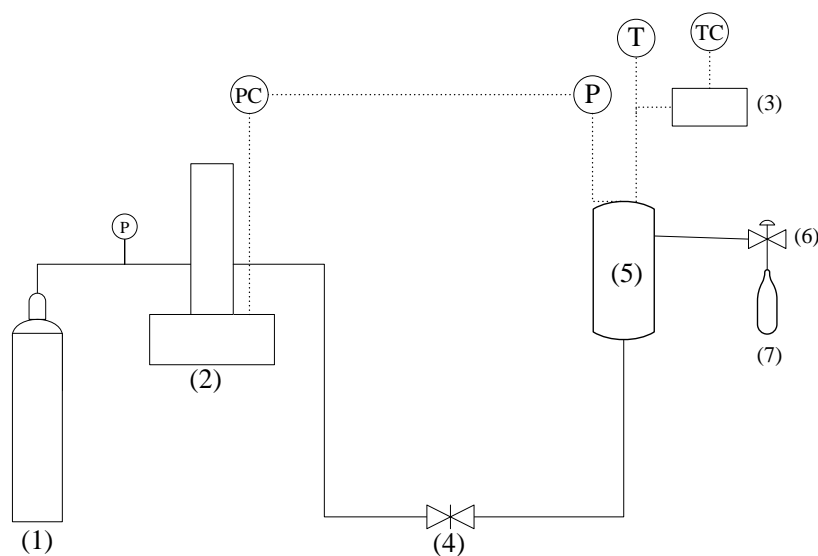
Figure 3.10: Schematic diagram of the batch apparatus used for lipid conversion to biodiesel

(1: CO_2 cylinder with dip tube, 2: Pump controller, 3: Temperature controller, 4: Pre-reaction valve, 5: reaction cell, 6: Metering-valve, 7: Collection vial)

3.2.5.2   Integrated semi-continuous extraction-reaction system

As explained earlier, in spite of the attractiveness of using SC-CO$_2$ as reaction medium, its commercial application is hampered by the high pumping cost. For an effective production of biodiesel, an integrated continuous process has to be used. The integrated system used in this study was a combination of extraction and reaction batch systems. Combining these two processes into a single process reduces processing cost, as the same medium of extraction and reaction is used, and the additional pumping costs are avoided. The optimum extraction and reaction conditions, determined from the separate batch experiments have been used, which were 50 ^{o}C and 200 bar. SC-CO$_2$ flow rate of 0.785 g min^{-1} that corresponds to 1 ml min^{-1} was used to ensure sufficient resident time in the reactor.

Figure 3.11 shows a schematic diagram of the integrated system. Supercritical fluid extraction unit (ISCO, SFX 220, USA), described earlier was used to extract lipids from the lyophilized biomass. 10 ml reaction cell, packed with 1.5 g of the enzyme, occupying 50 % of the reaction cell volume and supported with glass wools at both ends was used to transesterify extracted lipids. The CO$_2$ source was connected to ISCO-SFX 200 high pressure pump, and the pressurized CO$_2$ entered via the pre-extraction valve into the lipid extraction cell. Initially, extraction and reaction cells were sealed and pressurized at 200 bar. Then the product elution micro-metering valve was slightly opened to purge residual air in the cell and then closed immediately to maintain the pressure at 200 bar. The extraction cell, filled with 3 g of lyophilized biomass, was equilibrated for 20 min, and then dissolved lipids in SC-CO$_2$ were allowed to

flow out via the enriched stream micro-metering valve. The enriched lipid stream was mixed with a specified ratio of pressurized methanol–*tert*-butanol solution and the mixture then entered the packed bed bioreactor via reaction mixture valve. Methanol was diluted 32 times in *tert*-butanol to give the minimum 5:1 molar ratio at 1% modifier ratio, controlled via pump controller. The mixture then entered the packed reaction cell. The flow rate of dissolved products in SC-CO_2 emerged through product metering valve. The produced FAMEs were then separated from the CO_2 by depressurization and collected in 10 ml *n*-hexane in a volumetric. The effect of M:L molar ratios; in range of at 5:1 to 20:1 was studied by adjusting the modifier ratio in range of 1-4 %, respectively.
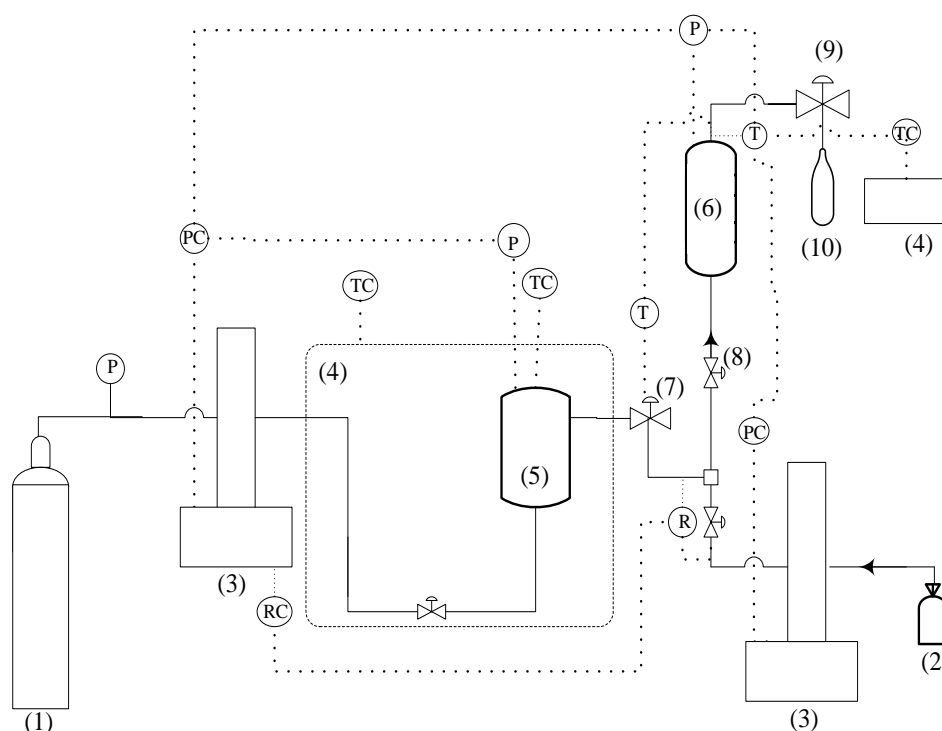
Figure 3.11: Schematic diagram of the integrated lipids extraction–reaction system used for continuous production

(1: CO_2 cylinder with dip tube, 2: Methanol-*tert*-butanol mixture, 3: Pump controller, 4: Temperature controller, 5: Extraction cell, 6: Reaction cell, 7:

Enriched stream metering valve, 8: reaction mixture valve, 9: product emerging valve and 10: Product collection vial)

After passing 80 ml of SC-CO$_2$, the lyophilized biomass was replaced with fresh new biomass, while keeping the same lipase in the reaction cell. This process was repeated six times to study the enzyme reusability and bed stability.

The production yield of FAME was determined from the ratio of pre-determined FAMEs production rate in each cycle to the lipid solubility in SC-CO$_2$, as given by Eq. (3.10). The lipid solubility in SC-CO$_2$ at 50 ^{o}C, 200 bar and 1 ml min^{-1} was determined experimentally from the slope of the initial linear part of the overall extraction curve, as described in section 2.5.2.3. The FAMEs production rate, in each cycle, was determined from the slope of cumulative FAMEs verses operation time.

$$\% \, Y_{FAME,c} = \frac{\dot{m}_{FAME}}{Y^*} \times 100$$

(3.10)

where, $Y_{FAME,c}$ is the continuous production yield of FAME in each cycle, $\dot{m}_{FAME}$ is the FAME production rate in mg min^{-1} and Y^* is the lipid solubility in SC-CO$_2$.

A further study was carried out to test the enzyme activity regeneration, in which the used enzymes after the six cycles, at pre-determined optimum M:L molar ratio of 10:1, were decanted and washed with *tert*-butanol and then reused again with fresh microalgae biomass in new batch under same conditions. *tert*-Butanol was selected as the washing solvent due to its ability to dissolve both methanol and glycerol, in addition to being an inert in the reaction, as lipase does not act on tertiary alcohols [22]. This process was repeated three more times and

the regeneration activity was determined based on the relative value of production rate in the first cycle of each batch to the rate in the first cycle were fresh enzyme was used, given by Eq. (3.11).

$$\% \, RA = \frac{\dot{m}_{i+1}}{\dot{m}_{i=1}} \times 100 \qquad\qquad (3.11)$$

where, RA is the regenerated activity due to *tert*-butanol washing, and $\dot{m}_{i+1}$ and $\dot{m}_{i=1}$ are the production rates in batches $i + 1 \, and \, i = 1$, respectively.

3.2.6 Experimental design and statistical analysis

To generate a relationship between the main responses; namely lipid extraction and FAMEs yields, with their process variables, an experimental design approach was carried out. Full factorial experimental designs (FFD) of three factors with three levels (3^3) and two factors with five levels (2^5) were employed in lipid extraction and FAME production, respectively. RSM was applied to evaluate the effects of temperature, pressure and CO_2 flow rate on the extraction yield and the effect of temperature and molar ratio on FAMEs production yield in batch systems. Independent process variables and their respective levels for both responses are listed in Tables (3.1 and 3.2). As mentioned earlier, these experiments were carried out at least in duplicate and performed in a random manner to eliminate the effect of unexpected variability and various types of biases in the response due to other extraneous factors. The average experimental data and measured uncertainties were considered. The measured uncertainty as for each experimental condition response was determined by considering the relative standard deviations of sampling and analysis as an estimate of standard uncertainty.

Table 3.1: Uncoded levels of independent variables used in the full (3^3) factorial design for lipid extraction

Independent variable	unit	Symbols	Key	Un-coded levels		
Temperature	^{o}C	T	X_1	35	50	65
Pressure	bar	P	X_2	200	350	500
Flow rate	ml min^{-1}	F	X_3	2	3	4

Table 3.2: Uncoded levels of independent variables used in the full (2^5) factorial design for FAME production

Independent variable	Unit	Symbols	Key	Un-coded levels				
M:L molar ratio	-	M:L	X_1	3:1	6:1	9:1	12:1	15:1
Temperature	^{o}C	T	X_2	35	40	45	50	55

A second order polynomial, defined in Eq (3.12), was used to express each process response as a function of the selected independent variables, and MiniTab 16 statistical software (MiniTab Inc.) was used for the statistical study. The analysis of variance (ANOVA) was employed to assess statistically the effect of the selected process factors and their interactions, using *F*-test and its associated probability,Whereas, *t*-test was performed to judge the significance of the estimated models coefficients. The test of statistical significance was based on the total error criteria within selected confidence level of 95%. The determination coefficient (R^2) and its adjusted value (adj.R^2) were used to evaluate the goodness of the fit to the regression model. In order to validate the model, an additional run at the optimum conditions, determined by the refined models, were carried out and then the experimental results were compared to

models prediction. Three dimensional surface response and contour plots were generated using sigma plot 10 (Systat Software, Inc.).

$$Y = a_0 + \sum_{i=1}^{n} a_i X_i + \sum_{i=1}^{n} a_{ii} X_i{}^2 + \sum_{i=1}^{n} \sum_{j=i+1}^{n+1} a_{ij} X_i X_j \qquad (3.12)$$

where, Y represent the responses, which are the lipid yield in extraction experiments and FAMEs yield in transesterification experiments, a_0 is a constant, $a_i a_{ii} a_{ij}$ are the linear, quadratic and interaction coefficients, respectively, n is number of factors, and X_i and X_j are the levels of the independent variables.

The cell pre-treatment experiments were conducted in random manner as well with at least duplicate treatments. The data were analyzed using one-way (unstacked) ANOVA followed by Fisher's Least Significant Differences (LSD), where p- values $\leq$ 5% (confidence level = 95 %) were considered.

3.2.7 FAME analysis

The fatty acids composition of the extracted lipid affects the properties of the produced FAMEs and their applicability to replace the petroleum fuel. The profile of extracted lipid was determined after rapid esterification to FAMEs using 14% boron tetraflouride–methanol mixture as described by Rule [405]. FAME were identified and quantified by GC-FID (Varian, CP-3800, USA), fitted with CP-Sil 88 FAME capillary column (100 m × 0.25 mm × 0.2 μm, Varian, USA), and equipped with auto-injector (CP 8410. Varian, USA). The oven initial temperature was 150 $^{\circ}$C during 1 min, and then increased to 220 $^{\circ}$C at 4 $^{\circ}$C.min^{-1}. Helium and zero air were used as the carrier gases with a split ratio of 40:1. Both

the injector and the detector temperature were set at 260 ^{o}C. FAMEs were identified by comparing their retention times with those obtained using the standard mixture. The TAGs contents of the lipids were determined from the total amount of produced FAMEs, which should be close to unity if 96-100 % of the TAGs contents were converted with the mentioned rapid esterification method. Similar analysis was carried out with produced FAMEs from reaction experiments. The production yields were determined from the weight percent of FAMEs produced divided by the lipid charged (in batch system) or flowed (in continuous system) to the bioreactor.

3.2.8   Fuel properties of FAMEs

The fuel properties of produced FAME were tested and compared to those of the commercial diesel fuel available at the petrol station (Abu Dhabi National Oil Company, UAE), and with those of ASTM and EN diesel standards. The determined properties were; density, kinematic viscosity, flash point, pour point, caloric value, acid value, and sulfur and free glycerol contents. The density and kinematic viscosity were tested at 40 ^{o}C using SVM300 Stabinger Viscometer (Anton Paar, Austria). The flash point, pour point and caloric values were determined using flash point analyzer (Stanhope Seta, England), Seta Cloud and Pour Point Cryostat (Stanhope Seta ltd, England) and bomb calorimeter (Parr Instrument Company, USA), respectively. The sulfur content was determined using Tanaka sulfur meter (RX-360 SH, Japan). The acid value was calculated by titration with KOH, and total free glycerol content was determined by spectrophotometric method [406]. Briefly in this analysis, a calibration curve between UV absorbance and glycerol standard solution was first prepared by

preparing a series of 0-2 ml standards and diluted them with solvent solution of 1:1 ratio deionized water and ethanol in a way to get a final volume of 2 ml in each tube. The final concentrations of glycerol were 0-18.75 mg kg^{-1}. 1.2 ml of sodium periodate (10 mM) was then added to each tube, shook and followed by the addition of 1.2 ml of acetylacetone (0.2 M). The solution was then heated at 70 ^{o}C in SI-300 shaker incubator for 1 min, and cooled down immediately by immersing in tap water at room temperature. The absorbance of the standards samples were read at a wavelength of 410 nm and the calibration curve was then generated. The same procedure was carried out with the fuel sample, and the absorbance was read against a blank sample contains no glycerol reference solution. The cetane number was calculated according to [407] using Eq. (3.13), .

$$CN = 46.3 + \frac{5458}{SV} - 0.225 \; IV \tag{3.13}$$

where CN is the cetane number, and SV and IV are the saponification and iodine values calculated, according to [408] from the chemical composition of produced FAMEs using Eqs. (3.14 and 3.15), respectively.

$$IV = \sum \frac{254 \; D \; A_i}{MW_i} \tag{3.14}$$

$$SV = \sum \frac{560 \; A_i}{MW_i} \tag{3.15}$$

where D, Ai and MWi are number of double bond, percent composition and the molecular weight of particular ester

3.3 KINETICS MODELS FITTING

3.3.1 Growth kinetics

In cell growth kinetics study, the experimental data of the specific growth rate in both nitrogen-sufficient and nitrogen-deficient media at tested CO_2 concentrations range (0.03 % to 2%) were modeled using Haldane model. As mentioned earlier (section 2.4.2.3), TIC was selected as the substrate. Obtained experimental results were fitted to the model equation (Eq 2.7) and the kinetics parameters were determined using Excel solver to minimize the objective function (OF) given by Eq (3.16), with a tolerance less than 10^{-5}.

$$OF = \frac{1}{m} \sum_{i}^{m} \left| \frac{Experimental - Predicted}{Experimental} \right| \tag{3.16}$$

where, m is the number of points used.

3.3.2 Extraction kinetics

The overall lipid extraction curve from the lyophilized biomass at specified condition was modeled using the Sovova model [380], given in Eqs. (2.21-2.23). The model parameters (Z, W and x_k) were determined by minimizing the errors between the experimental mass of the extract and the extracted mass calculated by the Sovova model using the OF shown earlier (Eq 3.16). The lipid solubility in SC-CO_2 at the specified operating condition was calculated using the pre-determined correlation (Eq. 2.29) established between the experimental solubility that was determined from the slope of the line in first portion of the extraction curve, SC-CO_2 density and process operating condition. A first guess

of the Z value was calculated from an empirical mass transfer correlation of Sherwood number presented in the work of Tan et al. [138] and shown in Table 2.19, which was then used to calculate the mass transfer coefficient in fluid phase, k_f, from which a new Z value was determined using Eq. (2.27). The bed characteristics necessary for the empirical correlation, namely d_p, ε and ρ_b were determined by the sieve, BET and gravimetric analysis, respectively and used to determine Reynold and Schemit numbers. The viscosity and density of the dissolved lipids in SC-CO$_2$ were assumed to be same as those for pure SC-CO$_2$, obtained from NIST chemistry database. In order to use the Solver tool in Excel, and to avoid the GRG non-linear algorithm of going beyond the solution range, x_o and q_m were restricted to be less than the highest amount of lipids extracted and SC-CO$_2$ per solute-free biomass utilized, respectively, in all tests.

3.3.3 Reaction kinetics

The initial reaction rates, expressed as the ratio of produced FAMEs per hour, were determined from the slope of the linear part of time course of FAMEs production. The effect of methanol mass concentration on the initial reaction rate was investigated by transesterifying fixed initial quantities of lipids with various initial concentrations of methanol at 50 ^{o}C. The kinetics parameters of the Ping Pong Bi Bi model were determined by the GRG non-linear optimization, as done with the growth kinetics and extraction models.

CHAPTER 4: RESULTS AND DISCUSSION

4.1   MICROALGAE PRODUCTION

Microalgae, as a source of lipid for biodiesel production, offer many advantages over traditional feedstocks, including their high growth rate and lipid content. The most important parameter to be considered for biodiesel production is the overall lipid productivity, which is a result of the biomass productivity and lipids content. For efficient biomass production, sufficient supply of the macro-nutrients (C, N and P) in dissolved form at optimal growth conditions is essential. For the photoautotrophic growth, the CO_2 supplementation as carbon source is required. In this work, air enriched with CO_2 has been used to supply excess CO_2. In addition to enhancing the growth rate, the growth under CO_2 enriched air has promising applications in CO_2 mitigation processes. The identification of a strain of high overall lipid productivity, CO_2 fixation rate and easy adaptation to the climate conditions such as high water salinities and temperatures could support the sustainable production of biodiesel.

In this work, the effect of growth condition and micronutrient concentrations on the biomass and lipid productivities were investigated in three different scales, namely 250 Erlenmeyer flasks, 5 L photobioreactor and 320 L open pond. The effect of different CO_2 enrichments and environment stresses; namely nitrogen starvation, NaCl stressing and high temperatures were studied in the 250 ml scale. A detail study on nitrogen starvation effect on cell; namely *Scenedesmus* sp. growth, and lipid accumulation was carried out in a 5-L

photobioreactor, and a 320 L open pond was used to obtain sufficient amount of biomass for subsequent experiments.

4.1.1 Growth in 250 ml scale

4.1.1.1 Effect of different CO2 enrichments

Freshwater strains, namely *Chlorella* sp., *Pseudochlorococcum* sp., *Scenedesmus.* sp*.,* and M.C. sp. were cultivated in +3N-BBM medium, and the marine strains; *Tetraselmis* sp, and *Nannochloropsis* sp. were grown in F/2 media at 27 ^{o}C and light intensity of 136 μmol m^{-2} s^{-1} for two continuous weeks under different CO_2 enrichments ranging from atmospheric air (0.04 %) to 2 % CO_2 (v/v). The effect of the different CO_2 enrichments on the specific growth rate, biomass productivity and lipid productivity were determined at tested conditions. The lipid content was assumed to be independent on CO_2 concentration in enriched air in the selected range, as reported by Chiu et al. [296].

Figure 4.1 shows the growth curves of the examined strains grown at different CO_2 enrichments in their corresponding media. At all tested conditions, an initial lag period of few days after the inoculation was observed, which was the time needed for the cells to adapt to the new environment, and synthesize the necessary growth enzymes. This period was followed by the exponential growth phase, where a rapid utilization of the substrate and cell division at constant rate occurred. This later phase, in most conditions, was followed by a stationary phase where cessation of division occurred. Considering that the light availability was provided in abundance due to low culture density, the growth was assumed to be

independent on the light intensity. Thus, the observed decrease in biomass growth was mainly due to the depletion of nutrients, which were supplied once at the beginning of the experiment. This suggests that for the larger scale system, nutrients concentrations should be taken in to consideration and should be continuously provided as time progress. It is worth mentioning that stock solutions of the investigated strains were maintained under controlled conditions during the study period, where cells in their exponential phase were transferred to afresh medium with constant growth rate.
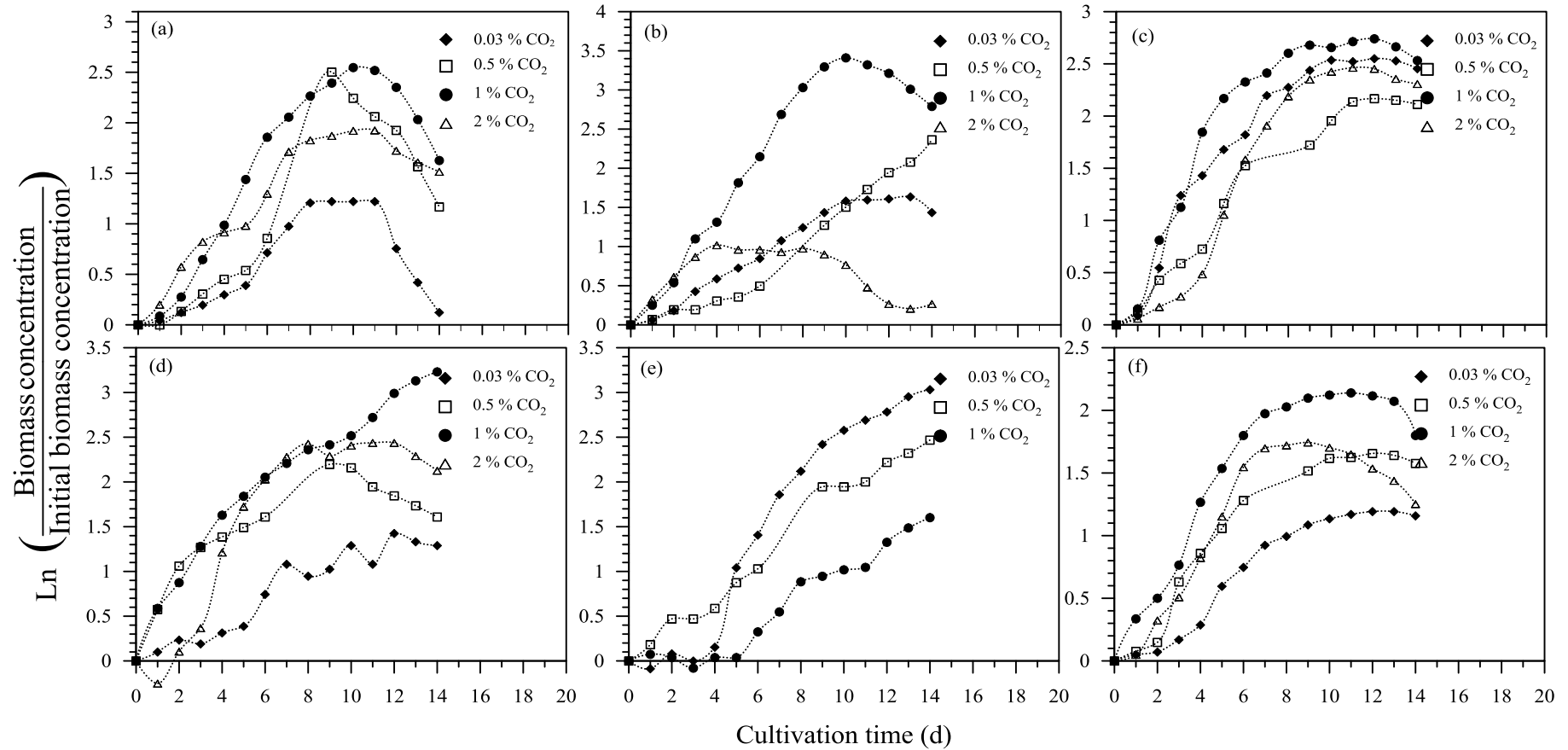
Figure 4.1: The growth curves of examined strains grown at 27 $^{\circ}$C and 140 r min^{-1} and different CO_2 enrichments [+3N-BBM (a: *Chlorella* sp., b: *Pseudochlorococcum* sp., c: *Scenedesmus.* sp. and d: M.C sp.) and on F/2 (d: *Tetraselmis* sp. and e: *Nannochloropsis* sp.)]

Culture pH was controlled using HEPES (50 mM, pH 7.4) buffer solution, which is well known for its ability to maintain the pH despite changes in CO_2 concentration [409]. To confirm the elimination of the pH effect, the pH value was monitored throughout the experiment. Figure 4.2 shows the pH fluctuation range for *Chlorella* sp. grown in +3N-NBBM and –N-BBM at 1% CO_2 enrichment. Indeed, the average culture pH value was 7.30 (shown as dashed line) with a *p*-value equal to 0.322 and sample standard uncertainty of 1.42 %, considered as the relative standard deviation, according to the ANOVA analysis by Minitab, using *t*-test. This value proves that the HEPES buffer solution effectively controlled any pH changes, where a *p*-value higher than 5% suggests that there were no difference in the means and the parameter shows insignificant effect. This further confirms that the drop in the growth was due to nutrients deficienct and not to the pH drop.
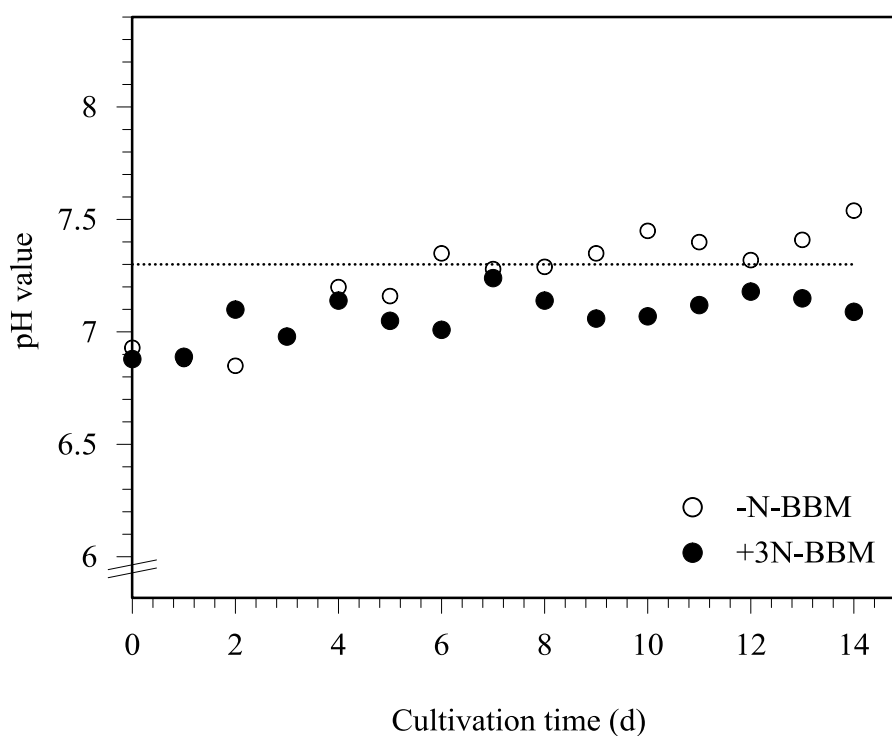
Figure 4.2: pH change of *Chlorella* sp. Culture maintained at 27 ^{o}C, 136 μmol m$^-$^{2} s^{-1} and 1 % CO_2 enrichment.

It was seen from Figure 4.1 that the biomass productivity tended to increase with the increase in CO_2 enrichment for most tested strains, until it reached its highest values at the optimum enrichment and then decreased. Table 4.1 lists the highest biomass productivities obtained for each examined strain.

Comparing obtained values with those at the control ambient air with 0.04 % CO_2 concentration, the biomass productivities at the optimum enrichment were the in range of 5-7 folds higher, depending on the strain. In the case of *Tetraselmis* sp.*,* however, the highest biomass productivity (0.457 g L^{-1} d^{-1}) was observed in atmospheric air, where increasing CO_2 concentration negatively affected the growth. Having said that, Ferriols et al. [410] work with *Tetraselmis* sp. resulted in higher adaptation to CO_2 enrichment reaching 10 % when grown in a different nitrogen source, namely NH_4Cl compared to the $NaNO_3$ in this work. This could be due to the strain superiority to uptake nitrogen from NH_4 at elevated CO_2 than from NO_3, which was proved by Meseck et al. [411].

Table 4.1: Obtained growth rate, lipid content and biomass and lipid productivities at optimum CO_2 enrichment and cultivation medium

Strain	Experimental results [a]								Litreature values [282]	
	Nitrogen sufficient				Nitrogen defficient					
	$\mu(d^{-1})$	% Lipid	P_M $(g\ L^{-1}d^{-1})$	P_L $(mg\ L^{-1}d^{-1})$	$\mu(d^{-1})$	% Lipid	P_M $(g\ L^{-1}d^{-1})$	P_L $(mg\ L^{-1}d^{-1})$	P_M $(g\ L^{-1}d^{-1})$	P_L $(mg\ L^{-1}d^{-1})$
Chlorella sp.[b]	0.29±0.03	13±0.6	0.87±0.05	115±5.32	0.21±0.07	20±1.2	0.17±0.08	33.3±2.22	0.17-0.23[d]	18-19[d]
Pseudochlorococcum sp.[b]	0.37±0.04	2.9±0.4	0.81±0.04	23.5±3.24	0.29±0.06	4.8±0.04	0.31±0.05	14.8±0.15	-	-
Scenedesmus sp.[b]	0.38±0.07	10±0.3	1.1±0.08	78.4±0.91	0.26±0.08	21±2.4	0.52±0.0	48.0±1.86	0.19-0.26[d]	18-21[d]
M.C sp.[b]	0.47±0.02	0.94±0.07	0.24±0.04	1.49±0.2	0.31±0.04	1.5±0.02	0.096±0.07	1.46±0.15	-	-
Nannochloropsis sp.[b]	0.30±0.04	14±0.8	0.38±0.03	37.7±2.16	0.24±0.07	21±0.8	0.38±0.14	43.1±1.77	0.17-0.21[e]	21-30[e]
Tetraselmis sp.[c]	0.27±0.04	0.91±0.06	0.46±0.06	4.14±0.6	0.23±0.09	1.2±0.06	0.098±0.03	1.21±0.09	0.28-0.32[e]	8-15[e]

μ: specific growth rate

P_M: Biomass productivity

P_L: Overall lipid productivity

[a] Average values with ± measured uncertainty

[b] At 1 % CO_2 enrichment

[c] At 0.5 % CO_2 enrichment

[d] Grown in BG11 medium at 25 ^oC under continuous illumination with CO_2 enriched air

[e] Grown in *F* medium of 30 g L^{-1} salinity at 25 ^oC under continuous illumination with CO_2 enriched air

At different CO_2 enrichments, the specific growth rate, μ, was determined from the slope of the growth curves, shown in Figure 4.1, in the exponential growth region, and the results are shown in Figure 4.3. It can clearly be seen that the specific growth rate increased with the increase of CO_2 concentration at the beginning until it reached its highest value at the optimal enrichment, which then dropped due to the high concentration inhibition to the growth.

Typically, in green algae, CO_2 and O_2 compete to access the RuBISCO enzyme that can fix both. The high concentration of CO_2 may lead to a high amount of O_2 release that accumulate and compete to access RuBISCO and catalyze an oxidase reaction [412, 413]. Previously reported results, showed that optimal growth rate in a range of 3-10 % CO_2 was observed for *Chlorella,* depending on species genus and growth environment [414]. Higher enrichment of 4% was reported by Bhola et al. [415] for *Chlorella vulgaris* grown in BG11 medium. Similarly, an optimum growth at 2 % enrichment was reported for *Nannochlorpsis oculata* grown in same media used in this study for this particular strain. The higher specific growth (0.571 d^{-1}) reported might be due to the higher (almost double) provided light intensity [296]. When cultivated in saline water, higher optimum CO_2 enrichment was usually observed [296, 416]. The higher inhibition onset concentration of CO_2 is mainly due to the decrease in CO_2 solubility with the increase in salinity depending on the ionic strength of the solution. Sodium chloride is reported to account for 73 % of seawater ionic strength [417]; therefore, higher partial pressure was needed, and a higher partial pressure of CO_2 can be tolerated by the microalgae.
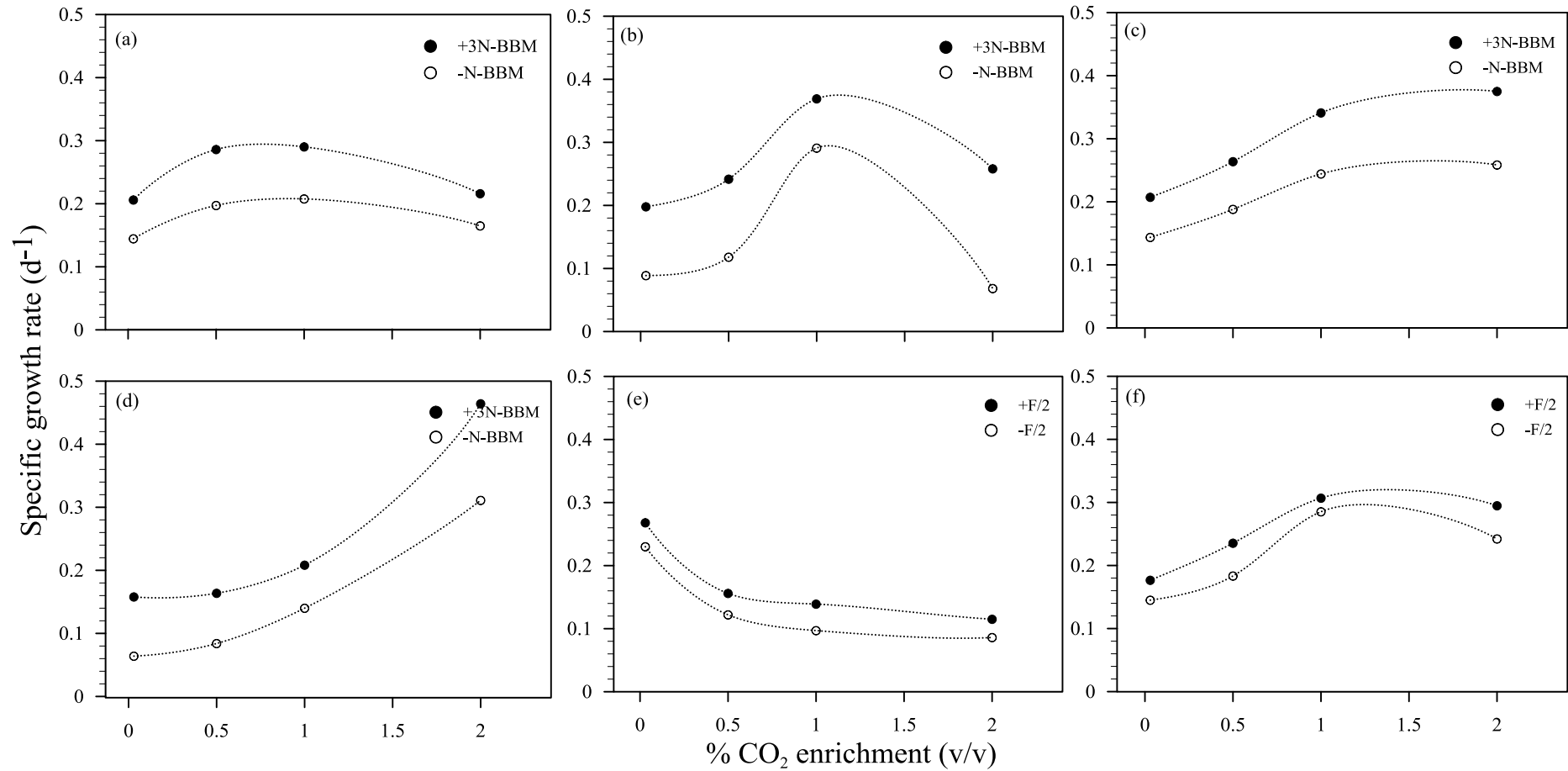
Figure 4.3: The specific growth rates of examined strains grown in in both nitrogen rich and deficient medium at different CO$_2$-air enrichments

(a: *Chlorella* sp., b: *Pseudochlorococcum* sp., c: *Scenedesmus* sp. d: M.C sp. e: *Tetraselmis* sp. and f: *Nannochloropsis* sp.)

4.1.1.2   Effect of nitrogen starvation

For an efficient production of biodiesel, it is important to utilize the species with high growth rate and lipid content yielding the highest lipid productivity. Recently, environment stressing to prompt lipid synthesis, has received considerable attention. Previous studies have verified that many microalgae strains can modify their metabolism in response to media changes, where the lipid contents were found to be increased by nitrogen deprivation [44, 282, 418, 419].

To study this effect, strains under investigation were grown in nitrogen stress (-N-BBM or –N-F/2) media for two continuous weeks, by removing the nitrate source ($NaNO_3$) from the control media. The specific growth rates of examined strains at different CO_2 enrichments are shown in Figure 4.3, and the highest growth rates and biomass productivities at optimum enrichment can be found in Table 4.1. The pH change was also monitored daily for *Chlorella* sp. grown in 1 % CO_2, as shown in Figure 4.2, and it was found insignificant with *p*-value of 0.653 and sample standard uncertainty of 3.03 %, determined from ANOVA *t*-test by Minitab. It is clearly shown in Figure 4.3 that under nitrogen stressing, lower growth rates were observed. However, it was the lipid enhancement by starvation which was of interest in this case. The lipid contents of the lyophilized cells were determined by supercritical CO_2 extraction at 50 ^{o}C, 300 bar, and 1.5 ml min^{-1}.

Table 4.1 shows the determined lipids contents after two weeks of starvation compared to that grown in controlled media. It was found that that lipid contents increased by 52, 64, 99, 61, 35 and 54 % for *Chlorella* sp.,

Pseudochlorococcum sp., *Scenedesmus* sp., M.C sp., *Tetraselmis* sp. and *Nannochloropsis sp*, respectively, under nitrogen deprivation. This is mainly due to the nitrogen unavailability that shifted the pathway from protein synthesis to lipid accumulation. The cell division was hence reduced and fatty acids synthesis, which was deposited in the cells as triglycerides, was enhanced.

The lipid productivities of tested strains were determined from the multiplication of biomass productivity by the lipid content. Figure 4.4 shows the overall lipid productivities calculated at different CO_2 concentrations for all examined strains. Despite the higher lipid content induced under high C/N ratio in the biomass grown in the N- deficient medium, the overall lipid productivity in the controlled media remained higher for most tested strains. This is mainly due to the fact that the conditions favoring high lipid accumulation are usually associated with low biomass productivity, and thus yielding a lower overall lipid productivity. However, that was not the case with *Nannochloropsis* sp*.,* which showed a higher productivity with starvation due to the lipid enhancement dominance on biomass production. The highest lipid productivities are shown in Table 4.1, which are comparable to values reported in literature.

The results obtained in this study suggest the use of a two stage cultivation, in which in the first stage the biomass production is enhanced followed by cells grown under stress condition to induce lipid accumulation, this cultivation strategy was studied thoroughly with *Scenedesmus* sp., which showed the highest lipid productivity when tested at 1 % enrichment of CO_2.
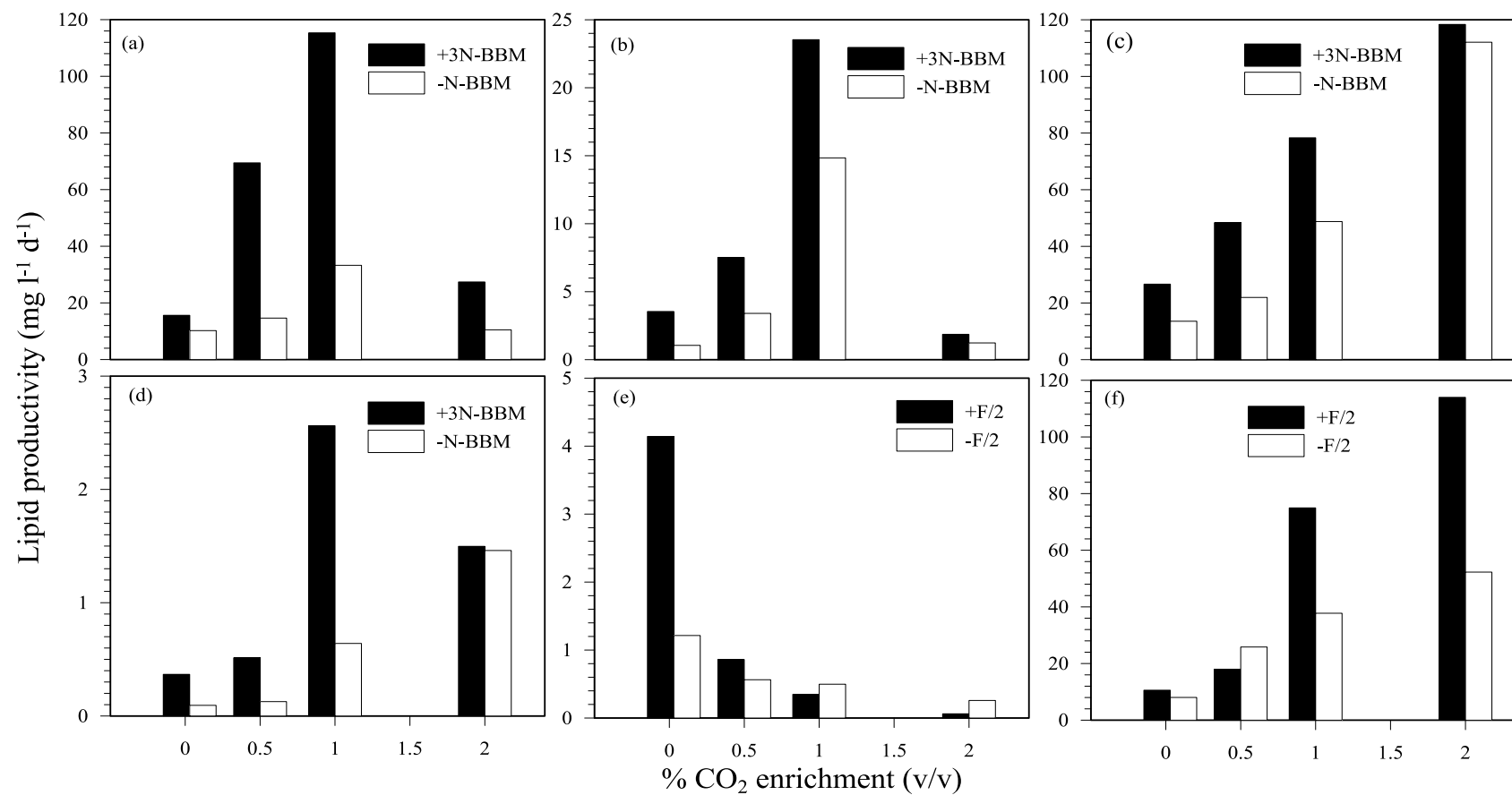
Figure 4.4: Overall lipid productivity of examined strains grown in; both control and starved medium

(a: *Chlorella* sp., b: *Pseudochlorococcum* sp., c: *Scenedesmus*. sp. d: M.C sp. e: *Tetraselmis* sp. and f: *Nannochloropsis* sp.)

4.1.1.3 Carbon fixation

As mentioned earlier, one of the promising features of microalgae production is their ability to mitigate CO_2. It has been reported that for each gram of produced microalgae biomass, between 1.6 and 2 g of CO_2 are captured [45] . To analyze the examined strains, the CO_2 fixation rate and capturing efficiency were determined using Eq. (3.2), using the carbon contents determined by the elemental analyzer. Table 4.2 shows the determined carbon content, fixation rates and CO_2 capturing efficiency for the examined strains. The high observed fixation rats of *Chlorella* sp. and *Scenedesmus* sp. makes them good choices for fuel production with CO_2 mitigation.

Table 4.2: Carbon content, CO_2 fixation rates of examined strains in the control medium

Strain	% Carbon content ($g\ g^{-1}$)	Fixation rate ($g\ L^{-1}\ d^{-1}$)	CO_2 Capture ($g\ g^{-1}$)
Chlorella sp.[a]	48.0±0.9	1.538±0.093	1.76±0.11
Pseudochlorococcum sp.[a]	39.7±0.7	1.182±0.062	1.45±0.08
Scenedesmus. sp. [a]	48.6±0.4	1.300±0.09	1.78±0.17
M.C sp.[a]	47.8±0.4	0.478±0.13	1.75±0.44
Nannochloropsis sp.[b]	47.6±0.3	0.46±0.09	1.745±0.35

[a] +3N-BBM medium

[b] F/2 medium

CO_2 fixation rates found in this study were close to those reported for *Aphanothece microscopic Nägeli* [420], *Tetraselmis subcordiformis* [41] and *Chlorella vulgaris* [421]. However, Yang et al. [421] reported a higher fixation rate reaching 2.78 g L^{-1} d^{-1} from *Chlorella pyrenoidosa*. The difference in results is mainly due to the adaptation of each strain to the growth conditions.

4.1.1.4   Effect on temperature and NaCl stressing

The ability of microalgae strains to grow in saline water reduces the freshwater load. To test the ability of fresh water strains to withstand high salinities, *Chlorella* sp. was grown in media of high salinities ranging from 0.49 to 680 mM NaCl at different temperatures ranging from 27 to 35 ^{o}C. Figure 4.5 shows the effect of salinity on the specific growth rate at the optimum CO_2 enrichment of 1%.
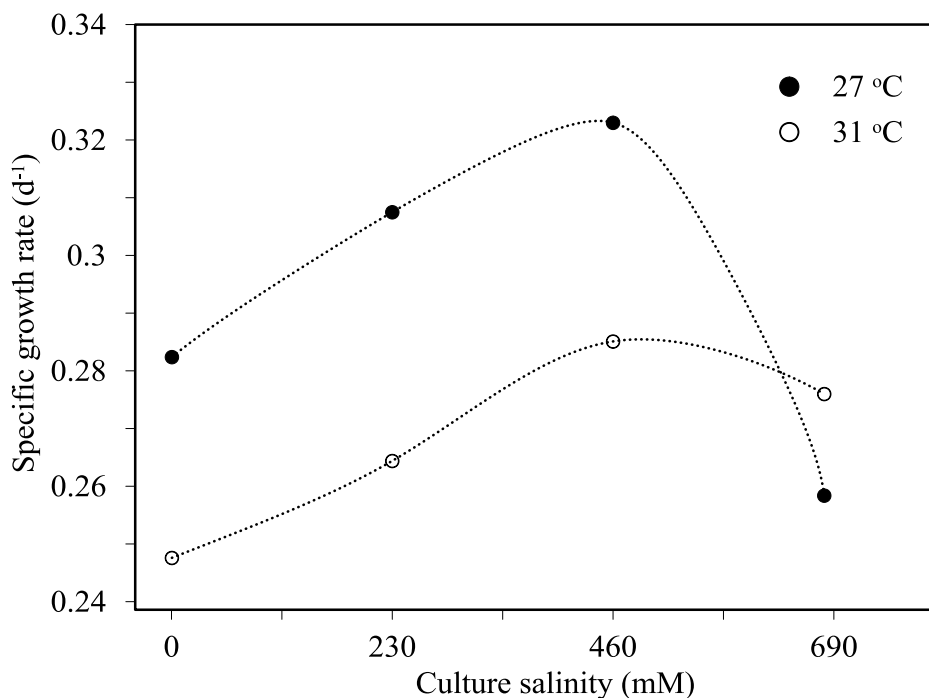
Figure 4.5: Specific growth rates of *Chlorella sp.* at different salinities

It was found that this freshwater strain was able to grow in marine environments of salinity levels up to 460 mM NaCl, with a growth rate reaching 0.323 and 0.285 d^{-1} at 27 and 31 ^{o}C, respectively. Further increase in the temperature resulted in a sharp decrease in the growth rate, and at 35 ^{o}C cell decay was observed within a few days, even at low salinities. This might be due to the low solubility of CO_2 in the culture medium of high temperatures and using higher concentrations of CO_2 would help to enhance the growth rate in this case.

Close results were reported for *C. vulgaris* growth with a 17% decrease in growth rate at 35 ^oC compared to 30 ^oC [305]. The ability of this fresh water strain to grow in a marine environment was achieved by the gradual increase in the solubility, which allowed the adaptation of the strain to the high salinities.

The lipid contents at tested conditions were determined and further used for lipid productivity determination. Table 4.3 shows the lipid content of the microalgae grown at different salinity levels and temperatures.

Table 4.3: % Lipids content and productivity of *Chlorella* sp. grown in both medium at different culture conditions

	Temperature (^oC)	Salinity (mM)		
		0.49	230	460
% Lipid content	27	13±0.6	13.5±0.3	25.9±0.2
	31	12±0.4	16.3±0.7	19.1±0.2
Lipid productivity	27	115±5.32	130±3.72	177±6.25
(mg L^{-1} d^{-1})	31	81.3±1.66	128±2.83	125±3.61

It was found that growing in saline environment induced the lipid production, and the highest content was observed at 460 mM. As further increase of the temperature to 31 ^oC reduced the content. However, at 230 mM, lipid content slightly increased (20 %) by the temperature, whereas, it decreased by 26 % at 460 mM. The increase at 230 mM might due to the low solubility of CO_2 in the culture that decreased the concentration of dissolved carbon leading to the utilization of the produced ATP and NADPH by photosynthesis in biomass production more than lipid accumulation; thus the rate of growth rate enhancement was higher than lipid enhancement.

Table 4.3 shows also the overall lipid productivity of *Chlorella* sp. grown at 27 and 31 ^{o}C under different salinities. The increase in temperature resulted in a decrease in the growth rate from 0.282 to 0.248 d^{-1} when the strain was grown in the controlled media, and since the lipid content was almost constant, the lipid productivity decreased from 101.2 to 81.3 mg L^{-1} d^{-1}. Similar results were obtained at higher salinities; but the drop in lipid productivity with temperature was steeper at 460 mM. The results suggest that the optimum conditions for lipid productivity are 27°C and 460 mM NaCl concentration. The trend obtained in this work agrees with that found for *Chlorella vulgaris* [305, 422].

4.1.1.5 Kinetic of cells growth

The basic model to describe cells growth is the Monond model (Eq. 2.6), which assumes that the specific rate is dependent on a particular limiting substrate. As mentioned earlier, Haldane model (Eq. 2.7) has been suggested to consider the substrate inhibition effect that is not considered in Monod model. In this work, the effect of CO_2 concentration on a range of atmospheric air to 2% CO_2 enrichment on the specific growth rate was studied in both +3N-BBM and-3N-BBM for *Chlorella* sp. and *Pseudochlorococcum* sp., the study was carried out at constant growth conditions of temperature, light intensity and nutrient concentration to eliminate their effects.

Due to the low solubility of CO_2 in freshwater, the TIC concentrations, determined using Eq. (2.8), were considered as growth substrate. The experimental data shown in Figures (1.2 a and b) were used to determine the kinetic model parameters using nonlinear least square method by minimizing the objective function given in Eq. (3.16) using Excel solver with 10 $^{-5}$ tolerance.

Table 4.4 shows estimated kinetic parameters for the species in +3N-BBM and -N-BBM.

Table 4.4: Kinetic parameters comparison of *Chlorella* sp. and *Pseudochlorococcum* sp. grown in +3N-BBM and –N-BBM

Parameter	*Chlorella* sp.		*Pseudochlorococcum* sp.	
	+3N-BBM	-N-BBM	+3N-BBM	-N-BBM
μ_{max}	0.875	0.706	1.012	0.99
K_s	3.23	2.97	3.88	5.65
K_I	3.34	2.84	4.36	2.03
R^2	0.982	0.978	0.836	0.692

It was found that the maximum specific growth rate and inhibition constant in +3N-BBM were higher than in -N-BBM for both tested species. Half saturation constant, however, was higher in -N-BBM for *Pseudochlorococcum* sp., which was not the case with *Chlorella* sp.. This might be due to the numerical uncertainty caused by the method iteration. The lower maximum growth rate obtained by nitrogen stressing, indicates that nitrogen unavailability had significant effect on total biomass production rate. Figures (4.6 and 4.7) show the comparison between the experimental and model predicted specific growth rates, for *Chlorella* sp. and *Pseudochlorococcum* sp., respectively. It can be clearly seen that the Haldane model predicted the experimental data well, which is confirmed by in the R^2 value shown in Table 4.4, although the prediction was poor with starved cells of *Pseudochlorococcum* sp.
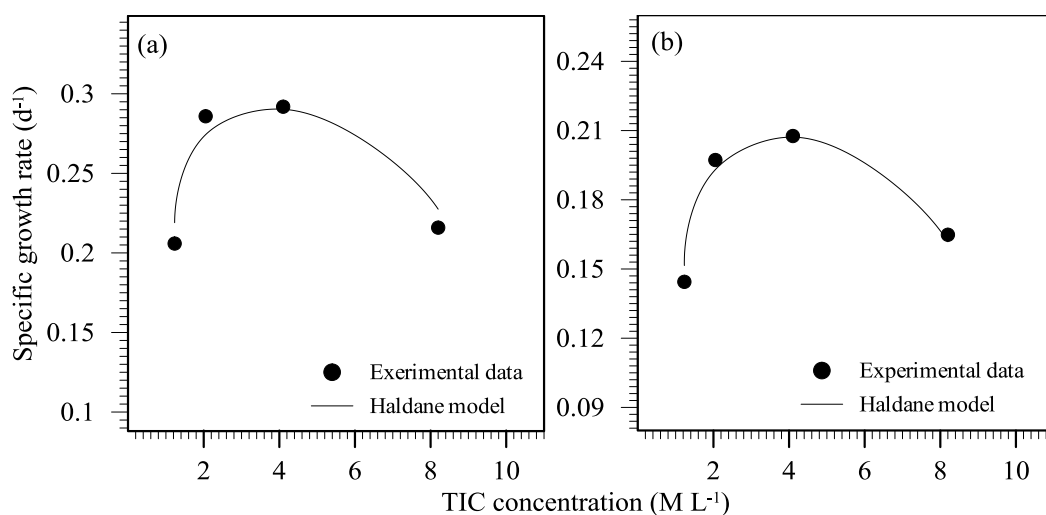
Figure 4.6: Effect of total inorganic carbon on *Chlorella* sp. specific growth rate at 27 ^{o}C in; (a) 3N-BBM and (b) –N-BBM
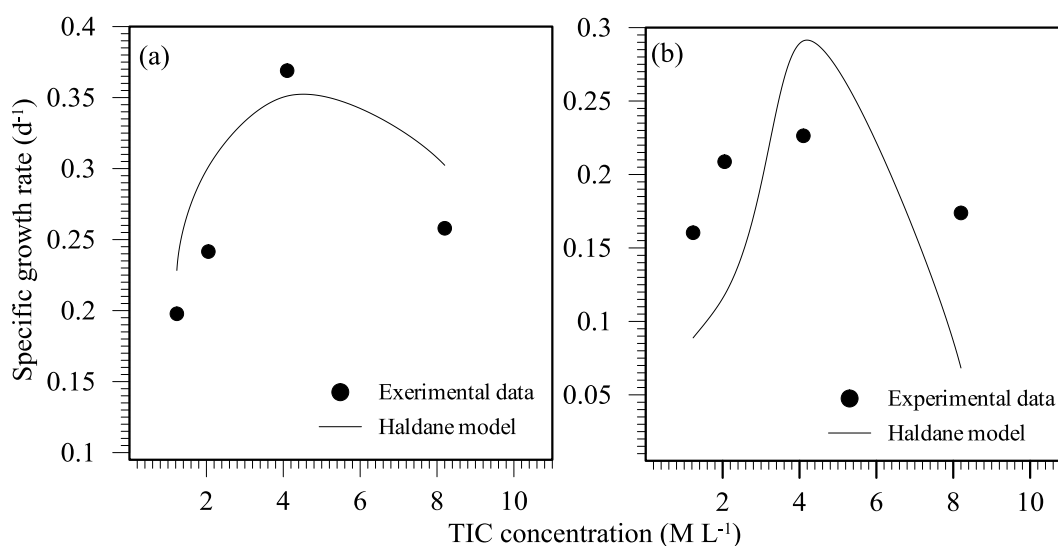
Figure 4.7: Effect of total inorganic carbon on *Pseudochlorococcum* sp. specific growth rate at 27 ^{o}C in; (a) 3N-BBM and (b) –N-BBM

4.1.2   Growth in 5L photobioreactor and indoor open pond

4.1.2.1   Strain growth and productivity

Scenedesmus sp. cultivation was carried in two stages: in the first the cells were allowed to grow in a nutrient rich media (+3N-BBM) for 14 days to enhance the biomass productivity, and in the second the cells were transferred to

nitrogen deficient medium (-N-BBM) to enhance the lipid accumulation. Figure 4.8 shows the growth and the correspondence time course of lipid accumulation in the two cultivation stages.
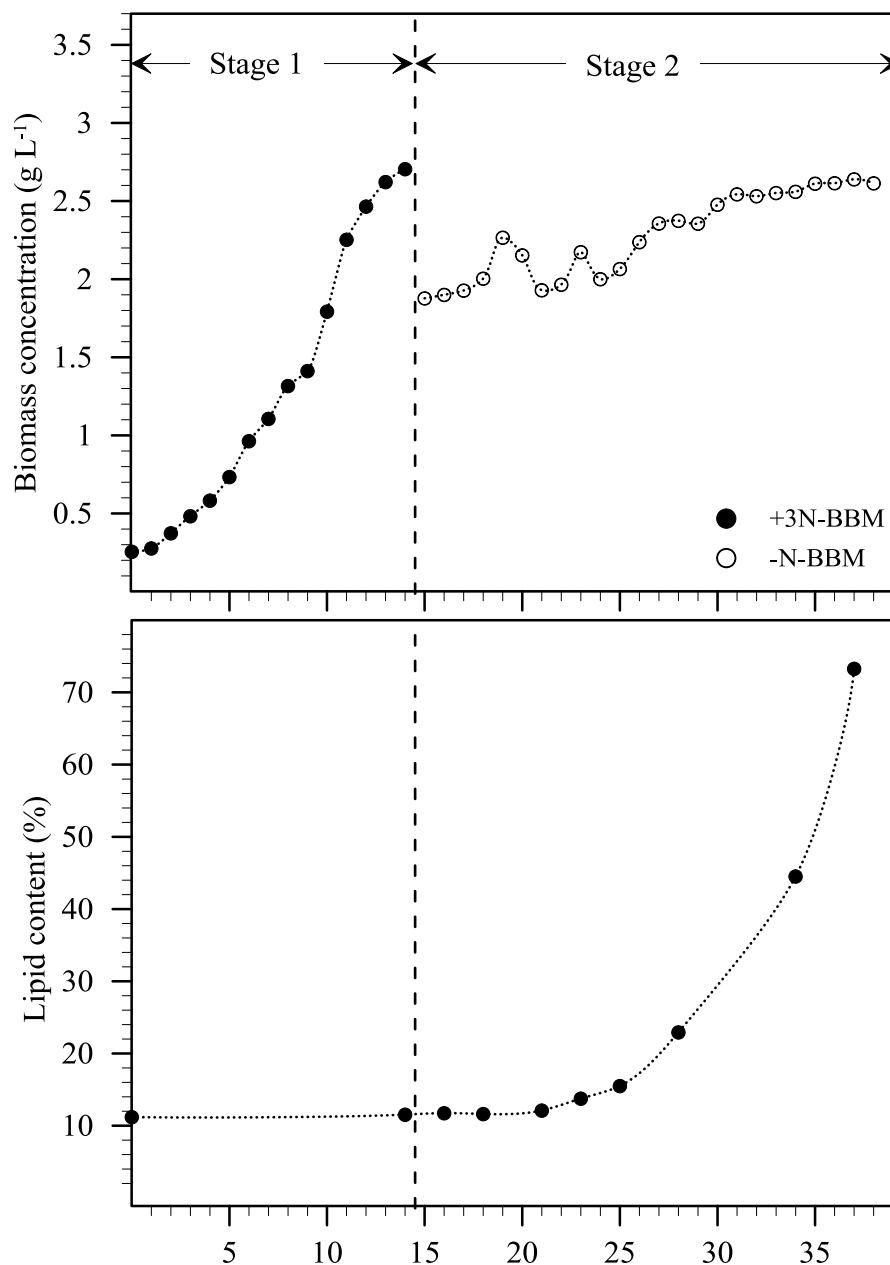
Figure 4.8: Cell growth and lipid accumulation curves of *Scenedesmus* sp. grown in 5L photobioreactor

The figure shows that the lag phase was short, and the growth entered the exponential growth phase almost immediately. As expected, the lag phase was

short as the inoculum into the photobioreactor was from the stock broth of cells grown in the same medium. In stage 1, the specific growth rate was 0.195 d^{-1}, determined from the slope of the logarithmic growth line. The lipid content was determined at the beginning and end of this stage and found to remain almost constant at 12.6±0.8 % (dry basis). The lipid content was determined after cells lyophilization at -54°Cand 0.02 mbar for 6 h in the freeze drier followed by y SC-CO_2 extraction at 50 ^{o}C, 500 bars and 3ml min^{-1} with 100ml total CO_2 passed. Multiplying the biomass productivity, determined from the slope of the growth curve, by lipid content resulted in overall lipid productivity of 19.5 mg L^{-1} d^{-1}. Similar lipid content was also reported in the work of Rodolfi et al. [282] done on a strain of a genus similar to the one used in this work. The exact species of the strain used in this work was not identified. However, slightly higher biomass productivity was obtained by Rodolfi et al. [282], which resulted in higher overall lipid productivity. This is mainly because the cultivation was done with 5 % CO_2 enrichment, whereas in this work, the cultivation was autotrophic with CO_2 being the sole carbon source. In addition, this slightly higher productivity is due to the preferable illumination intensity and duration, which were in this work 120 μmol m^{-2} s^{-1} under 12 h light/dark photoperiod, respectively, compared to 100 μmol m^{-2} s^{-1} under continuous illumination applied in [282]. These results are also comparable to those found by Ren et al. [423] for the same strain but grown heterotrophically.

4.1.2.2   Effect of nitrogen stressing on lipid productivity

In the second stage, cells were grown in a nitrogen deficient medium (-N-BBM), which resulted in a sharp drop in the specific growth rate to 0.0165 d^{-1}, as

shown in Figure 4.8. The slight drop in biomass concentration observed at the beginning of the second stage was due to loss of some cells during the harvesting, after collecting the cells and re-culturing them in the new medium. However, having grown in stage 1 to a sufficient concentration, the lipids accumulation was the main objective of this stage. This reduces the net energy and increases biodiesel productivity [332]. Furthermore, if the growth was carried in outdoor cultures, this proposed technique would still be applicable. The total lipid content in the first day of starvation was 12.6 % based on dried cell weight. The lipid accumulation was monitored by staining with Nile red. Figure 4.9 shows the fluorescence microscopic images in different days after starvation, where the brightness in the photos indicates the amount of lipids.

(a)   (b)   (c)   (d)   (e)
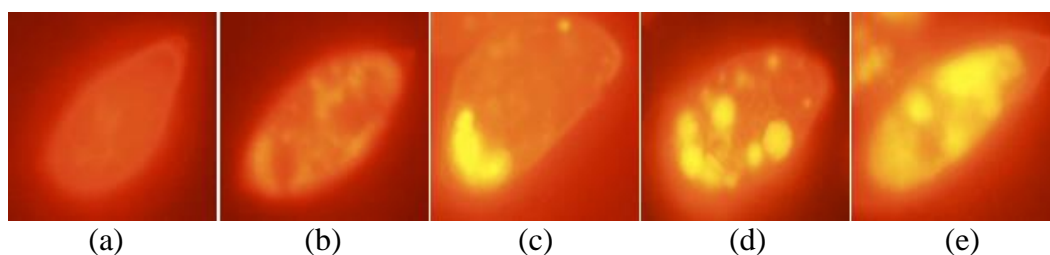
Figure 4.9: Fluorescence microscopy images of *Scenedesmus* sp. cells stained with Nile Red and showing lipid accumulation after 1 (a), 11 (b), 14 (c), 20 (d) and (e) 23 days of nitrogen starvation in cultures.

It is clearly seen that by day 11, cells started to accumulate the lipid, which enhanced further until day 23. This has been also proven by quantitative measurements using a micro-plate reader as shown in Figure 4.10. The lipid content was also determined gravimetrically by Soxhlet extraction from lyophilized samples and a calibration curve between the fluorescence intensity and lipid content was prepared. The results shown in Figure 4.10 further confirmed that lipid accumulation started after day 11 of starvation and increased

exponentially thereafter. After 3 weeks of starvation, a six-fold increase in lipid content was observed, reaching 73 % on a dry weight basis. This enhancement applicability may contribute farther in decreasing the harvesting cost.
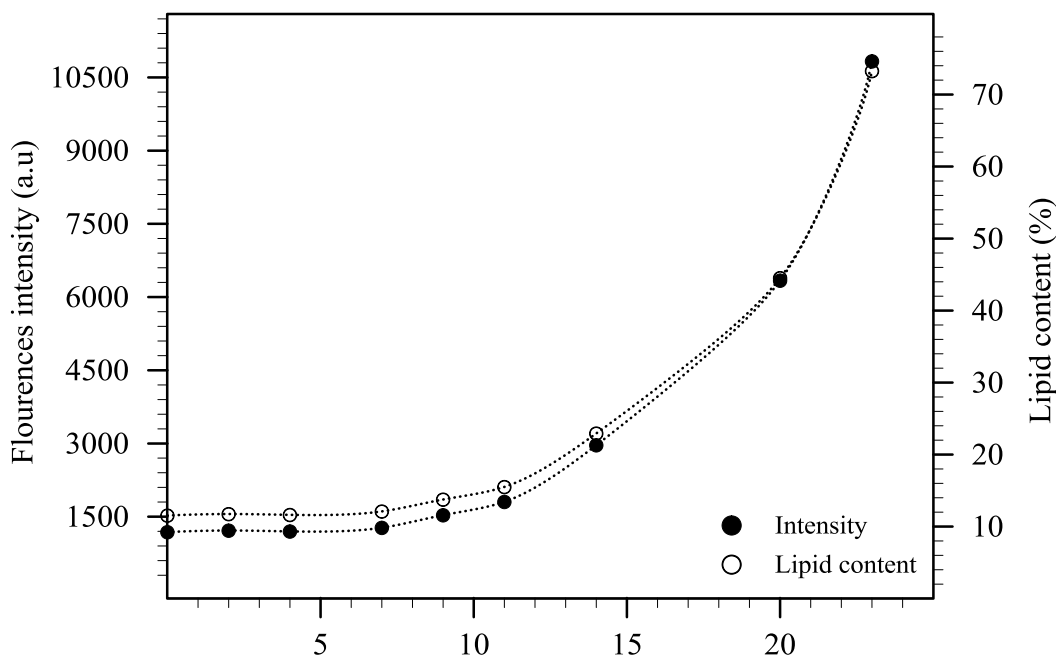
Figure 4.10: Relative fluorescence intensity and lipid content in the nitrogen starvation stage of *Scenedesmus sp.* grown in 5 L photobioreactor

Table 4.5 shows the fatty acids profile in extracted lipid, after SC-CO$_2$ extraction, rapid transesterification to FAME, and analysis using GC-FID, from the growth in nitrogen sufficient (+3N-BBM) and nitrogen deficient (-N-BBM) media. The results show that the compositions of the extracted lipid was almost similar, but the triglycerides content (fatty acid contents) was higher in the lipid extracted from cells grown in -N-BBM confirming that the natural lipid are accumulated by starvation.

Table 4.5: Fatty acid composition (% w/w) of cells lipids in nitrogen sufficient and nitrogen diffecient media

Fatty acid	Growth environment	
	+3N-BBM[a*]	-N-BBM[b*]
C14:0	3.50 ±0.04	3.20 ±0.03
C16:0	16.5 ±0.05	17.4 ±0.1
C18:0	4.70 ±0.37	6.30 ±0.11
C18:1	11.8 ±0.12	12.1 ±0.15
C18:1 (*trans-9*)	9.40 ±0.03	8.20 ±0.16
C18:2	-	0.60 ±1.9
C18:2 (*n6*)	44.7 ±0.25	40.7 ±0.04
C18:3 (*n3*)	7.10 ±0.08	8.40 ±0.27
C20:0	-	1.20 ±1.09
C22:0	2.40 ±0.42	1.90±0.004
Total fatty acids	69.6	78.2
U/S[c]	2.7	2.3

[a] In +3N-BBM
[b] In -N-BBM[*]
[*] Average values with ±measured uncertainty

4.2 MICROALGA LIPID EXTRACTION

The effectiveness of microalgae lipids extraction using SC-CO_2 was investigated and compared to different conventional extraction techniques. The effects of biomass pre-treatment and process operating conditions, namely temperature, pressure and fluid flow rate, on the extraction yield and quality were studied, optimized using 3^3 FFD and RSM, and modeled using Sovova [380] model. In addition, supercritical extraction from lyophilized biomass was tested at larger laboratory scale and results were compared. To avoid the high cost associated with the energy extensive drying, extraction from cell disrupted biomass using enzymes was tested.

4.2.1 Dried biomass

4.2.1.1 Comparison between different extraction techniques

Prior to any extraction, the lipid-containing cells were disrupted and thoroughly dried by lyophilization, which has been widely used with microalgae cells [329, 330]. Lipids can be extracted from solid matrices by several methods including organic solvents and SC-CO_2. The use of chemical solvents, such as *n*-hexane, has several drawbacks, which include the leftover biomass contamination with the solvent, long extraction time and the need for additional separation units. These drawbacks can be overcome by using SC-CO_2 extraction. For comparison, SC-CO_2 extraction of lipid from lyophilized biomass at 50 ^{o}C, 350 bar and a flow of 2.69 g min^{-1} (3 ml min^{-1}) was compared to that found by conventional solvent extraction methods. *n*-Hexane, chloroform/methanol/water (1:1:0.9) and *n*-hexane/*iso*-propanol (3:2), were used to extract lipids statically, and compared to the dynamic extraction using pure *n*-hexane in the Soxhlet apparatus. The latter was used as a baseline to evaluate the SC-CO_2 extraction efficiency. In the static extraction techniques, the cells were further disrupted using ultra-sonication. This step was not used for SC-CO_2 and Soxhlet extractions tests.

The effectiveness of each extraction technique was determined from the lipid extraction yields and the TAGs content of extracted lipids, which was used as a tool to assess the quality for extract. Figure 4.11 shows a comparison of the both yields between the tested methods. It is clearly seen that the highest lipid extraction yield was achieved using SC-CO_2. Although the solvating power of SC-CO_2 is similar to that of the liquid solvents, its diffusivity is higher and viscosity is lower, which allow the SC-CO_2 to penetrate deeper and faster within

the solid matrix. The static extraction using solvents mixture (n-hexane/*iso*-propanol and chloroform/methanol/water) were able to extract more lipids compared to pure n-hexane when carried out in a static mode. In addition, Soxhlet extraction was less effective than the static extraction techniques, which could be due to the positive effect of the ultra-sonication, used in the static techniques, which enhanced the cell wall disruption, and, therefore the yield.
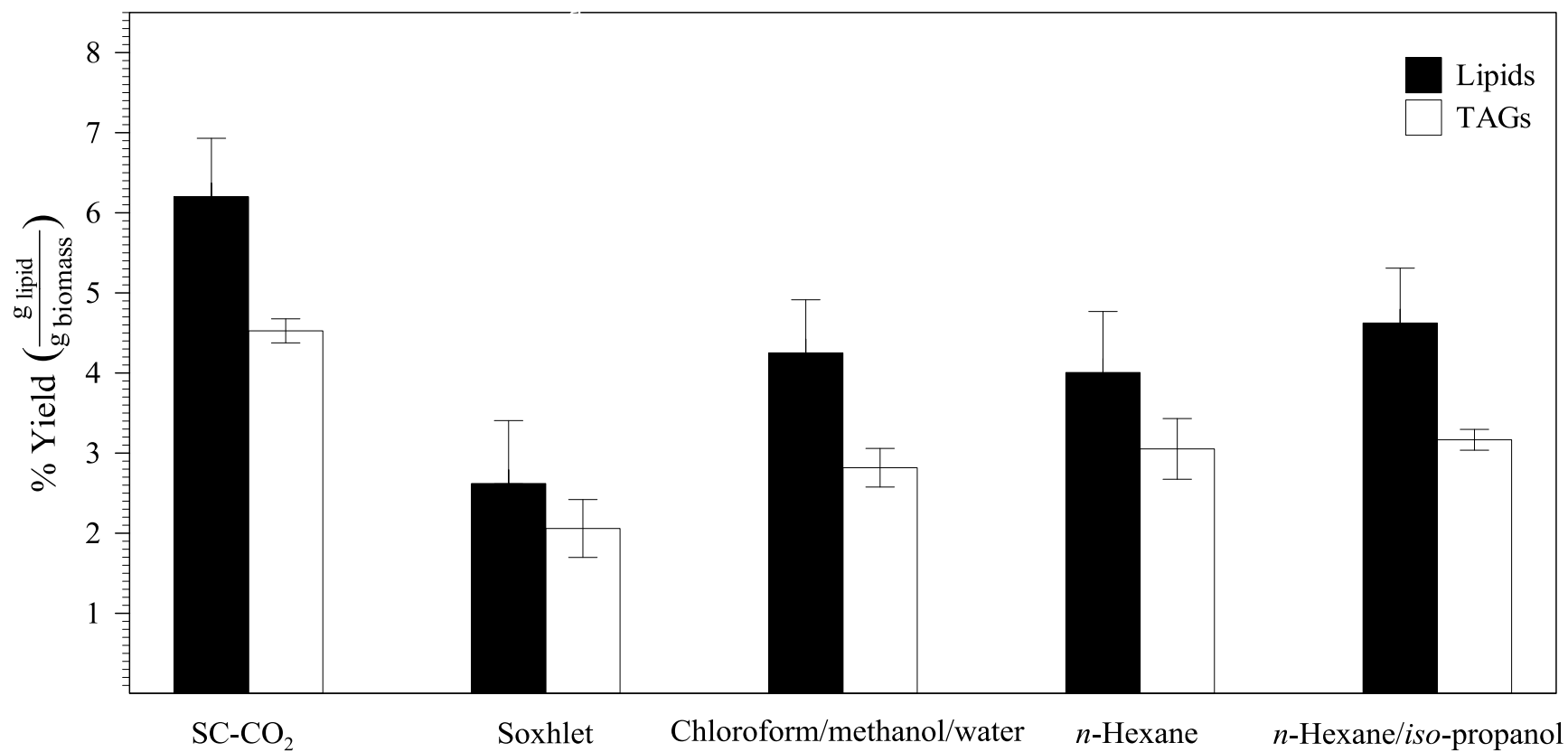
Figure 4.11: Comparison of lipid and triglyceride yield extracted using SC-CO_2 at 50 $^{\circ}$C, 350 bar and a flow of 2.69 g min^{-1} and other conventional methods

Table 4.5 shows extracted lipid profile determined using GC-FID. It is shown that extracted lipid in all tested methods mainly comprised of trans-9-elaidic acid (C18:1) followed by methyl linoleate (C18:2) and oleic methyl ester (C18:1), which are the important for best constitutes for better biodiesel quality . The results indicated that although chloroform/methanol/water and *n*-hexane/*iso*-propanol mixtures were able to extract more lipids compared to the *n*-hexane, the TAGs contents were less due to the co-extraction of other undesired compounds. In addition to extracting more lipids, using SC-CO$_2$ resulted in extracting lipids of higher TAGs contents than most of the solvent extraction methods, except for that extracted with pure *n*-hexane. These results clearly proved the superiority of SC-CO$_2$ extraction over conventional extraction techniques. Furthermore, SC-CO$_2$ extracted more than 90 % of the total extracted lipid in the first 20 min; compared to the conventional methods that required much longer extraction times. Besides that, organic solvents required a solvent separation step following the extraction, which was not required in the SC-CO$_2$ extraction, where the extract was collected by simply depressurizing the system.

Table 4.6: Fatty acid composition of extracted lipid using different extraction methods and treatments.

FAME	Static extractions [a]			Dynamic extractions [a]			
					SC-CO$_2$ (50 ^{o}C, 350 bar and 2.69 g min^{-1})		
	n-hexane	n-hexane/iso-propanol	chloroform/methanol/water	Soxhlet	lyophilized -grinded	lyophilized-ungrinded	control-grinded
C16:0	12.5±0.5	5.3±0.4	14.3±0.2	9.1±0.3	13.3±0.5	13±0.6	11.1±0.3
C18:0	6.30±0.1	10.5±0.6	5.4±0.1	9.1±0.5	5±0.2	2.9±0.4	3.7±0.7
C18:1-cis	12.5±0.3	15.8±0.7	10.7±0.4	18.2±0.3	16.7±0.2	17.4±0.4	18.5±0.4
C18:1-$trans$	43.8±1.2	42.1±0.3	46.4±0.2	45.5±0.8	38.3±0.8	40.6±0.9	44.4±0.8
C18:2	18.8±0.8	15.8±0.8	17.9±0.4	9.1±0.4	21.7±0.4	23.2±0.4	22.2±0.4
C18:3	-	-	1.8±0.2	-	-	-	-
C22:0	6.3±0.4	10.5±0.6	1.8±0.1	-	1.7±0.4	2.9±0.1	3.7±0.6
% TAGs	76±2	68±0.9	66±1.3	79±3.4	73±1.9	73±1.5	70±2.6

[a] Average values with ± measured uncertainty

4.2.1.2 Biomass characterization

Thermal gravimetric analysis (TGA) can be used to determine the proximate analysis of the biomass. In addition, it has been reported that TGA results can be used as a rapid, simple and accurate method for lipid quantification [424]. Thus, it was used to identify and characterize the lyophilized biomass of *Scenedesmus* sp. used in this work. Figures 4.12 (a and b) show the percentage of weight loss by temperature and its thermogravimetric derivative analysis (DTG), respectively. The derivative of the weight loss by time in Figure 4.12 (b) was scaled from 0-2 % min^{-1} to allow magnifying of the difference between the samples, which was insignificant compared to the sample weight loss shown in Figure (4.12 a). The results showed that the pyrolysis underwent three steps of decomposition, namely dehydration, devolatilization and solid decomposition, demonstrated as dot vertical lines in Figure (4.12a). The first stage began from the room temperature to around 180 ^{o}C, where moisture was released and weight loss of 4.8% was found on total loss of ignition (LOI) basis for the lyophilized biomass, corresponding to 8.2 % of the total biomass weight. This value agrees well with determined moisture content by the moisture analyzer. The major biomass degradation was observed in the second stage at temperatures between 180 and 530 ^{o}C, with weight loss of about 78.7 %, based on LOI. In this stage, the pyrolysis proceeded very rapidly with the maximum rate taking placed at about 275 ^{o}C. This temperature fell between T_i of 225 ^{o}C, which is the intermediate between the peaks of stages 1 and 2, and T_e of 530 ^{o}C, which is the next temperature at which DTG value was equal to that at T_i, shown in Figure (4b). Figures (4 a and b) also shows that the devolatilization went through the two

steps with two observed peaks. The former appeared at 275 ^{o}C and generally attributed to protein and carbohydrate devolatilization, whereas the second at around 475°C was for lipids [425], which was confirmed by characterizing the lipid-free sample. It is clearly seen from the peaks at 475 ^{o}C that lipid difference between lyophilized and leftover biomass, which is lipid free. In the third stage of decomposition, the carbonaceous solids underwent a slow degradation, which is a similar thermal behavior to those reported for other strains [426-428]. The total amount LOI was found to be 61.53 %, for the lyophilized biomass, which was used to convert the percentage weight loss based on LOI, reported in the TGA results to that based on the total biomass weight mentioned earlier.
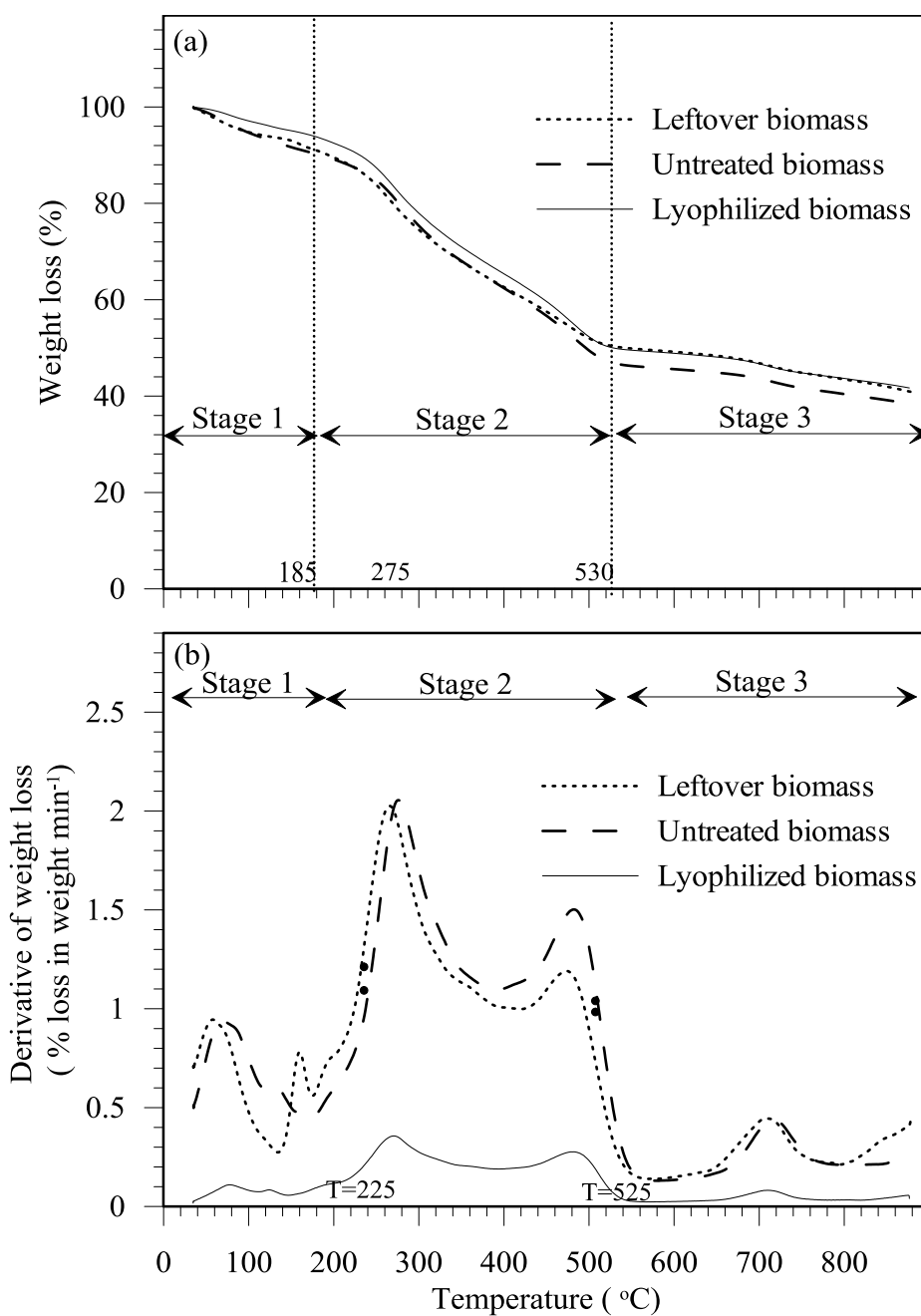
Figure 4.12: (a) Thermal Gravimetric Analysis and (b) thermogravimetric derivative analysis curves of *Scenedesmus* sp. at a heating rate of 10 ^{o}C min^{-1}

4.2.1.3 Supercritical CO2 extraction

A. Biomass pre-treatment effect on extraction yield

SC-CO$_2$ extraction of lipids depends strongly on the matrix pre-treatment. Due to microalgae cell wall rigidity and the negative reported effect of the water

on lipid extraction, cells should be dried and disrupted (lysised). In this work, cells lyophilizing (freeze drying) and mechanical grinding were employed, in which the lyophilization effect on sample general appearance, moisture content, surface area, pore size and extraction yield were investigated. Figure 4.13 shows the lipid extraction yield from the untreated (control) and lyophilized biomass of *Scenedesmus* sp. at 50 $^{\circ}$C, 500 bar and a flow of 2.88 g min^{-1} (3 ml min^{-1}). Generally, lipid extraction exhibits a step of constant extraction rate, which is followed by a rapid decrease in extraction rate.
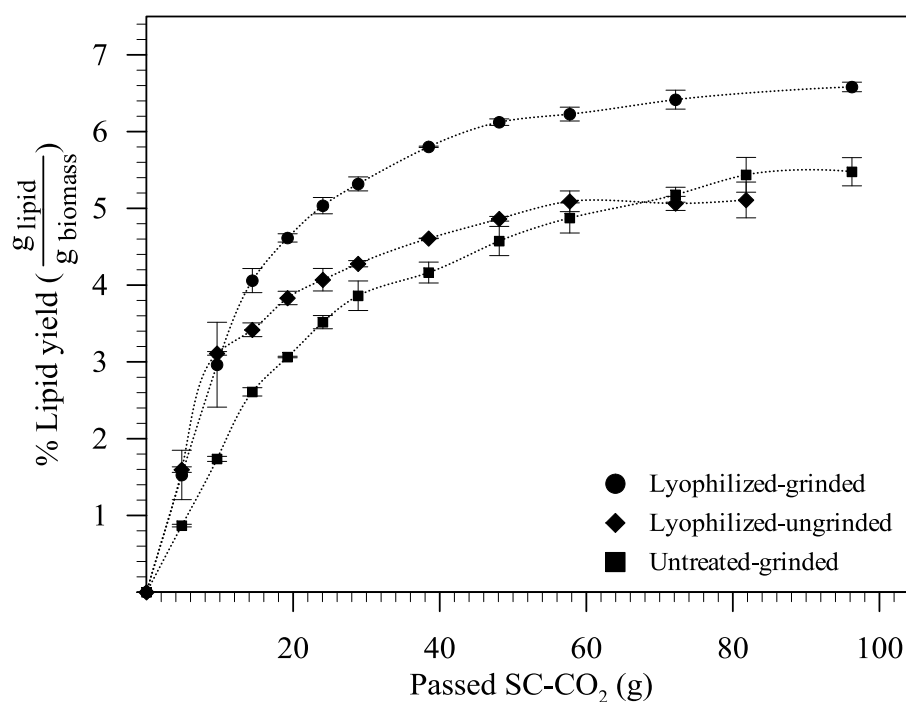
Figure 4.13: Effect of biomass pre-treatment on lipid extraction yield using SC-CO$_2$ at 50 $^{\circ}$C, 500 bar and 2.88 g min^{-1}.

At the beginning of the extraction process, easily accessible lipids were dissolved and extracted, and the extraction in this region was limited by the lipid solubility in the SC-CO$_2$. When the free lipids were depleted, SC-CO$_2$ had to diffuse into the particles, dissolve the lipids and then diffuse out, which was a slow process driven by the lipid diffusivity in the fluid. It is clearly seen from

Figure 4.13 that the highest extraction yield was attained using lyophilized-grinded samples. By lyophilizing, sample moisture content was reduced by 46% reaching 8.3%. In addition to the effective moisture removal by lyophilization, the freeze-thaw cycle improved SC-CO_2 accessibility through the sample. The control (untreated) sample of biomass appeared as clusters, whereas the lyophilized biomass appeared as flakes. The steady state lipid yield of lyophilized-ungrinded sample was almost similar to that of unlyophilized-grinded biomass, whereas, the solubility was high, which was evident in the lyophilization positive effect on enhancing the yield. Figure 4.14 shows eSEM morphological images of the control and treated samples. The comparison revealed that the sample rigidity was higher for the control biomass and decreased by the lyophilization. The effect of lyophilization on the porosity was further proved by surface area and pore size analysis using DR and BJH methods. The surface area results, shown in Table 4.7, revealed that by lyophilizing, the surface area and pore volume increased by about 165% and the pore size by 19%. These enhancements in the structure increased lipid disolvation in SC-CO_2, and, hence, the extraction yield. Therefore, all subsequence runs were carried out using lyophilized samples.
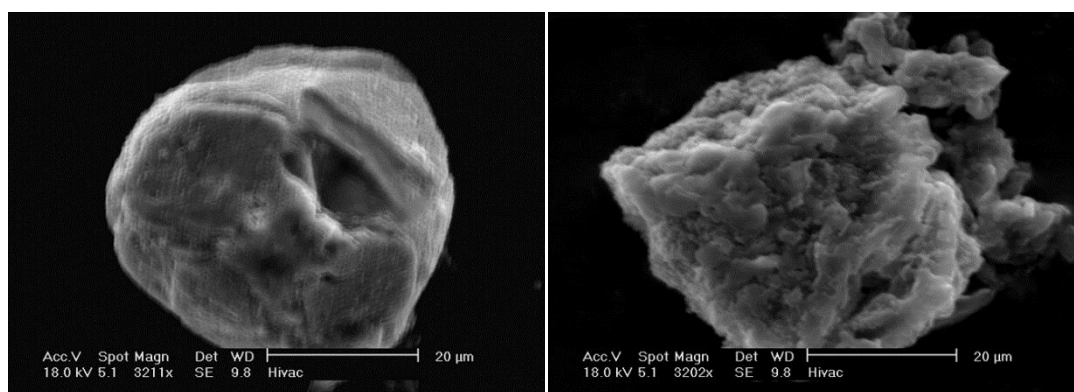
(a)   (b)

Figure 4.14: eSEM images of; (a) original biomass cell and (b) cell after lyophilization

Table 4.7: Surface characteristics of untreated, lyophilized and leftover biomass

Property	Control	Lyophilized	Leftover
Surface area (m^2 g^{-1})	0.5055	1.341	2.241
Micro pore volume (ml g^{-1})	1.796×10^{-4}	4.7×10^{-4}	7.96×10^{-4}
Micro pore size (^{o}A)	1.554×10^2	1.850×10^2	1.66×10^2

Figure 4.13 also shows the effect of particle size reduction, by grinding, on the extraction yield of lyophilized samples. It was found that the extraction yield dramatically increased for the grinded samples compared to un-grinded biomass. Since the extraction rate and yield depend on the internal mass transfer rate in the solid phase, particle size reduction increased the specific surface area and enhanced the SC-CO_2 contact with the soluble components. Mainly, the intra-particle diffusion resistance is smaller in smaller particles due to the shorter diffusion path [429]. Several investigators reported that in some cases decreasing the particle size may lead to solvent channeling [430], hence lowering extraction yield. This drawback, however, was not encountered within the operating conditions used in this work.

B. Parametric effects on extraction yield

The pressure, temperature and flow rate were studied as the key parameters affecting the extraction yield. Three levels were tested for each parameter as shown in Table 4.8. Figure 4.15(a and b) show the effect of temperature and pressure on the steady state extraction yield considered after passing 100 g of SC-CO_2 at a constant volumetric flow rate of 4 ml min^{-1}. Similar

behavior was observed at other SC-CO_2 flow rates, as can be seen in Figures C1 and C2, Appendix C.

Table 4.8: Experimental design conditions, and experimental and predicted yields

Run Number	Process variables			% Yield	
	Temperature (^{o}C)	Pressure (bar)	Mass flow (g min^{-1})	Experimental[*]	Predicted
1	65	350	1.69	4.43± 0.33	4.62
2	65	350	3.38	4.41± 0.16	4.62
3	35	500	2.01	5.03± 0.34	4.81
4	50	500	1.92	7.34± 0.0.11	7.05
5	35	200	3.46	2.92±0.47	3.31
6	50	350	3.60	6.00± 0.51	6.12
7	35	200	1.73	3.61± 0.26	3.32
8	35	500	3.02	4.97± 0.28	4.81
9	65	200	2.07	3.53± 0.42	3.52
10	65	200	1.38	3.67± 0.16	3.52
11	65	500	1.83	6.18± 18	5.72
12	50	200	3.14	5.10± 0.36	5.20
13	35	350	3.81	3.79± 0.28	4.07
14	50	500	2.89	6.81± 0.08	7.05
15	35	350	1.90	4.26± 0.22	4.07
16	50	200	2.35	5.30± 0.38	5.20
17	35	200	2.60	3.36± 0.15	3.32
18	65	350	2.53	4.44± 0.09	4.62
19	65	500	3.68	5.70± 0.25	5.72
20	50	350	1.80	6.62± 0.37	6.12
21	35	350	2.86	3.94± 0.21	4.07
22	50	500	3.85	6.38± 0.34	7.05
23	65	200	2.77	3.47± 0.5	3.51
24	65	500	2.76	5.73± 0.21	5.72
25	50	200	1.57	5.25± 0.21	5.20
26	50	350	2.70	6.30± 0.16	6.12
27	35	500	4.02	4.71± 0.35	4.81

[*] Average values with ±measured uncertanity
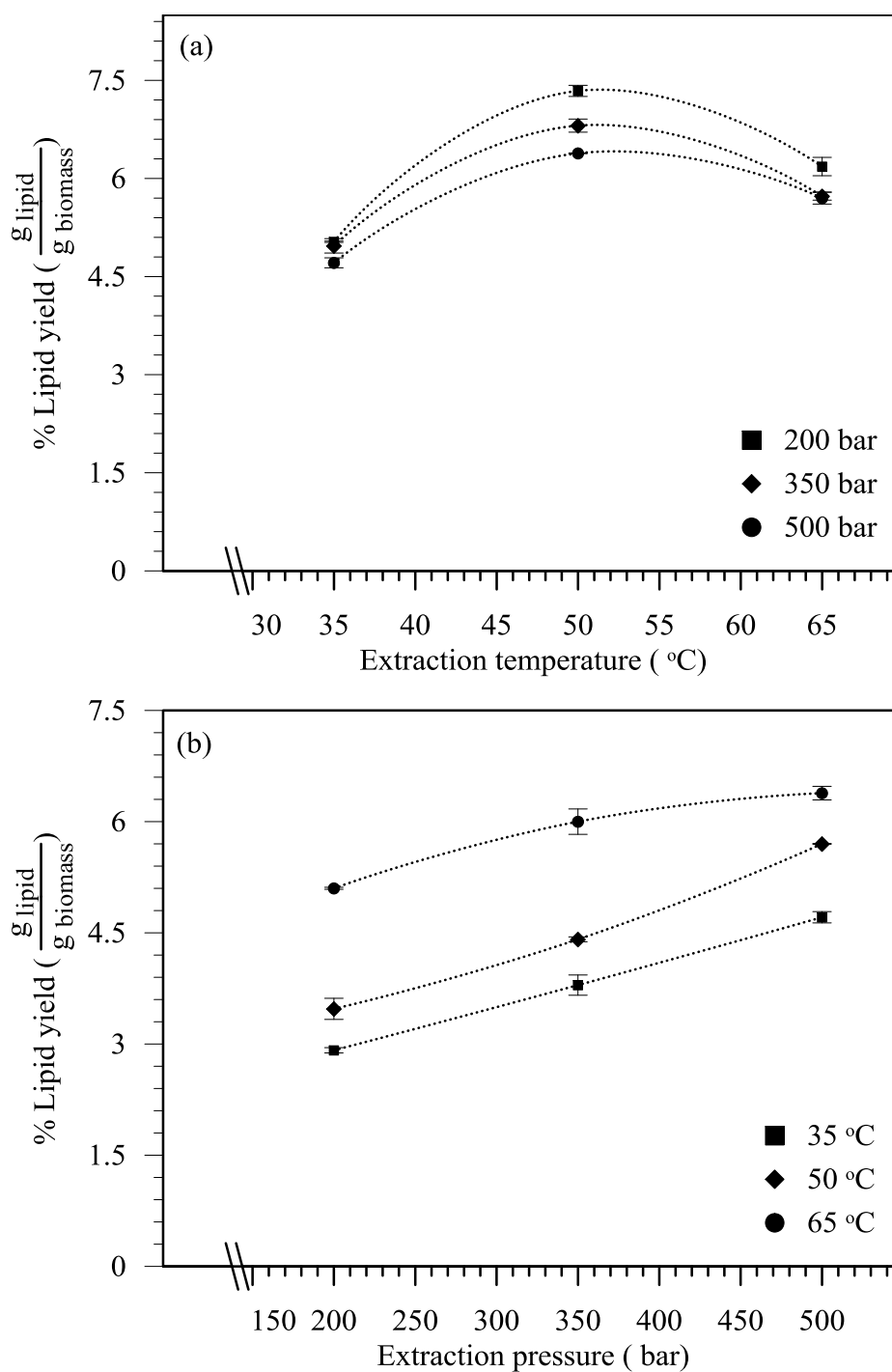
Figure 4.15: Effect of; (a) extraction temperature and (b) pressure variations at 4

ml min^{-1} on extraction yield after passing 100 g of SC-CO$_2$

Figure 4.15 (a) shows that increasing extraction temperature from 35 to

50 ^{o}C increased the extraction yield, whereas a decrease in the yield was

observed at higher temperatures. This is mainly due to the competing effects of

CO_2 solvation and lipid volatility on the solubility. At constant pressure, CO_2 density decreases with increasing temperature, but at the same time the volatility of the triglyceride increases [367]. This competing behavior is known as the crossover phenomenon, which is discussed further later. Figure 4.15 (b) shows lipid extraction yield at 4 ml min^{-1}, and different pressures. It is clearly shown that the extraction yield increased significantly with the increase in pressure leading to higher extraction yields at 500 bar. This was expected as the solubility increased with pressure at constant temperature due to the increase in solvent density, and therefore, increase in solvation power.

The lipid solubility in SC-CO_2 was determined from the initial straight line of the extraction curve between the lipid yield and consumed CO_2, mainly up to passing 10 g of SC-CO_2. Figure 4.16 shows the trend at a selected low flow rate of 0.5 ml min^{-1}, where the solubility at each temperature were plotted as a function of pressure. As shown, the lipid solubility in SC-CO_2 increased from 1.5 to 9.0 x10^{-3} kg m^{-3} at 50 $^{\circ}$C as the pressure increased from 200 to 500 bar, and similar behavior was observed at other temperatures. The crossover solubility, mentioned earlier, was observed at round 350 bar for the three temperatures tested. Above the crossover pressure, the effect of temperature on density becomes less than that on the lipid vapor pressure. A similar crossover phenomenon was observed with SC-CO_2 extraction of soybean oil [431], rice bran oil [27] and fats from lamb [35]. However, a lower crossover pressure, in the range of 200-300 bar was observed for the SC-CO_2 extraction of kernel oil [432].
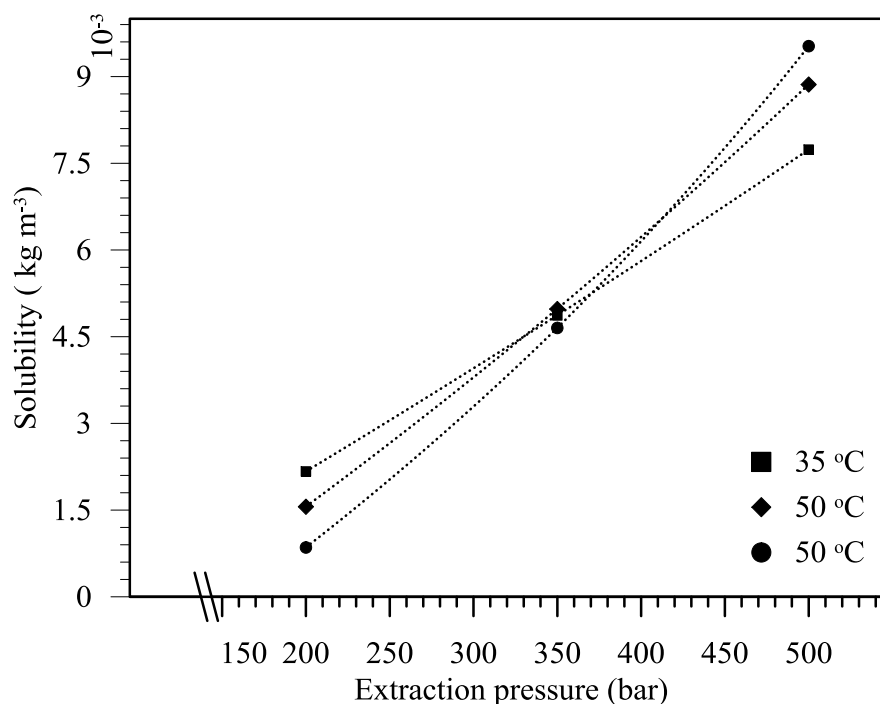
Figure 4.16: Effect of operating pressure on lipid solubility after passing 10 g of SC-CO2 at different operating temperatures and low flowrate of 0.5 ml min-1

The experimentally determined solubility data were used to fit the Chrastil [382] empirical correlation (Eq. 2.29). Table 4.9 shows the obtained parameters determined by non-linear regression technique, which were found to agree well with parameters found from extraction of other vegetable oils [52, 433, 434]

Table 4.9: Solubility model parameters determined by non-linear regression

Oil source	Fitting parameter			Reference
	k_o	a	b	
Microalgae biomass	8.48	-52.55	-3375.67	This study
Pumpkin seed	9.93	-5000.6	-49.25	[435]
Jack Prain Seeds	7.75	-7549.8	-29.90	[433]
Blackcurrant seed	12.6	-5270	-67.07	[52]
Pine kernel	9.29	-46.708	-4602.82	[434]

Figure 4.17 shows the effect of SC-CO_2 flow rate on the extraction yield considered also after passing 100 g of SC-CO_2 at 500 bar and different temperatures. It can be seen that the extraction yield decreased slightly as SC-CO_2 flow rate increased, with this effect increasing at higher temperatures. This is mainly due to the decrease of the residence time that resulted in a shorter contact time between the fluid and the lipid. Therefore, the SC-CO_2 leaving the extraction cell may not be saturated with the lipid, indicating that the intra-particle diffusion resistance controls the extraction at this condition, and a larger amount of CO_2 is needed to reach the steady state. Similar results were also observed at other pressures (shown in Figure C.3 and C.4). It was noted that as the pressure increased, the effect of the flow rate tended to be small. This is because increasing the pressure increased the solubility, and low flow rate provided the sufficient time to reach saturation.
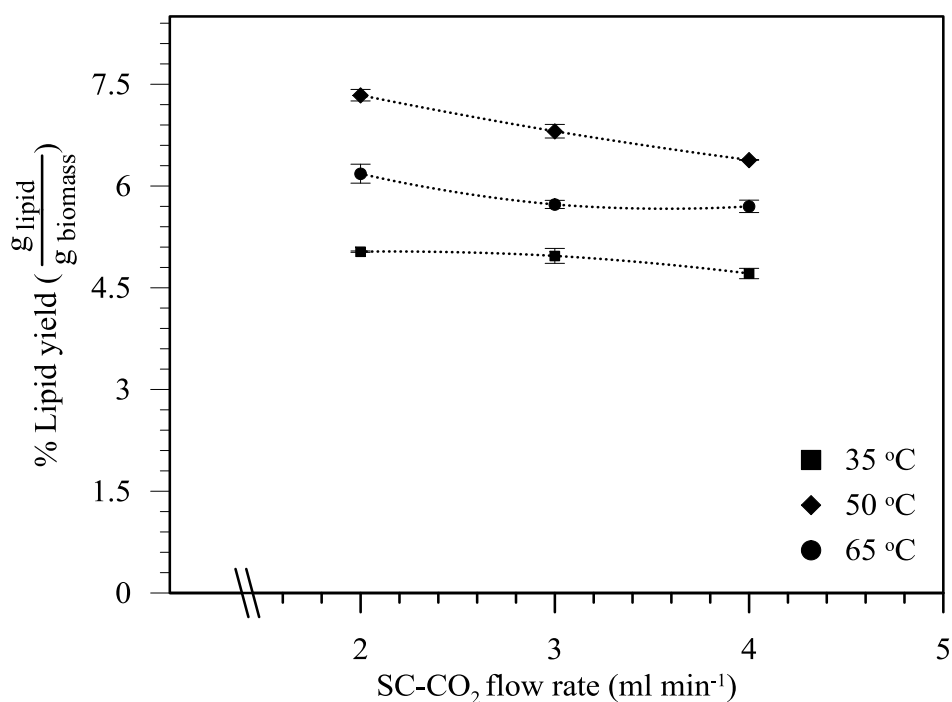
Figure 4.17: Effect of changing SC-CO_2 flow rate at 500 bar for and different temperatures on extraction yield

4.2.1.4   Process conditions optimization

The design of experiments was used to determine statistically the most significant factors that affect the extraction yield, and to optimize the process operating conditions. The effects of the selected three factors; namely pressure, temperature and flowr ate, were studied using 3^3 FFD, as shown in Table 4.8**.** The experimental results were used to determine the parameters of a second-order polynomial model by employing the least squares technique. The model presents the relationship between the lipid yield, at steady state, and process variables, which were temperature, pressure and flow rate. Equation (4.1) shows the regression model with the determined parameters. The degree of significance for each factor is represented by the *p*-value, obtained from MiniTab 16 statistical software and shown in Table 4.10**.** The large absolute value of the *t*-test and the small *p*-value (< 0.05) of any term indicates a more significant effect of that process variable.

$$Y = -14.33 + 0.768\ T + 0.0026\ P - 0.32150\ F - 0.0079\ T^2 + 1 \times 10^{-4}\ T \times P$$

$$+ 0.0033\ T \times F + 1.64 \times 10^{-5}\ P^2 - 0.0003\ P \times F + 0.0011\ F^2 \pm 0.2166 \tag{4.1}$$

Table 4.10: Regression model coefficients of the response surface polynomial
function of lipid extraction yield obtained by MiniTab 16

Coefficient	Value	Standard error	t-value	p-value
α_0	-14.33	1.509	-9.496	0.000
α_T	0.77	0.043	17.961	0.000
α_P	2.6×10^{-3}	3.3×10^{-3}	0.774	0.450
α_F	-0.32	0.623	-0.516	0.612
α_{TT}	-7.9×10^{-3}	3.9×10^{-4}	-20.287	0.000
α_{PP}	0.00	0.00	0.333	0.743
α_{FF}	1.1×10^{-3}	0.106	0.010	0.992
α_{TP}	1×10^{-4}	$3 \times 10\text{-}5$	2.562	0.020
α_{TF}	3.3×10^{-3}	5.23×10^{-3}	0.632	0.536
α_{PF}	-3×10^{-4}	6.0×10^{-4}	-0.445	0.662

From the statistical analysis of the regression coefficients, it was found that the extraction yield was highly affected by temperature and its square term, pressure and the interaction between the temperature and pressure. The coefficients that were insignificant were eliminated, and the final refined model was refitted. The refined model is shown in Eq (4.2).

$$Y = -15.3651 + 0.7822\ T + 0.0022\ P - 0.0079\ T^2 + 7.85 \times 10^{-5}\ T \times P \pm 0.278 \quad (4.2)$$

The analysis of variance (ANOVA) results, shown in Table 4.11 demonstrate that the refined model predictions were adequate, as indicated by ANOVA lack-of-fit analysis (*p-value*>0.2156; not significant). The coefficient of determination (R^2) and adjusted coefficient of determination (adj.R^2) were 95.48, and 94.66 %, respectively. These values also indicate that the model presents well the experimental data well. The suitability of the fit can also be seen in Figure 4.18, which shows a scatter plot of experimental verces predicted lipid yield.

Table 4.11: ANOVA results of the refined extraction model

Source	Degree of Freedom	Adjusted sum of squares	Adjusted mean square	F-test	p-value
Regression	4	36.15	9.04	116.30	<0.0001
Temperature	1	17.39	17.39	223.81	<0.0001
Pressure	1	0.11	0.11	1.48	0.24
Temperature x Temperature	1	19.02	19.02	244.78	<0.0001
Temperature x Pressure	1	0.37	0.37	4.82	0.04
Error	22	1.71	0.08		
Lack-of-Fit	4	0.45	0.11	1.60	0.21
Pure Error	18	1.26	0.07		
Total	26				
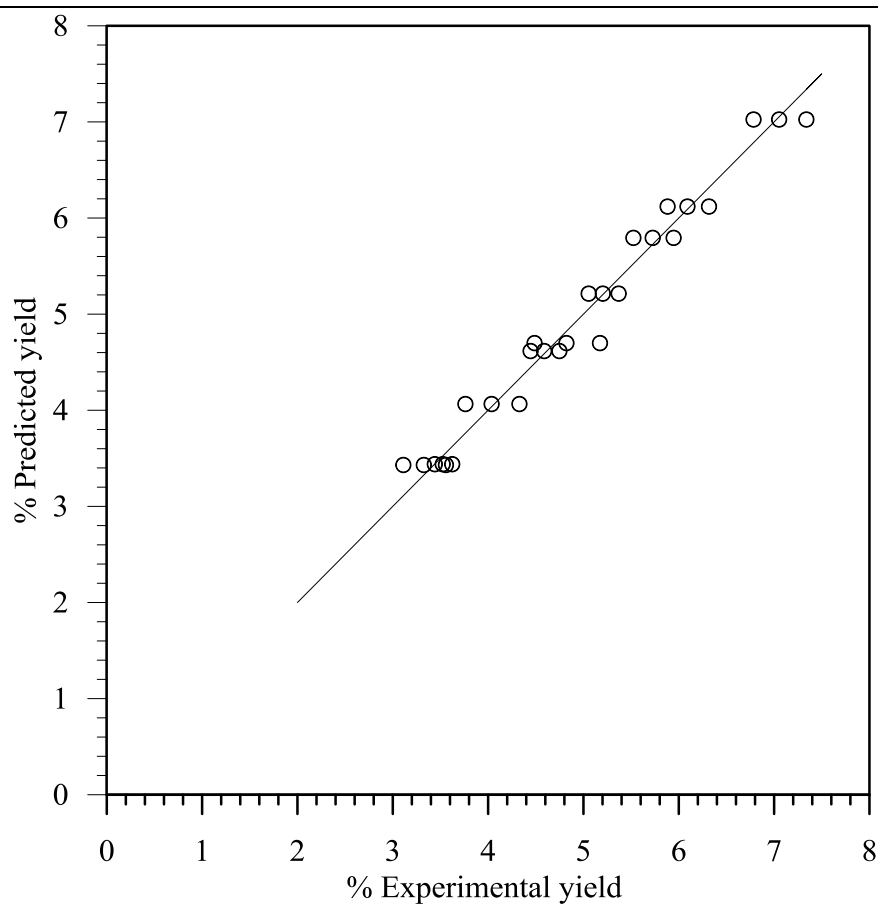
Figure 4.18: Comparison between experimentally determined extraction yield and the refined model predictions

A. Process optimization

To determine the optimum conditions in the range investigated in this work, the optimization tool in Minitab software was used based on the model equation (Eq. 4.2). The best operating conditions for lipid extraction were determined to be 53 ^{o}C, 500 bar and 1.9 g min^{-1} (2 ml min^{-1}), from which the yield was estimated to be 7.05 %. The model suitability was validated by performing an independent experiment at the selected best conditions in a duplicate. The extraction yield was found to be 7.41± 0.11 %, which is very close to that predicted by the model with less than 5 % deviation.

The influence of process variables on extraction yield was plotted in three dimensional (surface plot) and contour plots to visualize their combined effects. The response surface plot was developed using the refined quadratic model (Eq. 4.2). Figure 4.19 shows the effects of the two significant parameters, pressure and temperature, on the lipid extraction yield. It is clearly seen that the extraction yield was significantly affected by temperature variations. At a constant pressure, extraction yield increased with temperature to a certain value (just over 50 ^{o}C), then decreased, which also agrees with the experimental results.
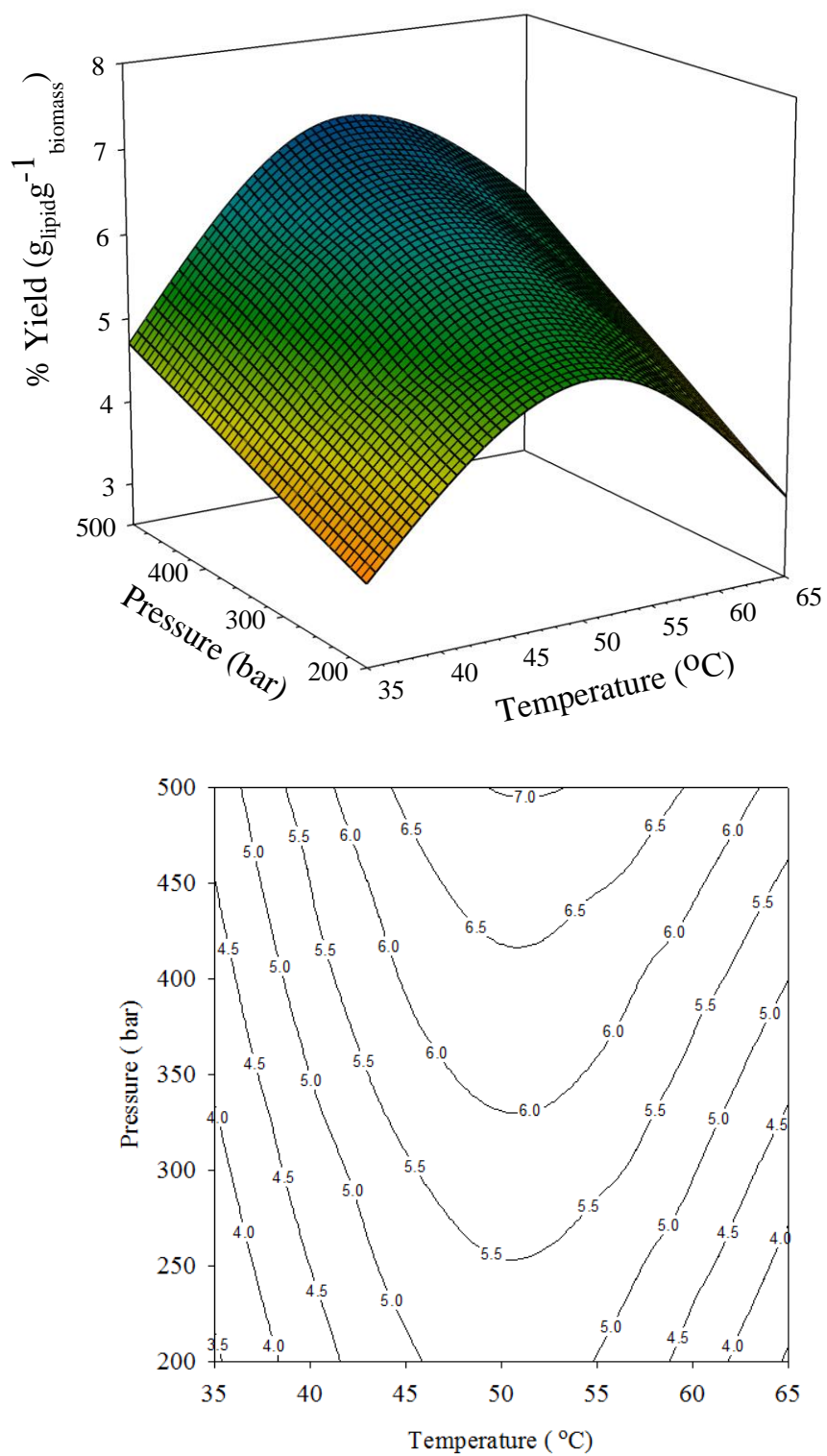
Figure 4.19: Extraction yield surface and contour plots as a function of temperature and pressure after passing 100g of CO_2 at flow rate of 3 ml min-1

4.2.1.5   Extraction from laboratory scaled-up unit

As mentioned in section 3.2.4.2, a laboratory scaled-up experiment was carried out at the optimum conditions, determined by RSM, namely at 53°C and 500 bar, with 25 g of lyophilized and grinded biomass. The process scaling-up was carried out by maintaining the bed height to diameter (H/D) ratio constant at 3.3 for the two scales. In addition, as suggested by Prado et al. [425] solvent flow rate to biomass (F/m) ratio in the two scales was kept the same. Thus, the flow rate in the scaled-up scale was 15.26 g min^{-1} (16 ml min^{-1}), compared to the 1.9 g min^{-1} (2 ml min^{-1}) used in the in small scale runs, with a total of 625 g of CO_2 passed. The total yield within 1 h of extraction was found to be 6.2%, which is close to that found in the small scale experiment and predicted by the refined model.

4.2.2   Wet biomass

4.2.2.1   Drying effect on the yield

As mentioned earlier, drying is a time consuming step and considered an energy intensive process. Thus, in this study the lipid extraction from lyophilized cells was compared to that from wet biomass, and Soxhlet extraction from lyophilized biomass of *Scenedesmus* sp. using *n*-hexane was used to determine the total lipid content of concentrated biomass from the 320 L open pond, which was found to be 21.1 ±1.5 %. The lipid extraction was also performed using static *n*-hexane, as a solvent and left overnight in an incubator at 50 $^{\circ}$C. Figure 4.20 shows the lipid extraction yield, on dry weight basis, for different pre-treatment and extraction techniques. As shown in the figure, lipid extraction yield from the wet sample was only 4 % compared to 12.6 % achieved from lyophilized

biomass. The lower lipid extraction yield from the wet sample was mainly due to the water film formed over the lipid, which prevents the solvent from contacting it, whereas, the higher value obtained from lyophilized biomass was mainly due to the drying and cell disruption effect mentioned earlier by lyophilization. This suggests further consideration of cell disruption on enhancement of lipid extraction. The reproducibility of the results was confirmed by doing the experiments at least in a duplicate, and the results presented in Figure 4.20. Avoiding this step would significantly enhance the microalgae-biodiesel production process.
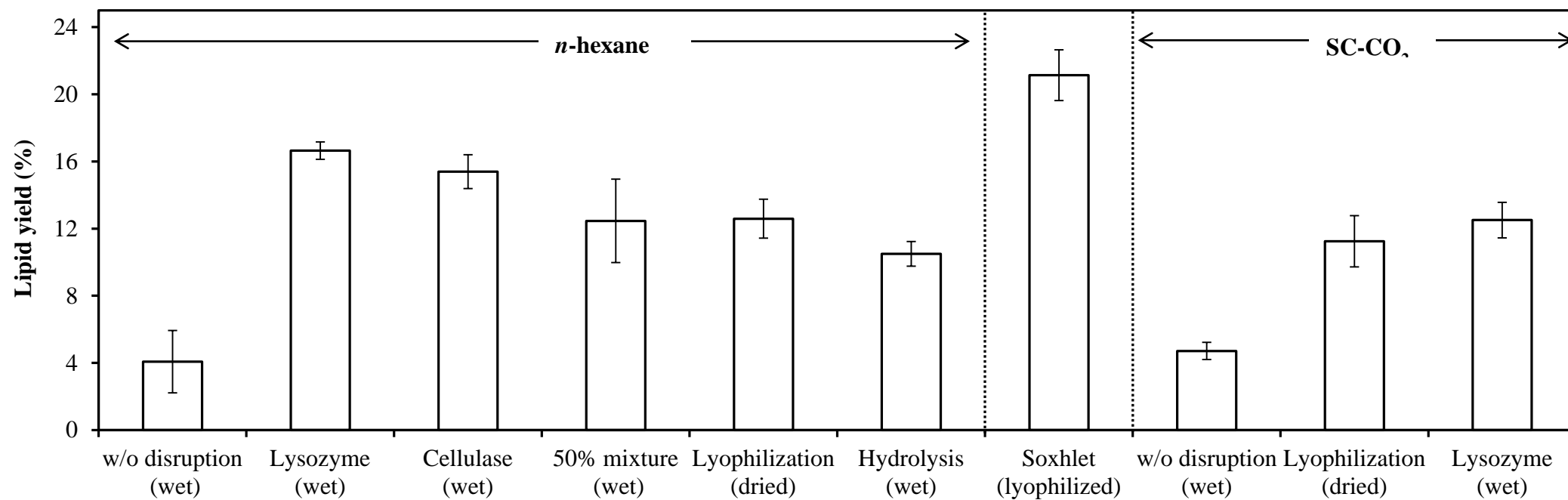
Figure 4.20: Yield of extracted lipid by *n*-hexane and SC-CO₂ with different treatments. The dashed horizontal line represents the total lipid content by determined by Soxhlet extraction from lyophilized biomass

4.2.2.2   Cell disruption effect on the yield

Microalga cells wall are rigid and tough, which acts as a barrier to efficient extraction. Thus, for efficient extraction of lipids, cells walls need to be disrupted. The main parameters that determine disruption method suitability are process cost, scalability and product contamination with other cell components. Lyophilization disrupts algal cell and makes cell walls more porous, in addition to the drying effect that enhanced the extraction yield [436]. However this technique requires high energy to freeze the samples and its operation and maintenance costs are relatively high, which is usually not justified in energy production processes.

Based on algae cells walls structure, which is mainly composed of 24–74 % neutral sugars [336], acid treatment has been suggested to liberate the lipid [343]. Pre-treatment using diluted sulfuric acid was tested in this work, and resulted in a lipid extraction yield of 10 %. However, using acids is neither recommended in fuel production nor for the leftover biomass applications. In addition, using acids require special materials of construction, which is not recomended for large-scale applications.

To test enzymatic treatment, two enzymes have been tested, namely lysozyme, naturally used to disrupt bacterial cell walls, and cellulase, which catalyzes the hydrolysis of cellulose. The latter was tested to disrupt the cellulosic structure of the cell walls. Figure 4.20 shows that lipid extraction yields from wet samples using both enzymes, separately, resulted in a better yield than even the lyophilized samples, with values of 16.6 and 15.4 % using lysozyme and cellulase,

respectively. This is a significant finding as it shows that using either enzyme, with lysozyme showing slightly better results, lipid can be extracted from awet sample without the need for the time consuming and energy intensive drying step. The result clearly shows the superiority of using lysozyme, or cellulase, in the extraction of lipid from wet microalgae, while avoiding the drying step. The synergic effect of both enzymes was tested using 50 % mixture of lysozyme and cellulase; however a lower yield of 12 % was achieved. This could be due to the formation of a product from one enzymatic reaction that inhibits the other enzymatic reaction. Cellulase, from the same source used in this study, has also been tested by Liang et al [437] to assist lipid extraction from pre-ultrasonicated wet cells of *Chlorella vulgaris*. Although the lipid extraction yield increased by increasing the enzymatic concentration, the recovery was only 15 % compared to that obtained in this study, which was 72 % compared to the total lipid extracted from lyophilized biomass using Soxhlet apparatus.

To study the pretreatment significance, one-way ANOVA was used, and it proved that there is a significant difference in the yield with *p*-value equal to 0.038 between the different disruption methods and the Fisher's (95 % confidence intervals) multiple comparison demonstrating that the yields of the individual enzymes use are close, whereas the enzyme mixture yield was not.

Although the use of the enzymes has shown to be effective, their industrial implementation for fuel production is often limited due to their high cost. Having said that, the price of lysozyme is relatively inexpensive, compared to other enzymes [438]. In addition, it can be repeatedly used for many cycles without any significant

loss of activity when used in an immobilized form. Immobilization of the enzyme also has the advantage of enhancing the recovery and purification steps. Lysozyme immobilized on extrudate-shaped NaY zeolite has been successfully used for 12 cycles [439].

Due to SC-CO_2 superiority over conventional solvent extraction, the application of enzymatic treatment with SC-CO_2 extraction from wet cells using lysozyme has been tested. The lipid extraction yield was 12.5 %, which is almost 75 % of that extracted using *n*-hexane. The significant difference in the yield was also confirmed by one way ANOVA, where a *p*-value of 0.033 was obtained. This relatively lower yield can be attributed to some free lipid that may have been lost in the enzymatic aqueous solution during the disruption step after centrifugation. This did not occur with *n*-hexane extraction, as the solvent was added before the centrifugation, which was not possible in the SC-CO_2 extraction. Nevertheless, due to its favorable features, the successful use of SC-CO_2 with wet biomass is still a major finding. When considering the extract yield, quality, costs and environmental impacts of using chemical solvents, the enzymatic disruption, followed by SC-CO_2 extraction, could probably be the most efficient for biodiesel production from wet biomass. This is especially true if the leftover, protein rich, biomass after lipid extraction is used in pharmaceutical or food industries.

Operation time and cost are the main concerns in the commercial process. SC-CO_2 method has a much shorter extraction time with less solvent consumption compared to organic solvents. Although the operation cost might be higher due to the pumping cost, this could be counterbalanced by lower down-streaming cost, as no

solvent recovery unit is required and the solvent can be separated by simple depressurizing and recycled back.

4.2.2.3 Analysis of extracted lipid

Complete analysis of the fatty acid composition of the extracted lipid by SC-CO_2 at different temperature and pressure combinations for lyophilized biomass were carried out using GC-FID. Mass fractions were normalized according to the total fatty acids found by the GC analysis. Table 4.12 shows the weight percentage of the main fatty acids in the extracted lipids. It was found that the main fatty acid in all cases was linoleic acid, which counted for more than 40 % of the total fatty acids. ANOVA analysis was used to assess the influence of the operating conditions on the fatty acid content and not much difference was observed. Similar analysis was carried for extracted lipid from wet biomass at different treatments and extraction solvents. Table 4.12 shows the lipid composition with different treatments. The obtained unsaturation ratio was in the range of 1.5-3. No significant change in composition was observed by using different treatments and extraction techniques. However, the total fatty acid of the lipid extracted by SC-CO_2 was slightly lower in all treatments, which is mainly due to the solubility of other pigments in SC-CO_2.

Table 4.12: Fatty acid composition (% w/w) of the lipid extracted using SC-CO_2 and *n*-hexane with different disruption methods

Fatty acid	*n*-hexane extraction [*]					SC-CO_2 Extraction [*]			
	lyophilization[a]	wet	acid treatment	lysozyme	cellulase	lyophilization[a]	wet	lysozyme	lyophilization[b]
C14:0	3.20 ±0.4	6.10 ±0.8	7.50 ±0.5	7.5 ±0.7	6.00 ±0.4	3.50 ±0.1	5.70 ±0.6	7.00 ±0.2	3.20 ±0.05
C16:0	21.0 ±0.09	12.2 ±0.5	15.1 ±0.2	16.4 ±0.08	11.9 ±0.3	16.5 ±0.4	14.3 ±0.3	18.6 ±0.2	17.4 ±0.7
C18:0	8.10 ±0.5	8.20 ±0.8	11.3 ±0.4	13.4 ±0.1	13.1 ±0.7	4.70 ±0.6	5.70 ±0.9	9.30 ±0.6	6.30 ±0.4
C18:1	12.9 ±0.1	2.00 ±0.9	-	6.0 ±0.7	4.80 ±0.9	11.8 ±0.54	-	4.70 ±0.1	12.1 ±0.9
C18:1 (*trans-9*)	8.10 ±0.4	12.2 ±0.7	9.40 ±0.7	7.5 ±0.96	7.10 ±0.4	9.40 ±0.1	11.4 ±0.4	-	8.20 ±0.5
C18:2	1.60 ±0.6	2.00 ±0.03	1.90 ±0.2	4.5 ±0.8	6.00 ±0.8	-	2.90 ±0.5	7.00 ±0.4	0.60 ±0.7
C18:2 (*n6*)	43.5 ±0.9	53.1 ±0.7	50.9 ±0.2	41.8 ±0.1	45.2 ±0.9	44.7 ±0.6	54.3 ±0.1	41.9 ±0.2	40.7 ±0.6
C18:3 (*n3*)	-	4.10 ±0.4	-	-	2.40 ±0.1	7.10 ±0.2	2.90 ±0.3	4.70 ±0.7	8.40 ±0.8
C20:0	-	-	1.90 ±0.8	-	3.60 ±0.4	-	2.90 ±0.6	4.70 ±0.3	1.20 ±0.6
C22:0	1.60 ±0.1	-	1.90 ±0.1	3.0 ±0.6	-	2.40 ±0.4	-	2.30±01	1.90±0.02
Total fatty acids	84.3	76.9	79.7	82.2	79.0	69.6	73.5	76.1	78.2
U/S[c]	2.0	2.8	1.7	1.5	1.9	2.7	2.5	1.4	2.3

[*] Average values with ±measured uncertainty

[a] extraction from lyophilized cell grown in +3N-BBM

[b] extraction from lyophilized cell grown in -N-BBM

4.2.3   Mathematical modeling of extraction

4.2.3.1   Extraction curve modeling

For the modeling the SC-CO_2 extraction process, the overall extraction curves (OECs) at the tested conditions were plotted, by considering the mass of the extracted lipids as a function of the specific CO_2 consumption, in lipid free basis as depicted in Figure 4.21. Each experimental data point shown is the result of the average of different two performed individual experiments. It is important to mention that in ISCO system capabilities, the volumetric flowrate is calculated from which the mass flowrate was determined from the density changes with temperature and pressure in real cases. The extraction curves at all tested conditions were modeled using the BIC model developed by Sovova [380], and shown in Eq. (2.21-2.23). The model curves have been drawn, as dot lines on Figure 4.21 to compare their prediction to the experimental data. The Z and W dimensionless parameters, and the intact cell concentration (x_k), were used as the adjustable parameters and determined by minimizing the errors between the experimental and predicted data. The initial guesses of Z values were estimated from the film mass transfer coefficient using the empirical correlation given by Tan et al. [138], shown in Table 2.19. The new values of Z were then determined by error minimization.

The model curves are determined and drawn as dotted lines in Figure 4.21. The results indicate that the BIC model showed a good representation of experimental data all tested conditions. The extraction curves indicate that the process was divided into three periods, as proposed by Sovova, which are the rapid, falling and slow extraction period. In the first period, the

easily accessible lipids were extracted and the convection was the dominant mechanism. The amount of lipids extracted in this period was limited by the solubility of the lipids in SC-CO$_2$. Then, the extraction took longer for the solute trapped inside particles to diffuse out compared to the lipids allocated on the particle surface, which resulted a reduction in mass transfer coefficient in the solid phase in the second region. In this stage, the diffusion mechanism starts to combine with convection resulting in a slower reaction rate. In the last stage the mass transfer occurred mainly by the diffusion.

Table 4.13 summarizes the fitted and calculated model parameters at all tested conditions. The OF's values ranged from 1.89×10^{-1} to 3.18×10^{-2} and R^2 was always above 97.5 %, which indicates that the model showed excellent agreement with the experimental data. The mass transfer coefficients in both phases (k_f and k_s) were evaluated, based on the determined Z and W parameters values. It was found that the values of mass transfer coefficient, k_f in the fluid phase were about four to five-orders of magnitude larger than those in the solid phase, k_s. This was expected as the convection in the fluid phase is the main transport mechanism in SFE. The small particles, with average particle diameter of 0.193 mm used in the work also favored this phase transfer over the solid phase. The very low k_s values, compared to k_f, is also due to their dependence on the diffusion of the unbroken cells, which are hardly accessible in microalgae because of the rigid cell walls. Similar coefficients ranges were also found, even extracting oil from paprika fruit [440] and rosehip seed [50]
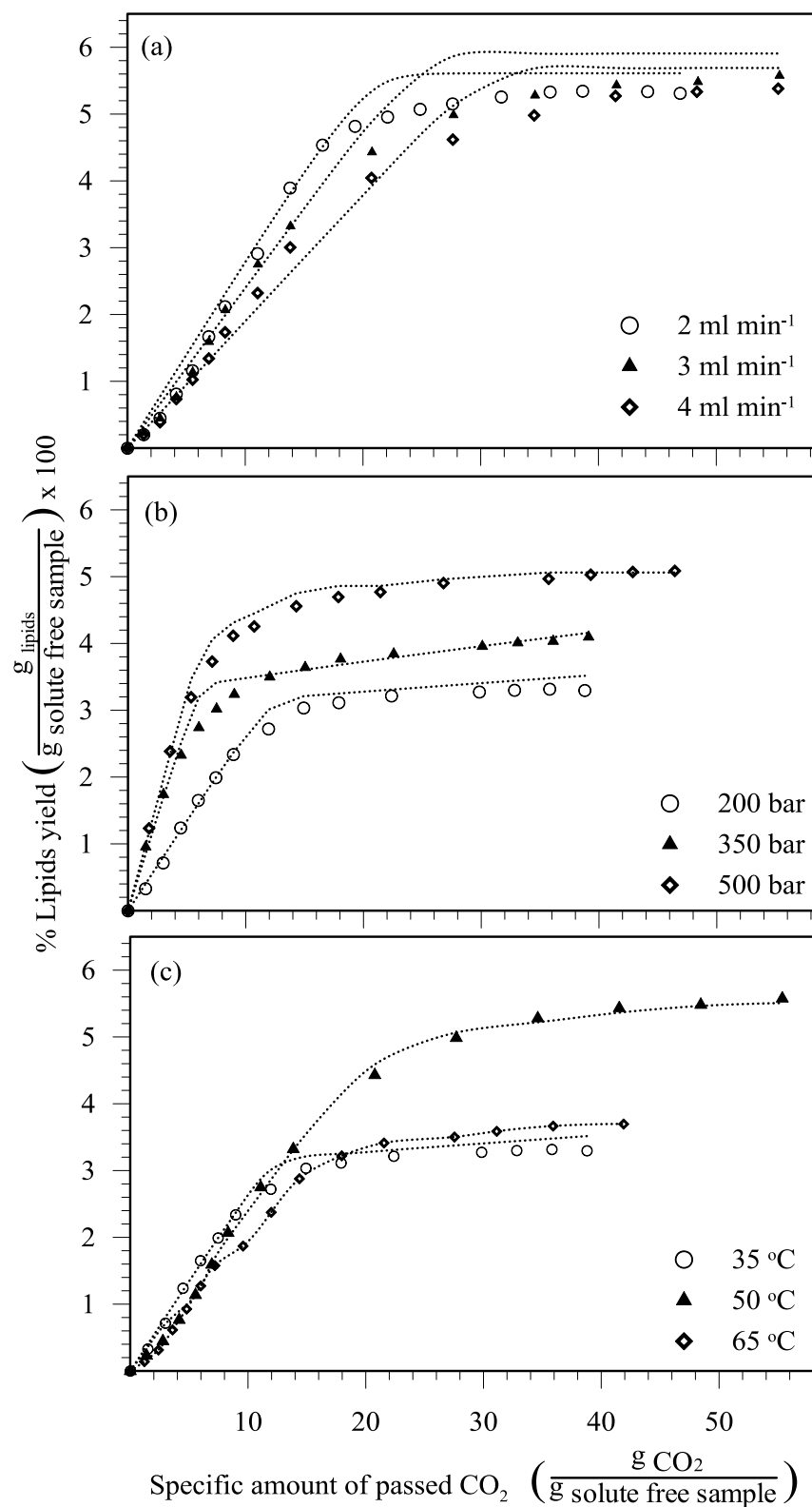
Figure 4.21: Overall extractive curves at 200 bar, 3 ml min^{-1} and different temperatures (a) 50 ^{o}C, 200 bar and different volumetric flow rates, (b) at 35 ^{o}C, 3 ml min^{-1} and different pressures, and (c)

Table 4.13: Experimental conditions, model parameters and accuracy and calculated mass transfer coefficients

Run number	Experimental conditions				Fitting parameters			Calculated parameters		Model accuracy	
	Temperature (^{o}C)	Pressure (bar)	Flow rate		Z	W	x_k	k_f ($\times 10^{-6}$)	ks ($\times 10^{-10}$)	R^2	OF
			(ml min^{-1})	(g s^{-1})							
1	35	200	2	104	4.8	0.48	0.014	7.14	2.63	99.5	0.081
2	35	200	3	156	5.9	0.36	0.013	13.08	2.97	99.8	0.041
3	35	200	4	208	6.9	0.34	0.013	20.23	3.70	99.8	0.040
4	35	350	2	114	4.6	0.39	0.012	6.85	2.39	99.0	0.064
5	35	350	3	171	5.2	0.31	0.018	11.44	2.81	99.2	0.069
6	35	350	4	229	6.6	0.31	0.017	19.47	3.81	98.9	0.060
7	35	500	2	121	4.5	0.32	0.020	6.65	2.08	99.8	0.034
8	35	500	3	181	5.7	0.27	0.021	12.57	2.57	99.6	0.047
9	35	500	4	241	6.5	0.26	0.022	19.18	3.33	98.7	0.091
10	50	200	2	94	0.6	0.67	0.018	9.11	3.36	0.1	0.000
11	50	200	3	141	7.5	0.63	0.023	16.63	4.73	99.6	0.106
12	50	200	4	188	0.8	0.64	0.021	23.91	6.38	0.1	0.000

Table 4.13: Experimental conditions, model parameters and accuracy and calculated mass transfer coefficients

13	50	350	2	108	6.1	0.45	0.027	9.00	2.5.9	99.7	0.032
14	50	350	3	162	7.6	0.39	0.028	16.82	3.32	99.4	0.075
15	50	350	4	216	8.6	0.45	0.026	25.38	5.14	97.5	0.102
16	50	500	2	115	5.9	0.40	0.028	8.71	2.45	99.1	0.122
17	50	500	3	173	7.3	0.32	0.029	16.05	2.89	99.2	0.067
18	50	500	4	231	8.4	0.32	0.027	24.64	3.90	98.6	0.094
19	65	200	2	83	7.2	0.92	0.015	10.64	4.05	99.7	0.117
20	65	200	3	125	8.9	0.99	0.015	19.70	6.54	99.7	1.891
21	65	200	4	166	10.0	1.50	0.014	29.58	13.21	99.1	0.096
22	65	350	2	101	7.4	0.68	0.017	10.85	3.68	99.3	0.064
23	65	350	3	152	8.9	0.61	0.018	19.74	4.92	99.1	0.113
24	65	350	4	203	10.5	0.95	0.018	30.86	10.25	98.8	1.036
25	65	500	2	110	7.2	0.59	0.025	10.66	3.47	98.0	0.098
26	65	500	3	165	8.7	0.51	0.023	19.28	4.47	98.4	0.086
27	65	500	4	221	10.2	0.57	0.023	29.95	6.68	98.3	0.080

4.2.3.2   Effects of process conditions

As mentioned earlier, Sovova had considered both the internal and external mass transfer resistances in the proposed model. Figure 4.22(a-c) shows the effect of the extraction conditions on the mass transfer coefficient in the fluid phase, k_f. The values obtained in this work ranged from 6.7×10^{-6} to 3.1×10^{-5} m s^{-1}, which is close to the reported values reported by [50, 440]. At a particular extraction temperature and pressure, increasing the fluid flow rate, resulted in increasing the interstitial fluid velocity, which in turn resulted in increasing k_f, as shown in Figure 4.22(a) at 50 $^{\rm o}$C and different operating pressure. This is mainly due to the increase in the convection at higher flowrate that causes reduction in the film layer surrounding the solid, and hence, decreasing the mass transfer resistance. A similar trend was reported for the extraction of oils from almond oil [441]. In addition, at a particular temperature and pressure, and for constant particle size, it was found that the values of x_k of intact cells were almost constant, as shown in Table 4.13, which is expected as the solid phase depends mainly on the particle structure and fluid conditions; namely temperature and pressure, and any changes in the flow rate and bed height should not affect this parameter.

A similar, but less significant, effect on k_f was found with temperature variation (Figure 4.22-b), which is mainly due to the decrease in the resistance and the increase of lipid solubility in SC-CO$_2$. On the other hand, the increase in pressure resulted in a slight decrease in the k_f due to the dominant negative effect of the diffusivity compared to the positive effect of the solubility with the

increase in pressure (Figure 4.22-c). Similar effects of pressure and temperature were also found at all tested flow rates.
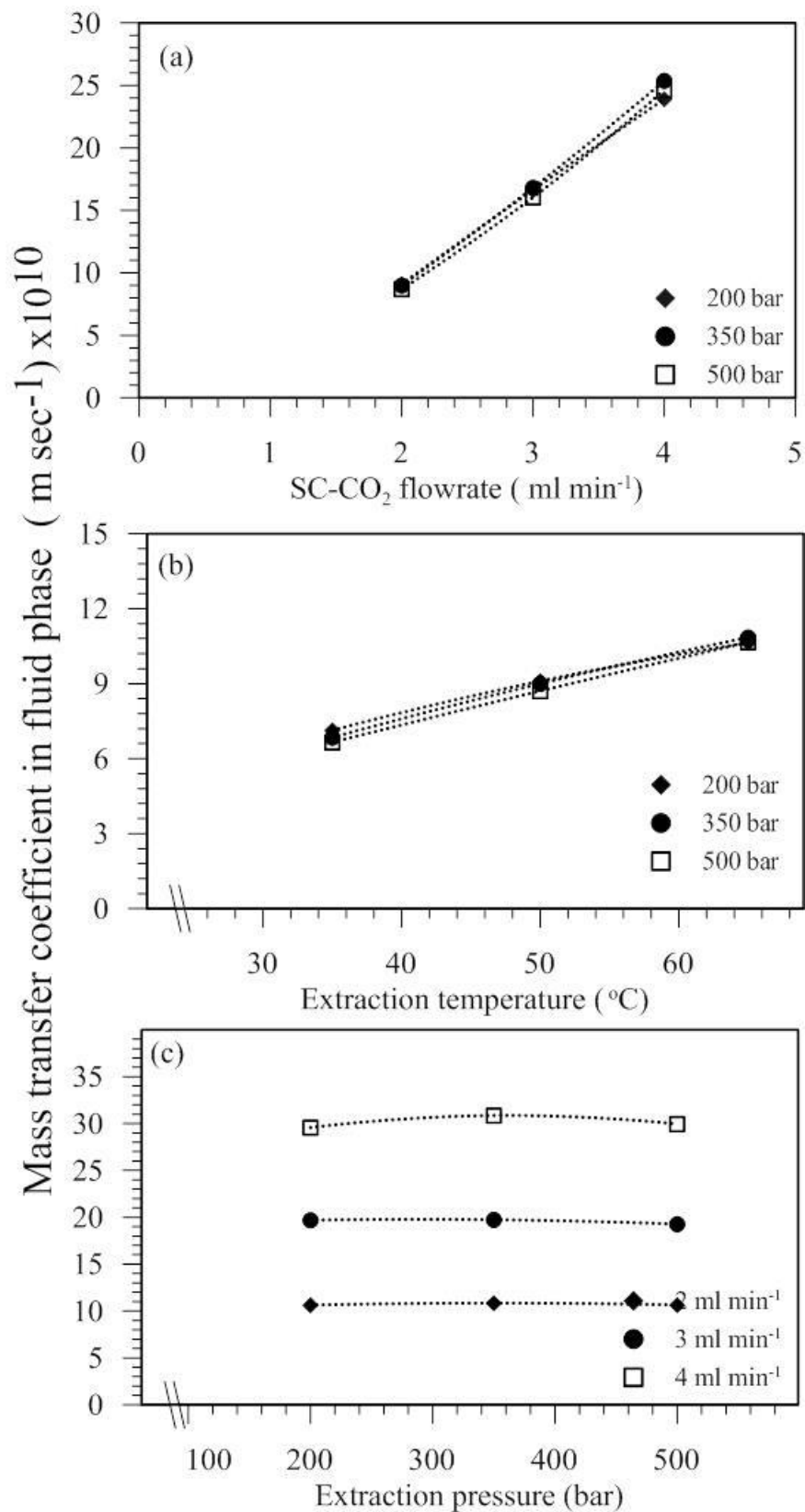
Figure 4.22: Effect of extraction conditions; (a) flow rate at 50 $^{\circ}$C and different pressures, (b) temperature at 2 ml nin^{-1} and different pressures and (c) pressure at 65 $^{\circ}$C and different flow rates and (c)

The solid phase mass transfer coefficient (k_s) is related to the diffusion of lipids enriched SC-CO$_2$ through the solids pores. Therefore, this coefficient depends on sample pretreatment, which affect the pore size. Figure (4.23 a-c) shows the effects of the process variables on k_s. The extraction pressure affects the solvent properties by increasing the density and, therefore, the increasing solubility, resulting in much lipids extraction, and therefore less k_f . In addition, the pressure may also affect the geometry of pore structure of the particles resulting in lower diffusivity of enriched SC-CO$_2$ to the bulk, and hence, resulted in decreasing k$_s$, as shown in Figure 4.23 (a). Increasing the flow rate, on the other hand, increased k_s, as shown in Figure 4.23(b), which is also due to the reduction in the film thickness surrounding that particle, but the effect was much less compared to k_f. Increasing the temperature also increased k_s by increasing lipids solubility in SC-CO$_2$ and diffusivity of the enriched SC-CO$_2$ to the bulk.
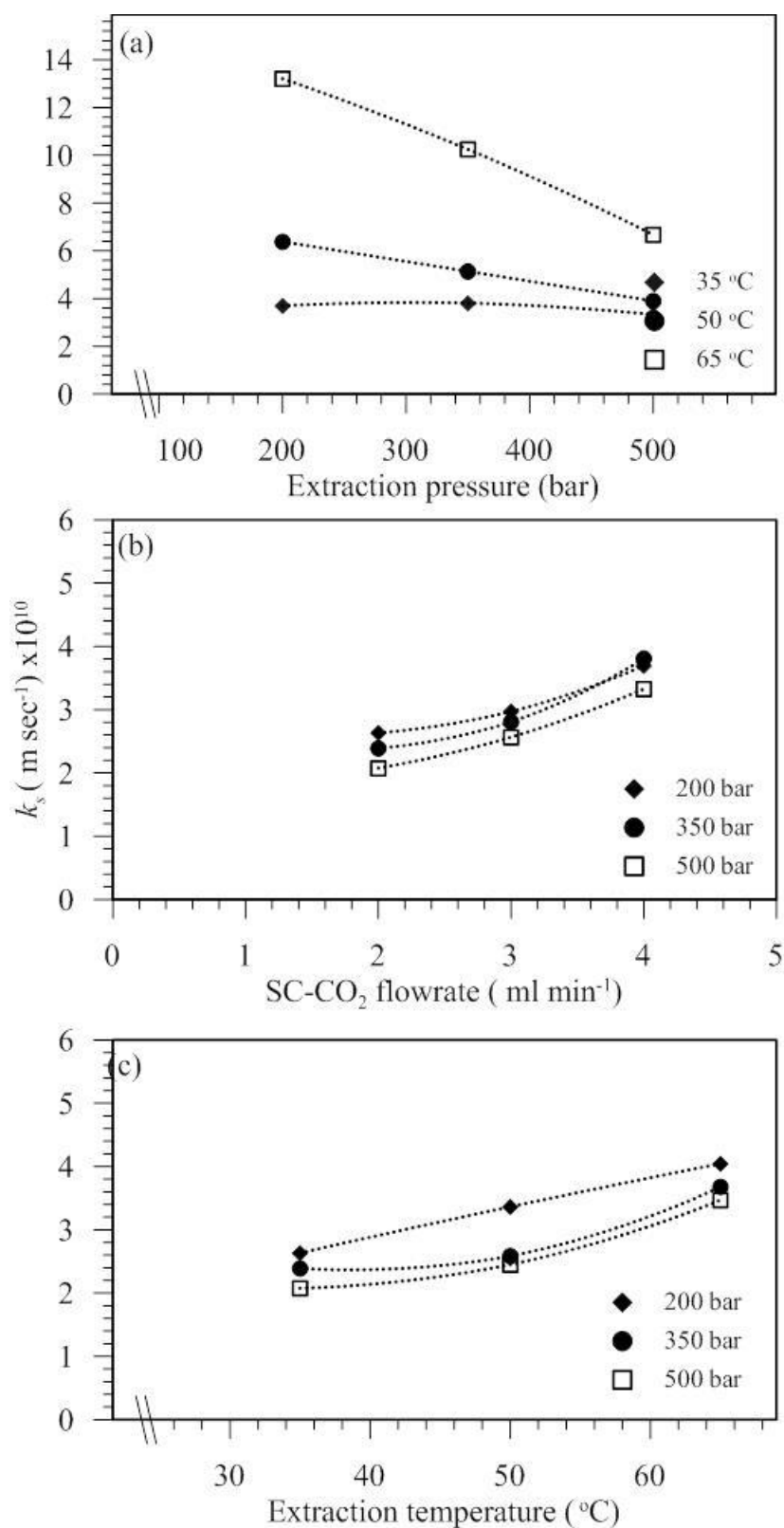
Figure 4.23: Effect of extraction conditions; (a) pressure at 4 ml min^{-1} and different temperatures, (b) flow rate at 35 ^{o}C and different pressures and (c) temperature at 2 ml nin^{-1} and different pressures

For the evaluation of SCF extraction effectiveness, the extraction rate is usually considered. To study the effect of specific passed SC-CO_2 on extraction rate, the extraction curves drawn verses the specific passed SC-CO_2 (Figure 4.21-a) were very close and the effect could not be clearly shown. To overcome this, the extraction curves were drawn against extraction times instead, as shown in Figure 4.24. The figure shows the time course of the extraction at 65 ^{o}C, 350 bar and different mass flow rates. As expected, the extraction rate increased with increasing solvent flow rate, resulting in a shorter time to reach the steady state yield. Similar observations were found at other conditions.
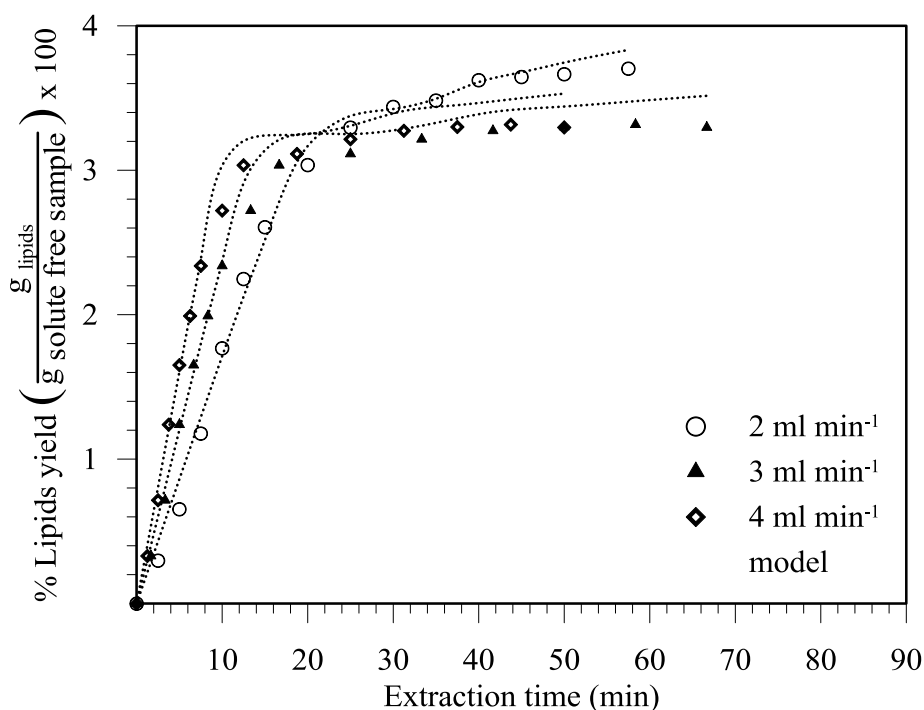
Figure 4.24: Time progress of lipid extraction at 65 ^{o}C, 350 and different SC-CO_2 flow rate

The effect of flowrate, pressure and temperature could be clearly seen Figure 4.21. As shown in Figure 4.21 (b), increasing the pressure at constant temperature of 35 ^{o}C and at 3 ml min^{-1}, resulted in increasing the extraction rate. However, it was mentioned earlier that increasing the pressure caused a slight

decrease in k_f; which should affect negatively the extraction rate. Nevertheless, increase in density, in this case makes the overall effect of pressure in favor of enhancing the extraction rate. As shown in Figure 4.21(c), as temperature increases from 35 to 50 ^{o}C, the extraction rate decreased due to the decrease in the solubility; however further increase resulted in an increase in the rate, which is mainly because of the higher lipid vapor pressure.

4.2.3.3 Mass transfer correlation

It is important to develop a correlation to predict the mass transfer coefficient, k_f, from easily measurable dimensionless numbers such as Re, Sc and Gr. The correlations available in literature, shown in Table 4.14 are for forced convections, Sh_F, which are limited to large Reynolds numbers that are not applicable to those found in this work. Therefore, it was important to develop a correlation that takes into consideration both forced and natural convections to account for the low Re numbers found in this work. Thus, in this part, the parameters in Eq. (2.36) were determined by minimizing the difference between predicted Sh and the experimentally determined one. Obtained k_f values from the OEC's model were used to calculate the experimental Sh . Table 4.14 shows the physical properties on SC-CO$_2$ and calculated Sh at the tested conditions. To consider the effect of natural convection, Gr numbers were calculated at the tested conditions, and the correlation parameters of Eq. (2.37) were determined.

Table 4.14: Physical properties, calculated dimensionless numbers predicted Sherwood number at different operating conditions

Run	Experimental conditions			SC-CO$_2$ properties				Calculated dimensionless numbers				Models predictions		
	Temperature (^{o}C)	Pressure (bar)	Flow rate (ml min^{-1})	Density (kg m^3)	Viscosity (Pa.s)	Diffusivity (m^2 s^{-1})	Velocity (m s^{-1})	Re	Sc	Gr	Sh^a	Sh^b	Sh^c	$\left(\dfrac{Sh_N}{Sh}\right)^d$
9	35	500	4	1005.7	12.3	3.31	5.29	0.41	36.9	108.6	0.552	0.522	0.415	0.21
19	65	200	2	691.71	5.61	10.54	2.64	0.31	7.69	75.5	0.096	0.110	0.166	0.31
15	50	350	4	899.23	9.13	5.81	5.29	0.5	17.47	89.4	0.417	0.390	0.378	0.17
1	35	200	2	865.72	8.36	4.32	2.64	0.26	22.35	34.9	0.158	0.189	0.193	0.23
11	50	200	3	784.29	6.87	7.06	3.97	0.43	12.4	27.5	0.225	0.249	0.286	0.12
13	50	350	2	899.23	9.13	5.81	2.64	0.25	17.47	89.4	0.148	0.147	0.170	0.36
14	50	350	3	899.23	9.13	5.81	3.97	0.37	17.47	89.4	0.276	0.260	0.271	0.24
22	65	350	2	844.57	7.98	8.28	2.64	0.27	11.4	96.2	0.125	0.119	0.159	0.37
7	35	500	2	1005.7	12.3	3.31	2.64	0.21	36.9	108.6	0.192	0.214	0.261	0.42

Continue on next page

Table 4.14: Physical properties, calculated dimensionless numbers predicted Sherwood number at different operating conditions (Cont.)

12	50	200	4	784.29	6.87	7.06	5.29	0.58	12.4	27.54	0.323	0.373	0.400	0.09
10	50	200	2	784.29	6.87	7.06	2.64	0.29	12.4	27.54	0.123	0.141	0.178	0.20
2	35	200	3	865.72	8.36	4.32	3.97	0.39	22.35	34.91	0.289	0.334	0.311	0.14
24	65	350	4	844.57	7.98	8.28	5.29	0.53	11.4	96.18	0.356	0.315	0.356	0.18
18	50	500	4	962.45	10.83	5.17	5.29	0.45	21.77	31.78	0.455	0.396	0.360	0.12
4	35	350	2	952.29	10.54	3.68	2.64	0.23	30.05	72.81	0.177	0.195	0.190	0.34
25	65	500	2	919.02	9.63	7.28	2.64	0.24	14.39	189.03	0.14	0.130	0.178	0.49
20	65	200	3	691.71	5.61	10.54	3.97	0.47	7.69	75.53	0.178	0.195	0.267	0.20
3	35	200	4	865.72	8.36	4.32	5.29	0.52	22.35	34.91	0.447	0.501	0.435	0.10
21	65	200	4	691.71	5.61	10.54	5.29	0.62	7.69	75.52	0.268	0.293	0.373	0.14
5	35	350	3	952.29	10.54	3.68	3.97	0.34	30.05	72.80	0.297	0.343	0.295	0.23
16	50	500	2	962.45	10.83	5.17	2.64	0.22	21.77	31.78	0.161	0.149	0.160	0.26

Continue on next page

Table 4.14: Physical properties, calculated dimensionless numbers predicted Sherwood number at different operating conditions (Cont.)

23	65	350	3	844.57	7.98	8.28	3.97	0.4	11.4	96.18	0.228	0.210	0.255	0.24
6	35	350	4	952.29	10.54	3.68	5.29	0.46	30.05	72.80	0.505	0.514	0.410	0.16
8	35	500	3	1005.7	12.3	3.31	3.97	0.31	36.9	108.62	0.362	0.352	0.324	0.29
17	50	500	3	962.45	10.83	5.17	3.97	0.34	21.77	31.78	0.296	0.264	0.257	0.17
26	65	500	3	919.02	9.63	7.28	3.97	0.36	14.39	189.03	0.253	0.218	0.255	0.34
27	65	500	4	919.02	9.63	7.28	5.29	0.48	14.39	189.03	0.393	0.324	0.347	0.26

[a] Based on calculated k_f from Sovova model [380]

[b] Using Eqs (4.3 and 4.4)

[c] Using Eq. (4.5 and 4.6)

[d] Sh_N was based on Eq. (4.6)

Two fitting strategies were considered to determine models parameters. According to the literature, the Sc number exponent C_2 (Eq. 2.32) should be fixed to 0.33 and C_o and C_1 were adjusted. This resulted in an estimate of 0.32 and 1.2 for C_o and C_1, respectively are the adjustable parameters. When this was applied, the estimated values of C_3 and C_4 were found to 1.5 and 6.3×10^7 as shown in Eq. (4.4), for natural convection. The R^2 was found to be 60 %, which indicates that the keeping the exponent of Sc constant at 1/3 is not appropriate in this case.

$$Sh_F = 0.32 \, Re^{1.2} \, Sc^{0.33} \tag{4.3}$$

$$Sh_N = 6.3 \times 10^{-7} \, (Gr \, Sc)^{1.54} \tag{4.4}$$

In a second fitting strategy the exponent of Sc was left as another estimated variable. The estimated values of C_o, C_1 and C_2 in this case were This resulted in 0.13, 1.4 and 0.75, respectively, as shown in Eq. (4.5) for forced convection. The estimated values of C_3 and C_4 were 0.001 and 0.56, respectively. as shown in Eq. (4.6) for natural convection, respectively. The R^2 in this case was much closer to 1, with value larger than 90 %.

$$Sh_F = 0.13 \, Re^{1.4} \, Sc^{0.75} \tag{4.5}$$

$$Sh_N = 0.001 \, (Gr \, Sc)^{0.56} \tag{4.6}$$

Figure 4.25 shows a scatter plot between experimental data and both models predictions. Table 4.14 also shows also the contribution of the natural convection to the overall Sh, which clearly show that the contribution of natural convection was less than 25 %, compared to the forced convection, and dropped as the flowrate increased.
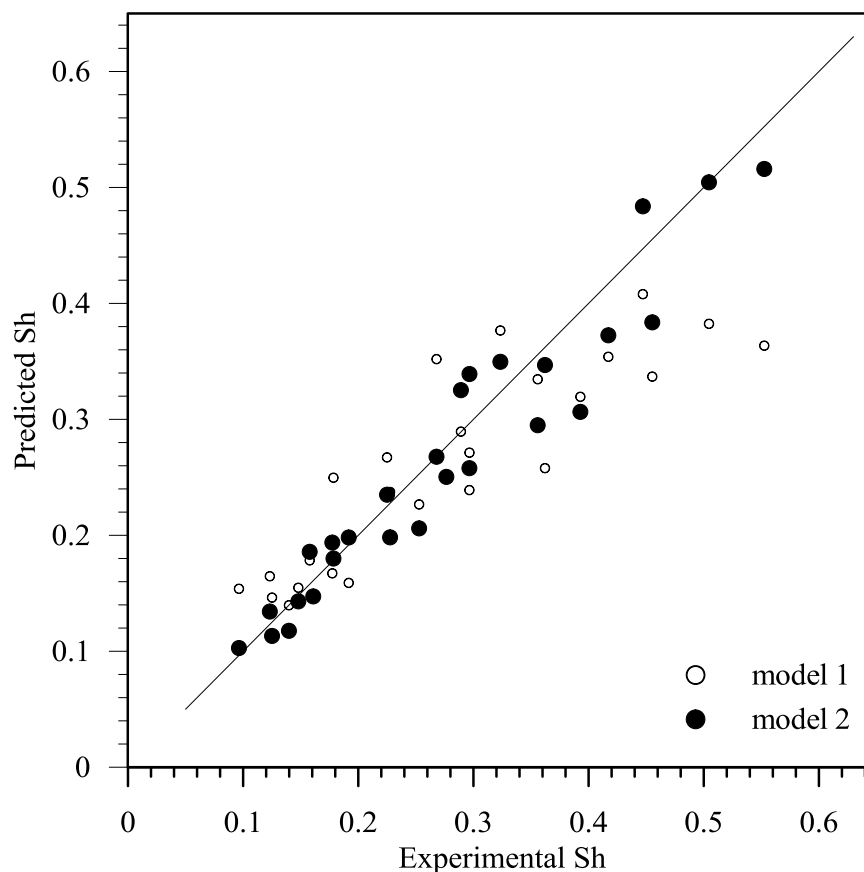
Figure 4.25: Experimental data and predictions from the two tested models

Although the second model showed better predictions of the experimental data, obtained fitting parameters were found to be different than those of correlations found in literature, shown in Table 2.19. The reason could be attributed to the small d_o of the particles and the low velocity of SC-CO$_2$ used in this work, which resulted in a much smaller Reynolds numbers compared to those used to develop the correlations in Table 4.14. It is important therefore to realize that the developed correlations (Eq. 4.5 and 4.6) are applicable for Re < 0.6 and 5 <Sc < 40.

As mentioned earlier, the scale up of the extraction process was studied from 10 ml to 60 ml at 53 ^{o}C and 500 bar. The scaling up criteria were based on keeping the bed height to diameter ($\frac{H}{D}$) and solvent flowrate to biomass weight

($\frac{F}{m}$) ratios constants for both scales. Figure 4.26 shows the OEC's of the lipids at the optimum conditions for the two scales. The model parameters mentioned earlier were determined from the experimental results of the small scale extraction cell. To verify the model, the mass transfer coefficient, k_f, at the optimum extraction conditions of 53 ^{o}C, 200 bar and 16 ml min^{-1} was determined for the extraction in the 60 ml cell. The developed correlations (Eqs 4.5 and 4.6 and 2.36) were used to predict the values of the mass transfer coefficients for the larger scale at the optimum conditions. This value was then used to predict the OEC's using the BIC model. Figure 4.26 shows the comparison between the model prediction and the experimental values.

The validity of the correlations is proven from their ability to predict the behavior of the large scale using the correlation parameters determined from the experimental data of the small scale. Although the scale up of the extraction was done using the criteria mentioned before, namely constant ($\frac{H}{D}$) and ($\frac{F}{m}$), yet the extraction yield of the larger scale was slightly lower. This could be explained by the higher interstitial velocity (3 folds higher) and larger diameter (almost 2 folds) of the larger extraction cell compared to the small cell. These both factors further enhance the channeling, which has a negative effect on the yield.
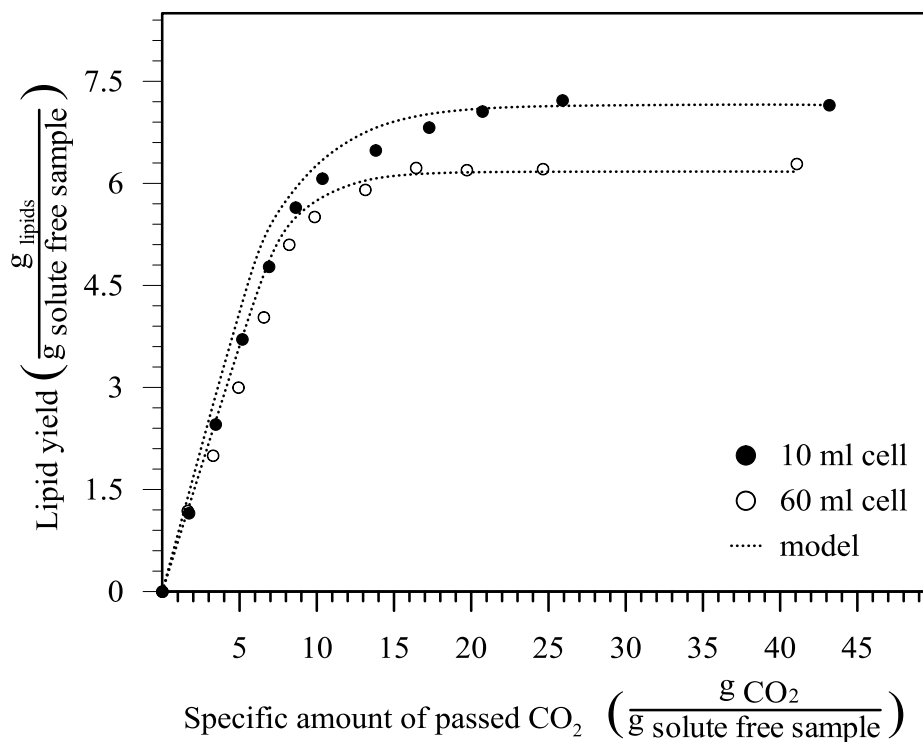
Figure 4.26: Experimental and predicted overall extraction curves for; (a) 10 ml extraction cell and (b) 60 ml extraction cell

4.3 TRANSESTERIFICATION REACTIONS IN BATCH SYSTEM

Generally, the main factors that affect an enzymatic reaction in SCFs are enzyme loading, temperature, pressure, substrates molar ratio, and water content. In esterification reaction catalyzed by immobilized lipase in $SC\text{-}CO_2$, it has been shown that pressure up to 300 bar has minimal effect on the enzyme activity and stability [442]. This should also be applicable in transesterification reactions, and a pressure of 200 bar was considered in this work. By using high pressure 10 ml view cell, sealed with O-ring, the miscibility of reaction mixture containing microalgae lipids and methanol (5:1 M:L molar ratio) at 50 ^{o}C, and different pressures were visualized, as shown in Figure 4.27.
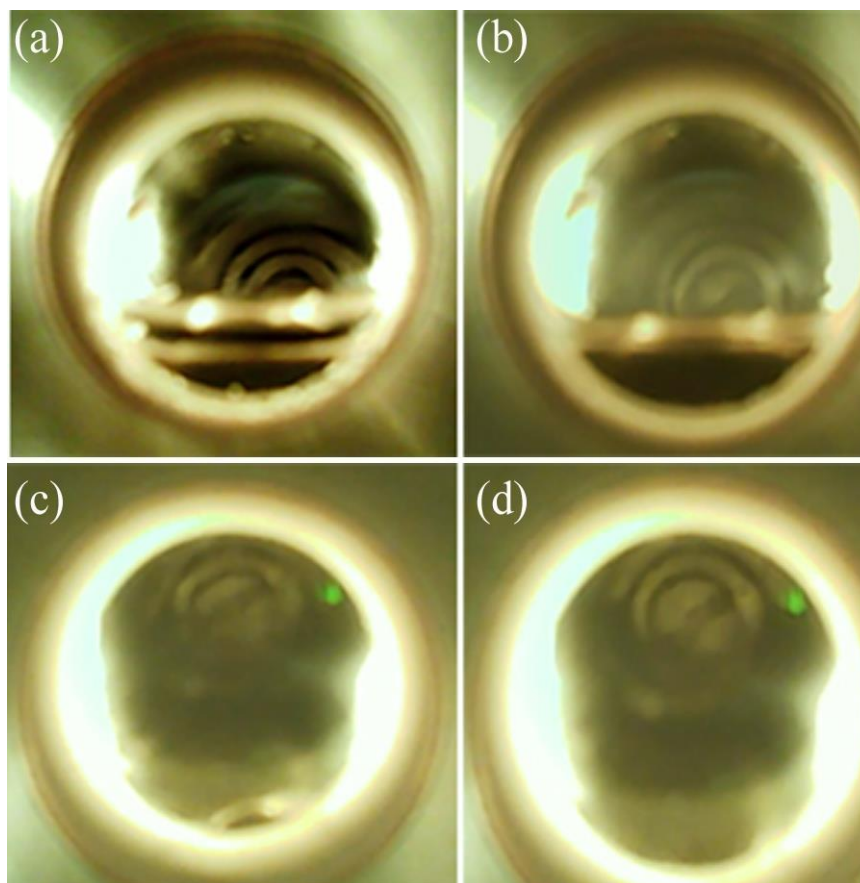
Figure 4.27: Mixture of microalgae lipids and methanol in 10 ml view cell at 50 oC, 5:1 molar ratio and [(a) atmospheric pressure, (b) 60 bar, (c) 150 bar and (d) 200 bar)]

It is clearly shown that at atmospheric pressure, the methanol and lipids are immiscible, and by pressurization the immiscible two liquid phases become one single liquid phase at 60 bar, which is close to CO_2 critical pressure. A further increase in pressure to 150 and 200 bar resulted in a homogeneous phase. In addition, for lipases to perform their functionalities and attain their activities, they require a certain amount of water, known as bound water, within their structure. Therefore, the presence of water is important or the reactions where water is one of the products that accumulates in the reaction medium and could lower the reaction yield. However, this is not the case in transesterification reactions, where glycerol is the by-product and Novozyme[®]435 used in this work

contains 2% water, and high production yield could be obtained without the need for any extra water [82]. Therefore, the effect of water content was not considered in this work. To reduce number of process variables, a preliminary study on enzyme loadings effect was fist considered to determine the optimum loading value, which was them used to carry out a parametric study on the effect of reaction temperature and M:L molar ratio in a batch system. The experimental data were used to determine the kinetic parameters of Ping-Pong Bi Bi model. The data were also used to generate second order regression model, where the effect of the significant factors were determined statistically by ANOVA. The dotted lines shown in the figures are connections between the experimental data shown to highlight the trend.

4.3.1 Parametric effects

4.3.1.1 Effect of lipase loading

The effect of enzyme loading on FAME yield was investigated in SC-CO$_2$ at levels of 15, 35 and 50 %, based on the initial TAGs quantity of 0.625 g that corresponds to 73 % of total lipid content in extracted lipids at conditions of 53 ^{o}C, 500 bar and 2 ml min^{-1}. Other variables were kept constant at 50 ^{o}C, 200 bar and 4:1 M:L molar ratio, which were selected based on a previous study results [35]. Figure 4.28 shows the FAME production yield, determined using Eq. (3.9), with time at different enzyme loads for a total of 15 h.
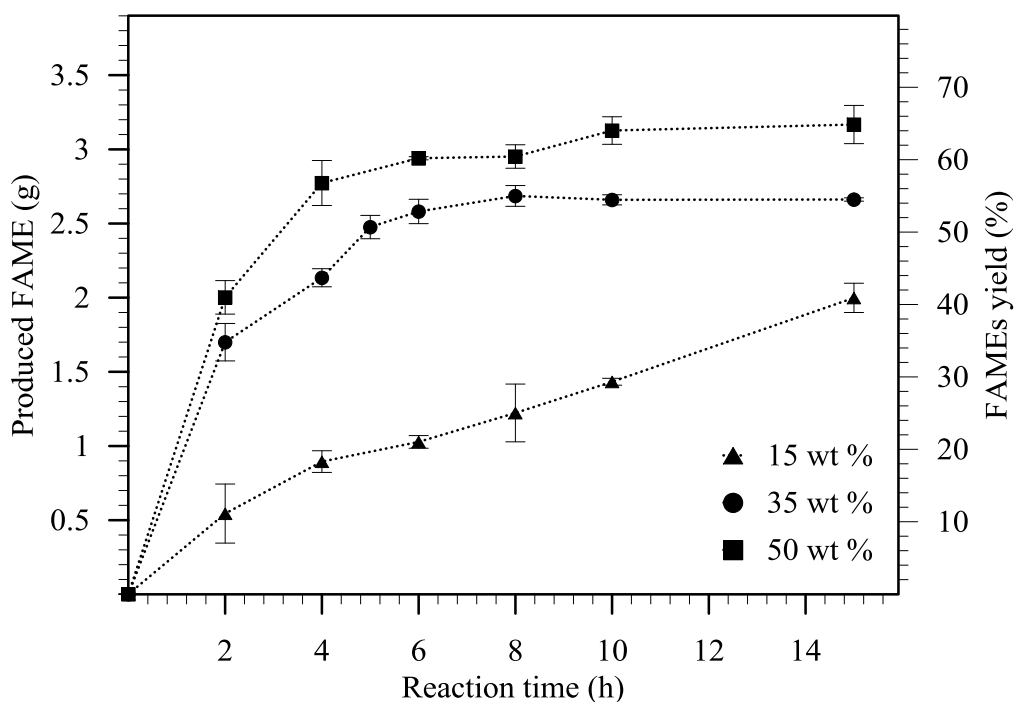
Figure 4.28: Amount of produced FAME and production yield versus reaction time using different enzyme loading at 50 °C, 200 bar and 4:1 molar ratio

It is clearly seen in the figure that the FAME yield increased significantly (*p*-value =0.000) with the increase in the enzyme load. The highest obtained yield was close to 65 % at the highest tested loading of 50 %. It was observed that the enzyme loading effect became less significants, as the loading increased. This was due to the enzyme saturation effect, where beyond that concentration any increase in enzyme loading would not affect the yield significantly. Moreover, the reaction rate increased with the increase in the enzyme concentration, where the reaction rate was almost constant at the low loading of 15 %. However, at higher loadings the reaction showed a linear increase in the yield in the first 4 h, then started to deviate, which is due to the equilibrium reached.

Although the lipid conversion increased with the increase in the enzyme loading, from an economical point of view and, due to the high cost of enzymes, the loading cannot be increased indefinitely. The results shown in Figure 4.28

suggest that it is not recommended to use enzyme loading higher than 35 %, as the enhancement in reaction yield was not significant beyond that loading (p-0.624). The results of this study agree with those obtained in a previous work done on a similar system with lamb fat [35]. Novozyme[®]435 loading of 30% was also found to be the optimum dosage by Madras et al. [143] and Rathore and Madras [34] when several edible and non-edible oils were transesterified at 45 ^{o}C, 200 bar and 5:1 molar ratio in SC-CO_2, with the highest conversion close to 60 % using refined palm oil. A lower enzyme loading of 20 % was reported by Varma and Medras [443] using castor oil in SC-CO_2 at 50 ^{o}C, 5:1 molar ratio and 200 bar, which could be due to the higher tested temperature and the high diffusivity of ricinoleate acid, which accounts for 85-90 % of total fatty acid content of castor oil, in SC-CO_2 at 200 bar, compared to linoleic acid, which accounts for 72 % of total fatty acids composition of sunflower oil tested at the same pressure [444]. Based on the above results, 35% enzyme load was selected for further investigations.

4.3.1.2   Effect of methanol to lipid molar ratio

The stoichiometric molar ratio for transesterification reaction is 3 moles of methanol for each mole of lipids. Further increase in the molar ratio, shifts the reaction toward more product formation. However, when the reaction is enzymatically catalyzed; by lipase, excess alcohol inhibits the reaction. This is because short alcohols have a low solubility in lipids and do not dissolve well. The solubility of methanol in lipid was found to be 1.5 of the stoichiometric ratio [187], and when alcohol appears at a different phase, it strips away the essential water molecules required to maintain the enzyme active [445]. In addition, due to

the high polarity of methanol, the excess amount binds to the active sites of the enzyme and prevents the substrate from reaching them. To enhance the solubility, organic solvents were suggested. It was reported that solvents with log P values higher than 3, such as n-hexane (log P=3.5), are suitable for transesterification reaction. Rodrigues et al. [446] showed a significant enhancement of ethyl ester yield at 7.5:1 when the reaction was carried in the presence of n-hexane, compared to solvent free system by Lipozyme TL IM. However, lower optimum ratio in the range of 4-5:1 has been reported when methanol and Novozyme[®]435 were used, where *tert*-butanol was used as a solvent.

The effect of M:L molar ratio in this work was studied in the range between 3:1 and 15:1, while holding the enzyme load, pressure and temperature constants at 35% wt, 200 bar and 50 ^{o}C, respectively. Figure 4.29 shows the reaction yield progress at different M:L molar ratios.
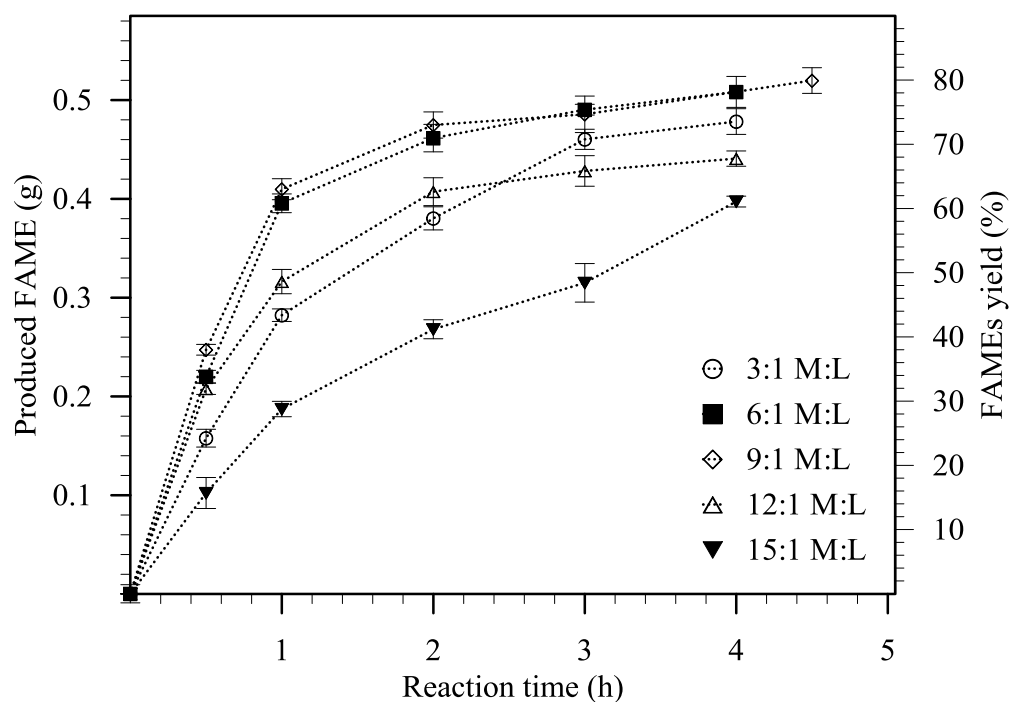
Figure 4.29: Time progress of FAME yield at 50 °C, 200 bar, 35% enzyme load and different M:L molar ratios

As can be seen, at all tested concentrations, FAME production yield was linear in the first hour of reaction, and then started to flatten after that. It can also be seen that the yield increased with the increase in the M:L molar ratio from 3:1 to 9:1 yielding a highest conversion of 80 % at 9:1 molar ratio. However, further increase to 15:1 resulted in a drop in the yield by 22 %. This drop in the yield is mainly due to the lipase inhibition. This was further confirmed from the initial reaction rates shown in Figure 4.30. The initial reaction rates were determined from the slope in the first hour of reaction.
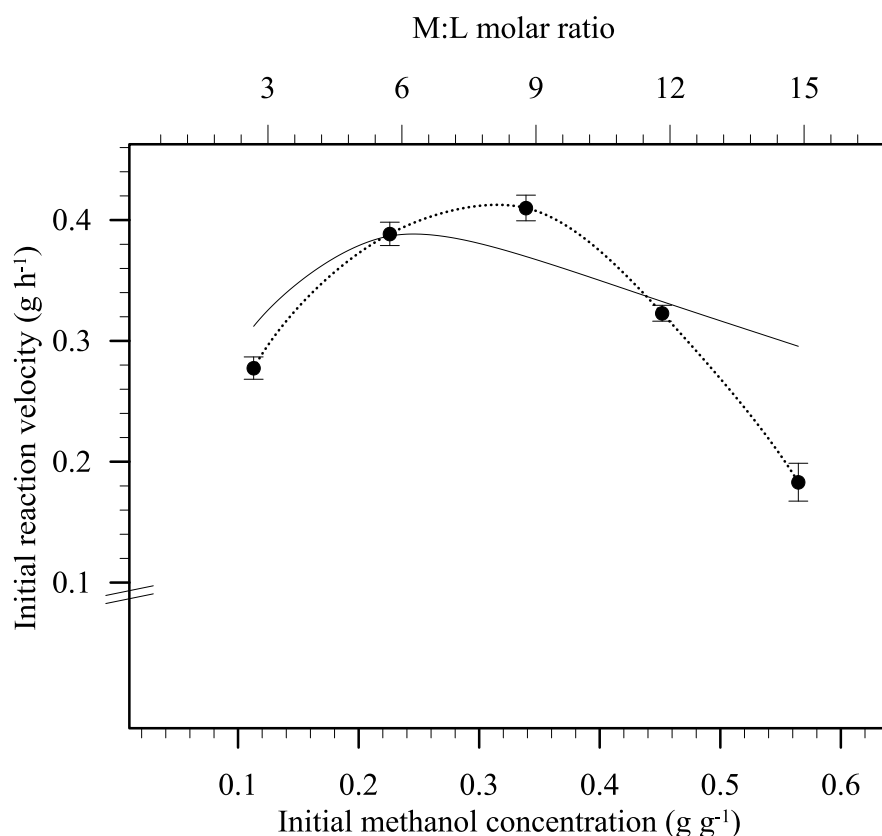
Figure 4.30: Effect of increasing the initial M:L molar ratio on the initial reaction rate at 50 °C, 200 bar and 35% enzyme loading

The figure clearly shows that the initial rate increased with the increase in methanol concentration reaching its highest value of 0.388 g h^{-1} at 9:1 M: L

molar ratio. Beyond this value, the rate decreased due to the inhibitory effect of the excess methanol. A similar trend was also found in a previous work using the same enzyme and alcohol with lamb fat [35]. However, the optimum ratio obtained was 4:1 when lamb fat was used, which is the same as that obtained in solvent free systems using oils. The lower molar ratio found when lamb meat was used could be due to the lower solubility of methanol in the highly saturated fat/SC-CO_2 mixture, compared to the unsaturated microalgae lipids used in this work. In addition, the diffusivity of the microalgae lipids used in this work is higher than that of lamb fats, which is mainly due to negative effect of C18 unsaturated fatty acids that account for more than 75 and 50% of total content in microalgae lipids and lamb fat, respectively [444].

4.3.1.3 Effect of temperature

Like all chemically catalyzed reactions, the reaction rate constants, and hence the reaction rate, increase with temperature. However, this is not always correct, with enzyme catalyzed reactions, due to the protein denaturation at high temperatures, which results in the substrate no longer fitting on the enzyme active sites. Therefore, a rapid decline in reaction rate, and conversion yield, are usually observed at high temperatures. The optimum working temperature range for Novozym$^{®}$435 is reported to be between 40 and 60 ^{o}C according to manufacturer. The effect of temperature on the reaction yield after 4 h was studied in SC-CO_2 in the range of 35–55 ^{o}C at 200 bar and 35% of enzyme loading, and Figure 4.31 shows the results at the optimal determined M:L ratio of 9:1
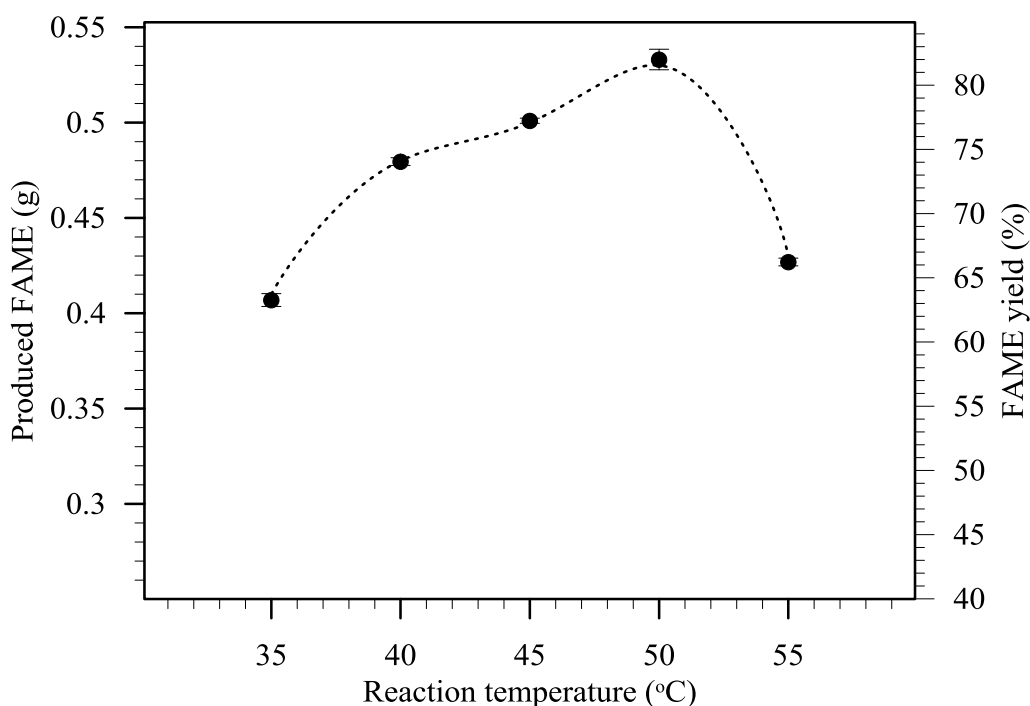
Figure 4.31: Effect of reaction temperature on FAME yield after 4 h reaction at 200 bar, 35% enzyme loading and 9:1 molar ratio.

As expected, an increase in the temperature resulted in an increase in the production of FAME and the maximum yield of 82 % was reached at 50 ^{o}C. A further increase resulted in a decrease in the yield by 19 % at 55 ^{o}C. The increase in production yield was mainly due to the increase in the reaction rate constants and in the mass transfer diffusion at higher temperatures, whereas, the sharp decrease in the yield is caused by the lipase denaturation. In addition, the presence of the inactive denatured particles at the lipid interface blocks the active enzyme from being utilized, which results in a further drop in the yield. This trend was observed in all studies that investigated the effect of temperature on the production of biodiesel using Novozym$^{®}$435 [35, 209]. The optimum temperature found in this study was close to other reported optimum temperatures using Novozym$^{®}$435[19, 35, 447]. However, a lower optimum temperature of 38 ^{o}C, which is below the manufacturer's claim, was observed by Chang et al. [448]

using canola oil with 42.3% loading, 7.2 % water, 3.5 molar ratio; this might be due to the high water concentration that acted as a competitive inhibitor to transesterification.

4.3.2   Optimization of process conditions

4.3.2.1   Statistical analysis and regression model development

The effect of temperature (35-55 ^{o}C) and M:L molar ratio (3-15:1) on FAME yield was studied using RSM. Table 4.15 shows the average yields at each experimental condition with measured uncertainties. It can be clearly seen that the highest FAME yield of 82% was obtained at 50 ^{o}C and 9:1 M:L molar ratio. A second order polynomial was used to model the system, in which regression coefficients of the predicted polynomial, shown in Eq. (4.7), were obtained by employing the least squares technique.

Table 4.15: Experimental conditions, and experimental and predicted yields

Run order	Temperature (^{o}C)	M:L molar ratio	FAME yield (%)	
			Experimental[*]	Predicted
1	50	12	74.0 ± 1.22	74.34
2	35	12	57.3 ± 3.98	48.75
3	40	3	41.2 ± 3.63	48.12
4	55	9	66.2 ± 1.10	72.04
5	45	15	52.3 ± 2.40	55.26
6	45	12	76.7 ± 2.43	74.56
7	50	6	76.8 ± 0.49	75.04
8	50	15	62.3 ± 0.57	55.04
9	55	15	45.0 ± 3.01	46.07
10	55	6	57.8 ± 2.98	66.07
11	45	6	74.2 ± 1.89	75.26
12	55	12	62.3 ± 0.312	65.37
13	35	6	45.0 ± 5.15	49.45
14	35	3	33.8 ± 5.99	30.84
15	40	15	40.0 ± 8.01	46.73
16	35	15	21.5 ± 2.56	29.45
17	40	9	74.1 ± 0.925	72.7
18	50	3	65.8 ± 1.82	56.43
19	40	6	54.7 ± 1.57	66.73
20	45	9	77.2 ± 0.87	81.23
21	55	3	51.2 ± 3.11	47.46
22	40	12	73.1 ± 0.97	66.03
23	35	9	63.3 ± 2.3	55.42
24	50	9	82.0 ± 2.59	81.01
25	45	3	54.5 ± 0.78	56.65

* Average values with ±measured uncertanity

$$Y = -371.225 + 16.695\,T + 13.041\,M{:}L - 0.175\,T^2 - 0.702\,M{:}L^2 \qquad (4.7)$$

$$- 0.011\,T \times M{:}L \pm 2.29$$

Table 4.16 shows the degree of significance of each factor. The *p*-values of the regression terms reveal that both tested variables have high significant effect (*p*-value=0.000) on conversion yield, whereas the interaction of the independent variables was insignificant (*p*-value=0.797). In addition, the significance of the second order terms indicates that the optimal conditions were located within the experimental range.

Table 4.16: Second order regression model coefficients of transesterification yield obtained by MiniTab 16.

Term	Coefficient	Standard error of Coefficient	*t*-test	*p*-value
Constant	-371.225	65.0533	-5.706	0.000
Temperature	16.695	2.8466	5.865	0.000
M:L	13.041	2.5270	5.161	0.000
Temperature $\times$ Temperature	-0.175	0.0313	-5.612	0.000
M:L $\times$ M:L	-0.702	0.0868	-8.085	0.000
Temperature $\times$ M:L	-0.011	0.0436	-0.260	0.798

Based on obtained data, the second order polynomial model was re-regressed, coefficients that are not significant were eliminated and the final model was refitted. The refined model is shown in Eq. (4.8). It was found that the linear individual terms have positive coefficients and the temperature effect was slightly higher than that of M:L molar ratio. The positive sign of these coefficients implies that the corresponding variables positively affect the production yield, whereas, the negative second order coefficient of these variables indicates the maximum region for the production is present in the selected conditions in this work.

$$Y = -366.64 + 16.6\,T + 12.53\,M{:}L - 0.175\,T^2 - 0.702\,M{:}L^2 \pm 2.30 \quad (\,4.8\,)$$

The coefficient of determination (R^2) and adjusted coefficient of determination (adj. R^2) were used to measure the ability of the obtained model to predict the experimental data. The results showed that the R^2 and *adj. R^2* were 85.87, and 83.04 %, respectively. The close values of the two coefficients to each other and to 100 % indicate that the model successfully presents the real relationship between the process variables, and insignificant terms are eliminated. Table 4.17 shows the ANOVA analysis of the model. The ability of the model to predict the experimental data was further presented by the graphical plot of predicted yield versus the experimental values, shown in Figure 4.32, where data points are fragmented consistently by the diagonal line.

Table 4.17: ANOVA of the refined regression model

Source	Degree of freedom	Sequential sum of squares	Adjusted sum of squares	Adjusted mean square	F-test	p-value
Regression	4	4954.19	4954.19	1238.55	30.39	0.000
Linear	2	813.08	4125.78	2062.89	50.61	0.000
Temperature	1	808.02	1480.63	1480.63	36.33	0.000
M:L	1	5.06	2645.15	2645.15	64.90	0.000
Square	2	4141.12	4141.12	2070.56	50.80	0.000
Temperature $\times$ Temperature	1	1346.41	1346.41	1346.41	33.03	0.000
M:L $\times$ M:L	1	2794.70	2794.70	2794.70	68.57	0.000
Residual Error	20	815.18	815.18	40.76		
Total	24	5769.38				
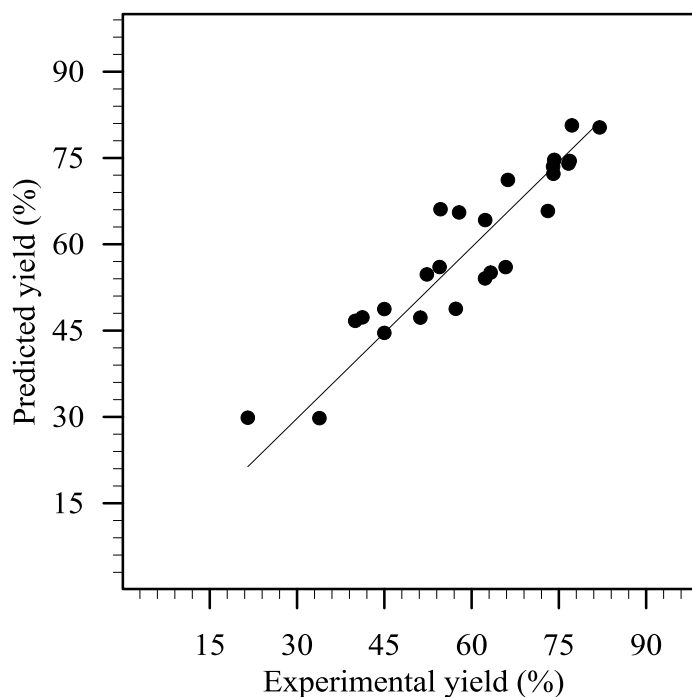
Figure 4.32: Comparison between experimentally determined extraction yield and the model predictions.

4.3.2.2 Process optimization

The influences of the selected process conditions on the conversion yield were plotted in a 3D (Figure 4.33-a) and contour (Figure 4.33-b) plots, to visualize their effects. Both plots were generated from the refined second order model (Eq. 4.8). The hump shape of both plots indicates that the FAME yield increased with the temperature reaching its optimum value and then decreased. A similar effect was also found for M:L molar ratio effect. From the observed shape, it can be deuced that the yield did not decrease steeply when the operation conditions changed slightly from its best value. This is a favorable process feature as it suggests a more robust production toward fluctuations in temperature during the process operation.
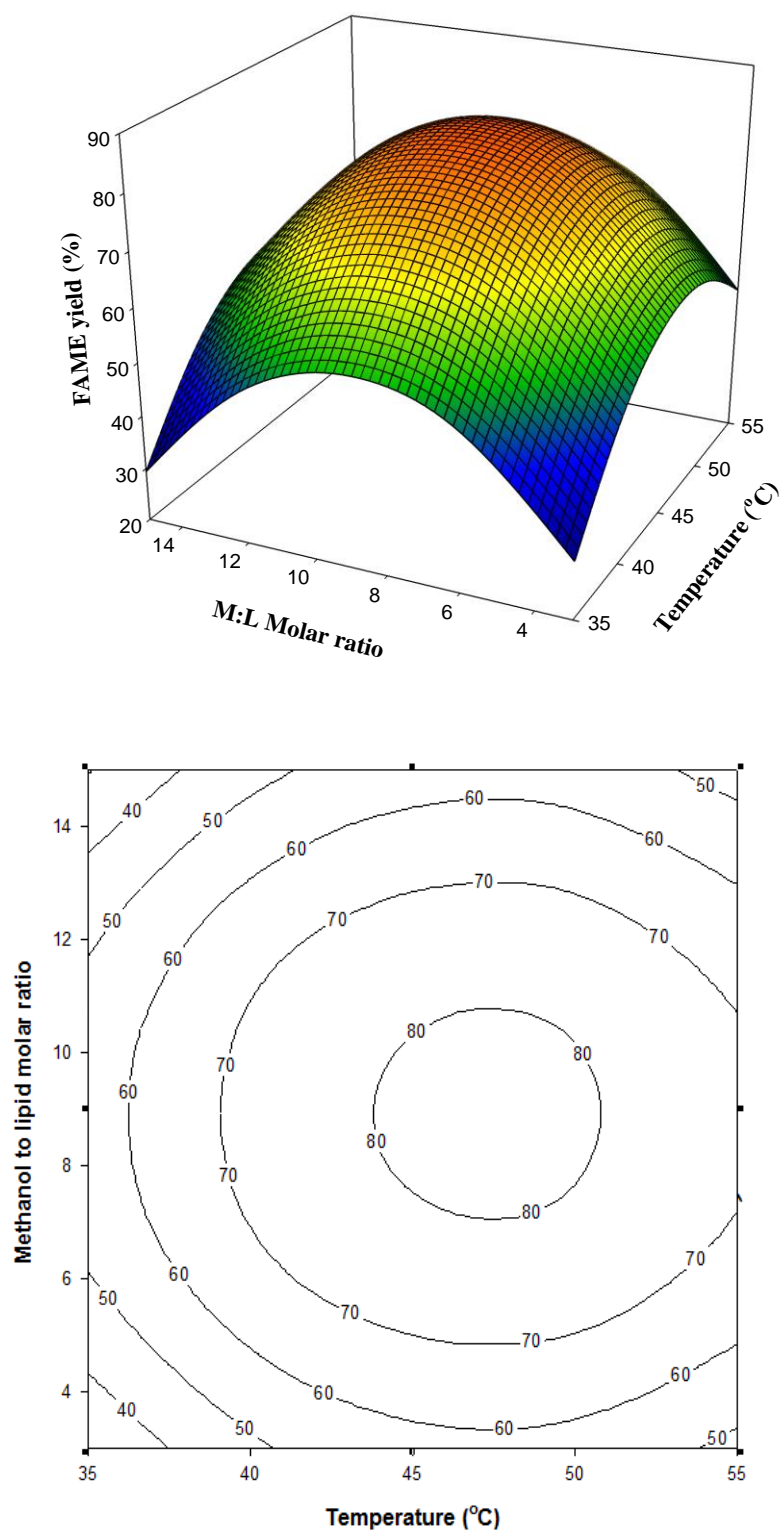
Figure 4.33: % FAME yield; (a) surface and (b) contour plots as a function if the process variables

Based on the refined model equation (Eq. 4.8), the optimum operating conditions were determined using the response optimizer tool to be 47 °C and 9:1 molar ratio, for which the yield was estimated to be 81.63 %. The model suitability was validated by performing an independent experiment at these optimum conditions in a duplicate. This gave production yield of 80.4 ± 1.97 %, which was very close to that predicted value by the model with less than 2 % deviation.

4.3.3 Kinetic study

Most kinetic studies of lipase catalyzed reactions are described by the Ping Pong kinetic model with competitive alcohol inhibition [192, 215, 216, 443]. In the kinetic study part of this work, the initial lipid concentration was kept constant and the concentration of methanol was changed, and expressed as initial amount of methanol per lipids used. The effect of methanol concentration in range of 0.11 to 0.56 g g^{-1} (equivalent to 3:1-15:1 M:L molar ratio) on the initial reaction rate was studied at 50 ^{o}C, 200 bar, 35% loading in the first 1 h of reaction, and shown in Figure 4.30. The kinetic model parameters were determined using the nonlinear least square method by minimizing the objective function given in Eq. (3.16). The model equation with estimated kinetic parameters is presented in Eq. (4.9). It was found that $K_{m,m}$ (5×10^{-1} g g^{-1}) was higher than $K_{m,l}$ ($8.\times10^{-3}$ g g^{-1}), which indicates that the affinity of the enzyme towards lipids was greater than that to methanol. The model curve was drawn in Figure 4.30, which clearly shows that the prediction of the reaction model using the Ping-Pong Bi Bi mechanism are acceptable and relatively close to the experimental points.

Table 4.18 shows a comparison between the estimated values of the kinetic parameters determined in this study and those previously obtained for lamb fat under SC-CO$_2$ [35] using the same model modifications. All apparent constants were lower and the maximum initial reaction rate was 10 times higher. The lower estimated value for the inhibition constant indicates that reaction is more inhibited by methanol. This is expected as the kinetic study in this work was carried out at a high molar ratio of 9:1 compared to 4:1 used in the lamb fat study.

$$v = \frac{2\,[M]^*}{[M]^* + 5 \times 10^{-1} + 8.6 \times 10^{-3}\,[M]^* \left\{ 1 + \frac{[M]^*}{9.9 \times 10^{-4}} \right\}} \qquad (4.9)$$

Table 4.18: Kinetic parameters comparison between algae oil and lamb meat fat in SC-CO$_2$.

	Lamb meat fat	Algae oil
Parameter	[35]	[This study]
v_{max}	1.35×10^{-1}	2.00
$K_{m,l}$	3.01×10^{-1}	8.56×10^{-3}
$K_{m,m}$	1.26	5.00×10^{-1}
K_{im}	9.00×10^{-3}	9.92×10^{-4}

4.4 INTEGRATED EXTRACTION−REACTION SYSTEM

An integrated extraction-reaction process was tested in a semi-continuous mode, in which 3 g of lyophilized biomass were charged into the extraction cell and extracted lipids were mixed with specified molar ratio of M:L before entering the reaction cell packed with 1.5 g of Novozym®435. Both systems were operated at 50 ^{o}C and 200 bar based on the obtained results in batch extraction and

reaction systems. Mixed substrates were then allowed to flow to the reaction cell at 1 ± 0.15 ml min^{-1} flow rate. The reaction was terminated after 80 min, which is the time the lipid extraction started to be diffusion limited at the operation conditions used. The solubility of the lipid in SC-CO$_2$ at the tested condition was determined from the slope of the linear part of the extraction curve, shown in Figure 4.16 , and was found to be 1.135×10^{-4} g ml^{-1}. Thus, lipid flow rate through the reaction cell was 1.135 mg min^{-1}. Due to the system limitation, methanol was diluted in *tert*-butanol, 32 times, using the lowest modifier ratio of 1% (volume ratio) that corresponds to 5:1 molar ratio of M:L. The M:L ratio was adjusted by changing the modifier ratio. It is worth mentioning that at the specified ratio of 32:1 (v/v) of *tert*-butanol:methanol mixture, the methanol dissolved well in the *tert*-butanol, hence the inhibition effect was minimized. Although high molar quantity of methanol is needed for the transesterification reaction, the volume is very small compared to the flowing enriched SC-CO$_2$. Therefore, the recovery of the *tert*-butanol:methanol mixture was not considered in this work.

4.4.1   Effect of substrates ratio on production and enzyme stability

The system was tested at different M:l molar ratios ranging from 5 to 20:1 by changing the modifier ratio from 1 to 4 %. The operational stability and reusability of the immobilized lipase, which are important factors affecting the production cost were tested. After 80 min of operation, lyophilized biomass was replaced with another fresh 3 g, while keeping the enzyme bed unchanged. This process was repeated six times. Figure 4.34 shows the cumulative FAME produced at different M:L ratios for the six different cycles of biomass replacements.
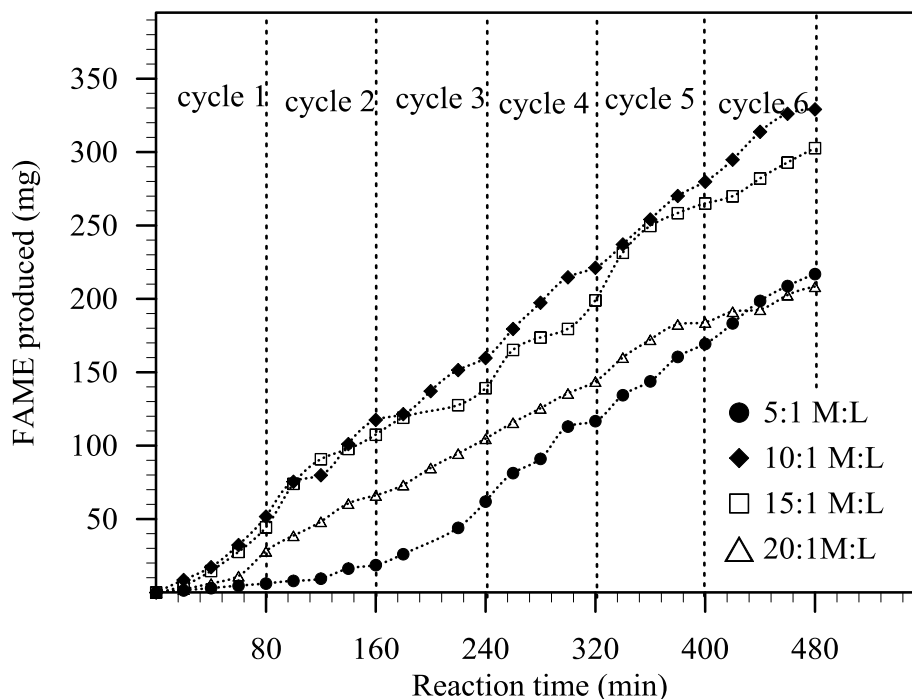
Figure 4.34: Time course production of FAME at different methanol to lipid

molar ratios with six biomass replacements at different M:L molar ratios

It was found that the amount of produced FAME increased 8 times when

the molar ratio was increased from 5 to 10:1 by the end of the first cycle.

However, further increase in the molar ratio reduced the production by 14.3 and

45.7% at 15:1 and 20:1, respectively, in the first cycle. In addition, it is clearly

shown in Figure 4.34 that the enzyme bed was successfully reused with the fresh

biomass and the highest produced FAME was 329.2 mg collected after 480 min

of operation at 10:1 molar ratio. The reduction in the production rate at the high

M: L was mainly due to the methanol inhibition effect. It can also be observed

that the production was almost linear at all tested ratios in the six cycles.

Figure 4.35 represents the average production rate during the six cycles at

different M:L molar ratios. It is clearly seen that the highest production rate and

yield were attained at 10:1 ratio, and both decreased with further increase beyond

this ratio.
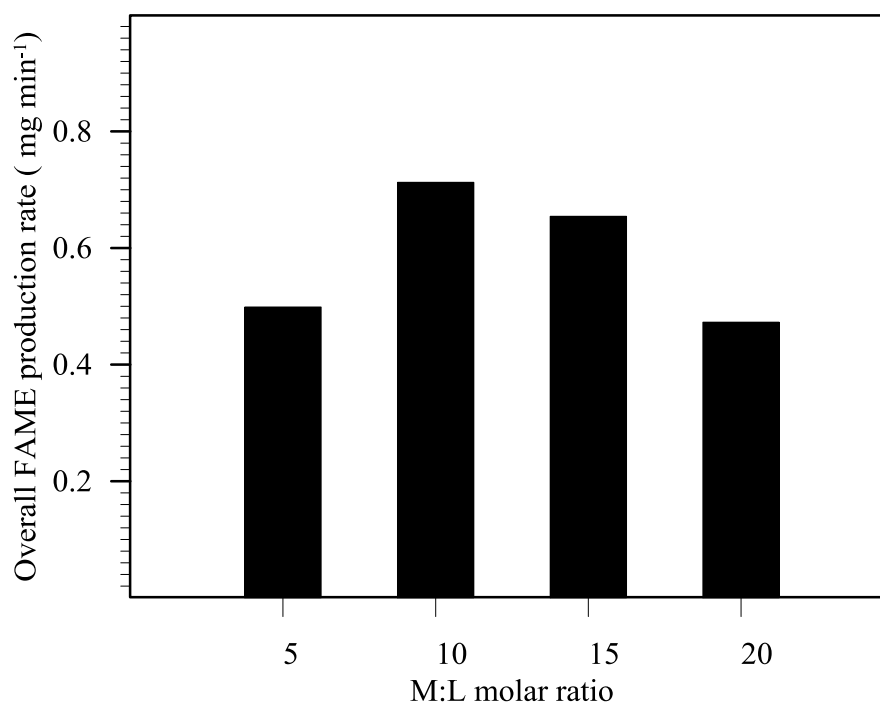
Figure 4.35: Overall production rate verses methanol to lipid molar ratio

The bed stability, defined as relative production rate in the sixth cycle to the maximum rate at each ratio, was determined and shown in Figure 4.36 for each molar ratio. It can be clearly seen that the bed was able to attain above 80% of its original activity at all tested ratios, except 20:1 ratio, which showed a significant drop of 41.7%. This is again due to the bed inhibition with the access methanol. The slightly lower stability at 10:1 ratio is due to the accumulation of excess glycerol produced, which formed a layer around the enzyme, and inhibited the substrate from reaching the enzyme. This was clearly observed in cycle 6 of 10:1 ratio, as faster production took place in previous steps compared to other M:L ratio, where the production rate was almost constant.
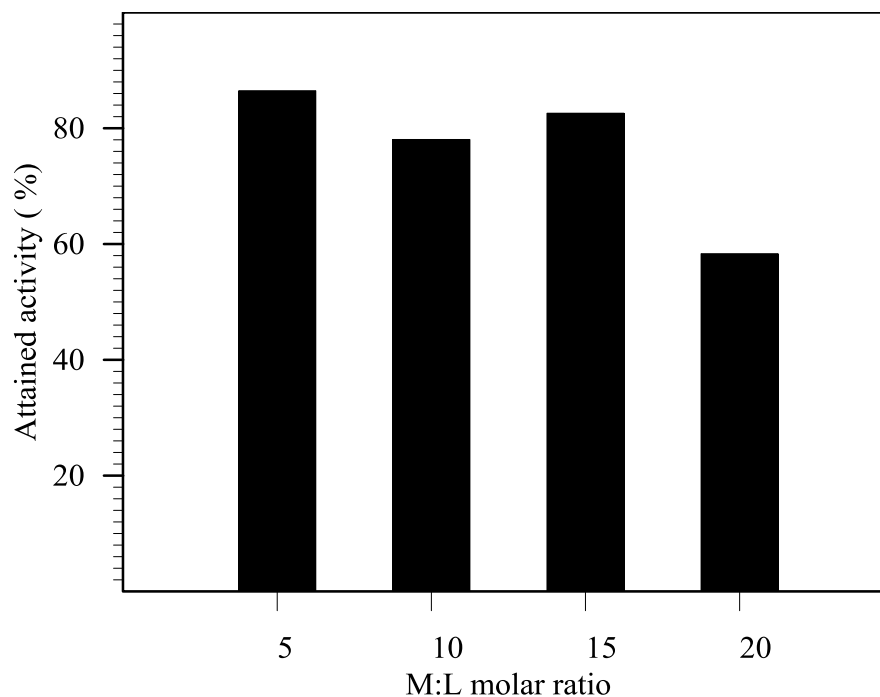
Figure 4.36: Attained enzyme bed activity by reusing at different methanol to lipid ratios

4.4.2 Enzyme bed activity regeneration by tert-butanol washings

Due to its high production rates, the enzyme bed at 10:1 molar ratio was further utilized with fresh lyophilized biomass in new sets of cycles, referred by batches, after washing the enzyme with 10 ml of *tert*-butanol. *tert*-Butanol was used due to it's ability to dissolves both methanol and glycerol and is not a substrate for the lipase, and based on the promising results obtained earlier [18], where 91% of enzyme activity was regenerated when washed with *tert*-butanol compared to 20 and 69 % obtained using water and *n*-hexane, respectively. Figure 4.37 shows the produced FAME in four batches. It was found that the *tert*-butanol enhances the enzyme stability and the bed was successfully reused after washing. The drop in FAME production, in second batch, after 6 cycles operation was 30 %.
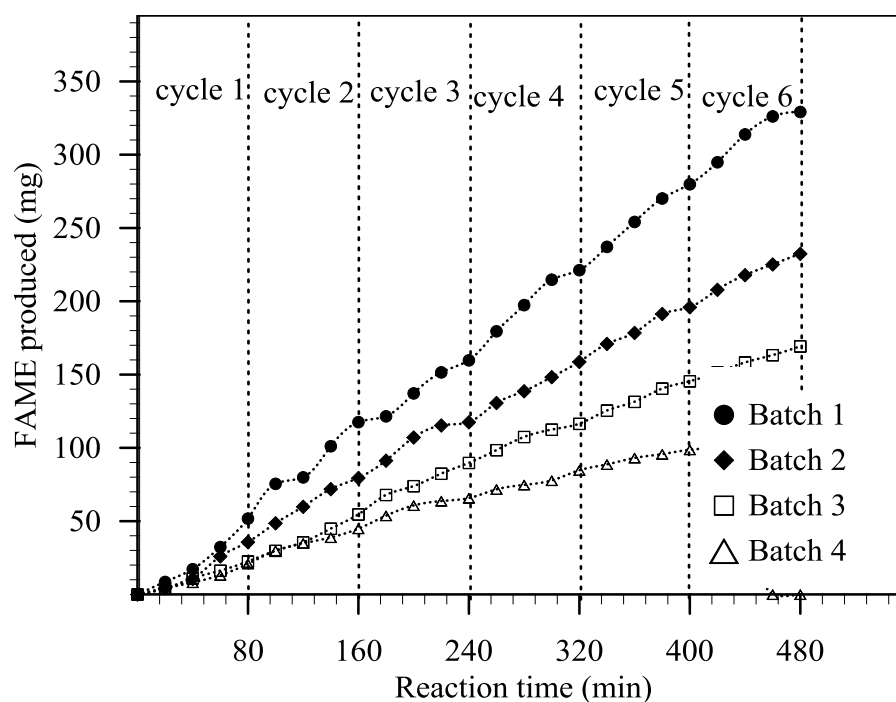
Figure 4.37: Amount of produce FAME with 6 replacements of the biomass in 4 consequence batches

These results further confirm the enzyme reusability, as each batch was successfully reused for six continuous cycles without a significant drop in the activity. The regenerated activity of the enzyme bed by washing was determined from the ratio of production rate in first cycle over that of sixth cycle of the preceding batch, as illustrated in Eq. (3.11). The results showed that the *tert*-butanol was able to regenerate 95, 75 and 93 % of the activity, in second, third and fourth batches, respectively. This favorable feature was due to the ability of *tert*-butanol to dissolve the inhibitors (methanol and glycerol) and increase the lipase activity [188].

The attained activity by reusing in each batch is shown in Figure 4.38. The lower obtained value in the second regeneration might be due to the particle loss during the washing and filtration steps.
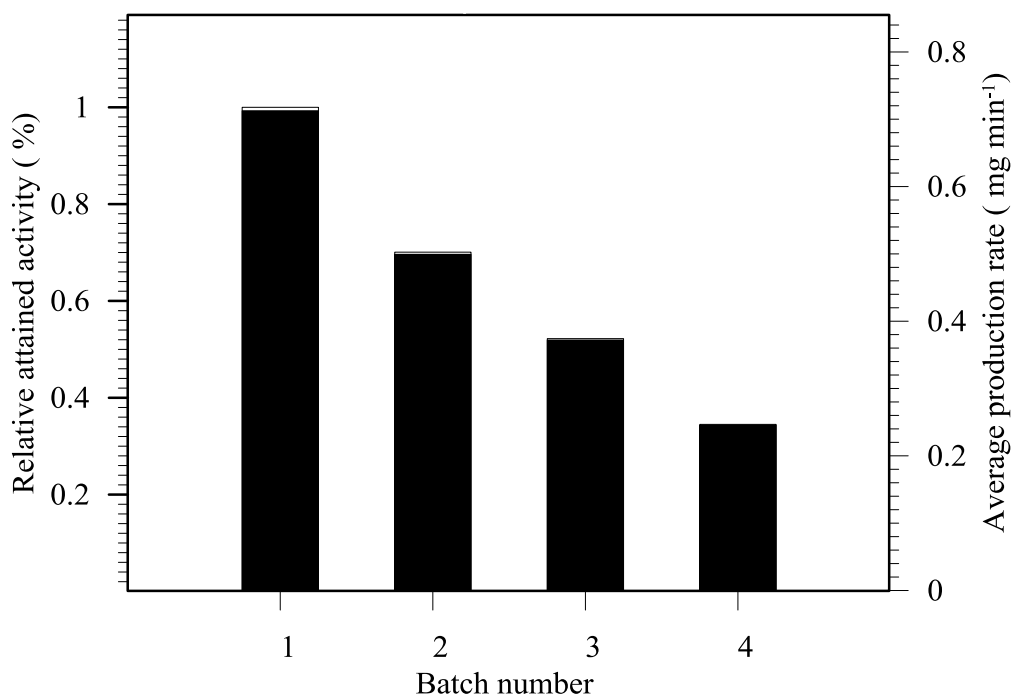
Figure 4.38: Average production rate and attained enzyme activity in the four
tested batches

    Table 4.19 summarizes and compares obtained results in this study, for
the first three cycles, with previously obtained results from lamb fat tested using
the same system. It can be seen that FAME productivity was higher from
microalgae lipids than that of lamb fat, although the lamb fat content was three
times higher than the microalgae lipid content. This is due to the higher mass
diffusivity of the unsaturated microalgae lipid compared to the saturated lipids in
lamb fat. These are promising results to the development of a cost effective
biodiesel production process.

Table 4.19: Comparison between production yield and bed activity with the recycling between lamb meat fat and microalgae oil .

Comparison		Lamb fat [18]				Algae lipids (this study)			
M:L ratio		5	10	15	20	5	10	15	20
FAME productivity	Cycle 1	13.5	53.5	32.5	12.5	7	64	59	37
	Cycle 2	13	19	20.5	9.5	17	65	47	42
	Cycle 3	10.7	10	1.9	0.08	51	57	28	16
Attained activity (%)		0.79	0.19	0.06	0.01	7.29	0.89	0.47	0.43

4.5 FUEL PROPERTIES OF MICROALGAE BIODIESEL

The fuel properties of enzymatically produced biodiesel from microalgae lipids extracted by SC-CO$_2$ are shown in Table 4.20 For comparison, the values of commercial diesel available in local petrol station have been also measured and shown in Table 4.20. The table also shows the standard limits.

Table 4.20: Properties of produced microalgae biodiesel and market diesel

Property	Algal biodiesel	Diesel	ASTM	EN
Viscosity (mP-s @ 40°C)	5.3	2.6	1.9-6	33.5-5
Flash point (°C)	105	68-72	93[a]	120[a]
Specific gravity	0.876	0.858	-	0.86-0.9
Higher heating value (MJ/kg)	39.842	42.2	-	-
Cetane number*	57.6	50.3	47[a]	51[a]
Acid value (mg KOH g^{-1})	0.32	-	0.5[b]	0.5[b]
Cloud point (°C)	7	-13	-	-

Table 4.20: Properties of produced microalgae biodiesel and market diesel

Pour point (^{o}C)	-1	-22	-	-
Sulfur content (wt %)	0.008	-	0.02	0.02
Free glycerol (mg kg^{-1})	33	-	0.02	0.02

[*] Calculated using Eq. (3.13)

[a] minimum limit

[b] maximum limit

The results show that the properties of produced FAMEs are close to those of the commercial diesel and of the diesel standard. The low viscosity of the produced biodiesel indicates that it can be directly used in existing engines. The slightly lower heating value was expected due to the oxygen content of the biodiesel, which is not present in conventional diesels. However, the presence of the oxygen may help to achieve complete combustion, which is advantageous. The flash point of the produced biodiesel was almost 45-54 % higher than that of diesel, which is safer for storage and transportation. Most importantly, the present results show that the produced biodiesel has low sulphur content below the fuel limit, according to ASTM D874 method, which is expected as biomass has very low sulfur content. This results in low SO_x emissions. The glycerol content is an important feature that determine the success of the process altogether. It was claimed that using immobilized lipase in SC-CO_2 would result in avoiding the need of glycerol separation step. The free glycerol content in the produced biodiesel was found to be very low, which proves this claim.

CHAPTER 5: CONCLUSIONS AND FUTURE WORKS

The use of $SC\text{-}CO_2$ in microalgae lipids extraction and enzymatic biodiesel production has been investigated. The work was divided in to three phases, which are biomass production, lipid extraction and biodiesel production.

In the first phase, the lipid productivity and carbon biofixation rate of different freshwater and marine microalgae strains were studied under different environmental conditions and the following conclusions were reached:

a. The strains were able to grow under aeration with enriched CO_2, and the optimum growths achieved for most strains were at 1 % CO_2 enrichment.

b. The highest lipid productivity was 115 mg L^{-1} d^{-1}, obtained from *Chlorella* sp. grown in nitrogen rich medium.

c. The freshwater strain, *Chlorella* sp. was able to grow at 27 ^{o}C in water of different salinities reaching up to 460 mM.

d. The highest carbon fixation rate was 1.7 g L^{-1} d^{-1}, achieved when *Chlorella* sp. was grown at 27 ^{o}C in water of 230 mM salinity.

e. *Scenedesmus* sp. showed the highest lipid induction by nitrogen starvation, but its growth rate dropped significantly compared to that obtained in nitrogen sufficient medium.

f. Two-steps culturing, combining high biomass productivity with high lipids content, were tested with *Scenedesmus* sp., and a six-fold increase in the

lipid content was achieved after three weeks of growing in nitrogen starvation medium.

g. Cell growth kinetics data, with respect to TIC concentration, were fitted to the Haldane model, which represented the system well.

The key findings of this phase suggest further studies CO_2 enrichment and its interaction with other process variables considering the two-stage culturing, photobioreactor design and cell growth and lipids content modeling .

In the second phase, lipids extraction from dried microalgae biomass using SC-CO_2 was studied, and the following conclusions were reached:

a. The extraction yield of lipids from lyophilized biomass was higher in SC-CO_2 compared to the yields achieved using conventional extraction methods.

b. SC-CO_2 extraction yield was enhanced by lyophilization, with insignificant effect on the TAG content of the lipids.

c. Extraction temperature and pressure were found to be the significant process variable affected by the extraction yield.

d. A statistically determined second order polynomial adequately predicted the steady state extraction yield

e. Based on the statistical RSM analysis, the optimum operating conditions were determined to be 53 ^{o}C and 500 bar, with the highest extraction yield of 7.4 %.

f. The process was successfully scaled-up by 8-folds, and the lipids extraction yield was 88% of that achieved in the small scale.

g. The overall extraction curves were used to determine the parameters of the BIC model. The predicted mass transfer coefficients determined from the BIC model were used to develop a mass transfer correlation that was verified against the results of the large-scale extraction system.

h. Lipids were successfully extracted from wet cells, which were enzymatically disrupted, using SC-CO$_2$, with insignificant effect on the TAGs content of the lipids.

The results of this phase suggest further studies on protein recovery and purification using SFE technology. The findings also suggest further studies on lipid extraction from enzymatically pre-treated wet cells.

In the third phase, biodiesel was enzymatically produced from extracted lipids under SC-CO$_2$, and the following conclusions were reached:

a. FAMEs were successfully produced from extracted microalgae lipids, within relatively short reaction time, using immobilized lipase in SC-CO$_2$ medium.

b. Reaction temperature and M:L molar ratio were shown to have a significant effect on the production yield.

c. The best FAMEs production yield of about 80 %, was obtained at 50 $^{\circ}$C, 9:1 molar ratio and 35 % loading within 4 h of reaction.

d. The robust FAMEs production against fluctuations in temperature during the process operation was confirmed by RSM results.

e. The experimental results were used to determine the parameters of the Ping Pong Bi Bi model with competitive methanol inhibition

f. The properties of the produced biodiesel were shown to meet the ASTM D6751 and EN 14214 fuel standards, and were comparable to those of commercial petroleum diesel.

g. A integrated continuous extraction-reaction system was tested and the highest FAMEs production yield was achieved at 10:1 M:L molar ratio.

h. The immobilized enzyme was successfully reused for 6 cycles; however, at high M:L ratio, the reusability was significantly reduced due to methanol inhibition.

i. The inhibition effect due to glycerol accumulation in the bed appeared more significant in the 6th cycle when operating at 10:1 M:L ratio.

j. *tert*-Butanol successfully regenerated 88 % of used bed , which allowed the bed to be used for 24 cycles operating at 10:1 M:L ratio.

The results of this phase suggest further optimization of the integrated developed process, considering the effect of other process variables, such as lipid content, lipids solubility in SC-CO_2, specific bed height and reaction temperature on the final biodiesel production yield, and enzyme reusability and regeneration.

REFERENCES

1. IPCC, *Climate Change 2001: the Scientific Basis. Contribution of Working Group I to the Third Assessment Report of the Intergovernmental Panel on Climate Change.*, J.T. Houghton, et al., Editors. 2001.

2. Zhang, Y., et al., *Biodiesel production from waste cooking oil: 1. Process design and technological assessment.* Bioresource Technology, 2003. **89**(1): p. 1-16.

3. Al-Zuhair, S., *Production of biodiesel:possibilities and challenges.* Biofuels, Bioproducts and Biorefining, 2007. **1**(1): p. 57-66.

4. Shay, E.G., *Diesel fuel from vegetable oils: status and opportunities.* Biomass and Bioenergy, 1993. **4**(44): p. 227-242.

5. Peterson, G. and W. Scarrah, *Rapeseed oil transesterification by heterogeneous catalysis.* Journal of the American Chemical Society, 1984. **61**(10): p. 1593-1597.

6. Demirbas, A., *Importance of biodiesel as transportation fuel.* Energy Policy, 2007. **35**(9): p. 4661-4670

7. Schumacher, L.G., et al., *Biodiesel Emissions Data From Series 60 DDC.* Transactions of the ASAE, 2001. **44**(6): p. 1465–1468.

8. Akoh, C.C., et al., *Enzymatic Approach to Biodiesel Production.* Journal of Agricultural and Food Chemistry, 2007. **55**(22): p. 8995–9005.

9. Darnoko, D. and M. Cheryan, *Kinetics of Palm Oil Transesterification in a Batch Reactor.* Journal of the American Oil Chemists' Society, 2000. **77**: p. 1263-1267.

10. Dossin, T.F., et al., *Simulation of heterogeneously MgO-catalyzed transesterification for fine-chemical and biodiesel industrial production.* Appl. Catal., B 2006. **67**(1-2): p. 136-148.

11. Freedman B., B.O., Butterfield E H., *Transesterification Kinetics of Soybean Oil.* Journal of the American Oil Chemists' Society, 1986. **63**: p. 1375-1380.

12. Xie, W., H. Peng, and L. Chen, *Calcined Mg-Al hydrotalcites as solid base catalysts for methanolysis of soybean oil.* Journal of Molecular Catalysis A: Chemical, 2006. **246**(1-2): p. 24-32.

13. Ma, F. and M.A. Hanna, *Biodiesel production: a review.* Bioresource technology, 1999. **70**(1): p. 1-15.

14. Nelson, L.A., T.A. Foglia, and W.N. Marmer, *Lipase-catalyzed production of biodiesel.* Journal of Americal Oil Chemist's Society, 1996. **73**(9): p. 1191-1195.

15. Hsu, A.-F., et al., *Production of alkyl esters from tallow and grease using lipase immobilized in a phyllosilicate sol-gel.* Journal of the American Oil Chemists' Society, 2001. **78**(6): p. 585-588.

16. De Paola, M.G., et al., *Factor analysis of transesterification reaction of waste oil for biodiesel production.* Bioresource technology, 2009. **100**(21): p. 5126–5131.

17. Kumar, R., G.v. Madras, and J. Modak, *Enzymatic Synthesis of Ethyl Palmitate in Supercritical Carbon.* Industrial & Engineering Chemistry Research, 2004. **43**(7): p. 1568-1573.

18. Al-Zuhair, S., et al., *Continuous production of biodiesel from fat extracted from lamb meat in supercritical CO_2 media.* Biochemical Engineering Journal, 2012. **60**(0): p. 106-110.

19. Chen, H.-C., et al., *Continuous production of lipase-catalyzedbiodiesel in a packed-bed reactor: Optimization and enzyme reuse study.* Journal of Biomedicine and Biotechnology, 2011. **2011**(Article ID 950725,): p. 1-6.

20. Garlapati, V.K., et al., *Lipase mediated transesterification of Simarouba glauca oil: a new feedstock for biodiesel production.* Sustainable Chemical Processes, 2013. **1**(11): p. 1-6.

21. Jeong, G.-T. and D.-H. Park, *Lipase-catalyzed transesterification of rapeseed oil for biodiesel production with tert-butanol.* Applied Biochemistry and Biotechnology, 2008. **148**(1-3): p. 131-139.

22. Royon, D., et al., *Enzymatic production of biodiesel from cotton seed oil using t-butanol as a solvent.* Bioresour. Technol., 2007. **98**(3): p. 648-653

23. Giebauf, A. and T. Gamse, *A simple process for increasing the specific activity of porcine pancreatic lipase by supercritical carbon dioxide treatment.* Journal of Molecular Catalysis B: Enzymatic, 2000. **9**(1â€"3): p. 57-64.

24. Wimmer, Z.k. and M. Zarevʲcka, *A review on the effects of supercritical carbon dioxide on enzyme activity.* International Journal of Molecular Sciences, 2010. **11**(1): p. 233-253.

25. Hammond, D.A., et al., *Enzymatic reactions in supercritical gases.* Applied Biochemistry and Biotechnology, 1985. **11**(5): p. 393-400.

26. Randolph, T.W., et al., *Enzymatic catalysis in a supercritical fluid.* Biotechnology Letters, 1985. **7**(5): p. 325-328.

27. Wang, C.-H., et al., *Designing supercritical carbon dioxide extraction of rice bran oil that contain oryzanols using response surface methodology.* Journal of Seperation Science, 2008. **31**(8): p. 1399-1407.

28. Kondo, M., et al., *On-line extraction-reaction of canola oil with ethanol by immobilized lipase in $SC\text{-}CO_2$.* Industrial & Engineering Chemistry Research, 2002. **41**(23): p. 5770-5774.

29. Tewari, Y.B., et al., *A thermodynamic study of the lipase-catalyzed transesterification of benzyl alcohol and butyl acetate in supercritical*

carbon dioxide media. Journal of Molecular Catalysis B: Enzymatic, 2004. **30**(3–4): p. 131-136.

30. Laudani, C.G., et al., *Lipase-catalyzed long chain fatty ester synthesis in dense carbon dioxide: Kinetics and thermodynamics.* Journal of Supercritical Fluids, 2007. **41**(1): p. 92-101

31. Laudani, C.G., et al., *Immobilized lipase-mediated long-chain fatty acid esterification in dense carbon dioxide: bench-scale packed-bed reactor study.* The Journal of Supercritical Fluids, 2007. **41**(1): p. 74-81.

32. Romero, M.D., et al., *Enzymatic synthesis of isoamyl acetate with immobilized Candida antarctica lipase in supercritical carbon dioxide.* Journal of Supercritical Fluids, 2005. **33**(1): p. 77-84.

33. Oliveira, D. and J.V. Oliveira, *Enzymatic alcoholysis of palm kernel oil in n-hexane and $SCCO_2$.* Journal of Supercritical Fluids, 2001. **19**: p. 141-148.

34. Rathore, V. and G. Madras, *Synthesis of biodiesel from edible and non-edible oils in supercritical alcohols and enzymatic synthesis in supercritical carbon dioxide.* Fuel, 2007. **86**(17–18): p. 2650-2659.

35. Taher, H., et al., *Extracted fat from lamb meat by supercritical CO_2 as feedstock for biodiesel production.* Biochemical Engineering Journal, 2011. **55**(1): p. 23-31.

36. Varma, M.N., P.A. Deshpande, and G. Madras, *Synthesis of biodiesel in supercritical alcohols and supercritical carbon dioxide.* Fuel, 2010. **89**: p. 1641-1646.

37. Varma, M.N. and G. Madras, *Synthesis of Biodiesel from Castor Oil and Linseed Oil in Supercritical Fluids.* Industrial & Engineering Chemistry Research, 2007. **46**(1): p. 1-6.

38. Lai, C.-C., et al., *Lipase-catalyzed production of biodiesel from rice bran oil.* Journal of Chemical Technology & Biotechnology, 2005. **80**(3): p. 331-337.

39. Phan, A.N. and T.M. Phan, *Biodiesel production from waste cooking oils.* Fuel, 2008. **87**(17-18): p. 3490-3496.

40. Taufiqurrahmi, N., A.R. Mohamed, and S. Bhatia, *Production of biofuel from waste cooking palm oil using nanocrystalline zeolite as catalyst: Process optimization studies.* Bioresource Technology, 2011. **102**(22): p. 10686-10694.

41. Zheng, Y., et al., *Optimization of carbon dioxide fixation and starch accumulation by Tetraselmis subcordiformis in a rectangular airlift photobioreactor.* African Journal of Biotechnology, 2011. **10**(10).

42. Chisti, Y., *Biodiesel from microalgae.* Biotechnology Advances, 2007. **25**(3): p. 294-306.

43. Demirbas, A., *Progress and recent trends in biofuels.* Progress in Energy and Combustion Science, 2007. **33**(1): p. 1-18.

44. Sheehan, J., et al., *A Look Back at the U.S. Department of Energy-Aquatic Species Program: Biodiesel from Algae*. 1998.

45. Brennan, L. and P. Owende, *Biofuels from microalgae-A review of technologies for production, processing, and extractions of biofuels and co-products.* Renewable & Sustainable Energy Reviews, 2010. **14**(2): p. 557-577.

46. Hannon, M., et al., *Biofuels from algae: challenges and potential.* Biofuels, 2010. **1**(5): p. 763–784.

47. Bligh, E.G. and W.J. Dyer, *A rapid method of total lipid extraction and purification.* Canadian Journal of Biochemistry and Physiology, 1959. **37**(8): p. 911-917.

48. Folch, J., M. Lees, and G.H. Sloane Stanley, *A simple method for the isolation and purification of total lipides from animal tissues.* Journal of Biological Chemistry, 1957. **226**(1): p. 497-509.

49. Ryckebosch, E., K. Muylaert, and I. Foubert, *Optimization of an Analytical Procedure for Extraction of Lipids from Microalgae.* Journal of Americal Oil Chemist's Society, 2012. **89**(2): p. 189-198.

50. Del Valle, J.M., et al., *Supercritical CO2 processing of pretreated rosehip seeds: effect of process scale on oil extraction kinetics.* The Journal of Supercritical Fluids, 2004. **31**(2): p. 159-174.

51. Reverchon, E. and C. Marrone, *Modeling and simulation of the supercritical CO_2 extraction of vegetable oils.* Journal of Supercritical Fluids, 2001. **19**(2): p. 161-175.

52. Sovova, H., et al., *Solubility of two vegetable oils in supercritical CO_2.* Journal of Supercritical Fluids, 2001. **20**(1): p. 15-28.

53. Mendes, R.L., et al., *Supercritical CO2 extraction of carotenoids and other lipids from Chlorella vulgaris.* Food Chemistry, 1995. **53**(1): p. 99-103.

54. Mendes, R.L., et al., *Supercritical carbon dioxide extraction of compounds with pharmaceutical importance from microalgae.* Inorganica Chimica Acta, 2003. **356**: p. 328-334.

55. Andrich, G., et al., *Supercritical fluid extraction of bioactive lipids from the microalga Nannochloropsis sp.* European Journal of Lipid Science and Technology, 2005. **107**(6): p. 381-386.

56. Andrich, G., et al., *Supercritical fluid extraction of oil from microalga Spirulina (arthrospira) platensis.* Acta Alimentaria, 2006. **35**(2): p. 195-203.

57. Couto, R.M., et al., *Supercritical fluid extraction of lipids from the heterotrophic microalga Crypthecodinium cohnii.* Engineering in Life Sciences, 2010. **10**(2): p. 158-164.

58. Mohn, H.F., *Improved Technologies for Harvesting and Processing of Microalgae and their impact on production costs.* Arch Hydrobiol Beih Ergeb Limnol, 1978. **11**: p. 228-253.

59. Dejoye Tanzi, C., M. Abert Vian, and F. Chemat, *New procedure for extraction of algal lipids from wet biomass: A green clean and scalable process.* Bioresource Technology, 2013. **134**(0): p. 271-275.

60. Yang, F., et al., *A Novel Lipid Extraction Method from Wet Microalga Picochlorum sp. at Room Temperature.* Marine Drugs, 2014. **12**(3): p. 1258-1270.

61. Bengtsson, L., *The global energy problem.* Energy and Environment, 2006. **17**(5): p. 755-765.

62. Bajpai, D. and V.K. Tyagi, *Biodiesel: Source, Production, Composition, Properties and its Benifits.* Journal of Oleo Science, 2006. **55**(10): p. 487-502.

63. Fellows, P., *Food Processing Technology: Principles and Practice*. 2000, USA: Woodhead Publishing Limited and CRC Press LLC.

64. Demirbas, A., *Progress and recent trends in biodiesel fuels.* Energy Conversion and Management, 2009. **50**: p. 14–34.

65. Fjerbaek, L., K.V. Christensen, and B. Norddahl, *A review of the current state of biodiesel production using enzymatic transesterification.* Biotechnology and Bioengineering, 2009. **102**(5): p. 1298-1315.

66. Fukuda, H., A. Kondo, and H. Noda, *Biodiesel Fuel Production by transesterification of oils.* Journal of Bioscience and Bioengineering, 2001. **92**(5): p. 405-416.

67. Ranganathan, S.V., S.L. Narasimhan, and K. Muthukumar, *An overview of enzymatic production of biodiesel.* Bioresource Technology, 2008. **99**(10): p. 3975-3981

68. Hess, M.A., et al., *Effect of Antioxidant Addition on NOx Emissions from Biodiesel.* Energy Fuels, 2005. **19**(4): p. 1749–1754.

69. Wang, W.G., et al., *Emissions from Nine Heavy Trucks Fueled by Diesel and Biodiesel Blend without Engine Modification.* Environmental Science & Technology, 2000. **34**(6): p. 933-939.

70. Basha, S.A., K.R. Gopal, and S. Jebaraj, *A review on biodiesel production, combustion, emissions and performance.* Renewable Sustainable Energy Rev. , 2009. **13**(6-7): p. 1628–1634.

71. Sharma, Y.C., B. Singh, and S.N. Upadhyay, *Advancements in development and characterization of biodiesel: A review.* Fuel, 2008. **87**(12): p. Volume 87, Issue 12, September 2008, Pages 2355-2373.

72. Demirbas, A., *Biodiesel from waste cooking oil via base-catalytic and supercritical methanol transesterification.* energy Conversion and Management, 2009. **50**(4): p. 923-927.

73. Robles-Medina, A., et al., *Biocatalysis: Towards ever greener biodiesel production.* Biotechnology Advances, 2009. **27**(4): p. 398–408.

74. Helwani, Z., et al., *Technologies for production of biodiesel focusing on green catalytic techniques: A review.* Fuel Process. Technol., 2009. **90**(12): p. 1502-1514

75. Fan, X. and R. Burton, *Recent Development of Biodiesel Feedstocks and the Applications of Glycerol: A Review.* The Open Fuels & Energy Science Journal, 2009. **1**: p. 100-109.

76. Rajan, K. and K.R. Senthilkumar, *Effect of Exhaust Gas Recirculation (EGR) on the Performance and Emission Characteristics of Diesel Engine with Sunflower Oil Methyl Ester.* Jordan Journal of Mechanical and Industrial Engineering, 2009. **3**(4): p. 306 - 311.

77. Sinha, S., A.K. Agarwal, and S. Garg, *Biodiesel development from rice bran oil: Transesterification process optimization and fuel characterization.* Energy Conversion and Management, 2008. **49**(5): p. 1248-1257

78. Lin, L., et al., *Biodiesel production from crude rice bran oil and properties as fuel.* Applied Energy, 2009. **86**: p. 681–688.

79. Gerpen, J.V., *Biodiesel processing and production.* Fuel Processing Technology, 2005. **86**: p. 1097– 1107.

80. Marchetti, J.M., V.U. Miguel, and A.F. Errazu, *Possible methods for biodiesel production.* Renewable Sustainable Energy Rev. , 2007. **11**: p. 1300–1311.

81. Meher, L.C., D.V. Saga, and S.N. Naik, *Technical aspects of biodiesel production by transesterification—a review.* Renewable Sustainable Energy Rev. , 2006. **10**(3): p. 248-268

82. Atadashi, I.M., et al., *The effects of water on biodiesel production and refining technologies: A review.* Renewable and Sustainable Energy Reviews, 2012. **16**(5): p. 3456-3470.

83. Ma, F., L.D. Clements, and M.A. Ha, *Biodiesel Fuel from animal fat.* Industrial and Engineering Chemistry Research, 1998. **37**(9): p. 3768–3771.

84. Sivasamy, A., et al., *Catalytic Applications in the Production of Biodiesel from.* ChemSusChem, 2009. **2**: p. 278 – 300.

85. Carelli, A., M.V. Brevedan, and G. Crapiste, *Quantitative determination of phospholipids in sunflower oil.* Journal of the American Oil Chemists' Society, 1997. **74**(5): p. 511-514.

86. Verleyen, T., et al., *Influence of the vegetable oil refining process on free and esterified sterols.* Journal of the American Oil Chemists' Society, 2002. **79**(10): p. 947-953.

87. Chung, K.-H., J. Kim, and K.-Y. Lee, *Biodiesel production by transesterification of duck tallow with methanol on alkali catalysts.* Biomass and Bioenergy, 2009. **33**(1): p. 155-158.

88. Vicente, G., M. Martínez, and J. Aracil, *Integrated biodiesel production: a comparison of different homogeneous catalysts systems.* Bioresource Technology, 2004. **92**(3): p. 297-305.

89. Meng, X., G. Chen, and Y. Wang, *Biodiesel production from waste cooking oil via alkali catalyst and its engine test.* Fuel Processing Technology, 2008. **89**(9): p. 851-857.

90. Leung, D.Y.C. and Y. Guo, *Transesterification of neat and used frying oil: Optimization for biodiesel production.* Fuel Processing Technology, 2006. **87**(10): p. 883-890.

91. Ji, J., et al., *Preparation of biodiesel with the help of ultrasonic and hydrodynamic cavitation.* Ultrasonics, 2006. **44**(Supplement 1): p. e411-e414.

92. Rashid, U., et al., *Production of sunflower oil methyl esters by optimized alkali-catalyzed methanolysis.* Biomass and Bioenergy, 2008. **32**(12): p. 1202-1205.

93. Marjanovic, A.V., et al., *Kinetics of the base-catalyzed sunflower oil ethanolysis.* Fuel, 2010. **89**(3): p. 665-671.

94. Kucek, K., et al., *Ethanolysis of Refined Soybean Oil Assisted by Sodium and Potassium Hydroxides.* Journal of the American Oil Chemists' Society, 2007. **84**(4): p. 385-392.

95. Meher, L.C., V.S.S. Dharmagadda, and S.N. Naik, *Optimization of alkali-catalyzed transesterification of Pongamia pinnata oil for production of biodiesel.* Bioresource Technology, 2006. **97**(12): p. 1392-1397.

96. Karmee, S.K. and A. Chadha, *Preparation of biodiesel from crude oil of Pongamia pinnata.* Bioresource technology, 2005. **96**(13): p. 1425-1429.

97. Barbosa, D.d.C., et al., *Biodiesel production by ethanolysis of mixed castor and soybean oils.* Fuel, 2010. **89**(12): p. 3791-3794.

98. Armenta, R., et al., *Transesterification of Fish Oil to Produce Fatty Acid Ethyl Esters Using Ultrasonic Energy.* Journal of the American Oil Chemists' Society, 2007. **84**(11): p. 1045-1052.

99. Refaat, A.A., et al., *Production optimization and quality assessment of biodiesel from waste vegetable oil.* International Journal of Environmental Science & Technology, 2008. **5**(1): p. 75-82.

100. Meneghetti, S.M.P., et al., *Biodiesel from Castor Oil-A Comparison of Ethanolysis versus Methanolysis.* Energy & Fuels, 2006. **20**(5): p. 2262-2265.

101. Moser, B.R. and S.F. Vaughn, *Coriander seed oil methyl esters as biodiesel fuel: Unique fatty acid composition and excellent oxidative stability.* Biomass and Bioenergy, 2010. **34**(4): p. 550-558.

102. Wang, Y., et al., *Comparison of two different processes to synthesize biodiesel by waste cooking oil.* Journal of Molecular Catalysis A: Chemical, 2006. **252**(1â€"2): p. 107-112.

103. Freedman, B., E.H. Pryde, and T.L. Mounts, *Variables affecting the yields of fatty esters from transesterified vegetable oils.* Journal of the American Oil Chemists Society, 1984. **61**(10): p. 1638-1643.

104. Zheng, S., et al., *Acid-catalyzed production of biodiesel from waste frying oil.* Biomass and Bioenergy, 2006. **30**(3): p. 267-272.

105. Zullaikah, S., et al., *A two-step acid-catalyzed process for the production of biodiesel from rice bran oil.* Bioresource Technology, 2005. **96**(17): p. 1889-1896.

106. Sharma, Y.C., B. Singh, and J. Korstad, *High Yield and Conversion of Biodiesel from a Nonedible Feedstock (Pongamia pinnata).* Journal of Agricultural and Food Chemistry, 2009. **58**(1): p. 242-247.

107. Fadhil, A.B., et al., *Biodiesel Production from Spent Fish Frying Oil Through Acid-Base Catalyzed Transesterification.* Pakistan Journal of Analytical & Environmental Chemistry, 2012. **13**(1): p. 9-15.

108. Patil, P., et al., *Conversion of waste cooking oil to biodiesel using ferric sulfate and supercritical methanol processes.* Fuel, 2010. **89**(2): p. 360-364.

109. Granados, M.L., et al., *Biodiesel from sunflower oil by using activated calcium oxide.* applied Catalysis B: Environmental, 2007. **73**(3-4): p. 317-326.

110. Ebiura, T., et al., *Selective transesterification of triolein with methanol to methyl oleate and glycerol using alumina loaded with alkali metal salt as a solid-base catalyst.* Appl. Catal., A 2005. **283**(1-2): p. 111-116.

111. Silva, C.C.C.M., et al., *Biodiesel production from soybean oil and methanol using hydrotalcites as catalyst.* Fuel Process. Technol., 2010. **91**(2): p. 205-210.

112. Zabeti, M., W.M.A. Wan Daud, and M.K. Aroua, *Activity of solid catalysts for biodiesel production: A review.* Fuel Processing Technology, 2009. **90**(6): p. 770-777.

113. Liu, X., et al., *Transesterification of soybean oil to biodiesel using CaO as a solid base catalyst.* Fuel, 2008. **87**(2): p. 216-221.

114. Kouzu, M., et al., *Calcium oxide as a solid base catalyst for transesterification of soybean oil and its application to biodiesel production.* Fuel, 2008. **87**(12): p. 2798-2806.

115. Meher, L.C., et al., *Transesterification of karanja (Pongamia pinnata) oil by solid basic catalysts.* European Journal of Lipid Science and Technology, 2006. **108**(5): p. 389-397.

116. Guan, G., K. Kusakabe, and S. Yamasaki, *Tri-potassium phosphate as a solid catalyst for biodiesel production from waste cooking oil.* Fuel Processing Technology, 2009. **90**(4): p. 520-524.

117. Park, Y.-M., et al., *The heterogeneous catalyst system for the continuous conversion of free fatty acids in used vegetable oils for the production of biodiesel.* Catalysis Today, 2008. **131**(1â€"4): p. 238-243.

118. Zhang, X., et al., *Heteropolyacid Nanoreactor with Double Acid Sites as a Highly Efficient and Reusable Catalyst for the Transesterification of Waste Cooking Oil.* Energy & Fuels, 2009. **23**(9): p. 4640-4646.

119. Jacobson, K., et al., *Solid acid catalyzed biodiesel production from waste cooking oil.* Applied Catalysis B: Environmental, 2008. **85**(1â€"2): p. 86-91.

120. Peng, B.-X., et al., *Biodiesel production from waste oil feedstocks by solid acid catalysis.* Process Safety and Environmental Protection, 2008. **86**(6): p. 441-447.

121. Lam, M.K., K.T. Lee, and A.R. Mohamed, *Sulfated tin oxide as solid superacid catalyst for transesterification of waste cooking oil: An optimization study.* applied Catalysis B: Environmental, 2009. **93**(1-2): p. 134-139.

122. Al-Zuhair, S., F.W. Ling, and L.S. Jun, *Proposed kinetic mechanism of the production of biodiesel from palm oil using lipase.* Process Biochemistry, 2007. **42**(6): p. 951-960.

123. Garcia, C.M., et al., *Transesterification of soybean oil catalyzed by sulfated zirconia.* Bioresour. Technol. , 2008. **99**(14): p. 6608-6613.

124. Zhang, S., et al., *Rapid microwave-assisted transesterification of yellow horn oil to biodiesel using a heteropolyacid solid catalyst.* Bioresour. Technol., 2010. **101**(3): p. 931-936.

125. Shibasaki-Kitakawa, N., et al., *Biodiesel production using anionic ion-exchange resin as heterogeneous catalyst.* Bioresour. Technol. , 2007. **98**(2): p. 416-421.

126. Lopez, D.E., J.G. Goodwin Jr, and D.A. Bruce, *Transesterification of triacetin with methanol on NafionÂ® acid resins.* Journal of Catalysis, 2007. **245**(2): p. 381-391.

127. Feng, Y., et al., *Biodiesel production using cation-exchange resin as heterogeneous catalyst.* Bioresource Technology, 2010. **101**(5): p. 1518-1521.

128. Shibasaki-Kitakawa, N., et al., *Biodiesel Production from Waste Cooking Oil Using Anion-Exchange Resin as Both Catalyst and Adsorbent.* BioEnergy Research, 2011. **4**(4): p. 287-293.

129. Canakci, M. and J.V. Gerpen, *biodiesel production from oils and fat with high free fatty acids.* American Society of Agricultural Engineers, 2001. **44**(6): p. 1429–1436.

130. Liu, Y., E. Lotero, and J.G. Goodwin Jr, *Effect of water on sulfuric acid catalyzed esterification.* Journal of Molecular Catalysis A: Chemical, 2006. **245**(1â€"2): p. 132-140.

131. Berchmans, H.J. and S. Hirata, *Biodiesel production from crude Jatropha curcas L. seed oil with a high content of free fatty acids.* Bioresource Technology, 2008. **99**(6): p. 1716-1721.

132. Chen, L., et al., *Biodiesel production from algae oil high in free fatty acids by two-step catalytic conversion.* Bioresource Technology, 2012. **111**(0): p. 208-214.

133. Ghadge, S.V. and H. Raheman, *Biodiesel production from mahua (Madhuca indica) oil having high free fatty acids.* Biomass and Bioenergy, 2005. **28**(6): p. 601-605.

134. Sathya, T. and A. Manivannan, *Biodiesel production from neem oil using two step transesterification.* International Journal of Engineering Research and Applications, 2013. **3**(3): p. 488-492.

135. Demirbas, A., *Biodiesel from vegetable oils via transesterification in supercritical methanol.* Energy Convers. Manage. , 2002. **43**(17): p. 2349-2356.

136. Saka, S. and D. Kusdiana, *Biodiesel fuel from rapeseed oil as prepared in supercritical methanol.* Fuel, 2001. **80**(2): p. 225-231.

137. Haas, M.J. and T.A. Foglia, *Alternate Feedstocks and Technologies for Biodiesel Production*, in *The Biodiesel Handbook*, G. Knothe, J.V. Gerpen, and J. Krahl, Editors. 2005, AOCS Press: Champaign, IL. p. 42-61.

138. Tan, C.-S., S.-K. Liang, and D.-C. Liou, *Fluid-solid mass transfer in a supercritical fluid extractor.* The Chemical Engineering Journal, 1988. **38**(1): p. 17-22.

139. Samniang, A., C. Tipachan, and S. Kajorncheappun-ngam, *Comparison of biodiesel production from crude Jatropha oil and Krating oil by supercritical methanol transesterification.* Renewable Energy, 2014. **68**(0): p. 351-355.

140. Vieitez, I., et al., *Continuous Production of Soybean Biodiesel in Supercritical Ethanolâˆ’Water Mixtures.* Energy & Fuels, 2008. **22**(4): p. 2805-2809.

141. Tan, K.T., et al., *An optimized study of methanol and ethanol in supercritical alcohol technology for biodiesel production.* The Journal of Supercritical Fluids, 2010. **53**(1-3): p. 82-87.

142. Demirbas, A., *Biodiesel fuels from vegetable oils via catalytic and non-catalytic supercritical alcohol transesterifications and other methods: a survey.* Energy Conversion and Management, 2003. **44**(13): p. 2093-2109.

143. Madras, G., C. Kolluru, and R. Kumar, *Synthesis of biodiesel in supercritical fluids.* Fuel, 2004. **83**(14â€"15): p. 2029-2033.

144. Taipa, M.A., M.R. Aires-Barros, and J.M.S. Cabral, *Purification of lipases.* Journal of Biotechnology, 1992. **26**(2-3): p. 111-142.

145. Hasan, F., A.A. Shah, and A. Hameed, *Industrial applications of microbial lipases.* Enzyme and Microbial Technology, 2006. **39**(2): p. 235-251.

146. Chahiniana, H. and L. Sarda, *Distinction Between Esterases and Lipases: Comparative Biochemical Properties of Sequence-Related Carboxylesterases* Protein & Peptide Letters. **16**(10): p. 1149-1161

147. Fojan, P., et al., *What distinguishes an esterase from a lipase: A novel structural approach.* Biochimie, 2000. **82**(11): p. 1033-1041.

148. Ghosh, M., S. Bhattacharyya, and D.K. Bhattacharyya, *Production of Lipase and Phospholipase Enzymes from Pseudomonas sp. and Their Action on Phospholipids.* Journal of Oleo Science, 2005. **54**(7): p. 407-411.

149. Cesarini, S., et al., *Combining phospholipases and a liquid lipase for one-step biodiesel production using crude oils.* Biotechnology for Biofuels, 2014. **7**(29): p. 1-12.

150. Antczak, M.a.S., et al., *Enzymatic biodiesel synthesis – Key factors affecting efficiency of the process.* Renewable Energy, 2009. **34**: p. 1185–1194.

151. Mittelbach, M., *Lipase catalyzed alcoholysis of sunflower oil.* Journal of the American Oil Chemists' Society, 1990. **67**(3): p. 168-170.

152. Haas, M.J., et al., *A process model to estimate biodiesel production costs.* Bioresource Technology, 2006. **97**(4): p. 671-678.

153. Caballero, V., et al., *Sustainable preparation of a novel glycerol-free biofuel by using pig pancreatic lipase: Partial 1,3-regiospecific alcoholysis of sunflower oil.* Process Biochemistry, 2009. **44**(3): p. 334-342

154. Jegannathan, K.R., et al., *Design an immobilized lipase enzyme for biodiesel production.* Journal of Renewable and Sustainable Energy, 2009. **1**(6): p. 063101.

155. Noureddini, H., X. Gao, and R.S. Philkana, *Immobilized Pseudomonas cepacia lipase for biodiesel fuel production from soybean oil.* Bioresource technology, 2005. **96**(7): p. 769-777.

156. Cao, L., *Immobilised enzymes: science or art?* Current Opinion in Biotechnology, 2005. **9**(2): p. 217-226.

157. Iso, M., et al., *Production of biodiesel fuel from triglycerides and alcohol using immobilized lipase.* Journal of Molecular Catalysis B - Enzymatic, 2001. **16**(1): p. 53-58.

158. Taher, H., et al., *A Review of Enzymatic Transesterification of Microalgal Oil-Based Biodiesel Using Supercritical Technology.* Enzyme Research, 2011. **2011**(Article ID 468292): p. 1-25.

159. Da Ros, P.C.M., et al., *Evaluation of the catalytic properties of Burkholderia cepacia lipase immobilized on non-commercial matrices to be used in biodiesel synthesis from different feedstocks.* Bioresource Technology, 2010. **101**(14): p. 5508-5516.

160. Du, W., et al., *Comparative study on lipase-catalyzed transformation of soybean oil for biodiesel production with different acyl acceptors.* Journal of Molecular Catalysis B - Enzymatic, 2004. **30**(3-4): p. 125-129.

161. Orçaire, O., P. Buisson, and A.C. Pierre, *Application of silica aerogel encapsulated lipases in the synthesis of biodiesel by transesterification reactions.* Journal of Molecular Catalysis B - Enzymatic, 2006. **42**(3-4): p. 106-113.

162. Lu, J., et al., *Enzymatic synthesis of fatty acid methyl esters from lard with immobilized Candida sp. 99-125.* Process Biochemistry, 2007. **42**(9): p. 1367-1370.

163. Modi, M.K., et al., *Lipase-mediated conversion of vegetable oils into biodiesel using ethyl acetate as acyl acceptor.* Bioresource Technology, 2007. **98**(6): p. 1260-1264

164. Shimada, Y., et al., *Conversion of vegetable oil to biodiesel using immobilized Candida antarctica lipase.* Journal of the American Oil Chemists' Society, 1999. **76**(7): p. 789-793.

165. Wang, L., et al., *Lipase-catalyzed biodiesel production from soybean oil deodorizer distillate with absorbent present in tert-butanol system.* Journal of Molecular Catalysis B: Enzymatic, 2006. **43**(1-4): p. 29-32.

166. Modi, M.K., et al., *Lipase-mediated Transformation of Vegetable Oils into Biodiesel using Propan-2-ol as Acyl Acceptor.* Biotechnology Letters, 2006. **28**(9): p. 637-640.

167. Kumari, V., S. Shah, and M.N. Gupta, *Preparation of Biodiesel by Lipase-Catalyzed Transesterification of High Free Fatty Acid Containing Oil from Madhuca indica.* Energy & Fuels, 2007. **21**(1): p. 368-372.

168. Shah, S. and M.N. Gupta, *Lipase catalyzed preparation of biodiesel from Jatropha oil in a solvent free system.* Process Biochemistry, 2007. **42**(3): p. 409-414.

169. Soumanou, M.M. and U.T. Bornscheuer, *Improvement in lipase-catalyzed synthesis of fatty acid methyl esters from sunflower oil.* Enzyme and Microbial Technology, 2003. **33**(1): p. 97-103.

170. Salis, A., et al., *Comparison among immobilised lipases on macroporous polypropylene toward biodiesel synthesis.* Journal of Molecular Catalysis B: Enzymatic, 2008. **54**(1-2): p. 19-26.

171. Devanesan, M.G., T. Viruthagiri, and N. Sugumar, *Transesterification of Jatropha oil using immobilized Pseudomonas fluorescens.* African Journal of Biotechnology, 2007. **6**(21): p. *2497-2501.*

172. Ha, S.H., et al., *Lipase-catalyzed biodiesel production from soybean oil in ionic liquids.* Enzyme and Microbial Technology, 2007. **41**(4): p. 480-483.

173. Xu, Y., et al., *A novel enzymatic route for biodiesel production from renewable oils in a solvent-free medium.* Biotechnology Letters, 2003. **25**(15): p. 1239-1241.

174. Samukawa, T., et al., *Pretreatment of immobilized Candida antarctica lipase for biodiesel fuel production from plant oil.* Journal of Bioscience and Bioengineering, 2000. **90**(2): p. 180-183

175. Kaieda, M., et al., *Effect of Methanol and water contents on production of biodiesel fuel from plant oil catalyzed by various lipases in a solvent-free system.* Journal of Bioscience and Bioengineering, 2001. **91**(1): p. 12-15.

176. Shah, S., S. Sharma, and M.N. Gupta, *Biodiesel Preparation by Lipase-Catalyzed Transesterification of Jatropha Oil.* Energy & Fuels, 2004. **18**(1): p. 154-159.

177. Salis, A., et al., *Biodiesel production from triolein and short chain alcohols through biocatalysis.* Journal of Biotechnology, 2005. **119**(3): p. 291-299.

178. Xu, W.D., Jing Zeng and Y. Dehua Liu, *Conversion of Soybean Oil to Biodiesel Fuel Using Lipozyme TL IM in a Solvent-free Medium.* Biocatalysis and Biotransformation, 2004. **22**(1): p. 45-48.

179. Li, X., H. Xu, and Q. Wu, *Large-scale biodiesel production from microalga Chlorella protothecoides through heterotrophic cultivation in bioreactors.* Biotechnology and Bioengineering, 2007. **98**(4): p. 764-771.

180. Li, L., et al., *Lipase-catalyzed transesterification of rapeseed oils for biodiesel production with a novel organic solvent as the reaction medium.* J. Mol. Catal. B: Enzym., 2006. **43**(1-4): p. 58-62

181. Klibanov, A.M., *Improving enzymes by using them in organic solvents.* Nature, 2001. **409**(6817): p. 241-246.

182. Zheng, Y., et al., *Lipase-catalyzed transesterification of soybean oil for biodiesel production in tert-amyl alcohol.* World Journal of Microbiology and Biotechnology, 2009. **25**(1): p. 41-46.

183. Santambrogio, C., et al., *Effects of methanol on a methanol-tolerant bacterial lipase.* Applied Microbiology and Biotechnology, 2013. **97**(19): p. 8609-8618.

184. Chen, J.-W. and W.-T. Wu, *Regeneration of immobilized Candida antarctica lipase for transesterification.* Journal of Bioscience and Bioengineering, 2003. **95**(5): p. 466-469.

185. Encinar, J.M., et al., *Biodiesel Fuels from Vegetable Oils: Transesterification of Cynara cardunculus L. Oils with Ethanol.* Energy & Fuels, 2002. **16**(2): p. 443-450.

186. Abigor, R.D., et al., *Lipase-catalysed production of biodiesel fuel from some Nigerian lauric oils.* Biochemical Society Transactions, 2000. **28**: p. 979–981.

187. Shimada, Y., et al., *Enzymatic alcoholysis for biodiesel fuel production and application of the reaction to oil processing.* Journal of Molecular Catalysis B: Enzymatic, 2002. **17**(3-5): p. 133-142.

188. Watanabe, Y., et al., *Continuous production of biodiesel fuel from vegetable oil using immobilized Candida antarctica lipase.* Journal of the American Oil Chemists' Society, 2000. **77**(4): p. 355-360.

189. Chen, G., M. Ying, and W. Li, *Enzymatic conversion of waste cooking oils into alternative fuel-Biodiesel.* Applied Biochemistry and Biotechnology, 2006. **132**(1-3): p. 911-921.

190. Bernardes, O.v., et al., *Biodiesel fuel production by the transesterification reaction of soybean oil using immobilized lipase.* Applied Biochemistry and Biotechnology, 2007. **137-140**(1-12): p. 105-114.

191. Lee, K.-T., T. Foglia, and K.-S. Chang, *Production of alkyl ester as biodiesel from fractionated lard and restaurant grease.* Journal of the American Oil Chemists' Society, 2002. **79**(2): p. 191-195.

192. Xu, Y., W. Du, and D. Liu, *Study on the kinetics of enzymatic interesterification of triglycerides for biodiesel production with methyl acetate as the acyl acceptor.* Journal of Molecular Catalysis B: Enzymatic, 2005. **32**(5-6): p. 241-245.

193. Radzi, S., et al. (2005) *High performance enzymatic synthesis of oleyl oleate using immobilised lipase from Candida antartica.* Electronic Journal of Biotechnology **8**.

194. Klibanov, A.M., *Improving enzymes by using them in organic solvents.* Nature, 2001. **209**: p. 241-246.

195. Zaks, A. and A. Klibanov, *Enzymatic catalysis in organic media at 100 degrees C.* Science, 1984. **224**: p. 1249-1251.

196. Laane, C., et al., *Rules for optimization of biocatalysis in organic solvents.* Biotechnology and Bioengineering, 1987. **30**(1): p. 81-87.

197. Khmelnitsky, Y.L., et al., *Denaturation capacity: a new quantitative criterion for selection of organic solvents as reaction media in biocatalysis.* European Journal of Biochemistry, 1991. **198**(1): p. 31-41.

198. Adamczak, M. and S.H. Krishna, *Strategies for Improving Enzymes for Efficient Biocatalysis.* Food Technology and Biotechnology, 2004. **42**(4): p. 251–264.

199. Eltaweel, M.A., et al., *An organic solvent-stable lipase from Bacillus sp. strain 42.* Annals of Microbiology, 2005. **55**(3): p. 187-192.

200. Hernández-Rodríguez, B., et al., *Effects of organic solvents on activity and stability of lipases produced by thermotolerant fungi in solid-state fermentation.* Journal of Molecular Catalysis B: Enzymatic, 2009. **61**(3â€"4): p. 136-142.

201. Kaar, J.L., et al., *Impact of Ionic Liquid Physical Properties on Lipase Activity and Stability.* Journal of the American Chemical Society, 2003. **125**(14): p. 4125-4131.

202. Ulbert, O., et al., *Thermal stability enhancement of Candida rugosa lipase using ionic liquids.* Biocatalysis and Biotransformation, 2005. **23**(3-4): p. 177-183.

203. Knez, !.e. and M. Habulin, *Compressed gases as alternative enzymatic-reaction solvents: a short review.* The Journal of Supercritical Fluids, 2002. **23**(1): p. 29-42.

204. Nakamura, K., et al., *Lipase Activity and Stability in Supercritical Carbon Dioxide* Chemical Engineering Communications, 1986. **45**(1-6): p. 207-212.

205. Palocci, C., et al., *Lipase-catalyzed regioselective acylation of tritylglycosides in supercritical carbon dioxide.* The Journal of Supercritical Fluids, 2008. **45**(1): p. 88-93.

206. Cameron, P.A., et al., *Direct transesterification of gases by "dry" immobilized lipase.* Biotechnology and Bioengineering, 2002. **78**(3): p. 251-256.

207. Nie, K., et al., *Lipase catalyzed methanolysis to produce biodiesel: Optimization of the biodiesel production.* Journal of Molecular Catalysis B: Enzymatic, 2006. **43**(1–4): p. 142-147.

208. Nakaya, H., O. Miyawaki, and K. Nakamura, *Determination of log P for pressurized carbon dioxide and its characterization as a medium for enzyme reaction.* Enzyme and Microbial Technology, 2001. **28**(2–3): p. 176-182.

209. Köse, Ö., M. Tüter, and H.A. Aksoy, *Immobilized Candida antarctica lipase-catalyzed alcoholysis of cotton seed oil in a solvent-free medium.* Bioresour. Technol. , 2002. **83**(2): p. 125-129

210. Klibanov, A.M., *Why are enzymes less active in organic solvents than in water?* Trends in Biotechnology, 1997. **15**(3): p. 97-101.

211. Doukyu, N. and H. Ogino, *Organic solvent-tolerant enzymes.* Biochemical Engineering Journal, 2010. **48**(3): p. 270-282.

212. Ruzich, N.I. and A.S. Bassi, *Investigation of enzymatic biodiesel production using ionic liquid as a co-solvent.* The Canadian Journal of Chemical Engineering, 2010. **88**(2): p. 277-282.

213. Michaelis, L. and M.L. Menten, *Kinetics of Invertase Action.* Biochemische Zeitschrift, 1913. **49**: p. 333-369.

214. Al-Zuhair, S., A. Dowaidar, and H. Kamal, *Dynamic modeling of biodiesel production from simulated waste cooking oil using immobilized lipase.* Biochemical Engineering Journal, 2009. **44**(2–3): p. 256-262.

215. Al-Zuhair, S., et al., *The effect of fatty acid concentration and water content on the production of biodiesel by lipase.* Biochemical Engineering Journal, 2006. **30**(2): p. 212-217.

216. Chulalaksananukul, W., et al., *Kinetic study of esterification by immobilized lipase in n-hexane.* FEBS Letters, 1990. **276**(1–2): p. 181-184.

217. Dossat, V.r., D. Combes, and A. Marty, *Lipase-catalysed transesterification of high oleic sunflower oil.* Enzyme and Microbial Technology, 2002. **30**(1): p. 90-94.

218. Hari, K.S. and N.G. Karanth, *Lipase-catalyzed synthesis of isoamyl butyrate: A kinetic study.* Biochimica et Biophysica Acta (BBA) - Protein Structure and Molecular Enzymology, 2001. **1547**(2): p. 262-267.

219. Al-Zuhair, S., *Production of Biodiesel by Lipase-Catalyzed Transesterification of Vegetable Oils: A Kinetics Study.* Biotechnology Progress, 2005. **21**(5): p. 1442-1448.

220. Naik, S.N., et al., *Production of first and second generation biofuels: A comprehensive review.* Renewable and Sustainable Energy Reviews, 2010. **14**(2): p. 578-597.

221. Walton, J., *The Fuel Possibilities of vegetable oils.* Gas Oil Power, 1938. **33**: p. 167-168.

222. Antunes, W.M., C.d.O. Veloso, and C.A. Henriques, *Transesterification of soybean oil with methanol catalyzed by basic solids.* Catalysis Today, 2008. **133-135**: p. 548-554.

223. Dubé, M.A., A.Y. Tremblay, and J. Liu, *Biodiesel production using a membrane reactor.* Bioresource Technology, 2007. **98**(3): p. 639-647

224. Abdullah, A.Z., et al., *Current status and policies on biodiesel industry in Malaysia as the world's leading producer of palm oil.* Energy Policy, 2009. **37**(12): p. 5440-5448.

225. Kalam, M.A. and H.H. Masjuki, *Biodiesel from palmoil--an analysis of its properties and potential.* Biomass Bioenergy 2002. **23**(6): p. 471-479.

226. Georgogianni, K.G., et al., *Conventional and in situ transesterification of sunflower seed oil for the production of biodiesel.* Fuel Processing Technology, 2008. **89**(5): p. 503-509.

227. Pereyra-Irujo, G.A., et al., *Variability in sunflower oil quality for biodiesel production: A simulation study.* Biomass Bioenergy 2009. **33**(3): p. 459-468.

228. Srivastava, A. and R. Prasad, *Triglycerides-based diesel fuels.* Renewable and Sustainable Energy Reviews, 2000. **4**(2): p. 111-133.

229. Demirel, G., et al., *Fatty acids of lamb meat from two breeds fed different forage: concentrate ratio.* Meat Science, 2006. **72**(2): p. 229-235.

230. Kamal-Eldin, A. and R. Andersson, *A multivariate study of the correlation between tocopherol content and fatty acid composition in vegetable oils.* Journal of the American Oil Chemists' Society, 1997. **74**(4): p. 375-380.

231. Sharma, Y.C. and B. Singh, *A hybrid feedstock for a very efficient preparation of biodiesel.* Fuel Processing Technology, 2010. **91**(10): p. 1267-1273.

232. Sharma, Y.C., B. Singh, and J. Korstad, *Application of an efficient nonconventional heterogeneous catalyst for biodiesel synthesis from pongamia pinnata oil.* Energy and Fuels, 2010. **24**(5): p. 3223-3231.

233. Balat, M., *Potential alternatives to edible oils for biodiesel production â€" A review of current work.* Energy Conversion and Management, 2011. **52**(2): p. 1479-1492.

234. Koh, M.Y. and T.I. Mohd. Ghazi, *A review of biodiesel production from Jatropha curcas L. oil.* Renewable and Sustainable Energy Reviews, 2011. **15**(5): p. 2240-2251.

235. Marmesat, S., et al., *Quality of used frying fats and oils: comparison of rapid tests based on chemical and physical oil properties.* International Journal of Food Science & Technology, 2007. **42**(5): p. 601-608.

236. Olmstead, I.L.D., et al., *A quantitative analysis of microalgal lipids for optimization of biodiesel and omega-3 production.* Biotechnology and Bioengineering, 2013. **110**(8): p. 2096-2104.

237. Wang, Y., P.L.S. Ou, and Z. Zhang, *Preparation of biodiesel from waste cooking oil via two-step catalyzed process.* Energy Conversion and Management, 2007. **48**(1): p. 184-188.

238. Wen, Z., et al., *Biodiesel production from waste cooking oil catalyzed by TiO$_2$-MgO mixed oxides.* Bioresource Technology, 2010. **101**(24): p. 9570-9576.

239. Santos, N., et al., *Thermo-oxidative stability and cold flow properties of babassu biodiesel by PDSC and TMDSC techniques.* Journal of Thermal Analysis and Calorimetry, 2009. **97**(2): p. 611-614.

240. Rutz, D. and R. Janssen, *BioFuel Technology Handbook.* 2007: WIP Renewable Energies.

241. Yin, J.-Z., M. Xiao, and J.-B. Song, *Biodiesel from soybean oil in supercritical methanol with co-solvent.* Energy Conversion and Management, 2008. **49**(5): p. 908-912.

242. Chen, Y., et al., *Synthesis of biodiesel from waste cooking oil using immobilized lipase in fixed bed reactor.* Energy Conversion and Management, 2009. **50**(3): p. 668-673.

243. Li, Y., et al., *Biofuels from Microalgae.* Biotechnology Progress, 2008. **24**(4): p. 815-820.

244. Watanabe, Y., et al., *Enzymatic conversion of waste edible oil to biodiesel fuel in a fixed-bed bioreactor.* Journal of the American Oil Chemists' Society, 2001. **78**(7): p. 703-707.

245. Halim, S.F.A., A.H. Kamaruddin, and W.J.N. Fernando, *Continuous biosynthesis of biodiesel from waste cooking palm oil in a packed bed reactor: Optimization using response surface methodology (RSM) and mass transfer studies.* Bioresource Technology, 2009. **100**(2): p. 710-716.

246. Maceiras, R., et al., *Effect of methanol content on enzymatic production of biodiesel from waste frying oil.* Fuel, 2009. **88**(11): p. 2130-2134.

247. Enweremadu, C.C. and M.M. Mbarawa, *Technical aspects of production and analysis of biodiesel from used cooking oilâ€"A review.* Renewable and Sustainable Energy Reviews, 2009. **13**(9): p. 2205-2224.

248. Goering, C.E., et al., *Fuel Properties of Eleven Vegetable Oils.* Transactions of teh ASAE, 1982. **25**(6): p. 1472-1483.

249. *Committee for Standardization Automotive fuels - fatty acid FAME (FAME) for diesel engines - requirements and test methods*. 2003, European Committee for Standardization.

250. Azam, M.M., A. Waris, and N.M. Nahar, *Prospects and potential of fatty acid methyl esters of some non-traditional seed oils for use as biodiesel in India.* Biomass and Bioenergy, 2005. **29**(4): p. 293-302.

251. Graboski, M.S. and R.L. McCormick, *Combustion of fat and vegetable oil derived fuels in diesel engines.* Progress in Energy and Combustion Science, 1998. **24**(2): p. 125-164.

252. Adamczak, M., U.T. Bornscheuer, and W. Bednarski, *The application of biotechnological methods for the synthesis of biodiesel.* European Journal of Lipid Science and Technology, 2009. **111**: p. 800-813.

253. Demirbas, A., *Use of algae as biofuel sources.* Energy Conversion and Management, 2010. **51**(12): p. 2738-2749.

254. Demirbas, A. and M. Fatih Demirbas, *Importance of algae oil as a source of biodiesel.* Energy Conversion and Management, 2011. **52**: p. 163-170.

255. Graham, L.E. and L.W. Wilcox, *Algae* 2000, Upper Saddle River: Prentice Hall, Inc.

256. Pokoo-Aikins, G., et al., *Design and analysis of biodiesel production from algae grown through carbon sequestration.* Clean Technologies and Environmental Policy, 2009. **12**(3): p. 239-254.

257. Vyas, A.P., J.L. Verma, and N. Subrahmanyam, *A review on FAME production processes.* Fuel, 2010. **89**(1): p. 1-9.

258. Lee, R.E., *Phycology.* Fourth ed. 2008, New York: Cambridge University Press.

259. Lee, Y.-K., *Microalgal mass culture systems and methods: Their limitation and potential.* Journal of Applied Phycology, 2001. **13**(4): p. 307-315.

260. Rosenberg, J.N., et al., *A green light for engineered algae: redirecting metabolism to fuel a biotechnology revolution.* Current Opinion in Biotechnology, 2008. **19**(5): p. 430-436.

261. Crane, K.W. and J.P. Grover, *Coexistence of mixotrophs, autotrophs, and heterotrophs in planktonic microbial communities.* Journal of Theoretical Biology, 2010. **262**(3): p. 517-527.

262. Hu, Q., et al., *Microalgal triacylglycerols as feedstocks for biofuel production: perspectives and advances.* The Plant Journal, 2008. **54**(4): p. 621-639.

263. Harwood, J.L. and I.A. Guschina, *The versatility of algae and their lipid metabolism.* Biochimie, 2009. **91**(6): p. 679-684.

264. Knauer, J. and P.C. Southgate, *A Review of the Nutritional Requirements of Bivalves and the Development of Alternative and Artificial Diets for Bivalve Aquaculture.* Reviews in Fisheries Science, 1999. **7**(3): p. 241 - 280.

265. Becker, W., ed. *Microalgae in Human and Animal Nutrition.* Handbook of Microalgal Culture: Biotechnology and Applied Phycology

ed. A. Richmond. 2004, Blackwell Science Ltd. 312-351.

266. Voltolina, D., M.d.P. Sﺎnchez-Saavedra, and L.M. Torres-Rodrﻱguez, *Outdoor mass microalgae production in Bahia Kino, Sonora, NW Mexico.* Aquacultural Engineering, 2008. **38**(2): p. 93-96.

267. Natrah, F., et al., *Screening of Malaysian indigenous microalgae for antioxidant properties and nutritional value.* Journal of Applied Phycology, 2007. **19**(6): p. 711-718.

268. Renaud, S.M., et al., *Effect of temperature on growth, chemical composition and fatty acid composition of tropical Australian microalgae grown in batch cultures.* Aquaculture, 2002. **211**(1-4): p. 195-214.

269. Miao, X. and Q. Wu, *High yield bio-oil production from fast pyrolysis by metabolic controlling of Chlorella protothecoides.* Journal of Biotechnology, 2004. **110**(1): p. 85-93.

270. Miao, X. and Q. Wu, *Biodiesel production from heterotrophic microalgal oil.* Bioresource Technology, 2006. **97**(6): p. 841-846.

271. Miao, X., Q. Wu, and C. Yang, *Fast pyrolysis of microalgae to produce renewable fuels.* Journal of Analytical and Applied Pyrolysis, 2004. **71**(2): p. 855-863.

272. Fábregas, J., et al., *The cell composition of <i>Nannochloropsis</i> sp. changes under different irradiances in semicontinuous culture.* World Journal of Microbiology and Biotechnology, 2004. **20**(1): p. 31-35.

273. Repka, S., M.v.d. Vlies, and J. Vijverberg, *Food quality of detritus derived from the filamentous cyanobacterium Oscillatoria limneticafor Daphnia galeata.* Journal of Plankton Research, 1998. **20**(11): p. 2199-2205.

274. Singh, Y. and H.D. Kumar, *Lipid and hydrocarbon production by Botryococcus spp. under nitrogen limitation and anaerobiosis.* World Journal of Microbiology and Biotechnology, 1992. **8**(2): p. 121-124.

275. Spolaore, P., et al., *Commercial applications of microalgae.* Journal of Bioscience and Bioengineering, 2006. **101**(2): p. 87-96.

276. Vijayaraghavan, K. and K. Hemanathan, *Biodiesel Production from Freshwater Algae.* Energy & Fuels, 2009. **23**(11): p. 5448-5453.

277. Meng, X., et al., *Biodiesel production from oleaginous microorganisms.* Renewable Energy, 2009. **34**(1): p. 1-5.

278. Patil, V., K.-Q. Tran, and H.R. Giselrød, *Towards Sustainable Production of Biofuels from Microalgae.* International Journal of Molecular Sciences, 2008. **9**: p. 1188-1195.

279. Huang, Z., X.-h. Shi, and W.-j. Jiang, *Theoretical models for supercritical fluid extraction.* Journal of Chromatography A, 2012. **1250**(0): p. 2-26.

280. Richmond, A., ed. *Handbook of Microalgal Culture: Biotechnology and Applied Phycology.* Microalgae in Human and Animal Nutrition, ed. W. Becker. 2004, Blackwell Science Ltd. 312-351.

281. Vasudevan, P. and M. Briggs, *Biodiesel production—current state of the art and challenges.* Journal of Industrial Microbiology and Biotechnology, 2008. **35**(5): p. 421-430.

282. Rodolfi, L., et al., *Microalgae for oil: Strain selection, induction of lipid synthesis and outdoor mass cultivation in a low-cost photobioreactor.* Biotechnology and Bioengineering, 2009. **102**(1): p. 100-112.

283. Harun, R., et al., *Bioprocess engineering of microalgae to produce a variety of consumer products.* Renewable and Sustainable Energy Reviews, 2010. **14**(3): p. 1037-1047.

284. Richmond, A., *Open systems for the mass production of photoautotrophic microalgae outdoors: physiological principles.* Journal of Applied Phycology, 1992. **4**(3): p. 281-286.

285. Schenk, P., et al., *Second Generation Biofuels: High-Efficiency Microalgae for Biodiesel Production.* BioEnergy Research, 2008. **1**(1): p. 20-43.

286. Slade, R. and A. Bauen, *Micro-algae cultivation for biofuels: Cost, energy balance, environmental impacts and future prospects.* Biomass and Bioenergy, 2013. **53**(0): p. 29-38.

287. Tredici, M. and R. Materassi, *From open ponds to vertical alveolar panels: the Italian experience in the development of reactors for the mass cultivation of phototrophic microorganisms.* Journal of Applied Phycology, 1992. **4**(3): p. 221-231.

288. Chaumont, D., *Biotechnology of algal biomass production: a review of systems for outdoor mass culture.* Journal of Applied Phycology, 1993. **5**(6): p. 593-604.

289. Scragg, A.H., *Biofuels, Production, Application and Development.* 2009, Cambridge: Cambridge University Press.

290. Zaborsky, O.R., et al., *An Automated Helical Photobioreactor Incorporating Cyanobacteria for Continuous Hydrogen Production*, in *BioHydrogen*. 1999, Springer US. p. 431-440.

291. Vasudevan, P. and B. Fu, *Environmentally Sustainable Biofuels: Advances in Biodiesel Research.* Waste and Biomass Valorization, 2010. **1**(1): p. 47-63.

292. Huntley, M. and D. Redalje, *CO_2 Mitigation and Renewable Oil from Photosynthetic Microbes: A New Appraisal.* Mitigation and Adaptation Strategies for Global Change, 2007. **12**(4): p. 573-608.

293. Illman, A.M., A.H. Scragg, and S.W. Shales, *Increase in Chlorella strains calorific values when grown in low nitrogen medium.* Enzyme and Microbial Technology, 2000. **27**(8): p. 631-635.

294. Scragg, A.H., et al., *Growth of microalgae with increased calorific values in a tubular bioreactor.* Biomass and Bioenergy, 2002. **23**(1): p. 67-73.

295. Widjaja, A., C.-C. Chien, and Y.-H. Ju, *Study of increasing lipid production from fresh water microalgae Chlorella vulgaris.* Journal of the Taiwan Institute of Chemical Engineers, 2009. **40**(1): p. 13-20.

296. Chiu, S.-Y., et al., *Lipid accumulation and CO2 utilization of Nannochloropsis oculata in response to CO2 aeration.* Bioresource Technology, 2009. **100**(2): p. 833-838.

297. Tang, H., et al., *Potential of microalgae oil from Dunaliella tertiolecta as a feedstock for biodiesel.* Applied Energy, 2011. **88**: p. 3324-3330.

298. Muffler, K. and R. Ulber, eds. *Downstream Processing in Marine Biotechnology*. 1st ed. Marine Biotechnology II ed. Y.L. Gal and R. Ulber. 2005, Springer. 261.

299. O'Grady, J. and J. Morgan, *Heterotrophic growth and lipid production of Chlorella protothecoides on glycerol.* Bioprocess and Biosystems Engineering, 2010: p. 1-5.

300. Xu, H., X. Miao, and Q. Wu, *High quality biodiesel production from a microalga Chlorella protothecoides by heterotrophic growth in fermenters.* Journal of Biotechnology, 2006. **126**(4): p. 499-507.

301. Cheng, Y., et al., *Biodiesel production from Jerusalem artichoke (Helianthus Tuberosus L.) tuber by heterotrophic microalgae Chlorella protothecoides.* Journal of Chemical Technology & Biotechnology, 2009. **84**(5): p. 777-781.

302. Lu, Y., et al., *Biodiesel production from algal oil using cassava (Manihot esculenta Crantz) as feedstock.* Journal of Applied Phycology, 2010. **22**(5): p. 573-578.

303. Liu, J., et al., *Differential lipid and fatty acid profiles of photoautotrophic and heterotrophic Chlorella zofingiensis: Assessment of algal oils for biodiesel production.* Bioresource Technology. **102**(1): p. 106-110.

304. Liang, Y., N. Sarkany, and Y. Cui, *Biomass and lipid productivities of <i>Chlorella vulgaris</i> under autotrophic, heterotrophic and mixotrophic growth conditions.* Biotechnology Letters, 2009. **31**(7): p. 1043-1049.

305. Converti, A., et al., *Effect of temperature and nitrogen concentration on the growth and lipid content of Nannochloropsis oculata and Chlorella vulgaris for biodiesel production.* Chemical Engineering and Processing: Process Intensification, 2009. **48**(6): p. 1146-1151.

306. Hsieh, C.-H. and W.-T. Wu, *Cultivation of microalgae for oil production with a cultivation strategy of urea limitation.* Bioresource technology, 2009. **100**(17): p. 3921-3926.

307. Liu, Z.-Y., G.-C. Wang, and B.-C. Zhou, *Effect of iron on growth and lipid accumulation in Chlorella vulgaris.* Bioresource technology, 2008. **99**(11): p. 4717-4722.

308. Zemke, P.E., B.D. Wood, and D.J. Dye, *Considerations for the maximum production rates of triacylglycerol from microalgae.* Biomass Bioenergy, 2010. **34**(1): p. 145-151.

309. Tornabene, T.G., et al., *Lipid composition of the nitrogen starved green alga Neochloris oleoabundans.* Enzyme and Microbial Technology, 1983. **5**(6): p. 435-440.

310. Amaro, H.M., A.C. Guedes, and F.X. Malcata, *Advances and perspectives in using microalgae to produce biodiesel.* Applied Energy, 2011. **88**(10): p. 3402-3410.

311. Dragone, G., et al., *Nutrient limitation as a strategy for increasing starch accumulation in microalgae.* Applied Energy, 2011. **88**(10): p. 3331-3335.

312. Li, Y., et al., *Effects of nitrogen sources on cell growth and lipid accumulation of green alga Neochloris oleoabundans.* Applied Microbiology and Biotechnology, 2008. **81**(4): p. 629-636.

313. Millero, F.J., et al., *Dissociation constants of carbonic acid in seawater as a function of salinity and temperature.* Marine Chemistry, 2006. **100**(1â€"2): p. 80-94.

314. Dong, L.E., NY, US), Drury, Kenneth Joseph (Big Flats, NY, US), Fadeev, Andrei Gennadyevich (Elmira, NY, US), *Methods For Harvesting Biological Materials Using Membrane Filters.* 2010: United States.

315. Lamers, A., *Algae oils from small scale low input water remediation site as feedstock for biodiesel conversion.* Guelph Engineering Journal, 2009. **2**: p. 24-38.

316. Danquah, M.K., et al., *Dewatering of microalgal culture for biodiesel production: exploring polymer flocculation and tangential flow filtration.* Journal of Chemical Technology & Biotechnology, 2009. **84**(7): p. 1078-1083.

317. Mata, T.M., A.n.A. Martins, and N.S. Caetano, *Microalgae for biodiesel production and other applications: A review.* Renewable and Sustainable Energy Reviews, 2010. **14**(1): p. 217-232.

318. Grima, M., E., et al., *Recovery of microalgal biomass and metabolites: process options and economics.* Biotechnology Advances, 2003. **20**(7-8): p. 491-515.

319. Uduman, N., et al., *Dewatering of microalgal cultures: A major bottleneck to algae-based fuels.* Journal of Renewable and Sustainable Energy, 2010. **2**: p. 012701.

320. Oh, H.-M., et al., *Harvesting of Chlorella vulgaris using a bioflocculant from Paenibacillus sp. AM49.* Biotechnology Letters, 2001. **23**(15): p. 1229-1234.

321. Tenney, M.W., et al., *Algal Flocculation with Synthetic Organic Polyelectrolytes* Applied and Environment Microbiology, 1969. **18**(6): p. 965-971.

322. Shelef, G., A. Sukenik, and M. Green, *Microalgae harvesting and processing: a literature review*. 1984. p. Medium: ED; Size: Pages: 70.

323. Rawat, I., et al., *Dual role of microalgae: Phycoremediation of domestic wastewater and biomass production for sustainable biofuels production.* Applied Energy, 2011. **88**(10): p. 3411-3424.

324. Sim, T.S., A. Goh, and E.W. Becker, *Comparison of centrifugation, dissolved air flotation and drum filtration techniques for harvesting sewage-grown algae.* Biomass, 1988. **16**(1): p. 51-62.

325. Ahlgren, G. and L. Merino, *Lipid analysis of freshwater microalgae : a method study.* Archiv für Hydrobiologie, 1991. **121**(3): p. 295-306.

326. Belarbi, E.-H., E. Molina, and Y. Chisti, *Retracted : A process for high yield and scaleable recovery of high purity eicosapentaenoic acid esters from microalgae and fish oil.* Process Biochemistry, 2000. **35**(9): p. 951-969.

327. Grima, E., et al., *Comparison between extraction of lipids and fatty acids from microalgal biomass.* Journal of the American Oil Chemists' Society, 1994. **71**(9): p. 955-959.

328. Fajardo, A.R., et al., *Lipid extraction from the microalga Phaeodactylum tricornutum.* European Journal of Lipid Science and Technology, 2007. **109**(2): p. 120-126.

329. Chen, C.-Y., et al., *Strategies to enhance cell growth and achieve high-level oil production of a Chlorella vulgaris isolate.* Biotechnology Progress, 2010. **26**(3): p. 679-686.

330. Morist, A., et al., *Recovery and treatment of Spirulina platensis cells cultured in a continuous photobioreactor to be used as food.* Process Biochemistry, 2001. **37**(5): p. 535-547.

331. Ehimen, E.A., et al., *Energy recovery from lipid extracted, transesterified and glycerol codigested microalgae biomass.* GCB Bioenergy, 2009. **1**(6): p. 371-381.

332. Sander, K. and G. Murthy, *Life cycle analysis of algae biodiesel.* The International Journal of Life Cycle Assessment, 2010. **15**(7): p. 704-714.

333. Razon, L.F. and R.R. Tan, *Net energy analysis of the production of biodiesel and biogas from the microalgae: Haematococcus pluvialis and Nannochloropsis.* Applied Energy, 2011. **88**(10): p. 3507-3514.

334. Lardon, L., et al., *Life-Cycle Assessment of Biodiesel Production from Microalgae.* Environmental Science & Technology, 2009. **43**(17): p. 6475-6481.

335. Chisti, Y. and M. Moo-Young, *Disruption of microbial cells for intracellular products.* Enzyme and Microbial Technology, 1986. **8**(4): p. 194-204.

336. Blumreisinger, M., D. Meindl, and E. Loos, *Cell wall composition of chlorococcal algae.* Phytochemistry, 1983. **22**(7): p. 1603-1604.

337. Ottens, M., J.A. Wesselingh, and L.A.M.V.d. Wielen, eds. *Downstream processing.* 3rd Edition ed. Basic Biotechnology, ed. C. Ratledge and B. Kristiansen. 2006, Cambridge University Press. 666.

338. Shen, Y., et al., *Effect of nitrogen and extraction method on algae lipid yield.* International Journal of Agricultural and Biological Engineering, 2009. **2**(1): p. 51-57.

339. Sostaric, M., et al., *Growth, lipid extraction and thermal degradation of the microalga Chlorella vulgaris.* New Biotechnology, 2012. **29**(3): p. 325-331.

340. Suarsini, E. and S. Subandi. *Utilization ultrasonic to increase the efficiency of oil extraction for microalgae indigenous isolates from pond gresik, east java.* in *Clean Energy and Technology (CET), 2011 IEEE First Conference on.* 2011.

341. Lee, J.-Y., et al., *Comparison of several methods for effective lipid extraction from microalgae.* Bioresource Technology, 2010. **101**(1, Supplement): p. S75-S77.

342. Surendhiran, D. and M. Vijay, *Effect of Various Pretreatment for Extracting Intracellular Lipid from Nannochloropsis oculata under Nitrogen Replete and Depleted Conditions.* ISRN Chemical Engineering, 2014. **2014**: p. 9.

343. Sathish, A. and R.C. Sims, *Biodiesel from mixed culture algae via a wet lipid extraction procedure.* Bioresource technology, 2012. **118**(0): p. 643-647.

344. Cho, H.-S., et al., *Effects of enzymatic hydrolysis on lipid extraction from Chlorella vulgaris.* Renew Energy, 2013. **54**(0): p. 156-160.

345. Chuchird, N., et al., *Digestion of Chlorella Cells by Chlorovirus-encoded Polysaccharide Degrading Enzyme.* Microbes Environ, 2001. **16**(4): p. 206-212.

346. Fu, C.-C., et al., *Hydrolysis of microalgae cell walls for production of reducing sugar and lipid extraction.* Bioresour Technol, 2010. **101**(22): p. 8750-8754.

347. Gerken, H.G., et al., *Enzymatic cell wall degradation of Chlorella vulgaris and other microalgae for biofuels production.* Planta, 2013. **237**(1): p. 239-253.

348. Kates, M., *Techniques of Lipidology: Isolation, Analysis, and Identification of Lipids.* 1986: Elsevier.

349. Medina, A.R., et al., *Downstream processing of algal polyunsaturated fatty acids.* Biotechnology Advances, 1998. **16**(3): p. 517-580.

350. Hara, A. and N.S. Radin, *Lipid extraction of tissues with a low-toxicity solvent.* Analytical Biochemistry, 1978. **90**(1): p. 420-426.

351. Ranjan, A., C. Patil, and V.S. Moholkar, *Mechanistic Assessment of Microalgal Lipid Extraction.* Industrial & Engineering Chemistry Research, 2010. **49**(6): p. 2979-2985.

352. Samori, C., et al., *Extraction of hydrocarbons from microalga Botryococcus braunii with switchable solvents.* Bioresource Technology, 2010. **101**(9): p. 3274-3279.

353. Santana, A., et al., *Supercritical Carbon Dioxide Extraction of Algal Lipids for the Biodiesel Production.* Procedia Engineering, 2012. **42**(0): p. 1755-1761.

354. D'Oca, M.G.M., et al., *Production of FAMEs from several microalgal lipidic extracts and direct transesterification of the Chlorella pyrenoidosa.* Biomass and Bioenergy, 2011. **35**(4): p. 1533-1538.

355. Halim, R., et al., *Oil extraction from microalgae for biodiesel production.* Bioresource Technology, 2011. **102**: p. 178-185.

356. Cheng, C.-H., et al., *Comparative study of lipid extraction from microalgae by organic solvent and supercritical CO2.* Bioresource Technology, 2011. **102**(21): p. 10151-10153.

357. Berg, H., et al., *Development of a supercritical fluid extraction method for determination of lipid classes and total fat in meats and its comparison with conventional methods.* Journal of Chromatography A, 1997. **785**(1-2): p. 345–352. .

358. Liao, X., H. Zhang, and T. He, *Preparation of Porous Biodegradable Polymer and Its Nanocomposites by Supercritical CO$_2$ Foaming for Tissue Engineering.* Journal of Nanomaterials, 2012. **2012**: p. 12.

359. Dean, J.R., *Extraction Methods for Environmental Analysis*. Vol. Third 1998, England: John Wiley & Sons Ltd.

360. Henry, J.D., et al., *Alternative Separation Processes*, in *Perry's chemical engineers' handbook*. 1997, McGraw-Hill: New York. p. 22.14-22.19.

361. Mukhopadhyay, M., *Natural extracts using supercritical carbon dioxide*. 2000, USA: CRC Press LLC.

362. Brunner, G., *Supercritical fluids: technology and application to food processing.* Journal of Food Engineering, 2005. **67**(1-2): p. 21-33.

363. Berk, Z., *Extraction*, in *Food Process Engineering and Technology*, Z. Berk, Editor. 2009, Academic Press: San Diego. p. 259-277.

364. Hashim, I., et al., *Quality Characteristics of Low Fat Lamb Meat Produced by Supercritical Carbon Dioxide Extraction.* Global Journal of Biology, Agriculture and Health Sciences, 2013. **2**: p. 5-9.

365. Reverchon, E. and C. Marrone, *Supercritical extraction of clove bud essential oil: isolation and mathematical modeling.* Chemical Engineering Science, 1997. **52**(20): p. 3421-3428.

366. Reverchon, E. and F. Senatore, *Supercritical carbon dioxide extraction of chamomile essential oil and its analysis by gas chromatography-mass*

spectrometry. Journal of Agricultural and Food Chemistry, 1994. **42**(1): p. 154-158.

367. King, J.W., et al., *Fat and cholesterol content of beef patties as Affected by supercritical CO$_2$ extraction.* Journal of Food Science, 1993. **58**(5): p. 950-952.

368. Valderrama, J.O., M. Perrut, and W. Majewski, *Extraction of Astaxantine and Phycocyanine from Microalgae with Supercritical Carbon Dioxide.* Journal of Chemical & Engineering Data, 2003. **48**(4): p. 827-830.

369. Kitada, K., et al., *Supercritical CO2 extraction of pigment components with pharmaceutical importance from Chlorella vulgaris.* Journal of Chemical Technology & Biotechnology, 2009. **84**(5): p. 657-661.

370. Wu, Z., S. Wu, and X. Shi, *Supercritical fluid extraction and determination of lutein in heterotrophically cultivated Chlorella pyrenoidosa.* Journal of Food Process Engineering, 2007. **30**(2): p. 174-185.

371. Sarker, M.Z.I., et al., *Optimization of supercritical CO$_2$ extraction of fish oil from viscera of african catfish (Clarias gariepinus).* International Journal of Molecular Science, 2012. **13**(9): p. 11312-11322.

372. Tonthubthimthong, P., et al., *Extraction of nimbin from neem seeds using supercritical CO$_2$ and a supercritical CO$_2$-methanol mixture.* Journal of Supercritical Fluids, 2004. **30**(3): p. 287-301.

373. Brewer, W.E., et al., *Analysis of Cocaine, Benzoylecgonine, Codeine, and Morphine in Hair by Supercritical Fluid Extraction with Carbon Dioxide Modified with Methanol.* Analytical Chemistry, 2001. **73**(11): p. 2371-2376.

374. Aghel, N., et al., *Supercritical carbon dioxide extraction of Mentha pulegium L. essential oil.* Talanta, 2004. **62**(2): p. 407-411.

375. Mendes, R.L., A.D. Reis, and A.n.F. Palavra, *Supercritical CO2 extraction of [gamma]-linolenic acid and other lipids from Arthrospira (Spirulina)maxima: Comparison with organic solvent extraction.* Food Chemistry, 2006. **99**(1): p. 57-63.

376. Lundstedt, T.r., et al., *Experimental design and optimization.* Chemometrics and Intelligent Laboratory Systems, 1998. **42**(1â€"2): p. 3-40.

377. Bezerra, M.A., et al., *Response surface methodology (RSM) as a tool for optimization in analytical chemistry.* Talanta, 2008. **76**(5): p. 965-977.

378. Ragonese, R., M. Mulholland, and J. Kalman, *Full and fractionated experimental designs for robustness testing in the high-performance liquid chromatographic analysis of codeine phosphate, pseudoephedrine hydrochloride and chlorpheniramine maleate in a pharmaceutical preparation.* Journal of Chromatography A, 2000. **870**(1â€"2): p. 45-51.

379. Bartle, K.D., et al., *A model for dynamic extraction using a supercritical fluid.* The Journal of Supercritical Fluids, 1990. **3**(3): p. 143-149.

380. Sovova, H., *Rate of the vegetable oil extraction with supercritical CO2â€"I. Modelling of extraction curves.* Chemical Engineering Science, 1994. **49**(3): p. 409-414.

381. Sovova, H., *Mathematical model for supercritical fluid extraction of natural products and extraction curve evaluation.* The Journal of Supercritical Fluids, 2005. **33**(1): p. 35-52.

382. Chrastil, J., *Solubility of solids and liquids in supercritical gases.* The Journal of Physical Chemistry, 1982. **86**(15): p. 3016-3021.

383. Sparks, D.L., R. Hernandez, and L.A. Estevez, *Evaluation of density-based models for the solubility of solids in supercritical carbon dioxide and formulation of a new model.* Chemical Engineering Science, 2008. **63**(17): p. 4292-4301.

384. Adachi, Y. and B.C.Y. Lu, *Supercritical fluid extraction with carbon dioxide and ethylene.* Fluid Phase Equilibria, 1983. **14**(0): p. 147-156.

385. Del Valle, J.M. and J.M. Aguilera, *An improved equation for predicting the solubility of vegetable oils in supercritical carbon dioxide.* Industrial & Engineering Chemistry Research, 1988. **27**(8): p. 1551-1553.

386. Shi, J., et al., *Correlation of mass transfer coefficient in the extraction of plant oil in a fixed bed for supercritical CO_2.* Journal of Food Engineering, 2007. **78**(1): p. 33-40.

387. Lim, G.B., G.D. Holder, and Y.T. Shah, *Solid?Fluid Mass Transfer in a Packed Bed Under Supercritical Conditions*, in *Supercritical Fluid Science and Technology*. 1989, American Chemical Society. p. 379-395.

388. Mongkholkhajornsilp, D., et al., *Supercritical CO2 extraction of nimbin from neem seedsâ€"â€"a modelling study.* Journal of Food Engineering, 2005. **71**(4): p. 331-340.

389. King, M.B., T.R. Bott, and O. Catchpole, *Physico-chemical data required for the design of near-critical fluid extraction process*, in *Extraction of Natural Products Using Near-Critical Solvents*. 1993, Springer Netherlands. p. 184-231.

390. King, J.W., M. Cygnarowicz-Provost, and F. Favati, *Supercritical fluid extraction of evening primrose oil kinetic and mass transfer effects.* Italian journal of food science., 1997. **9**(3): p. 193-204.

391. Puiggene, J., M.A. Larrayoz, and F. Recasens, *Free liquid-to-supercritical fluid mass transfer in packed beds.* Chemical Engineering Science, 1997. **52**(2): p. 195-212.

392. Churchill, S.W., *A comprehensive correlating equation for laminar, assisting, forced and free convection.* AIChE Journal, 1977. **23**(1): p. 10-16.

393. Valle, J.M.D. and J.C. De La Fuente, *Supercritical CO_2 Extraction of Oilseeds: Review of Kinetic and Equilibrium Models.* Critical Reviews in Food Science and Nutrition, 2006. **46**(2): p. 131-160.

394. Lanza, M., et al., *The effect of temperature, pressure, exposure time, and depressurization rate on lipase activity in SCCO2.* Applied Biochemistry and Biotechnology, 2004. **113**(1-3): p. 181-187.

395. Prasanth, S. and T.E. Abraham, *ffect of Compression Pressure on the Activity of Lipase.* Hygeia journal for drugs and medicines', 2009. **1**(1): p. 11-18.

396. Dalla Rosa, C., et al., *Continuous lipase-catalyzed production of fatty acid ethyl esters from soybean oil in compressed fluids.* Bioresource Technology, 2009. **100**(23): p. 5818-5826.

397. Ciftci, O.N. and F. Temelli, *Continuous production of fatty acid methyl esters from corn oil in a supercritical carbon dioxide bioreactor.* The Journal of Supercritical Fluids, 2011. **58**(1): p. 79-87.

398. Ciftci, O.N. and F. Temelli, *Continuous biocatalytic conversion of the oil of corn distiller's dried grains with solubles to fatty acid methyl esters in supercritical carbon dioxide.* Biomass and Bioenergy, 2013. **54**(0): p. 140-146.

399. Lubary, M., et al., *Integrated synthesis and extraction of short-chain fatty acid esters by supercritical carbon dioxide.* AIChE Journal, 2009. **56**(4): p. 1080-1089.

400. Rodrigues, A.R., et al., *Continuous enzymatic production of biodiesel from virgin and waste sunflower oil in supercritical carbon dioxide.* The Journal of Supercritical Fluids, 2011. **56**(3): p. 259-264.

401. Siaut, M., et al., *Oil accumulation in the model green alga Chlamydomonas reinhardtii: characterization, variability between common laboratory strains and relationship with starch reserves. .* BMC Biotechnol, 2011. **11**(1): p. 7-21.

402. Strober, W., *Monitoring Cell Growth*, in *Current Protocols in Immunology*. 2001, John Wiley & Sons, Inc.

403. Allen, T., *Particle size measurement*. third ed. 1981, London: Chapman and Hall.

404. Prado, J.M., G.H.C. Prado, and M.A.A. Meireles, *Scale-up study of supercritical fluid extraction process for clove and sugarcane residue.* Journal of Supercritical Fluids, 2011. **56**(3): p. 231-237.

405. Rule, D.C., *Direct transesterification of total fatty acids of adipose tissue, and of freeze-dried muscle and liver with boron-trifluoride in methanol.* Meat Science, 1997. **46**(1): p. 23-32.

406. Bondioli, P. and L. Della Bella, *An alternative spectrophotometric method for the determination of free glycerol in biodiesel.* European Journal of Lipid Science and Technology, 2005. **107**(3): p. 153-157.

407. Krisnangkura, K., *A simple method for estimation of cetane index of vegetable oil methyl esters.* Journal of the American Oil Chemists Society, 1986. **63**(4): p. 552-553.

408. Kalayasiri, P., N. Jeyashoke, and K. Krisnangkura, *Survey of seed oils for use as diesel fuels.* Journal of Americal Oil Chemist's Society, 1996. **73**(4): p. 471-474.

409. Baicu, S.C. and M.J. Taylor, *Acid-base buffering in organ preservation solutions as a function of temperature: new parameters for comparing buffer capacity and efficiency.* Cryobiology, 2002. **45**(1): p. 33-48.

410. Ferriols, V.M.E.N., et al., *Effect of Elevated Carbon Dioxide and Phosphorus Levels on Nitrogen Uptake, Lipid Content and Growth of Tetraselmis sp.* Journal of Fisheries and Aquatic Science, 2013(659-672).

411. Meseck, S., et al., *Nutrient interactions between phytoplankton and bacterioplankton under different carbon dioxide regimes.* Journal of Applied Phycology, 2007. **19**(3): p. 229-237.

412. Heldt, H.-W. and F. Heldt, *8 - Photosynthesis implies the consumption of water*, in *Plant Biochemistry (Third Edition)*. 2005, Academic Press: Burlington. p. 213-242.

413. Ridge, I. and O. University, *Plants*. 2002: Oxford University Press, Incorporated.

414. Fulke, A.B., et al., *Bio-mitigation of CO$_2$, calcite formation and simultaneous biodiesel precursors production using Chlorella sp.* Bioresource Technology, 2010. **101**(21): p. 8473-8476.

415. Bhola, V., et al., *Effects of parameters affecting biomass yield and thermal behaviour of Chlorella vulgaris.* Journal of Bioscience and Bioengineering, 2011. **111**(3): p. 377-382.

416. Sasi, D., et al., *Growth kinetics and lipid production using Chlorella vulgaris in a circulating loop photobioreactor.* Journal of Chemical Technology and Biotechnology, 2011. **86**(6): p. 875-880.

417. Al-Anezi, K. and N. Hilal, *Scale formation in desalination plants: effect of carbon dioxide solubility.* Desalination, 2007. **204**(1â€"3): p. 385-402.

418. Ben-Amotz, A., T.G. Tornabene, and W.H. Thomas, *Chemical Profile of Selected Species of Microalgae with Emphasis on Lipids.* Journal of Phycology, 1985. **21**(1): p. 72-81.

419. Goldman, J.C. and D.G. Peavey, *Steady-State Growth and Chemical Composition of the Marine Chlorophyte Dunaliella tertiolecta in Nitrogen-Limited Continuous Cultures.* Applied and Environment Microbiology, 1979. **38**(5): p. 894-901.

420. Jacob-Lopes, E., et al., *Effect of light cycles (night/day) on CO$_2$ fixation and biomass production by microalgae in photobioreactors.* Chemical Engineering and Processing, 2009. **48**(1): p. 306-310.

421. Yun, Y.-S., et al., *Carbon Dioxide Fixation by Algal Cultivation Using Wastewater Nutrients.* Journal of Chemical Technology and Biotechnology, 1997. **69**(4): p. 451-455.

422. Chen, G.-Q., Y. Jiang, and F. Chen, *Salt-induced alteration in lipid composition of diatom Nitzchia Laevis (Bacillariophyceae) under*

heterotrophic culture condition. Journal of Phycology, 2008. **44**(5): p. 1309-1314.

423. Ren, H.-Y., et al., *A new lipid-rich microalga Scenedesmus sp. strain R-16 isolated using Nile red staining: effects of carbon and nitrogen sources and initial pH on the biomass and lipid production.* Biotechnology for Biofuels, 2013. **6**(6): p. 143-153.

424. Liu, J., et al., *Supercritical fluid extraction of flavonoids from Maydis stigma and its nitrite-scavenging ability.* Food and Bioproducts Processing, 2011. **89**(4): p. 333-339.

425. Peng, W., Q. Wu, and P. Tu, *Pyrolytic characteristics of heterotrophic Chlorella protothecoides for renewable bio-fuel production.* Journal of Applied Phycology, 2001. **13**(1): p. 5-12.

426. Marcilla, A., et al., *Characterization of microalgal species through TGA/FTIR analysis: Application to nannochloropsis sp.* Thermochimica Acta2009. **484**(1-2): p. 41-47.

427. Porphy, S.J. and M.M. Farid, *Feasibility study for production of biofuel and chemicals from marine microalgae Nannochloropsis sp. based on basic mass and energy analysis.* ISRN Renewable Energy, 2012. **2012**(Article ID 156824): p. 1-11.

428. Rizzo, A.M., et al., *Characterization of microalga Chlorella as a fuel and its thermogravimetric behavior.* Applied Energy, 2013. **102**(0): p. 24-31.

429. Snyder, J.M., J.P. Friedrich, and D.D. Christianson, *Effect of moisture and particle size on the extractability of oils from seeds with supercritical CO2.* Journal of Americal Oil Chemist's Society, 1984. **61**(12): p. 1851-1856.

430. Eggers, R., *Supercritical fluid extraction (SFE) of oilseeds/ lipids in natural products*, in *Supercritical Fluid Technology in Oil and Lipid Chemistry*, J.W. King and G.R. List, Editors. 1996, American Oil Chemists Society press: Champaign. p. 35-64.

431. Stahl, E., E. Schuetz, and H.K. Mangold, *Extraction of seed oils with liquid and supercritical carbon dioxide.* Journal of Agricultural and Food Chemistry, 1980. **28**(6): p. 1153-1157.

432. Özkal, S.G., M.E. Yener, and L. Bayındırlı, *The solubility of apricot kernel oil in supercritical carbon dioxide.* Internaltional Journal of Food Science and Technology, 2006. **41**(4): p. 399-404.

433. Che Yunus, M.A., et al., *Effect of supercritical carbon dioxide condition on oil yield and solubility of Pithecellobium Jiringan (Jack) Prain seeds.* Jurnal Teknologi, 2013. **60**: p. 45-50.

434. Salgin, U. and S. Salgin, *Effect of main process parameters on extraction of pine kernel lipid using supercritical green solvents: Solubility models and lipid profiles.* Journal of Supercritical Fluids, 2013. **73**(0): p. 18-27.

435. Salgin, U. and H. Korkmaz, *A green separation process for recovery of healthy oil from pumpkin seed.* Journal of Supercritical Fluids, 2011. **58**(2): p. 239-248.

436. Wiltshire, K., et al., *Extraction of pigments and fatty acids from the green alga Scenedesmus obliquus (Chlorophyceae).* Aquatic Ecology, 2000. **34**(2): p. 119-126.

437. Liang, K., Q. Zhang, and W. Cong, *Enzyme-Assisted Aqueous Extraction of Lipid from Microalgae.* Journal of Agricultural and Food Chemistry, 2012. **60**(47): p. 11771-11776.

438. Kubiak-Ossowska, K. and P.A. Mulheran, *Mechanism of Hen Egg White Lysozyme Adsorption on a Charged Solid Surface.* Langmuir, 2010. **26**(20): p. 15954-15965.

439. Chang, Y.K. and L. Chu, *A simple method for cell disruption by immobilization of lysozyme on the extrudate-shaped NaY zeolite.* Biochemical Engineering Journal, 2007. **35**(1): p. 37-47.

440. Nagy, B. and B.l. SimÃ¡ndi, *Effects of particle size distribution, moisture content, and initial oil content on the supercritical fluid extraction of paprika.* The Journal of Supercritical Fluids, 2008. **46**(3): p. 293-298.

441. Mezzomo, N.l., J. MartÃnez, and S.R.S. Ferreira, *Supercritical fluid extraction of peach (Prunus persica) almond oil: Kinetics, mathematical modeling and scale-up.* The Journal of Supercritical Fluids, 2009. **51**(1): p. 10-16.

442. Novak, Z., et al., *Silica aerogels as supports for lipase catalyzed esterifications at sub- and supercritical conditions.* The Journal of Supercritical Fluids, 2003. **27**(2): p. 169-178.

443. Varma, M.N. and G. Madras, *Synthesis of biodiesel from castor oil and linseed oil in supercritical fluids.* Industrial & Engineering Chemistry Research, 2006. **46**(1): p. 1-6.

444. Yang, Y., et al., *Diffusion coefficients of C18 unsaturated fatty acid methyl esters in supercritical carbon dioxide containing 10% mole fraction ethanol as modifier.* The Journal of Supercritical Fluids, 2013. **83**(0): p. 146-152.

445. Ganesan, D., A. Rajendran, and V. Thangavelu, *An overview on the recent advances in the transesterification of vegetable oils for biodiesel production using chemical and biocatalysts.* Review Environmental Science Biotechnology, 2009. **8**: p. 367-394.

446. Rodrigues, R., et al., *Two step ethanolysis: A simple and efficient way to improve the enzymatic biodiesel synthesis catalyzed by an immobilized-stabilized lipase from Thermomyces lanuginosus.* Process Biochemistry, 2010. **45**: p. 1268-1273.

447. Shaw, J.F., et al., *Continuous enzymatic synthesis of biodiesel with Novozym 435.* Energy & Fuels, 2008. **22**(2): p. 840-844.

448.   Chang, H.-M., et al., *Optimized synthesis of lipase-catalyzed biodiesel by Novozym 435.* Journal of Chemical Technology & Biotechnology, 2005. **80**(3): p. 307-312.

APPENDIX A:
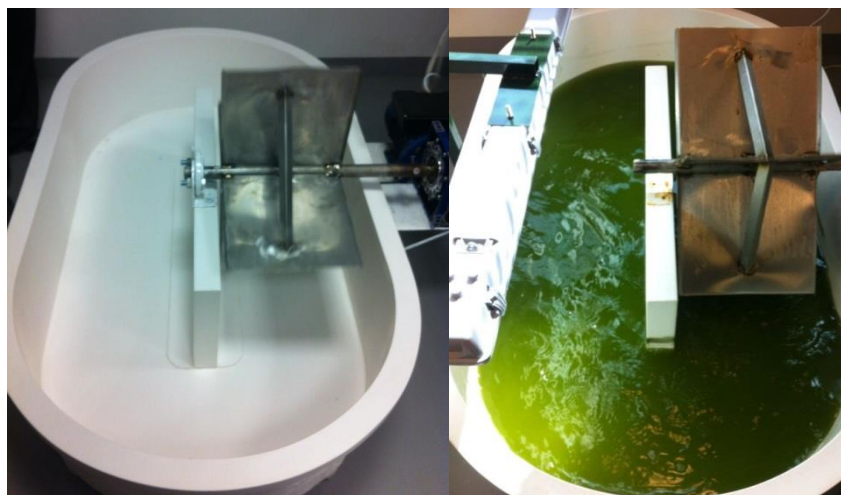
PHOTOS OF ALGAE CULTURES

Figure A.1: Stock cultures prior to growth study

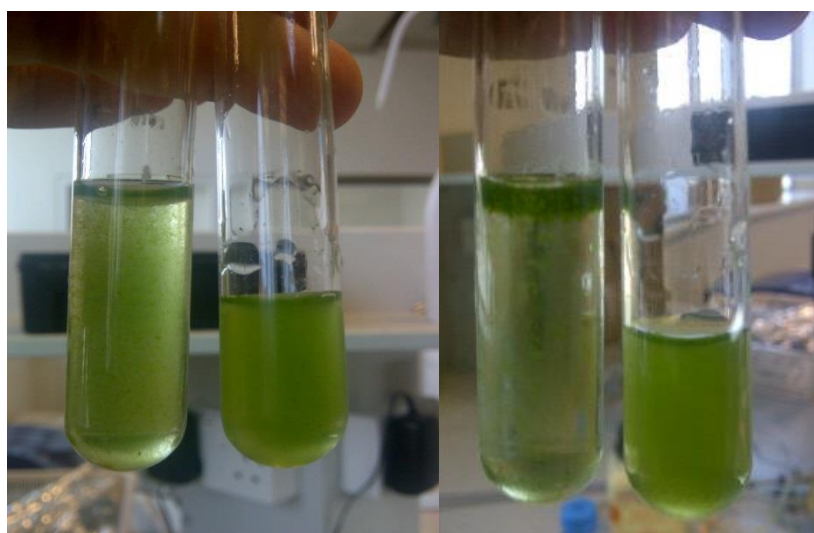Figure A.2: Sides view of the 250 ml scale cultivation system

Figure A.3: Photographs on the 5 L photobioreactos with different culture densities

(a)   (b)

Figure A.4: photographs of; (a) empty and (b) filled open pond

(a)   (b)

Figure A.5: Effectivness on NaOH in seperting algae cells from culture media

(a) after 30 s and (b) after 2 min

Figure A.6: Wet biomass used for cell disruption study

APPENDIX B:

PARTICLE SIZE DISTRIBUATION

Table B.1: Particle size distribution

Tyler Equivalent	Screen size (mm)	Cumulative residue (%)	Normalized Cumulative residue (%)		
			Experimental	Prediction	% Difference
42 mesh	0.355	5.2	5.2	5.2	3×10^{-06}
100 mesh	0.15	46.7	51.9	52.8	3×10^{-04}
200 mesh	0.075	34.2	86.1	83.0	1×10^{-03}
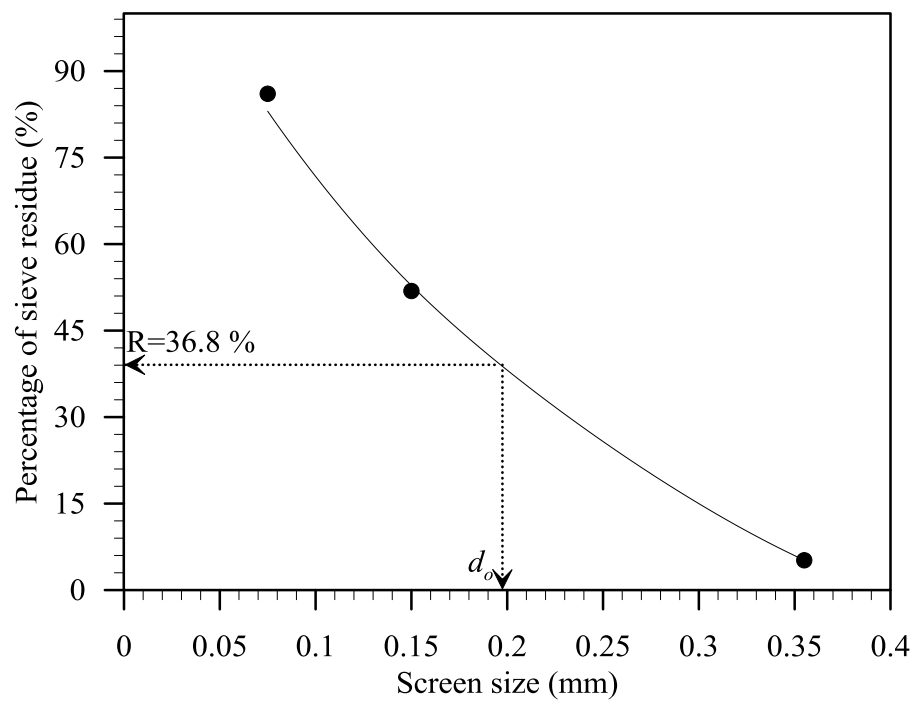
Figure B.1: Residual particle size distribution as function of screen size

APPENDIX C:

STEADY STATE YIELDS
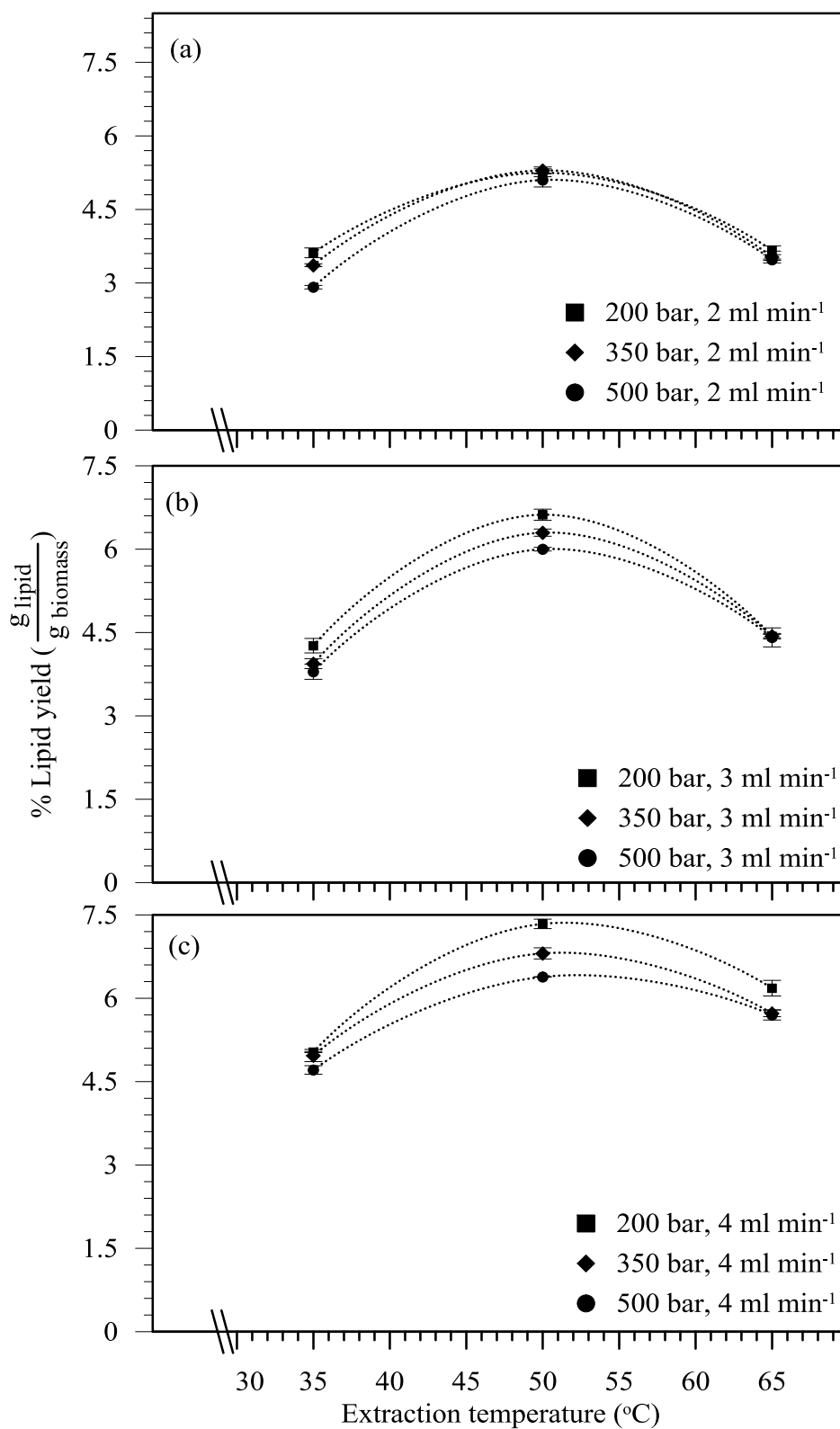
Figure C.1: Effect of the temperature on the steady sate lipids extraction yield after passing 100 g of SC-CO_2 at different pressures ((a) 2 ml min^{-1}, (b) 3 ml min^{-1} and (c) 4 ml min^{-1})
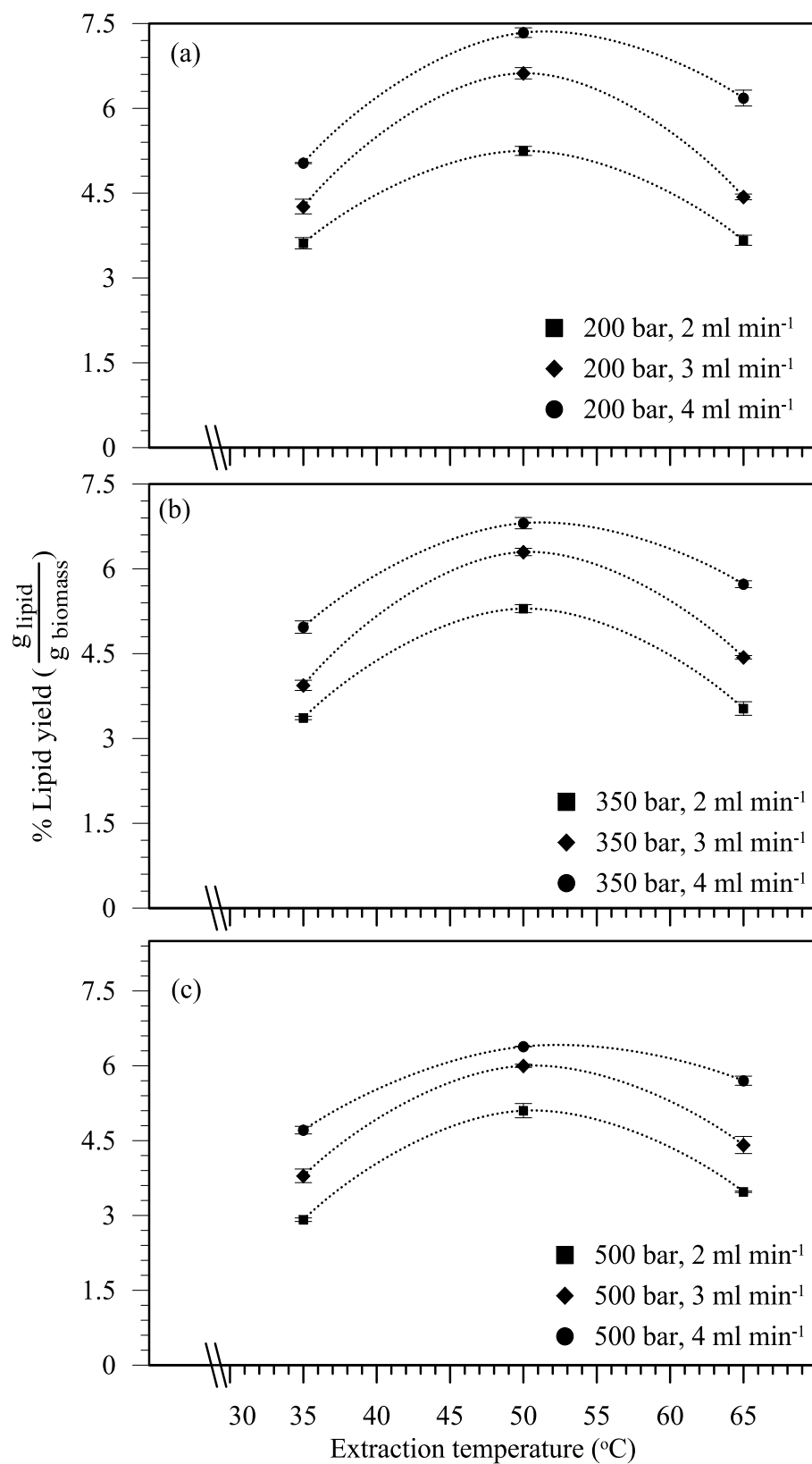
Figure C.2: Effect of the temperature on the steady sate lipids extraction yield

after passing 100 g of SC-CO$_2$ at different flow rates

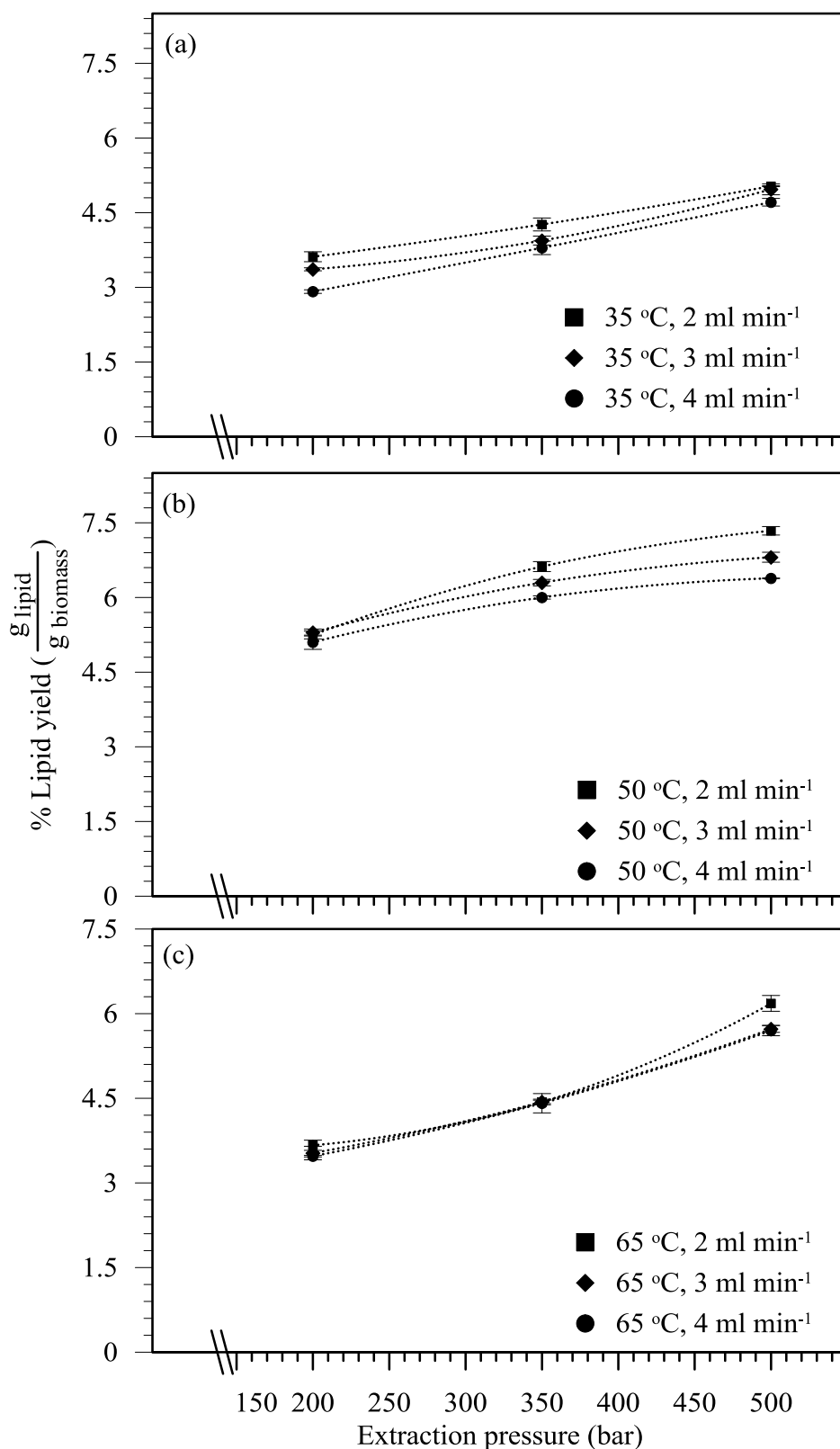((a) 200 bar , (b) 350 bar and (c) 500 bar)

Figure C.3: Effect of the pressure on the steady sate lipids extraction yield after passing 100 g of SC-CO$_2$ at different flow rates ((a) 35 ^{o}C , (b) 50 ^{o}C and (c) 65 ^{o}C)
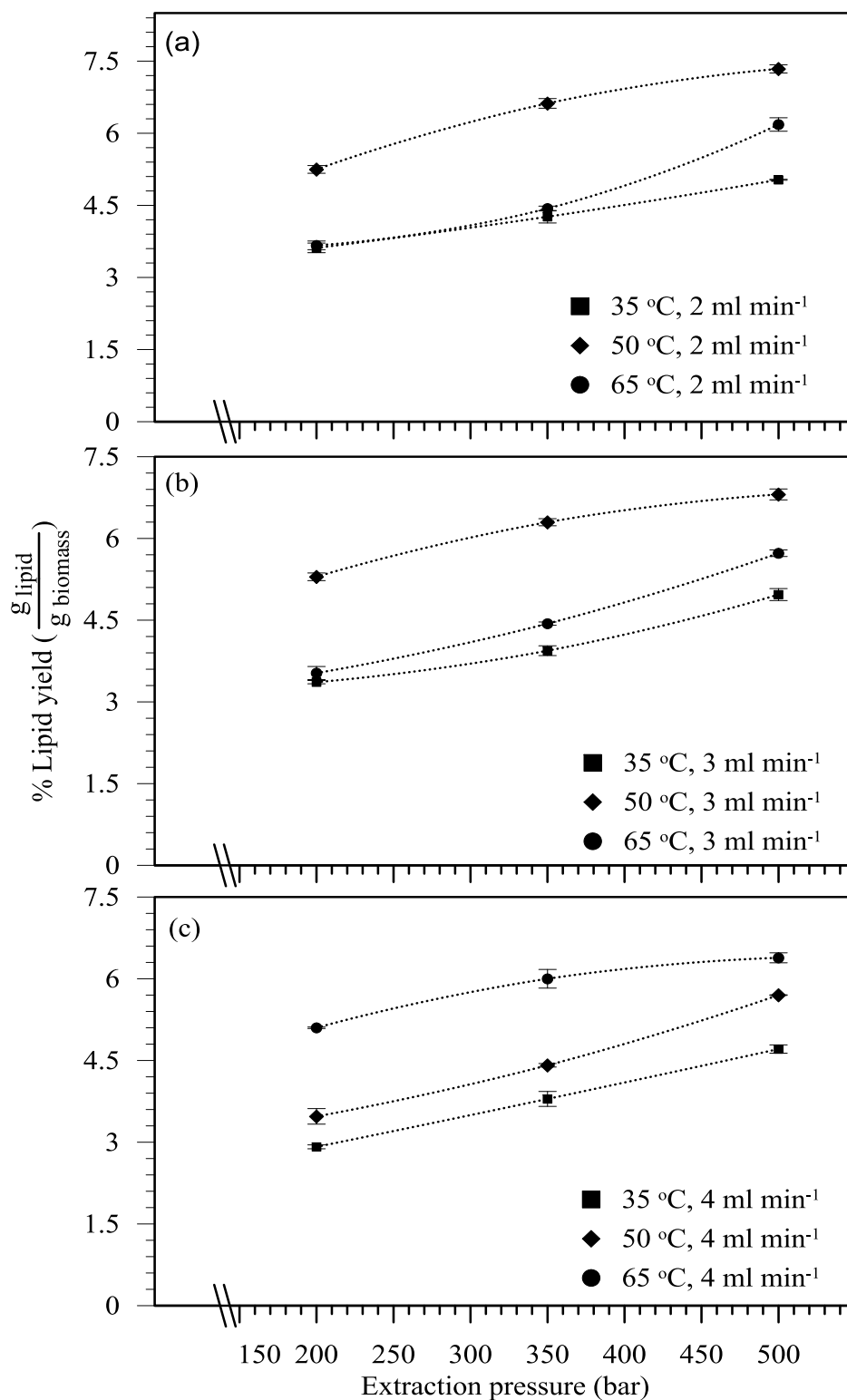
Figure C.4: Effect of the pressure on the steady sate lipids extraction yield after

passing 100 g of SC-CO$_2$ at different temperatures

((a) 2 ml min^{-1}, (b) 3 ml min^{-1} and (c) 4 ml min^{-1})